This document is the intellectual property of the fib – International Federation for Structural Concrete. All rights reserved.
This PDF of fib Bulletin 92 is intended for use and/or distribution solely within fib National Member Groups.

fib
CEB-FIP

Bulletin 92



Serviceability Limit State of Concrete Structures

Technical report

This document is the intellectual property of the fib – International Federation for Structural Concrete. All rights reserved.
This PDF of fib Bulletin 92 is intended for use and/or distribution solely within fib National Member Groups.

fib CEB-FIP

Bulletin 92

Serviceability Limit States of Concrete Structures

Technical Report

Task Group 2.1

September 2019

This document is the intellectual property of the fib – International Federation for Structural Concrete. All rights reserved.
This PDF of fib Bulletin 92 is intended for use and/or distribution solely within fib National Member Groups.

Approval for this bulletin

Subject to priorities defined by the Technical Council and the Presidium, the results of the *fib*'s work in commissions and task groups are published in a continuously numbered series of technical publications called *bulletins*. The following categories are used:

Category:	**Approval by**:
Technical report	Task group and chairpersons of the commission
State-of-the-art report	Commission
Manual / Guide to good practice / Recommendation	Technical Council
Model code	General Assembly

Any publication not having met the above requirements will be clearly identified as a preliminary draft.

fib Bulletin 92 was approved as a technical report by Commission 2 *Analysis & Design* in 2017.

This report was drafted by Task Group 2.1 Serviceability limit states within *fib* Commission 2

Jan L. Vítek (Convener and co-ordinating author; Metrostav a.s. and Czech Technical University in Prague, Czech Republic)

György L. Balázs (Previous convener, Budapest University of Technology & Economics, Hungary)

Cristina Barris (Universitat de Girona, Spain) Philippe Bisch (EGIS Industries, France), Clare Burns (Walt & Galmarini AG, Switzerland), Alejandro Perez Caldentey (Polytechnic University of Madrid and FHECOR, Spain), Vladimir Červenka (Cervenka Consulting, Czech Republic), Pier Giorgio Debernardi (Politecnico Torino, Italy), Frederic Duprat (INSA Toulouse, France), Noemi Duarte (Universitat Politecnica de Catalunya, Spain), Lars Eckfeldt (Deutsches Institut fuer Bautechnik, Germany), Mamdouh El-Badry (University of Calgary, Canada), Ekkehard Fehling (University of Kassel, Germany), Diane Gardner (Cardiff University, UK), Viktor Gribniak (Vilnius Gediminas Technical University, Lithuania), Matteo Guiglia (Studio AITEC, Torino, Italy), Ginatris Kaklauskas (Vilnius Gediminas Technical University, Lithuania), Alena Kohoutkova (Czech Technical University in Prague, Czech Republic), Laurie Lacarriere (INSA Toulouse, France), Robert Lark (Cardiff University, UK), Michel Lorrain (MLORRAIN Consultant, SAS, France), Antonio Mari (Universitat Politecnica de Catalunya, Spain), Philippe Menétrey (INGPHI, Switzerland), Eva Oller (Universitat Politecnica de Catalunya, Spain), Jean-Philippe Sellin (Bouygues, France), Helder Sousa (University of Surrey, UK), Maurizio Taliano (Politecnico Torino, Italy), Jean-Michel Torrenti (IFSTTAR, France), Lluis Torres (Universitat de Girona, Spain), Lukas Vrablik (Czech Technical University in Prague, Czech Republic), Roman Wan-Wendner (Ghent University, Belgium), Adorjan Borosnyoi (Budapest University of Technology and Economics, Hungary), Olivier Burdet (EPFL, Switzerland), Francesca Ceroni (Universita del Sannio, Italy), Mario Alberto Chiorino (Politecnico di Torino, Italy), Amin Ghali (University of Calgary, Canada), Josko Ozbolt (Universitaet Stuttgart, Germany), Marisa Pecce (Univerita del Sanio, Italy), Francois Toutlemonde (IFSTTAR, France), Damir Tkalčič (Civil Engineering Institute of Croatia, Croatia) Tamon Ueda (Hokkaido University, Japan), Andor Windisch (Germany).

Cover image: Experiment on bond of a prestressing steel at prestressed concrete beam. Author: Jan L. Vitek

© Fédération internationale du béton (*fib*), 2019

Although the International Federation for Structural Concrete / Fédération internationale du béton (*fib*) does its best to ensure that all the information presented in this publication is accurate, no liability or responsibility of any kind, including liability for negligence, is accepted in this respect by the organisation, its members, employees or agents.

All rights reserved. No part of this publication may be reproduced, modified, translated, stored in a retrieval system or transmitted in any form or by any means – electronically, mechanically, through photocopying, recording or otherwise – without prior written permission from the *fib*.

ISSN 1562-3610
ISBN 978-2-88394-135-9
doi.org/10.35789/fib.BULL.0092
Proofreading by Gordon Clark. Layout by Marie Reymond (*fib*).
Printed by DCC Document Competence Center Siegmar Kästl e.K., Germany

This document is the intellectual property of the fib – International Federation for Structural Concrete. All rights reserved.
This PDF of fib Bulletin 92 is intended for use and/or distribution solely within fib National Member Groups.

Acknowledgements

Authors:

Jan L. Vítek (Convener of TG2.1/Editor)
Metrostav a.s. and Czech Technical University in Prague, Czech Republic

György L. Balázs (Previous Convener/Editor)
Budapest University of Technology & Economics, Hungary

Philippe Bisch
EGIS Industries, France

Adorjan Borosnyoi
Budapest University of Technology and Economics, Hungary

Clare Burns
Walt & Galmarini AG, Switzerland

Alejandro Perez Caldentey
Polytechnic University of Madrid and FHECOR, Spain

Vladimir Červenka
Cervenka Consulting, Czech Republic

Pier Giorgio Debernardi
Politecnico Torino, Italy

Noemi Duarte
Universitat Politecnica de Catalunya, Spain

Ekkehard Fehling
University of Kassel, Germany

Matteo Guiglia
Studio AITEC, Torino, Italy

Antonio Mari Bernat
Universitat Politecnica de Catalunya, Spain

Maurizio Taliano
Politecnico Torino, Italy

Lluis Torres
Universitat de Girona, Spain

Lukas Vrablik
Czech Technical University in Prague, Czech Republic

Roman Wan-Wendner
Ghent University, Belgium

Andor Windisch
Germany

Contact details of Task Group members can be found in the members only section of the *fib* website, www.fib-international.org.

Authors by chapter

Chapters	Main Authors	DOI
1	Vítek	doi.org/10.35789/fib.BULL.0092.Ch01
2	Balázs and Vítek	doi.org/10.35789/fib.BULL.0092.Ch02
3	Balázs and Vítek	doi.org/10.35789/fib.BULL.0092.Ch03
4	Bisch, Caldentey, Duarte, Debernardi, Fehling, Guiglia, Mari Bernat, Taliano , Torres, Vítek and Vrablik	doi.org/10.35789/fib.BULL.0092.Ch04
5	Burns, Caldentey, Duarte, Fehling, Mari Bernat, Torres, Vítek and Vrablik	doi.org/10.35789/fib.BULL.0092.Ch05
6	Borosnyoi , Caldentey, Debernardi, Guiglia, Taliano, and Windisch	doi.org/10.35789/fib.BULL.0092.Ch06
7	Červenka	doi.org/10.35789/fib.BULL.0092.Ch07
8	Vítek	doi.org/10.35789/fib.BULL.0092.Ch08

This document is the intellectual property of the fib – International Federation for Structural Concrete. All rights reserved.
This PDF of fib Bulletin 92 is intended for use and/or distribution solely within fib National Member Groups.

Preface

The *fib* Model Code 2010 was published finally in 2013. The somewhat limited space in that document resulted in the publication of this Bulletin which should serve as a supplementary source of knowledge in the field of serviceability limit states (SLS). The design philosophy of limit states requires the check of two kinds of limit states. The ultimate limit states guarantee the safety of structures. The serviceability limit states guarantee the proper function, durability and favourable appearance of concrete structures. If the serviceability limit states are not satisfied, the user will complain that the structure was not built correctly, since it will suffer from cracking, deformations or vibrations. If the criteria of ultimate limit states are not satisfied, in many cases, the user will not realize that the safety of his structure is not as good as he expected. Although there is no intention to denigrate the importance of ultimate limit states, the serviceability limit states have great importance for the correct design of durable concrete structures.

In the last decades, there has been great pressure for cost savings in load-carrying concrete structures. Although the costs of a concrete structure of a typical building are about 20 to 25% of the total costs, there is a permanent pressure to save the cost of the steel and concrete resulting in the minimization of dimensions. The safety of structures can usually be kept within the code requirements, but the serviceability criteria are quite often violated, which may result in an incorrect function of structures in the future. The correct check of SLS criteria is rather sensitive if structures become more and more slender due to the reasons mentioned above.

This Bulletin provides explanation and extensive knowledge of the MC2010 sect. 7.6. The methods included in the following text should highlight the importance of SLS criteria and show in detail, how the brief information from MC2010 should be used. The detailed explanation of individual partial problems is supplemented by examples. Finally, additional information is provided above the scope of MC2010.

The members of *fib* TG2.1 "Serviceability limit states", who put this document together, had long discussions on individual parts of this Bulletin. Now the final version is available, but it does not mean that all problems are solved. As an example, the shear effects on deflections, particularly in prestressed structures, are not solved completely. The economic design of watertight structures requires more precise criteria. The application of new materials such as fibre reinforced concrete and ultra-high performance concrete (UHPC) will require further adjustments in SLS criteria. The concrete cover layer of structures made of UHPC, to name one example, certainly need not follow the criteria of Eurocodes and MC2010. Further research in cooperation with other groups within the *fib* will define new values. It will be covered by the work of working groups of the *fib* in the future.

Members of the TG2.1 believe that this Bulletin will contribute to improved design of concrete structures, in terms of SLS criteria, and that it will contribute to a better understanding of design approaches and methods included in MC2010.

Jan L. Vítek

Chair of Commission 2 *Analysis & Design*

This document is the intellectual property of the fib – International Federation for Structural Concrete. All rights reserved.
This PDF of fib Bulletin 92 is intended for use and/or distribution solely within fib National Member Groups.

Contents

Preface i
1. Introduction 1
2. Requirements for concrete structures in terms of SLS 3
2.1 Introduction 3
2.2 Serviceability limit states criteria 3
2.2.1 Stress limitation 3
2.2.2 Cracking and crack width 4
2.2.3 Deformations of concrete structures 5
2.2.4 Vibrations 5
2.3 Analysis of Serviceability Limit States 5
2.3.1 Stress analysis 6
2.3.2 Crack width analysis 6
2.3.3 Deformation analysis 7
3. Design criteria of serviceability limit states 9
3.1 Stress limits 9
3.2 Crack width 10
3.3 Deformation criteria 11
3.4 Vibrations 12
4. Rules and explanations 13
4.1 Calculation of stresses 13
4.1.1 RC sections 14
4.1.2 PC sections 21
4.2 Cracking 30
4.2.1 Bending cracks 30
4.2.2 Shear cracks 48
4.2.3 Cracks induced by deformation restraint 52
4.2.4 Cracks in prestressed concrete structures 56
4.2.5 Control of cracking without calculation 60
4.2.6 Cracks in orthogonally reinforced elements 63
4.3 Deflections of concrete structures 70
4.3.1 Calculation of deflections due to bending 72
4.3.2 Deflection due to shear 91
5. Examples 93
5.1 Stress and deflection analysis of a prestressed concrete beam 93
5.1.1 Stress analysis 93
5.1.2 Deflection analysis 96
5.2 Partially prestressed beam – cracking 99

This document is the intellectual property of the fib – International Federation for Structural Concrete. All rights reserved.
This PDF of fib Bulletin 92 is intended for use and/or distribution solely within fib National Member Groups.

5.3 Cracking due to shear 101
5.3.1 Experiment - Description of the structure 101
5.3.2 Numerical analysis of the formation of the first shear crack 102
5.3.3 Comparison of numerical and experimental results 103
5.3.4 Conclusions 104
5.4 Example for Combination of Restraint and Load Action 105
5.5 Design of watertight wall 109
5.5.1 Assumptions 110
5.5.2 SLS Design according to Model Code 2010 7.6.4.4 111
5.5.3 Discussion 114
5.5.4 Evenly spaced construction joints 114
5.5.5 On-site experience 115
5.6 Deflection analysis 115
5.6.1 Example of application of the general method 115
5.6.2 Example of application of simplified methods. Deflection control of a reinforced concrete slab 120
5.6.3 Solution of the problem by the General Sectional Method 124
5.6.4 General Method and Comparison of results 127
6. Outlook on serviceability limit states 130
6.1 Deflections of prestressed concrete beams 130
6.1.1 Slenderness limits 131
6.1.2 Basic assumptions for the parametric analysis 131
6.1.3 Parametric analysis 133
6.1.4 Conclusions 143
6.2 Shear effects on deflections 144
6.2.1 Introduction 144
6.2.2 Experimental background 145
6.2.3 Review of theoretical models for the calculation of the deformation of a macro-element of the beam block due to bending and shear 150
6.2.4 Calculation of the deflection of the beam due to bending and shear 155
6.2.5 Practical evaluation of the influence of shear on deflection 155
6.3 Slenderness limits 163
6.3.1 How slenderness limits are determined 163
6.3.2 Refining the model 164
6.4 The crack width along the concrete cover of reinforced concrete 171
6.4.1 General considerations of crack width and bond in concrete 171
6.4.2 Crack width along the concrete cover 176
6.4.3 Conclusions and recommendations 186

This document is the intellectual property of the fib – International Federation for Structural Concrete. All rights reserved.
This PDF of fib Bulletin 92 is intended for use and/or distribution solely within fib National Member Groups.

7. Verification of serviceability limit states by numerical simulation 188
7.1 Introduction 188
7.2 Crack model based on fracture mechanics 189
7.3 Crack model based on tension stiffening 192
8. Conclusions 194
References 196
Chapter 2 196
Chapter 3 196
Chapter 4 196
Chapter 5 199
Chapter 6 200
Chapter 7 201
Chapter 8 202

This document is the intellectual property of the fib – International Federation for Structural Concrete. All rights reserved.
This PDF of fib Bulletin 92 is intended for use and/or distribution solely within fib National Member Groups.

This document is the intellectual property of the fib – International Federation for Structural Concrete. All rights reserved.
This PDF of fib Bulletin 92 is intended for use and/or distribution solely within fib National Member Groups.

1. Introduction

Serviceability limit states criteria provide the limits which should guarantee the function, favourable appearance and the durability of concrete structures. They were developed within the limit state philosophy of design and they are used in the series of European codes. Members of *fib* commissions and task groups evaluated the rules of European codes and also the development of knowledge since completion of the CEB-FIP Model Code 1990 and wrote the *fib* Model Code 2010, which covers the knowledge until 2010, although the final edition of MC2010 was printed in 2013. The authors of MC2010 required the text to be clear, but reasonably short and transparent for everyday application. Therefore, there is a great amount of knowledge and technical opinions, which could not be included in the Model Code directly. The members of TG2.1 "Serviceability limit states" decided to collect the knowledge which was discussed in the group during writing the MC2010 in the form of a separate Bulletin of *fib*, which is focused on the extension of the MC2010 and which contains the background knowledge on criteria of serviceability limit states.

The Bulletin is divided into seven chapters. The major part is covered by chapters 4, 5 and 6. Chapter 4 explains the rules which are included in the MC2010. It extends the knowledge and provides more detailed explanation to individual criteria which could not be included in MC2010.

Chapter 5 illustrates the application of the rules of MC2010 in examples. Six examples cover stress analysis and deflection analysis of a prestressed beam, crack width analysis of a partially prestressed beam, cracking due to shear, an example on cracking due to restrained deformation in interaction with mechanical loading, the design of a wall exposed to restrained deformation with respect to the crack width and finally examples of deflection analysis using general and simplified methods.

Chapter 6, called "Outlook in Serviceability Limit States" forms an extension of knowledge slightly above the contents of MC2010. The discussion on deflections of prestressed concrete beams takes into account also the shear effects and shows when the shear becomes more important. The criteria of slenderness limits used for preliminary estimates of deflections are specified in MC2010 for selected frequent combination of parameters. Section 6.3 provides wider view on the slenderness limits and shows its dependence on different input parameters.

Crack width criteria should also guarantee the durability of concrete structures. Section 6.4 is focused on mutual relation of concrete cover and crack width. Usually thicker cover layer results in larger crack width, which need not mean reduced durability of the structure.

Finally, chapter 7 illustrates numerical analysis of serviceability limit states. Detailed analysis of cracked concrete structures requires sophisticated numerical models, so that reasonably correct values can be obtained. A successful application of numerical methods requires detailed knowledge of the computer codes used so that the correct input parameters are used and finally so that the obtained results can be correctly interpreted. It is important to note that sometimes the philosophy of limit states may be confusing, since there are characteristic, mean and design values of mechanical properties on one side and a great variety of load combinations on the other side. It is necessary to choose the right combinations, which provide the results which are then applicable for serviceability

This chapter was mainly authored by Vítek.

doi.org/10.35789/fib.BULL.0092.Ch01

This document is the intellectual property of the fib – International Federation for Structural Concrete. All rights reserved.
This PDF of fib Bulletin 92 is intended for use and/or distribution solely within fib National Member Groups.

criteria. It is expected that numerical methods will see a further development in the future leading to even more powerful tools. In the near future, the numerical methods are becoming a part of the wider system which is now known as BIM (Building Information Modelling). However, the role of a structural engineer, who is responsible for the design, is to find a reasonable balance between the computing effort and engineering judgment which should ensure the correct and robust design of structures.

This document is the intellectual property of the fib – International Federation for Structural Concrete. All rights reserved.
This PDF of fib Bulletin 92 is intended for use and/or distribution solely within fib National Member Groups.

2. Requirements for concrete structures in terms of SLS

2.1 Introduction

Serviceability limit states aim to ensure that concrete structures work without any problems for a complete length of their assumed service life. The basic requirements are briefly described in MC2010 sect. 3.3.1.1[2-1]. While ultimate limit states deal with safety, where a necessary reserve is required, SLS deals with everyday function of structures. If requirements of SLS are not satisfied, the clients will recognise such a situation very quickly in contrary to violation of ULS, where the reduction of safety reserve may not be recognised at all, even for a long time period. If some of serviceability criteria are not satisfied, the structure remains safe, but can be repaired. However, on the other hand excessive deflections, which also can be observed also in completely safe structures, may disturb the use of the structure significantly, and the repair may be very sophisticated and expensive and also limiting for future use of the structure.

Additionally, the serviceability criteria may be closely connected with durability of structures. In such cases, although the serviceability criteria are not satisfied, the structure may work completely correctly, but over time, corrosion of steel or any similar damage may result in reduction of service life.

The serviceability criteria are therefore essential for a correct and reliable design of concrete structures. Their importance is very high; on the same level as the ultimate limit state criteria, or durability criteria, etc. Violation of them results in problems reported by the users, and eventually in large costs for repair. Also, the reputation of the consultant and building company suffers if the structure is built without satisfying the SLS criteria.

2.2 Serviceability limit states criteria

According to MC2010 four groups of SLS criteria are applied in design.

1. Limitation of stresses
2. Cracks in concrete elements
3. Deformations (deflections, rotations, etc.) of concrete elements
4. Vibrations of elements or structures

Depending on the character of the structure all or at least some of them have to be checked.

2.2.1 Stress limitation

Stress in concrete, reinforcing steel and prestressing steel has to be limited. The concrete stress in compression should not exceed the limit of about $0.45f_c$ which is sometimes called a limit of microcracking of concrete. Internal damage may occur in concrete if the stress becomes higher. Although no visible damage is observed, the internal processes could reduce the strength of concrete under long-term load. Creep which is normally

This chapter was mainly authored by Balázs and Vítek.

doi.org/10.35789/fib.BULL.0092.Ch02

This document is the intellectual property of the fib – International Federation for Structural Concrete. All rights reserved.
This PDF of fib Bulletin 92 is intended for use and/or distribution solely within fib National Member Groups.

assumed to be linear with respect to the stress may become larger, i.e. non-linear. It can also happen that at higher long-term load, creep may increase after some time and result in failure of the concrete element.

High compression in one direction may result in tension in the other direction. If the compressive stress is high, the tensile stress in the other direction may exceed the tensile strength of concrete and cracks may appear.

Normally the stresses are calculated under simplified assumptions. The effects of eigenstresses in concrete sections due to non-uniform shrinkage and due to temperature distribution are not usually taken into account, but actually they contribute to the stresses developed by loads or by restrained shrinkage. Therefore, it is reasonable to keep the stress low which is guaranteed by the SLS criteria. The tensile stress in concrete is not limited, cracking is considered to be usual in areas exposed to tension. Exceptions may be expected for prestressed concrete structures, where cracking is sometimes excluded and compression reserve is prescribed (e.g. segmental structures without conventional reinforcement in joints).

Stress in reinforcement also has to be limited. High stress in steel may result in high tension in concrete and to extensive cracking. The stress in steel is often calculated on the basis of the factor α ($\alpha = E_s/E_c$). For long term load it is allowed to use a simplified approach, where $\alpha = 15$, while α is actually variable (see sect. 4.1.1). The stress in steel also has to be limited due to the simplified analysis, but mainly it is necessary to avoid plasticity in steel ($\sigma_s \leq 0.8 f_{yk}$). On the other hand, if an imposed deformation is applied the stress in steel may be allowed to be higher ($\sigma_s \leq f_{yk}$), since stress relaxation is assumed to take place over time.

Stress in prestressing steel should be also within reasonable limits. The limit of linearity should not be exceeded, which is given by the limit derived from the tensile strength or from the yield strength. Relaxation of stress and induced prestress losses represent a major threat for prestressed structures. In order to keep the stress relaxation reasonably low, it is worth to define the stress limits in prestressing steel rather conservatively ($\sigma_p \leq \{0.75 f_{pk}; 0.85 f_{p0.1k}\}$). The prestress losses, which are essential for correct function of prestressed structures mainly with respect to the long-term performance, can be reliably defined if the stress is limited.

2.2.2 Cracking and crack width

Cracking is an inevitable feature associated with concrete and concrete structures. The three main reasons for the need to limit crack widths are appearance of the structure, function and durability of the structure. The first reason is preferably psychological, but it is very important for the clients who use concrete structures. The other two reasons are technical and the crack limits should ensure that the structure will work properly for the expected service life.

It is important to note that the mechanism of crack origin and their development are sophisticated processes dependent on many material and structural parameters and environmental conditions. It is not possible to provide procedures for exact analysis of cracking. The procedures which are described in the following sections should be considered as practical and simplified approaches which should provide an approximate estimate of possible crack widths and which should indirectly ensure that the structure will satisfy the performance required by the client.

This document is the intellectual property of the fib – International Federation for Structural Concrete. All rights reserved.
This PDF of fib Bulletin 92 is intended for use and/or distribution solely within fib National Member Groups.

2.2.3 Deformations of concrete structures

Concrete structures developed originally from stone and masonry structures, which were considered to be rather stiff and which exhibited small deformations. Over time concrete parameters improved, and spans were significantly increased followed by reduction of dimensions, which resulted in slender beams and slabs. The criteria for deflections and rotations at the support areas then become essential for a correct design. Increasing strength of concrete and steel make it possible to design flexible and safe structures, where the criteria for deflection are governing for the dimensions design (similarly as is sometimes the case for steel structures). The stiffness of concrete structures and elements is also extremely important for redistribution of stresses in statically indeterminate structures.

For prestressed structures the final performance is a result of the difference between the effect of loads and the effect of prestressing, which works in the opposite direction. The deformation of prestressed structures is therefore extremely sensitive to the level of prestressing, which must be carefully analysed. Many factors with a large statistical scatter influence the performance of structures. Typically creep and shrinkage of concrete, stress relaxation of steel, etc., have to be carefully considered. The uncertainty given by the nature of these phenomena should lead to a reasonably conservative design, which has a reduced sensitivity to these uncertain phenomena, which is called a robust design.

Unfortunately, the reduction of costs, which is required by some clients, and insufficient experience of some consultants, result in design of extremely slender structural elements (typically the floors slabs and beams in buildings). Although they may satisfy the criteria of ultimate limit states, their insufficient stiffness may lead to damage in internal non-bearing structures. The deflections increase during the time, which requires repeated repairs of interior structures. A repair of concrete structures in terms of increasing stiffness is usually very costly or sometimes even impossible. The savings resulting in reduced stiffness are therefore rather dangerous, and finally may lead to depreciation of a complete structure.

The deformations must be limited because of appearance, proper function of a complete structure (including integrity of non-structural parts) and because of cracking which may appear if deflections become large.

2.2.4 Vibrations

Vibrations are typical for slender structures. They may result in discomfort of the occupants, in operation of machines and structural damage. It is necessary to keep vibrations within the limits specified for the structure under consideration. The dynamic modelling of the structure will determine natural frequencies and the critical performance of the structure may be determined on the basis of their comparison with excitation frequencies.

2.3 Analysis of Serviceability Limit States

In the MC2010, principles of design are described in section 4. The majority of design procedures are based on the partial safety format. However, this formulation is more suitable for ultimate limit state design. In the serviceability limit states the structural analysis is usually simplified using an assumption of the elastic behaviour, and the load combinations are close to the realistic load acting on structures. The load combinations are derived from the probabilistic analysis. However, most of loadings, especially in building structures,

This document is the intellectual property of the fib – International Federation for Structural Concrete. All rights reserved.
This PDF of fib Bulletin 92 is intended for use and/or distribution solely within fib National Member Groups.

are defined by experience (residential buildings, offices), or they are defined by the user (e.g. business centres, archives, storage areas). Combinations of actions for serviceability limit states are defined in MC2010[2-1] sect. 4.5.2.5. The characteristic, frequent, and quasi-permanent combinations are usually used. A simplification is proposed (Eq. 4.5-24 and 4.5.-25).

Using a philosophy of partial safety factors, the action side is multiplied by safety factors equal to 1. The resistance of the structure also uses safety factors of unity, but sometimes the characteristic values of the strength are used (concrete in compression and steel), and the strength of concrete in tension is usually considered by the mean value (f_{ctm}).

Prestressing is considered as a kind of loading, i.e. prestressing forces are regarded as an action on the structure. The prestressing level is basically given by the prestressing force reduced by the prestress losses. Prestress losses are calculated from the usual formulas and are assumed as mean values. For purposes of verification of serviceability limit states, the mean value of prestressing force is taken as design value (MC 2010[2-1], sect. 5.4.7.2). If the prestressing force is known (e.g. from the site measurements) the mean value of the prestressing force can be also used for the crack width analysis. In post-tensioned structures, the prestressing force is always measured on the site during the prestressing process, and the mean value can be used. For pretensioned elements, the production control in the precasting plant should also guarantee the prestressing level of the products, which could be used when the prestressing force is known.

In cases where the design value of the prestressing force or any variation on site would influence the behaviour of the structure in an over-proportionate way, the designer must take adequate precautions, e.g. providing spare ducts and anchorages for additional prestressing units (internal or external), which could be installed and stressed later during the service life of the structure.

2.3.1 Stress analysis

Stresses in the individual structural elements are usually calculated using elastic analysis. Non-linear analysis may be also used, but then the principle of superposition cannot be used and the analysis becomes sophisticated which is not necessary in most cases. Stresses in cracked elements are calculated under the assumption of the effective section in the stage II (i.e. the area of concrete under tension is excluded). The stresses induced by long-term load may be analysed using an effective modular ratio $\alpha_{e,ef} = E_s/E_{c,ef}$, which may be taken simply $\alpha_{e,ef} = 15$. Stress analysis is described in detail in the sect. 4.1.

2.3.2 Crack width analysis

Cracks in concrete are inevitable and their width is highly variable and dependent on many factors. The analysis takes into account only the most important of them. The theory of analysis of crack widths is partly based on the physical mechanism and partly on experimental results and experience. The calculated crack width according to the sections (4.2.1 – 4.2.6) represents so called design crack width (w_d), which is calculated under the appropriate load combination and compared with a nominal limit value (w_{lim}), which is specified as a design criterion. However, this procedure should ensure that the crack width will be in most of cases smaller than the limit value w_{lim}, but some cracks may exceed this value.

This document is the intellectual property of the fib – International Federation for Structural Concrete. All rights reserved.
This PDF of fib Bulletin 92 is intended for use and/or distribution solely within fib National Member Groups.

It is also important to note that crack width analysis is based on very simplified approaches which do not take into account the detailed properties of concrete, the stresses due to non-uniform shrinkage and temperature distribution along the section of the concrete element, etc. The empirical models are based on a large number of experiments, where the specimens were loaded by forces and the crack widths were measured. The cracks induced by restrained deformations are important for appearance as well as for function of concrete structures; however, their analysis is rather unreliable due to a large variety of influencing factors, especially the degree of restraint. The design of e.g. watertight structures requires very detailed analysis and design (including technological and structural details). Some recommended procedures are described in the sect. 4.2.3, 5.4 and 5.5., but also in specialist recommendations.

Cracks, which are important for appearance and durability, will be present for a long time, i.e. they are induced by long-term load in the analysis represented by a quasi-permanent combination for reinforced concrete structures or by a frequent combination for prestressed structures.

2.3.3 Deformation analysis

Analysis of deformations (deflections and rotations) is significantly influenced by cracks in concrete elements. If no cracking is assumed (prestressed structures) elastic analysis is completely appropriate. If the structure is cracked, the linear or non-linear analysis may be used. Non-linear numerical methods represent a higher level of analysis and the results are dependent on the accuracy of the applied procedure. General non-linear methods take into account the actual distribution of stiffnesses along the structure and then the distribution of internal forces as well as the deformations are analysed together. The application of non-linear methods is not usual or necessary for ordinary structures. Routine structural analysis used to be based on elastic analysis, which results in internal forces distribution (bending moments, shear forces and axial forces). When these forces are known, the stiffness is reduced depending on the loading level and is analysed in individual sections or parts of the structure and then the deformations are calculated using the reduced stiffnesses of the structural system. Stiffnesses are reduced depending on cracking and creep of concrete. The shrinkage induced deformation should not be neglected particularly in elements with asymmetrical reinforcement at the top and bottom surface.

Deformations of reinforced concrete structures are significantly influenced by cracking, which has to be correctly considered in the analysis. In buildings deformations are often analysed in three stages. i) Total deflection which is a deflection of the structural element at the end of the service life related to the initial (designed) shape. ii) Long-term deflection increment from the time after the internal non-bearing structures are installed until the end of the service life. These two values of deflections are analysed under the long-term load i.e. the quasi-characteristic load combination. iii) The short-term deflection induced by short-term (applied load). This value is important for an instantaneous deformation of the structure.

The serviceability check results in a statement that the calculated deformation $v_c \leq v_{lim}$, where v_c is a calculated deflection and v_{lim} is an appropriate limit value. The simplifications accepted in some methods should provide results which are overestimated, i.e. their results are greater than the actual deformation of the structure. Then the criterion limiting the calculated deflection will guarantee that the actual deflection should be also smaller than the limiting value.

This document is the intellectual property of the fib – International Federation for Structural Concrete. All rights reserved.
This PDF of fib Bulletin 92 is intended for use and/or distribution solely within fib National Member Groups.

Cracking represents damage of the structural element which is a reason for reduction of stiffness and increase of deformations. Cracking may occur due to different reasons. Some cracks may appear during the construction process, then the structure is open to operation and it can be exposed to the maximum allowable load (e.g. characteristic combination of loads). After removing such a rather unfavourable load combination the cracks partly close. If the long-term deflection is calculated, the load under consideration (e.g. quasi permanent load combination) may be smaller than the load which could induce cracks earlier. Therefore, it is important for correct deformation analysis to take into account the most severe load which could have been active on the structure before or after and to consider the cracks induced by such load, when the stiffness is calculated. In the opposite case, it could be concluded that the long-term load would induce no or very little cracking and the stiffness would be overestimated and the deformations underestimated. It is also important to note, that the deflection analysis should provide an upper limit for the deflection, which should not be exceeded. If the long-term deformation is calculated, creep and shrinkage have to be taken into account. A detailed explanation of the deformation analysis is described in the sections 4.3 and 5.6.

This document is the intellectual property of the fib – International Federation for Structural Concrete. All rights reserved.
This PDF of fib Bulletin 92 is intended for use and/or distribution solely within fib National Member Groups.

3. Design criteria of serviceability limit states

Design criteria for verification of serviceability limit states were developed many years ago and they are based partly on experience, research results and sometimes on agreement between the client, consultant and contractor.

3.1 Stress limits

Stress limits are specified almost exactly. The criteria are based on reasonable use of the material capacity.

Concrete short-term stress should not exceed $0.6f_{ck}$. The long term stress in concrete should not exceed the limit $0.4f_{ck}$. The mean strength is defined by Eq. 5.1-1 and 5.1-2 (MC 2010[3-1]) $f_{cm} = f_{ck} + 8$ [MPa]. Table 3.1 shows the stress limits for short-term and long-term loads. and their comparison with the mean concrete strength. The stress limit of $0.6f_{ck}$ for short-term load should avoid microcracking in concrete and also any development of cracks in the perpendicular direction. The stress limit of $0.4f_{ck}$ for long-term load should avoid the non-linear creep of concrete, which would lead to accelerated deformations of concrete elements.

Table 3.1: Stress limits for selected concretes classes

Concrete Class	C25/30	C35/45	C50/60	C120/140
f_{ck} [MPa]	25	35	50	120
f_{cm} [MPa]	33	43	58	128
$0.6\ f_{ck}$ [MPa]	15	21	30	72
$0.4\ f_{ck}$ [MPa]	10	14	20	48

Stress limits for concrete in tension are not specified, since it is assumed that cracking is allowed, and therefore instead of a tensile stress limit, crack width limits are used. If cracks have to be avoided the decompression limit is required, i.e. no tension is allowed in the concrete section.

Stress limits in steel are specified depending on the steel yield strength. If the stress is induced by characteristic load combination the tensile stress in steel reinforcement should not exceed $0.8f_{yk}$. If the stress is induced due to entirely imposed deformation the stress limit may be increased to $1.0f_{yk}$. Stress verifications should be carried out for fatigue effects in partially prestressed members.

Stress limits for prestressing steel are defined in two stages (sect. 5.4.4.2 MC 2010[3-1]). Stage 1 specifies the maximum stress in prestressing steel before transfer of prestressing force to concrete (i.e. during prestressing operation). The lower of the following values is limiting.

$$\sigma_{p0,\max} = 0.8f_{pk} \quad \text{or} \quad \sigma_{p0,\max} = 0.9f_{p0.1k} \tag{3-1}$$

In exceptional cases it is possible in stage 1 to allow even higher stress, up to $0.95f_{p0.1k}$. This allowance may be used if unexpected deviation of frictional behaviour on the site occurs, such that it may be impossible to obtain the required prestressing force under the limitation specified normally for stage 1.

This chapter was mainly authored by Balázs and Vítek.

doi.org/10.35789/fib.BULL.0092.Ch03

This document is the intellectual property of the fib – International Federation for Structural Concrete. All rights reserved.
This PDF of fib Bulletin 92 is intended for use and/or distribution solely within fib National Member Groups.

Maximum stress in prestressing steel should not exceed the lower of the following values after transfer of the prestressing force to concrete (stage 2).

$$\sigma_{p0,\max} = 0.75 f_{pk} \quad \text{or} \quad \sigma_{p0,\max} = 0.85 f_{p0.1k} \tag{3-2}$$

This limit should ensure that permanent deformations will not occur in prestressing steel and also that the stress relaxation remains in reasonable limits.

3.2 Crack width

The factors influencing allowable crack widths are not exactly defined as the limits of stresses. The maximum crack width is defined by appearance, by functional requirements, and by durability requirements. Appearance criteria are typically subjective and it is normally required that cracks should not be visible from a certain distance.

Durability of structures requires limiting the crack width at the level of reinforcement, since there is a risk of corrosion. Depending on the concrete cover the crack width on the surface may be larger than that at the level of reinforcement. The crack width can be measured only at the concrete surface, which leads to the requirement of the limited crack width at the concrete surface. But both limits of the crack width (appearance and durability) are to a certain extent subjective and should be agreed with the owner.

Functional limits of the crack width are important for structures which should be water or gas tight. In such cases special recommendations should be used for design (e.g. DAfStb[3-2], DAfStb[3-3], ÖVBB[3-4], EN 1992-3[3-5]). The crack width can be limited to smaller values 0.10 mm to 0.25 mm. Normally in dry conditions the cracks which would influence the structural performance of a typical structure would be significantly larger than the limits due to appearance and durability.

The crack width limits are a subject of discussion among technical experts. The actual cracks observed in some structures are often larger than limits recommended by codes or by MC2010[3-1]. Some experts propose to allow cracks up to 0.5 to 0.6 mm. On the other hand, the methods of crack width analysis have a very limited accuracy and sometimes in spite of the design limiting the crack width, the measured cracks are much wider than expected. The experts who wrote the MC2010 decided to keep the limits of the crack width similar to those in European codes. Experience with corrosion of steel and with consequences of severe environmental conditions on concrete structures is a good reason for smaller allowable crack width. The crack width for RC structures under quasi-permanent load combination is limited to 0.3 mm in cases of exposure classes of environment (XC, XD, XF, XS, w_{lim} = 0.3 mm). For exposure class X0 larger cracks limited by other criteria are allowed. When de-icing agents are used on the top of the tension zones, the limiting crack width should be discussed with the client.

The crack width limits for prestressed concrete members were agreed in MC2010[3-1] (Table 7.6-1), if no more precise data are available. The allowable crack width varies from 0.2 to 0.3 mm, depending on the exposure class of the environment and on the protection level of the prestressed reinforcement. In some more severe conditions, decompression is not allowed in the zone of the prestressing tendons.

This document is the intellectual property of the fib – International Federation for Structural Concrete. All rights reserved.
This PDF of fib Bulletin 92 is intended for use and/or distribution solely within fib National Member Groups.

3.3 Deformation criteria

Deformation criteria are based on requirements which were briefly described in sect. 2.2.3. Three criteria may be necessary.

1. The total allowed deformation of the structural member subjected to long-term load (quasi-permanent load combination)

2. The deformation increment from the time of installation of internal non-bearing structures until the end of the service life induced by long-term load (quasi permanent load combination should be used)

3. Instantaneous deformations induced by applied load (a suitable load combination should be discussed between the client and designer. If no information is available the characteristic or frequent load combination may be used (See sect. 7.6.2 MC2010[3-1]).

In buildings usually criteria 1 and 2 are essential; in bridges rather criteria 1 and 3 become more important.

In order to satisfy the limits of deformations, all effects which can influence the deflection development have to be considered, cracking in particular. I.e., if the structure is cracked due to previous loading (during construction, or during earlier service life), the cracks have to be taken into account. E.g. if the structure is subjected to a maximum load which is allowed immediately after opening (i.e. characteristic load combination) the corresponding damage due to cracking should be considered in the deformation analysis.

The calculated deformation which is compared with the deformation limit need not necessarily be a real deformation which can be expected to be measured on the site. It should be a limit which takes into account all effects which can realistically appear during the service life of the structure. It is the usual approach accepted for all verifications. The unfavourable combination of loads and other effects have to be checked and the limit criteria should be satisfied.

The deformation criteria should be specified by the owner in agreements with the consultant and the contractor. Appearance of the structure is a purely subjective issue; the function of the structure depends on the equipment inside the building or other structure and integrity with non-structural elements is also dependent on specific features of the structure under consideration.

In ordinary buildings the integrity with non-structural parts of the structure seems to be the most severe limit for deformation of the concrete structure. Therefore, it is extremely important to check what materials and what structures will be used inside and then to specify the limits of deformation. The verification of deformations according to item 2 is important.

Often there is an objection that the necessary criteria are not known in advance. Then it is a possibility to use the specific criteria which are rather moderate and which are prescribed in MC2010[3-1] and also in Eurocode 2[3-5]. The total deflection of beams or slabs should not exceed the value of span/250 measured relatively to supports. In case of the cantilever, this limit is not applicable. It may be recommended before application of this rule to multiply the span of the cantilever by a factor of 2). This criterion is derived from the appearance of the structure. Long term deformation can be balanced by precambering, which is usual for bridges, but in buildings it is used only

This document is the intellectual property of the fib – International Federation for Structural Concrete. All rights reserved.
This PDF of fib Bulletin 92 is intended for use and/or distribution solely within fib National Member Groups.

sometimes for large spans. It is important to note that precambering does not contribute to compliance with item 2.

If no data are available for the criterion under item 2, the MC2010[3-1] and Eurocode 2[3-5] recommend value of span/500 (integrity with non-structural elements). This value is not conservative at all, and may not guarantee, that cracks (e.g. in partition walls) will not appear. Therefore, it is strongly recommended to check which structures and materials will be used inside the building. If there are doubts it is always recommended to satisfy the recommendations for the minimum depth of beams or thickness of the slab which is mentioned in the table 7.6-6 MC2010[3-1].

Deformation limits for bridges are given in the specific codes.

3.4 Vibrations

Structures should be designed to avoid large deformations, large velocities and large accelerations during vibrations. It is necessary to design a concrete structure in such manner so that the unfavourable effects would be minimised. The natural frequencies of the structure should be outside the range of frequencies induced by possible loadings. Then the interference of the natural and forced vibration could be avoided. The natural frequencies of the designed structure can be calculated using its stiffness and weight distribution. The forced vibrations are briefly given in the table 7.6-7 MC2010[3-1] for most common situations. The comfort criteria and limit values for footbridges are given more in detail e.g. in *fib* Bull. 32[3-6] (2005), sect. 5.5.

This document is the intellectual property of the fib – International Federation for Structural Concrete. All rights reserved.
This PDF of fib Bulletin 92 is intended for use and/or distribution solely within fib National Member Groups.

4. Rules and explanations

This chapter will explain in more detail the background of individual rules applied in MC2010[4-1]. Knowledge which could not be included in the MC2010 is presented here to a larger extent. It should help to understand the meaning of individual clauses in MC2010.

4.1 Calculation of stresses

In service conditions Model Code 2010 requires the calculation of stresses in concrete and steel to avoid high levels of creep or unacceptable cracking. Under the quasi-permanent load combination, limiting the concrete compressive stresses to a value equal to $0.4f_{ck}(t)$ means preventing non-linear creep that can lead to excessive long term deformations and serious consequences on prestress losses. Further cracks parallel to reinforcing bars may be observed when, in the presence of sustained and short term loads (or with the characteristic combination of actions), the stress level exceeds a critical value of $0.6f_{ck}(t)$. Limitation of the tensile stress in the ordinary steel to a limit of $0.8f_{yk}$ allows inelastic strains and large, permanently open, cracks to be avoided. In partially prestressed members stress verifications should be carried out for fatigue effects. Last but not least, the calculation of stresses in steel is also required for the calculation of crack widths, when these are determined directly or are checked indirectly, and deflections.

Stresses can be calculated applying the principle of superposition of effects if the section is uncracked, as often happens in the case of members subjected to an axial force with or without a moderate eccentricity (RC columns and walls) or whenever the maximum concrete tensile stress obtained on the basis of an uncracked section under the characteristic load combination does not exceed the mean concrete tensile strength, f_{ctm}. This is the case for fully PC beams which have to remain uncracked under the characteristic load combination or for partially PC beams under the quasi-permanent load combination. In aggressive environments, partially PC beams should also respect a limit state of decompression under the frequent load combination.

However, greater difficulties can arise in cracked sections in the presence of creep, shrinkage and variations in the elastic modulus of the concrete because of the non-conservative nature of the system. The final configuration of the structure therefore depends on the evolution of the various phenomena, the histories of the actions involved and the need to satisfy compatibility conditions which, in indeterminate structures, continuously change the load effects along the structure. As a consequence, the relationships between actions and load effects, stresses and strains are not directly proportional and it is not possible to apply the principle of superposition of effects without losing the possibility of obtaining the solution in a closed form.

In literature this problem of the calculation of stresses is solved through various methods with different levels of refinement[4-2]. In the following the various aspects that are involved in the calculation of stresses in structures are considered taking into account, first, the case of RC sections and, after, PC sections.

This chapter was mainly authored by Bisch, Caldentey, Duarte, Debernardi, Fehling, Guiglia, Mari Bernat, Taliano, Torres, Vítek and Vrablik.

doi.org/10.35789/fib.BULL.0092.Ch04

This document is the intellectual property of the fib – International Federation for Structural Concrete. All rights reserved.
This PDF of fib Bulletin 92 is intended for use and/or distribution solely within fib National Member Groups.

4.1.1 RC sections

4.1.1.1 Load and creep effects on an uncracked RC section in composed bending

The effects of the load and the creep on an uncracked RC section can be evaluated through the effective modulus method and combined with those due to shrinkage by applying the superposition of the effects, because the reacting sections remain unchanged.

4.1.1.2 Creep effects on a cracked RC section in composed bending

The creep effect on a cracked, simply reinforced, RC section subjected to bending is demonstrated in Fig. 4-1, where the stress and strain configurations at times t_0 and t are shown. Times t_0 and t represent the age of concrete at the time of loading and the time being considered, respectively. The analysis is carried out under the main hypothesis of linear concrete stresses of the compressed zone of the section. Because of creep, the compressive strains of concrete fibres increase in time leading to an increase of the curvature of the section and the strain of steel. The higher tensile strains are associated with a higher stress on steel and, therefore, a greater resultant stress in the concrete is required for equilibrium. But, if the bending moment remains constant between t_0 and t, e.g. due to quasi-permanent loads, the internal lever arm of the tensile and compressive resultants have to be reduced. This means that the neutral axis moves towards the bottom, the compressive depth of concrete increases and the maximum concrete stress decreases. Finally, at time t the neutral axis (the level where the concrete stresses are equal to zero) does not coincide with the level where the strains are equal to zero. The presence of compressive steel is however favourable to the behaviour of the RC section, reducing the increase of deformations of the section and partly providing the required compressive resultant.

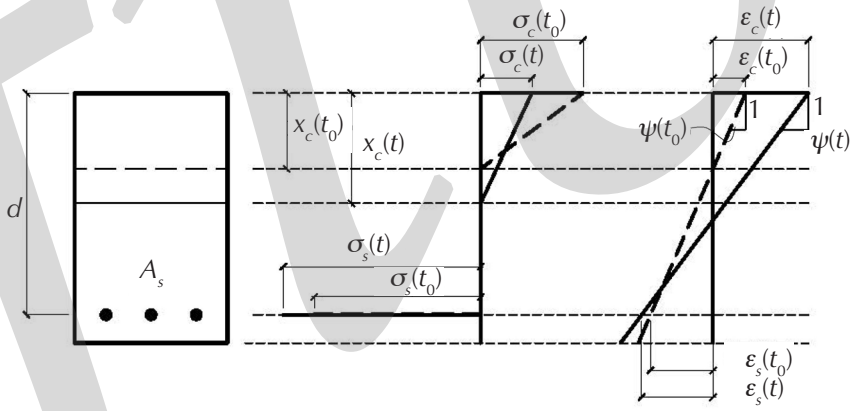


Fig. 4-1 Stresses and strains at times t_0 and t, due to creep effect, in presence of constant load effects

4.1.1.3 General method and refined approach

The most general and refined approach for the evaluation of creep and shrinkage effects consists of the incorporation of the constitutive relation for concrete for each part of the section into a step-by-step incremental numerical solution (see MC2010[4-1], sect. 7.2.4.11). For each time-step, the solution is achieved by imposing the equilibrium and congruence conditions and requires an iterative calculation. This method leads to laborious analyses and a consequent calculation effort that is in general justified only in structures sensitive to the time-dependent behaviour of concrete, where a particular accuracy is required.

This document is the intellectual property of the fib – International Federation for Structural Concrete. All rights reserved.
This PDF of fib Bulletin 92 is intended for use and/or distribution solely within fib National Member Groups.

A more affordable solution of the problem consists of the method proposed in the CEB Bulletin d'Information no. 235[4-2]. In this case the problem is solved through a calculation method of stresses on RC and PC cracked or uncracked sections developed by means of a refined analytical model, based on the method of imposed deformations, able to properly take into account the presence of various stages of the construction and several tendons prestressed in different phases.

The basic assumptions include:

- if the tensile stress (positive sign) in the concrete does not exceed the strength value f_{ct}, the section is uncracked.
- if the section is cracked, the concrete in tension is neglected.
- the traditional hypothesis of superposition and linearity of creep apply.
- in service conditions, steel has linear elastic behaviour characterized by the modulus E_s, and the prestressing tendons are also subjected to relaxation.
- plane section before loading remain plane after loading.
- the stress diagram in the uncracked concrete is linear.

The analysis is carried out by the method A.A.E.M. (Age Adjusted Effective Modulus – one study addresses this[4-4] (MC2010[4-1], sect. 7.2.4.10), represents an approximate algebraic formulation that offers a very good accuracy in particular in the case of evermore increasing stresses in the concrete.

4.1.1.4 Simplified n-method

In practice, the calculation of stresses is usually performed with a simplified method, commonly known as the "n-method". It consists of considering the effects of permanent and variable actions in a single stage, applying the customary elastic formulae and modifying the modular ratio, $\alpha_e = E_s/E_{cm}$, in order to take into account in a global way the elastic and creep effects. Because the time-dependent effects play a different role depending on the type of the loads (permanent and variable loads, instantaneous and sustainable loads) the modular ratio α_e can assume different values as a function of the load combination considered.

In the presence of long term loads (quasi-permanent load combination), an effective modular ratio $\alpha_{e,ef}$ may be adopted on the basis of the definition of the effective elastic modulus of concrete, $E_{c,ef}$, according to the Effective Modulus method[4-5]:

$$E_{c,ef} = \frac{E_c\left(t_0\right)}{1+\frac{E_c\left(t_0\right)}{E_{c,28}}\cdot\varphi\left(t;t_0\right)} \tag{4-1}$$

The approximation of this approach is due to the fact that the maximum concrete stress on the section is assumed constant between t_0 and t and equal to the final value as well as the geometry of the section (position of the neutral axis). This brings the n-method to underestimate the effects of creep. This means that the final value of the concrete stress is higher than the corresponding value obtained with the general method.

When long and short term loads act simultaneously (characteristic load combination) it is not possible to calculate separately the effects of long and short term loads with the relevant values of the modular ratio and then apply the principle of superposition of

This document is the intellectual property of the fib – International Federation for Structural Concrete. All rights reserved.
This PDF of fib Bulletin 92 is intended for use and/or distribution solely within fib National Member Groups.

effects. In fact, the basic assumption for the application of the principle of superposition, that means the linearity of the behaviour, is not valid anymore. The application of the n-method requires adoption of a new value of the modular ratio, which is intermediate between the values pertaining for long and short term loadings, intended to represent in a global way the effects on the section due to both long and short term loads. This intermediate value should take into account the influence of the elastic modulus of concrete and the expected creep deformation (creep coefficient φ), thus it should be fixed as a function of the strength of concrete. Moreover, the redistribution of the stresses is significantly affected by the different amount of sustained and short term loads, therefore the modular ratio should be defined on the basis of the variable-to-permanent load ratio.

In order to take into account the creep effects under the characteristic load combination, Model Code 2010[4-1] (on the left hand side, which includes comments, page. 476) allows consideration of a constant conventional value of the modular ratio, equal to 15, where more than 50% of the stress arises from the quasi-permanent load. Otherwise, creep effects may be neglected.

The effect of shrinkage represents an additional difficulty of calculation because of its complex interaction with the elastic and time-dependent effects of the loads, in particular for cracked sections. A drastic simplification can be obtained by calculating separately the effects of creep and shrinkage[4-5]. Under this assumption the n-method can be applied. The shrinkage acts on the section as an imposed deformation uniformly distributed on the compressed concrete, which actually varies in time due to the effect of creep. This leads to another uncertainty on the most appropriate height of the compression zone to be used. In accordance with the simplified method for the calculation of the curvature due to shrinkage (MC2010[4-1], sect. 7.6.5.2.2), in the presence of quasi-permanent loads the effect of creep and shrinkage can be calculated adopting the effective modular ratio $\alpha_{e,ef}$. The resulting approximation is due to the fact that the depth of the compressed zone is assumed to be constant and equal to that which is defined at time t. However, this methodology allows taking into account the interaction between creep and shrinkage, although in an implicit and simplified form. Finally, the stresses due to creep and shrinkage are determined by applying the principle of superposition of effects and this introduces a further approximation to the n-method because the principle of superposition of effects is actually no longer valid for cracked sections. On the other hand, in the presence of the characteristic loads the effects of creep, sustainable and instantaneous loads and shrinkage are obtained referring to a conventional value of 15 of the modular ratio. Finally, as above, the stresses due to creep and shrinkage are determined by applying the principle of superposition of effects.

4.1.1.5 Critical aspects connected to the n-method and to the choice of the conventional modular ratio

The use of the n-method associated with these values of the modular ratio leads to non-negligible differences in the calculation of the maximum concrete stress, if compared to the refined method. In this respect, let us consider a rectangular cross section with b = 300 mm, h = 500 mm, d' = 50 mm, A_s = 1500 mm^2, A'_s = 500 mm^2, assuming the constant ratios M_{qp}/M_{Rd} = 0.53, M_{char}/M_{Rd} = 0.69, where M_{qp}, M_{char}, M_{Rd} are the applied bending moment in the quasi-permanent, characteristic and ultimate limit stat combinations respectively. In order to allow for the effect of creep, the shrinkage is not considered here.

This document is the intellectual property of the fib – International Federation for Structural Concrete. All rights reserved.
This PDF of fib Bulletin 92 is intended for use and/or distribution solely within fib National Member Groups.

Three concrete strengths are considered (f_{ck} = 20, 50, 90 N/mm^2); for each example, the stresses on the concrete, the tension reinforcement and the compression reinforcement obtained by means the n-method are compared with those obtained with the refined calculation. The calculation is here based on the above mentioned refined approach proposed in the CEB Bulletin d'Information n. 235[4-3] and adopts the Age Adjusted Effective Modulus method.

For each of the three concrete strengths considered, the final creep coefficient at time t_1 at which the quasi-permanent load combination is applied ($\varphi(t_1; t_0)$ = 2.90, 1.55, 0.95 respectively) is determined assuming a conventional value of the nominal size h_0 equal to 100 mm and a relative humidity of 60 %. At time t_2, that occurs immediately after time t_1, it is assumed that the characteristic load combination is applied.

First example:

$f_{ck} = 20$ N/mm^2 $\Rightarrow E_{cm} = 30$ kN/mm^2, $\alpha_e = E_s/E_{cm} = 6.7$, $\varphi(t_1; t_0) = 2.90$, $\varepsilon_{cs}(t_1; t_0) = -0.50$ mm/m

M_{Rd} = 258.3 kN/m, M_{qp} = 141.5 kN/m, M_{char} = 184.5 kN/m

From the effective modulus method (EMM), Eq. (4.1.1-1): $\alpha_{e,ef}$ = 26.0

Stresses (in N/mm^2) and per cent differences compared to the refined method are:

Table 4-1 Results of the first example

	Quasi-permanent load combination			Characteristic load combination		
	$t = t_1$, $M = M_{qp}$			$t = t_2$, $M = M_{char}$		
	Refined method	E.M. Method		Refined method	α_e = 15	
	Stress	Stress	% difference	Stress	Stress	% difference
	N/mm^2	N/mm^2	%	N/mm^2	N/mm^2	%
$\sigma_c(t)$	**-7.7**	-8.7	+13.5 %	**-12.5**	-14.7	+17.3 %
$\sigma_s(t)$	**242.6**	237.5	-2.1 %	**312.0**	307.2	-1.5 %
$\sigma'_s(t)$	**-266.4**	-264.0	-0.9 %	**-287.5**	-251.1	-12.7 %

Second example:

$f_{ck} = 50$ N/mm^2 $\Rightarrow E_{cm} = 37$ kN/mm^2, $\alpha_e = E_s/E_{cm} = 5.4$, $\varphi(t_1; t_0) = 1.55$, $\varepsilon_{cs}(t_1; t_0) = -0.36$ mm/m

M_{Rd} = 272.8 kN/m, M_{qp} = 149.4 kN/m, M_{char} = 194.8 kN/m

Table 4-2 Results of the second example

	Quasi-permanent load combination			Characteristic load combination		
	$t = t_1$, $M = M_{qp}$			$t = t_2$, $M = M_{char}$		
	Refined method	E.M. Method		Refined method	α_e = 15	
	Stress	Stress	% difference	Stress	Stress	% difference
	N/mm^2	N/mm^2	%	N/mm^2	N/mm^2	%
$\sigma_c(t)$	**-11.7**	-12.3	9.0 %	**-17.2**	-15.5	-10.1 %
$\sigma_s(t)$	**251.2**	248.8	-1.6 %	**325.0**	327.1	0.6 %
$\sigma'_s(t)$	**-188.4**	-187.7	-0.6 %	**-206.8**	-233.6	13.0 %

Stresses (in N/mm^2) and per cent differences compared to the refined method are – see Table 4-2.

This document is the intellectual property of the fib – International Federation for Structural Concrete. All rights reserved.
This PDF of fib Bulletin 92 is intended for use and/or distribution solely within fib National Member Groups.

Third example:

$f_{ck} = 90$ N/mm^2 $\Rightarrow E_{cm} = 44$ kN/mm^2, $\alpha_e = E_s/E_{cm} = 4.5$, $\varphi(t_1; t_0) = 0.95$, $\varepsilon_{cs}(t_1; t_0) = -0.23$ mm/m

$M_{Rd} = 278.9$ kN/m, $M_{qp} = 152.7$ kN/m, $M_{char} = 199.2$ kN/m

From the effective modulus method (EMM), Eq. (4-1): $\alpha_{e,ef} = 8.9$

Stresses (in N/mm^2) and per cent differences compared to the refined method are:

Table 4-3 Results of the third example

	Quasi-permanent load combination			Characteristic load combination		
	$t = t_1$, $M = M_{qp}$			$t = t_2$, $M = M_{char}$		
	Refined method	E.M. Method		Refined method	$a_e = 15$	
	Stress	Stress	% difference	Stress	Stress	% difference
	N/mm^2	N/mm^2	%	N/mm^2	N/mm^2	%
$\sigma_c(t)$	-14.8	-15.2	3.0 %	-20.8	-15.7	-24.5 %
$\sigma_s(t)$	253.4	252.3	-0.4 %	328.7	336.5	2.4 %
$\sigma'_s(t)$	-132.9	-132.7	-0.2 %	-149.0	-213.4	43.2 %

Some general considerations can be derived from the analysis of the results of the three examples:

a) The application of the simplified method allows for evaluating stresses in the tension reinforcement with a good accuracy the, in both the quasi-permanent and characteristic load combination;

b) Under the quasi-permanent load combination the simplified method leads to an over-estimation of the concrete stress, in particular for cases with low concrete strength; the scattering on the stress of the compressive reinforcement is generally not significant;

c) Under the characteristic load combination, the simplified method leads to an under-estimation of the concrete stress and an over-estimation of the stress of the compressive reinforcement; the scattering is increasingly significant for high concrete strength.

A more general comparison between the simplified and refined calculation can be carried out by means of a parametric analysis that takes into account all the main involved parameters, as performed in this study[4-6]. The main results are shown in Fig. 4-2, in term of per cent differences in case of a RC simply reinforced section, for different values of the concrete strength. The calculation methods are applied on the basis of non-dimensional parameters of the width and the height of the section, the depth of the compressed zone, the areas of tensile and compressive reinforcements and the load effects. The quasi-permanent load is assumed equal to the 70 % of the characteristic one, the geometric reinforcement ratio of tension steel is 0.5 %, the creep coefficient is varying from 2.9 to 0.9 as a function of concrete strength, while shrinkage is absent. The corresponding concrete stresses are overestimated by the n-method based on the effective modular ratio, under the quasi-permanent load combination, up to 20 % for low strength concretes. Under the characteristic load combination, they are usually underestimated, up to more than 20% for high strength concretes. As far as the stresses on steel are concerned, the results show small differences that are on average smaller than 3 %.

This document is the intellectual property of the fib – International Federation for Structural Concrete. All rights reserved.
This PDF of fib Bulletin 92 is intended for use and/or distribution solely within fib National Member Groups.

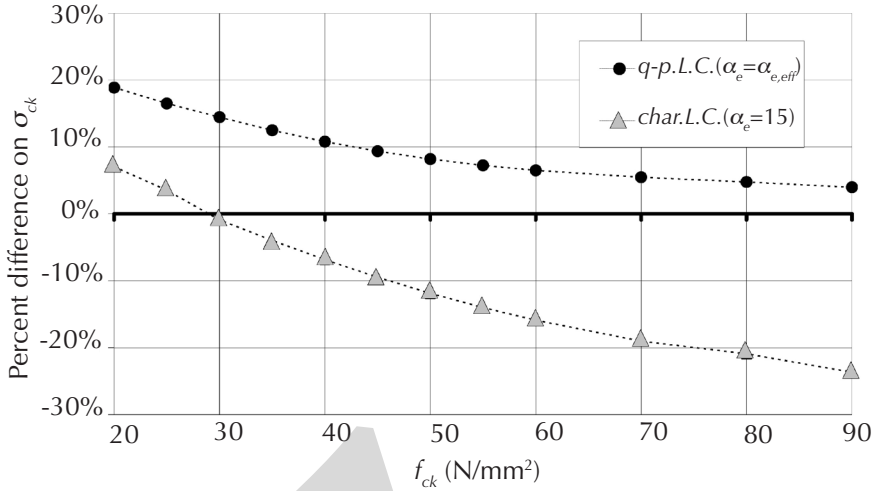


Fig. 4-2 Differences on concrete stresses (in %) using the n-method and the refined method as a function of the concrete strength (quasi-permanent and characteristic load combinations)

Moreover, it is interesting to note that the "traditional" value of the modular ratio equal to 15 under the characteristic load combination does not take into account that for high strength concrete the instantaneous value of modular ratio reduces and at the same time the creep effect decreases.

These aspects lead to exploration of the possibility of the definition of a more gradual variation, under the characteristic load combination, of conventional modular ratio α_{char} as a function of the concrete strength, in order to reduce the scattering of the n-method if compared to the refined one, in particular for the characteristic combination.

On the basis of experimental and theoretical research, the École des Ponts et Chaussées published a guideline for the extension of the calculation rules to the high strength concrete[4-7] in which a different value of modular ratio is proposed respectively for normal (α_{char} = 15) and high (α_{char} = 9) strength concrete (see Table 4-4).

Moreover, in one study[4-6], a recalibration of the modular ratio values as a function of the main parameters involved is proposed, based on an extensive and refined numerical analysis. The basic idea was to find appropriate values of the modular ratio suitable for the quasi-permanent or the characteristic load combinations which, applying the n-method, lead to reduction of the differences in the stresses on concrete between the "improved n-method" and the refined method. Therefore, the general expressions of the conventional value of the modular ratio a for the two load combinations are given as a function of the following parameters: the E_s/E_{cm} ratio, the creep coefficient $\varphi(t_1, t_0)$ and the quasi-permanent load-to-characteristic load ratio λ. In particular for the characteristic load combination, a simplification can be obtained referring to the values of the creep coefficient $\varphi(t_1, t_0)$ shown in Fig. 4.1.3 for each concrete strength and a given quasi-permanent load–to–characteristic load ratio λ (here λ equal to 0.4 - 0.6 - 0.8): in this way the modular ratio α_{char} can be further simplified and expressed as a function of the strength of the concrete for each λ-value, as shown in Table 4-4 (in the following called "improved modular ratio").

The comparison of the above mentioned proposals is shown in Fig. 4-3, in which the conventional value of the modular ratio α_{char} (characteristic load combination) as a function of the concrete strength, according to the Model Code 2010[4-1], the Bulletin des laboratoires

This document is the intellectual property of the fib – International Federation for Structural Concrete. All rights reserved.
This PDF of fib Bulletin 92 is intended for use and/or distribution solely within fib National Member Groups.

des Ponts et Chaussées – n. s. XIX, 1996[4-7] and the "improved modular ratio" based on this study[4-6] is represented. The conventional values are also compared with the instantaneous value $\alpha_{ist} = \frac{E_S}{E_{cm}}$ and the effective value $\alpha_{ef} = \frac{E_S}{\frac{E_{c,28}}{1+\varphi(t_1,t_0)}}$ of the modular ratio.

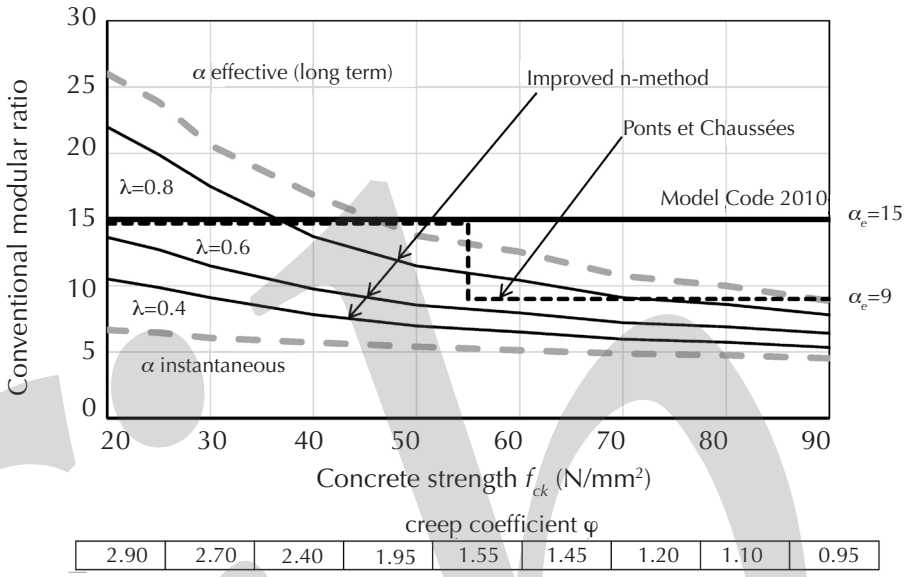


Fig. 4-3 Conventional value of the modular ratio α_{char} (calculation of stresses under the characteristic load combination) as a function of the concrete strength and the relevant creep coefficient, according to: MC2010[4-1], Bulletin des laboratoires des Ponts et Chaussées – n. s. XIX[4-7] and "improved modular ratio"[4-6]. Comparison with the instantaneous and the effective value of the modular ratio

In synthesis the calculation of stresses in service conditions can be made, in a simplified manner, adopting the n-method according to the following procedure (see Table 4-4):

- quasi-permanent load combination: the effective modular ratio $\alpha_{e,ef}$ may be adopted on the basis of the definition of the effective elastic modulus of concrete, $E_{c,ef}$, according to the Effective Modulus method.

- characteristic load combination: the conventional value of the modular ratio α_{char} may be defined with different levels of accuracy, according to the above mentioned different proposals, as a constant value or as a function of the concrete strength.

The Table 4-4 describes the procedure of calculation in the two load combinations and shows the practical values of modular ratio to be applied according to the different proposals.

This document is the intellectual property of the fib – International Federation for Structural Concrete. All rights reserved.
This PDF of fib Bulletin 92 is intended for use and/or distribution solely within fib National Member Groups.

Table 4-4 Effective value of the modular ratio $\alpha_{e,ef}$ for the calculation of stresses under the quasi-permanent load combination. Conventional value of the modular ratio α_{char} for the calculation of stresses under the characteristic load combination, according to Model Code 2010[4-1], Bulletin des laboratoires des Ponts et Chaussées – n. s. XIX[4-7] and "improved modular ratio"[4-6] proposal

calculation of stresses under the quasi-permanent load combination	$\alpha_{e,ef} = E_S / E_{c,ef}$									
calculation of stresses under the characteristic load combination	f_{ck} (N/mm^2)		20	25	30	40	50	60	70	80	90
	Model Code 2010		15(*)								
	Bulletin n. XIX Lab.P.C.1996		15					9			
	"improved modular ratio"	$\lambda = 0.4$	10.5	9.9	9.1	7.8	7.0	6.5	6.0	5.7	5.4
		$\lambda = 0.6$	13.7	12.7	11.5	9.8	8.6	8.0	7.2	6.9	6.4
		$\lambda = 0.8$	22.0	19.9	17.5	13.7	11.5	10.4	9.1	8.6	7.8

(*) (if more than 50% of the stress arises from the quasi-permanent load)

4.1.2 PC sections

4.1.2.1 General aspects

In general terms the calculation of stresses in PC sections can be carried out with the same conceptual approaches of RC sections and thus shares the same difficulties. The effect of time-dependent losses of prestressing represents an additional difficulty of calculation because of its complex interaction with the effects of the loads. The effects of the rheological properties of the materials can show a significant influence on the prestress losses and thus can severely affect the long-term deflection and service behaviour. Long-span prestressed elements can be particularly sensitive to prestress losses because the dead load is large if compared to the total load. For this reason, the theoretical evaluation of the effects due to creep and shrinkage of concrete and relaxation of prestressing steel is a very important aspect of the design in order to ensure proper service behaviour of the structure.

The stress limitation in prestressed structures at SLS involves the compressive stress in concrete, the tensile stress in ordinary and prestressing steel and the tensile stress in concrete.

Limiting the concrete compressive stresses to a value equal to $0.4f_{ck}(t)$ under the quasi-permanent load combination means preventing non-linear creep that can lead to excessive long term deformations and serious consequences to prestress losses. Furthermore, the formation of cracks parallel to reinforcing bars may be generally avoided when, in the presence of sustained and short term loads (or with the characteristic combination of actions), the stress level does not exceed a critical value of $0.6f_{ck}(t)$.

The limitation of the tensile stress in the prestressing steel to a limit of $0.75f_{pk}$ allows large inelastic strains to be avoided.

Further stress limits should be respected for transient situations (i.e. transfer of prestressing and construction phases): the stress limits for the prestressing reinforcements are given in Model Code 2010[4-1], sect. 5.4.4.2, while the maximum compressive stress on the concrete,

This document is the intellectual property of the fib – International Federation for Structural Concrete. All rights reserved.
This PDF of fib Bulletin 92 is intended for use and/or distribution solely within fib National Member Groups.

in general, have to be limited within the value of $0.4 \div 0.6 f_{ck}(t)$ depending on the duration of the loading.

In the sect. 7.6.3.2 of Model Code 2010[4-1] the "limit state of decompression" is introduced, defined as the state where the section under consideration of a beam is compressed and the extreme fibre concrete stress is equal to zero. The limit state of decompression should be required if cracking or reopening of cracks has to be avoided, under a given load combination, for specific design purposes. Nevertheless, tensile stresses in concrete or even cracking in PC members are in some cases admitted by Model Code 2010[4-1], according to the experimental evidence that a properly limited cracking does not reduce their functionality, durability and appearance. In particular, cracking is allowed for unbonded prestressing steel in presence of all exposure classes and for bonded prestressing steel in exposure classes X0, XC (MC2010[4-1], sect. 7.6.4.3). For bonded prestressing steel type PL1 (i.e. post-tensioned or pre-tensioned reinforcement without special layers for corrosion protection, see MC2010[4-1], sect. 5.4.3.3) subjected to aggressive exposure classes (XD, XF, XS) and bending, no tension is allowed in a distance of 100 mm from the duct or the perimeter of the prestressed reinforcement towards the tension face (this value may be reduced for thin elements).

It is important to consider that the ordinary reinforcement is more effective than prestressing steel to control the cracks width. For this reason, at all regions where tension is expected to develop in the concrete in the SLS (due to imposed or restrained deformation, combined or not combined with direct loading), a minimum amount of ordinary reinforcement should be placed, to ensure that the reinforcement does not yield immediately after cracking in the SLS. Furthermore, the cracking has to be limited, where permitted, by applying the procedures and the limits described in 7.6.4 of Model Code 2010[4-1] and considering the ordinary reinforcement.

In synthesis the calculation of stresses relates to sections which are uncracked under the characteristic load combination (this is the case of fully PC beams) or cracked (partially PC beams).

The distribution of stresses in a section of a PC element is significantly influenced by the various phases of construction and application of prestress and by the typology of prestressing reinforcement (i.e. pre-tensioned reinforcement, bonded or unbounded post-tensioned reinforcement). Therefore, the calculation requires considering different steps in which the active section changes and the various actions are applied, referring to a more or less complex scenario that includes most of the following phases:

- Time t_0 is the time in which the prestressing is applied to the element. Prestressing and self-weight are simultaneously acting on the beam. In pre-tensioned members the active section comprises the concrete and the ordinary and prestressing reinforcement. In post-tensioned members the active section comprises the concrete and the ordinary reinforcement and the calculation is performed assuming that the duct is not yet grouted. The section is usually uncracked.

- Time t_1 is the time in which the remaining quasi-permanent load is applied on the beam; for bonded post-tensioned members this step is generally considered after the grouting of the duct, thus the prestressing steel is bonded to the concrete; therefore the centroid, the area and the second moment of inertia of the section in this case is changed. The section is generally uncracked.

This document is the intellectual property of the fib – International Federation for Structural Concrete. All rights reserved.
This PDF of fib Bulletin 92 is intended for use and/or distribution solely within fib National Member Groups.

- Time t_2 represents the final time when the time-dependent effects (prestressing losses due to creep, shrinkage and relaxation) are completely developed (quasi-permanent load combination). The section is generally uncracked.

- At the time t_3, the variable load is applied. The section can be cracked or uncracked depending on whether a fully PC or a partially PC beam is considered. In general, the verification should consider the most unfavourable condition determined in short and in long terms respectively. Usually the most unfavourable time t_3 corresponds to the end of the service life, when the prestressing is minimized due to the maximum prestress losses.

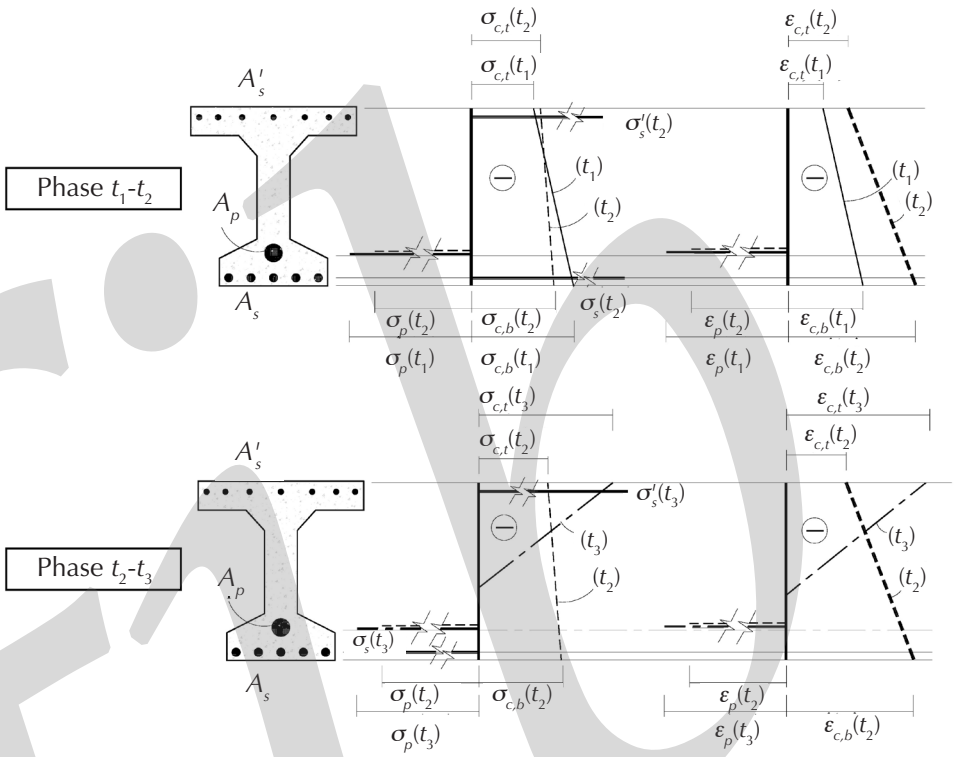


Fig. 4-4 Stresses and strains at times t_1 (application of quasi-permanent load just after the grouting of the duct), t_2 (after long term development of time-dependent effects) and t_3 (application of variable loads), in a section of a partially-prestressed post-tensioned beam

The evolution of stresses and strains in a section subjected to bending of partially-prestressed beam with bonded prestressing reinforcement is exemplified in Fig. 4-4, where the phases between time t_1, t_2 and t_3 are considered. The applied bending moment in the period t_1 - t_2 is considered as constant.

At time t_3, just after the time t_2, an increase of external bending moment ΔM, corresponding to short-term variable load, is applied. In the phase t_1 - t_2, because of creep and relaxation of prestressing steel, the strain of concrete fibres increases in time while in prestressing steel decreases, leading to an increase of the curvature of the section. It can be noted that in this phase the evolution in time of the stresses and strains in concrete due to the creep are affected by the variation of the stress in prestressing steel due to relaxation. In a reciprocal manner, the stress in prestressing steel varies according to a relaxation law that depends on the initial stress and thus is affected by the variation of stresses and strains in the concrete. Therefore the creep of concrete and the steel relaxation interact in a complex manner with each other and with the effects of the loads.

This document is the intellectual property of the fib – International Federation for Structural Concrete. All rights reserved.
This PDF of fib Bulletin 92 is intended for use and/or distribution solely within fib National Member Groups.

At the time t_3 the instantaneous increase of bending moment DM due to variable load is applied and the section is cracked. The variation of the stresses on the section should balance the variation of the external bending moment but, due to the change of the active section, the stresses are not linear.

According to Model Code 2010[4-1], sect. 7.2.4.2, the level of refinement of the analysis has to be appropriate to a series of design aspects such as the design stage, the sensitivity of the structure to time-dependent effects, and the reliability of the information on material properties.

In general terms the calculation can be based on the general assumptions of visco-elastic behaviour of materials, uncracked or fully-cracked section depending on whether the tensile stress in concrete exceeds the mean concrete tensile strength, f_{ctm}, and perfect bond between concrete and ordinary or bonded prestressing steel after grouting. The hypothesis that plane section before loading remains plane after loading is generally accepted in a large number of cases, except for particular situations such as, for example, bridge box sections in which a significant shear-lag effect is expected.

4.1.2.2 General method and refined approach

In rigorous terms, according to the considerations exposed in the previous paragraph, the calculation of the variation of stresses and strains from the time t_1 should take into account an evolution that occurs over time in the materials. For this purpose it is necessary to refer to the general approach that incorporates the constitutive relation for creep and shrinkage of concrete and steel relaxation for each part of the section, considering a series of time-steps, and performing for each step a numerical solution that matches both the equilibrium and congruence conditions. This method can be typically incorporated in the FEM approach and allows consideration in a detailed manner of not only the complex interaction between the load effects and the time-dependent properties of materials but also the redistribution of the effects due to external loads that occurs in statically indeterminate structures. Nevertheless, it must be considered such laborious analyses and consequent calculation effort is in general justified only in structures sensitive to the time-dependent behaviour of concrete, where a particular accuracy is required.

A more affordable solution can be obtained by adopting the method proposed in the CEB Bulletin d'Information No. 235[4-3], already described in the present text in the section about RC sections. The creep effects are treated with an approximate algebraic formulation of A.A.E.M. method (Age Adjusted Effective Modulus – Model Code 2010[4-1], sect. 7.2.4.10) and the analysis of the section is carried out by the method of imposed deformations. In this form the calculation procedure is rather general and able to properly consider a series of cases not covered by more simplified approaches, such as:

- the presence of various stages of the construction;
- the presence of several tendons set in different levels and prestressed in different phases;
- the presence of a section made with different mechanical and thermo-hygrometric properties.

The solution is in closed form in the case of uncracked sections but it requires an iterative calculation with one unknown when the section is cracked. Nevertheless, the calculation procedure can be easily implemented in an automatic spreadsheet and represents an

This document is the intellectual property of the fib – International Federation for Structural Concrete. All rights reserved.
This PDF of fib Bulletin 92 is intended for use and/or distribution solely within fib National Member Groups.

affordable tool for cases in which the simplified methods are not applicable or a particular accuracy is required.

4.1.2.3 Simplified method

In order to reduce the calculation efforts required by the refined approaches described in the previous paragraph, in many practical cases it is possible to introduce further simplified assumptions that lead to a more affordable solution while maintaining an acceptable accuracy.

The basic idea is to consider a series of phases from the initial time t_0 to the long-term time t_3 (when the time-dependent effects are completely developed), through a series of elastic analyses of the uncracked section and applying the superposition of the effects. The creep effects can be treated with an approximate formulation of A.A.E.M. method and, under certain geometrical and mechanical simplified assumptions, the prestressing losses can be derived in a closed form. After the time t_3, the application of the variable loads can lead to an increase of stresses without exceeding the mean concrete tensile strength, f_{ctm}, and thus the phase can be interpreted as a further elastic phase on which the superposition of the effects applies, or can lead to the cracking of the section: in this latter case a means of calculation can be adopted in order to assimilate the nonlinear redistribution of the stresses over the section to a pseudo linear-elastic behaviour. In the following a short description of the different phases and their simplified treatment is carried out.

4.1.2.3.1 Calculation of stresses after the application of the prestress

After the evaluation of the initial prestress losses (just the transfer of prestress for pre-tensioned members and after the release from the anchorages for pre-tensioned members) it is possible to define the effective stress in each point along the cable. The calculation of stresses on the section at time t_0 is carried out considering the elastic behaviour of concrete, taking into account the effective value of the elastic modulus of concrete at the considered time $E_c = E_c(t_0)$.

After the time when the prestressing reinforcement is bonded to the concrete, no differences between the post-tensioned and pre-tensioned elements are considered, except for the anchorage zones. When further loads are applied (i.e. the remaining quasi-permanent load, time t_1), the section is generally required to be uncracked: if such a hypothesis is satisfied, the increment of stress can be evaluated on the basis of the elastic formulae referring to the transformed section (considering both the ordinary and the prestressing reinforcement) and, according to the superposition of the effects, the final stress can be determined as the sum of the two contributions.

In the case of statically-indeterminate structures the external bending moment in each section does not depend only on the applied load but also on the hyperstatic effect of prestressing. Nevertheless, this contribution can be easily evaluated with the usual computational techniques, if linear elastic behaviour of the structure is assumed.

4.1.2.3.2 Calculation of stresses due to long-term effects

Let us consider that the stresses on the section at the previous step t_1 are known (due to the quasi-permanent load, see stresses in time t_1 of Fig. 4-4) and that in the time t_1-t_2 the external load remains constant. Due to the effects of creep and shrinkage, with concrete and steel relaxation, losses in the prestressing steel and a redistribution of stresses over the section occur.

This document is the intellectual property of the fib – International Federation for Structural Concrete. All rights reserved.
This PDF of fib Bulletin 92 is intended for use and/or distribution solely within fib National Member Groups.

If the prestressing steel consists of only one bonded cable set at the distance z_{cp} from the centroid of the concrete section and no ordinary reinforcement is present, the application of the A.A.E.M. method and the consideration of the perfect bond of prestressing reinforcement as well as the equilibrium conditions allow determination of the prestressing loss $\Delta\sigma_{p,c+s+r}$ through the following equation (CEB-FIP Model Code 1990, 1993[4-8]):

$$\Delta\sigma_{p,c+s+r} = \frac{\varepsilon_{cs}\cdot E_p + \sigma_c\left(t_1\right)\dfrac{E_p\cdot\varphi\left(t_1,t_2\right)}{E_c} + \Delta\sigma_{rel}\left(t_1,t_2\right)}{1+\dfrac{E_p}{E_c}\dfrac{A_p}{A_c}\left(1+\dfrac{A_c}{J_c}z_{cp}^2\right)\left[1+\chi\cdot\varphi\left(t_1,t_2\right)\right]} \tag{4-2}$$

where:

ε_{cs} is the shrinkage strain, in absolute value;

$\varphi(t_2;t_1)$ is the creep coefficient at a time t_2 and load application at time t_1;

χ is the ageing coefficient (can be assumed equal to 0.8);

$\Delta\sigma_{rel}$ is the absolute value of the variation of stress in the tendons, at time t_2, due to the relaxation of the prestressing steel;

E_p is the modulus of elasticity for the prestressing steel; E_c: modulus of elasticity for the concrete;

A_c is the area of the concrete section; A_p: area of the prestressing tendons;

J_c is the second moment of area of the concrete section;

z_{cp} is the distance between the centre of gravity of the concrete section and the tendons.

The variation of the stress in the prestressing reinforcement obtained with Eq. 4-2 causes a change of the stress distribution on the section: the equilibrium condition requires a variation of the resultant of stresses on the section equal to the variation of the prestressing force caused by the stress losses $\Delta P = \Delta\sigma_{p,c}\cdot A_p$.

The stress variation on the concrete at y level can be determined by applying the variation of the prestressing force, at the distance z_{cp} from the centroid, on the section (excluding the area of the prestressing reinforcement)

$$\Delta\sigma_c\left(y\right) = \frac{\Delta P}{A_P^*} + \frac{\Delta P\cdot z_{cp}}{J_C^*}y \tag{4-3}$$

being A^*_P and J^*_C the transformed area and second order moment of the section (excluding the area of the prestressing reinforcement). The superposition of the effects of this stress variation with the stress distribution at t_1 allows determination of the final stresses on the section at t_2.

Eq. 4-2 is derived for an uncracked section with bonded prestressing reinforcement set at distance z_{cp} from the centroid of the concrete section (without ordinary reinforcements); in a simplified way it can be extended to cases in which several prestressing reinforcements are set in different levels but they can be represented by a unique resultant reinforcement.

In the case of the presence of several tendons set at the top and the bottom levels of the section or if they are prestressed in different phases, Eq. 4-2 cannot be applied and a more refined approach has to be adopted.

This document is the intellectual property of the fib – International Federation for Structural Concrete. All rights reserved.
This PDF of fib Bulletin 92 is intended for use and/or distribution solely within fib National Member Groups.

Moreover Eq. 4-2 is not valid for sections made from different concretes and does not take into account the ordinary reinforcements.

4.1.2.3.3 Calculation of stresses due to variable loads

Variable loads act on the structure with higher intensity (characteristic combination) varying in each section the previous stress distribution due to the quasi-permanent actions, that we assume are known. The characteristic load combination thus produces an increment of the axial force and bending moment on the section ΔN, ΔM in addition to the quasi-permanent load combination that causes the stress variation in concrete:

$$\Delta\sigma_c(y) = \frac{\Delta N}{A_{C,trans}} + \frac{\Delta M}{J_{C,trans}} y \tag{4-4}$$

where $A_{C,trans}$ and $J_{C,trans}$ represent the transformed area and second order moment of the section (including the area of the prestressing reinforcement and referring to the instantaneous value of the elastic modulus $E_c(t_3)$ at the time t_3 being considered).

The resultant total stress distribution on the concrete can be obtained, according to the superposition of the effects, by the sum of this contribution with the previous stress $\Delta\sigma_c + \sigma_c(t_2)$ and, in an analogous way, on the reinforcements. If the maximum positive stress on the concrete does not exceed the mean concrete tensile strength f_{ctm}, the section is uncracked and the solution previously found is applicable. If not, the section is cracked and the previous solution has to be considered no more valid. At the same time a solution can be determined by applying a superposition of fictitious load effects[2] according the following procedure.

Let us consider the known distribution of stresses on concrete $\sigma_c(t_2)$ and on the reinforcements $\sigma_s(t_2)$, $\sigma_p(t_2)$ at time t_2 (Fig. 4-5a); it can be seen that, due to creep and shrinkage, the diagram of stresses in the uncracked concrete continues to be linear while the diagram relative to steel stresses is no longer such.

The latter distribution of stresses can be broken down into an initial linear portion consisting of the stresses $\overline{\sigma}_c(t_2)$ and $\overline{\sigma}_s(t_2)$, $\overline{\sigma}_p(t_2)$ (Fig. 4-5b), $\overline{\sigma}_s(t_2)$, $\overline{\sigma}_p(t_2)$ which are proportional to the concrete stress at the same level through the modular ratio (α_e) and another portion including the stress in the reinforcements $\Delta\overline{\sigma}_p(t_2) = \overline{\sigma}_s(t_2) - \overline{\sigma}_s(t_2)$ (Fig. 4-5c).

The "elastic" portion of diagram of Fig. 4-5b has as resultant the axial force $\overline{N}$ and the bending moment $\overline{M}$ with respect to the external load effect reference axis. The final stress distribution on the concrete can thus be evaluated by means of an elastic calculation, applying on the cracked section the fictitious axial force $N^* = \overline{N} + \Delta N$ and the bending moment $M^* = \overline{M} + \Delta M$ (Fig. 4-5d). The final stresses in the reinforcements are given by:

$$\sigma_s(t_3) = \overline{\sigma}_s(t_3) + \Delta\overline{\sigma}_s(t_2) \tag{4-5}$$

$$\sigma_p(t_3) = \overline{\sigma}_p(t_3) + \Delta\overline{\sigma}_p(t_2) \tag{4-6}$$

This document is the intellectual property of the fib – International Federation for Structural Concrete. All rights reserved.
This PDF of fib Bulletin 92 is intended for use and/or distribution solely within fib National Member Groups.

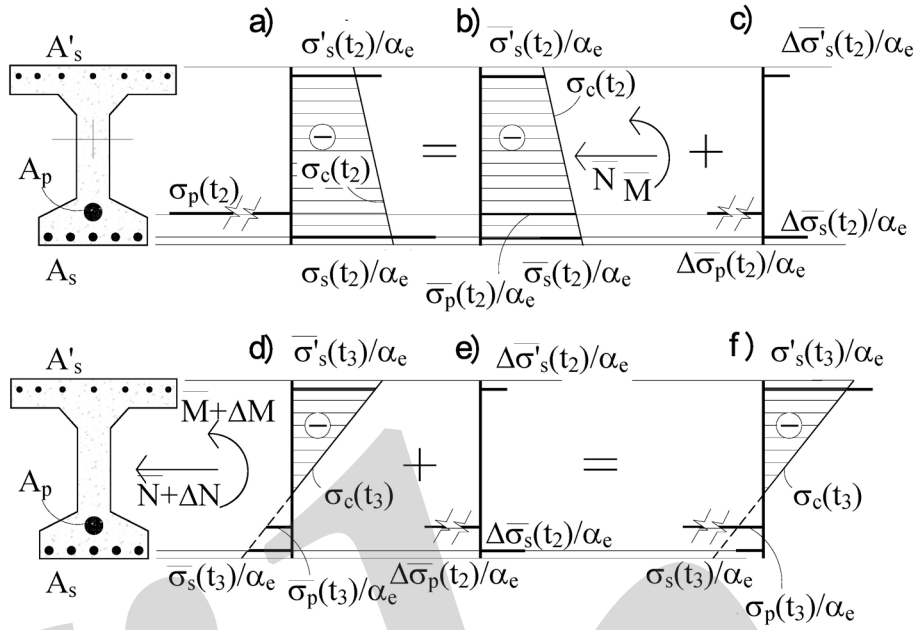


Fig. 4-5 Stresses due to the variable load in a cracked section

4.1.2.4 Particular cases

4.1.2.4.1 Load in different stages

In the previous paragraphs the time-dependent effects are considered in a unique time-step t_1-t_2; actually in several practical cases the quasi-permanent actions are applied in a series of time-steps t_{1a}, t_{1b}, etc. that should be taken into account in the calculation. In rigorous terms, the calculation of the variation of stresses and strains from the time t_1 should consider the evolution that occurs with continuity in time in the materials, requiring the application of a general iterative method. However the simplified calculation can be applied if, as a major simplification, the total creep coefficient $\varphi(t_1, t_2)$ and the shrinkage strain $\varepsilon_{sh}(t_1, t_2)$ are divided into partial shares relative to each time-step:

step t_1-t_{1a}: (t_1, t_{1a}); $\varepsilon_{sh}(t_1, t_{1a})$;

step t_{1a}-t_{1b}: $\varphi(t_{1a}, t_{1b}) = \varphi(t_1, t_{1b})$- (t_1, t_{1a}); $\varepsilon_{sh}(t_{1a}, t_{1b}) = \varepsilon_{sh}(t_1, t_{1b})$- $\varepsilon_{sh}(t_1, t_{1a})$;

step t_{1b}-t_2: $\varphi(t_{1b}, t_2) = \varphi(t_1, t_2)$- (t_1, t_{1b}); $\varepsilon_{sh}(t_{1b}, t_2) = \varepsilon_{sh}(t_1, t_2)$- $\varepsilon_{sh}(t_1, t_{1b})$;

As regards to prestressing losses, it is possible to determine the variation of stress in the tendons due to relaxation in each time-step $\Delta\sigma_{rel}(t_1, t_{1a})$, $\Delta\sigma_{rel}(t_{1a}, t_{1b})$, $\Delta\sigma_{rel}(t_{1b}, t_2)$ and to calculate the total losses in the different phases by application to each step Eq.4-2. This procedure does not take into account the influence of the variation of stresses in the prestressing tendons due to external load effects.

The simplified method described in the previous paragraphs considers a time-step t_1-t_2 where the effects of the sustained loads are assumed as constant, as happens in statically-determinate structures. To the contrary, in a statically-indeterminate structure the effects of the external loads and the reactions in general depend on the stiffness of the structure and thus, due to the rheological properties of the materials, vary in time. In order to take this aspect into account it is necessary to adopt a general methodology, dividing the time-step in an appropriate series of ranges in which the effects can be considered as constant. For each range the solution should be determined by means of an iterative calculation that

This document is the intellectual property of the fib – International Federation for Structural Concrete. All rights reserved.
This PDF of fib Bulletin 92 is intended for use and/or distribution solely within fib National Member Groups.

satisfies both the equilibrium and compatibility conditions. However in some practical cases, as a simplification, it is possible to refer to the principles of linear viscoelasticity valid for homogeneous structures. With this assumption, in a statically-indeterminate structure with rigid restraints and constant load the load effects are constant in time and the calculation of stresses described in the previous paragraphs can be adopted.

4.1.2.4.2 Structures with unbonded tendons

In the previous section the calculation of stresses and the evaluation of losses due to long-term effects were illustrated with reference to the case of bonded prestressing reinforcement.

In the case of use of unbonded prestressing reinforcement, the calculation of stresses and the evaluation of losses due to long-term effects must take into account that the stress variation in the tendon is no longer linked to the local strain variation in each section but depends on the total length variation that is produced on the entire cable, between anchorages.

For this purpose the calculation of the stresses on the section can be developed by referring to the RC section without prestressing reinforcement, taking into account the equivalent effect of the prestress (axial force and bending moment).

Due to the effects of creep and shrinkage, with concrete and steel relaxation, losses in the prestressing steel and a redistribution of stresses over the section occur.

According to Model Code 2010[4-1], sect. 5.4.6.1, the time-dependent losses are calculated by considering both the reductions of stress due to the steel relaxation and to the reduction of strain, caused by the deformation of concrete due to creep and shrinkage, under quasi-permanent actions, occurring along the whole structure between the anchorages of the tendons.

The prestressing loss $\Delta\sigma_{p,c+s+r}$ can thus be evaluated through the following equation:

$$\Delta\sigma_{p,c+s+r} = \frac{E_p \int \Delta\varepsilon_x \cdot dx}{l_p} + \Delta\sigma_{rel}\left(t_1, t_2\right) \tag{4-7}$$

being:

E_p is the modulus of elasticity for the prestressing steel;

$\Delta\sigma_{rel}$ is the absolute value of the variation of stress in the tendons, at time t_2, due to the relaxation of the prestressing steel;

l_p is the total length of unbonded prestressing tendons, between the anchorages;

$\Delta\varepsilon_x$ is the concrete strain variation at the tendon level due to creep and shrinkage (after the application of prestress); the concrete strain variation can be evaluated by applying the AAEM method, through the following equation:

$$\Delta\varepsilon_x\left(x\right) = \varepsilon_{c,creep}\left(x\right) + \varepsilon_{cs} = \sigma\left(t_1\right)\frac{\varphi\left(t_1,t_2\right)}{E_c} + \frac{\Delta\sigma_c}{E_c}\left[1+\chi\cdot\varphi\left(t_1,t_2\right)\right] + \varepsilon_{cs} \tag{4-8}$$

ε_{cs} is the shrinkage strain, in absolute value;

$\varphi(t_2;t_1)$ is the creep coefficient at a time t_2 and load application at time t_1.

The integrations are made over the projected length of the unbonded tendons from anchor to anchor.

This document is the intellectual property of the fib – International Federation for Structural Concrete. All rights reserved.
This PDF of fib Bulletin 92 is intended for use and/or distribution solely within fib National Member Groups.

The variation of the stress in the prestressing reinforcement causes a change of the stress distribution on the section. It can be noted that, in the same way of the case of bonded prestressing reinforcement, the evolution in time of the stresses and strains in concrete due to the creep and the steel relaxation interact with each other in a complex manner and with the effects of the loads.

In a simplified way, in many practical cases it is possible to introduce the analogous simplified assumptions considered in the section 4.1.2.3. The stresses are thus calculated with the elastic analysis of the uncracked section and applying the variation of the prestressing force $\Delta P = \Delta\sigma_{p,c} \cdot A_p$, at the distance z_{cp} from the centroid, on the section of concrete excluding the area of the prestressing reinforcement.

4.2 Cracking

This section 4.2 deals with cracks induced by bending and shear in reinforced and prestressed structures. Attention is given also to the avoidance of cracks without calculation and to cracking in orthogonally reinforced elements. Cracks induced by deformation restraint are also mentioned.

4.2.1 Bending cracks

4.2.1.1 Background

The main background to the MC 2010 formulation for crack width goes back to the drafting of EN 1992-1-1[4-9] and the discussions which took place within the Project Team when drafting chapter 7 Serviceability Limit States (SLS) with respect to the influence of cover on crack width. At that time, two established formulations were competing side by side: the formulation of MC 1990[4-8] which took no explicit account of cover and the formulation of ENV 1992-1-1[4-10] which provided a formulation consisting of a sum of terms, dating back to the formulation originally proposed by Ferry-Borges. This second formulation took into account cover, implicitly assuming a fixed value of 25 mm and the ϕ/ρ_{ef} ratio.

MC 1990 was a rational expression based on theory. Its formulation could be derived from the equilibrium of the bar between the cracked cross section and the point of zero slip.

$$w_k = l_{s,\max}\left(\varepsilon_{sm} - \varepsilon_{cm} - \varepsilon_{cs}\right) \tag{4-9}$$

In Eq. (4-9), $l_{s,\max}$ denotes the maximum length over which slip between steel and concrete occurs and is taken as twice the transfer length, l_s, ε_{sm} is the mean tensile strain of reinforcement within $l_{s,\max}$, ε_{cm} is the mean tensile strain of concrete within $l_{s,\max}$, and ε_{cs} is the shrinkage strain. This last term increases the crack width since ε_{cs} is to be taken as a negative strain.

The formulation for the transfer length can be derived from simple equilibrium conditions. From equilibrium of the bar (see Fig. 4-6), it is possible to derive Eq. (4-10).

This document is the intellectual property of the fib – International Federation for Structural Concrete. All rights reserved.
This PDF of fib Bulletin 92 is intended for use and/or distribution solely within fib National Member Groups.

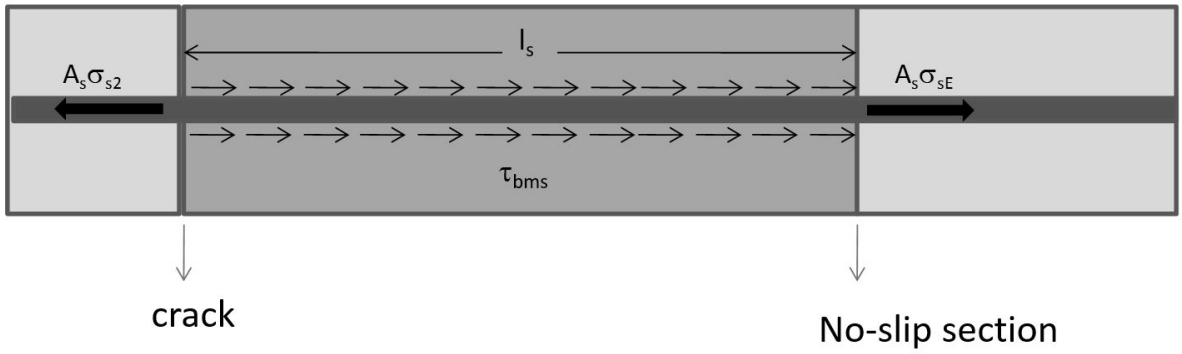


Fig. 4-6 Equilibrium of the bar between the section of the crack and the section of no-slip

$$\left.\begin{aligned} &A_s \cdot \sigma_{s2} = A_s \cdot \sigma_{sE} + \tau_{bms}\pi \cdot \phi_s \cdot l_s \\ &A_s = \frac{\pi\phi_s^2}{4} \end{aligned}\right\} \rightarrow l_s = \frac{\sigma_{s2} - \sigma_{sE}}{4\tau_{bms}}\phi_s$$
$$\rightarrow \sigma_{s2} - \sigma_{sE} = \frac{4l_s \cdot \tau_{bms}}{\phi_s} \qquad (4\text{-}10)$$

In Eq. (4-10), σ_{s2} is the tensile stress of reinforcement determined assuming a fully cracked (State II) section, σ_{sE} is the tensile stress of reinforcement at the section of no slip, *As* is the bar area, ϕ the bar diameter, l_s the transfer length and τ_{bms} the bond stress. The transfer length is defined as the distance from the crack in which a stress equal to the tensile strength of concrete is transferred to the effective concrete area surrounding the reinforcement. The concept of effective area takes into account the fact that it is not necessary to transfer to concrete by bond a force equal to the full area of concrete times the concrete tensile strength to generate a new crack, when the area of concrete is very large. This is because the distribution of stresses is not uniform in the concrete surrounding the bar. A crack can originate due to high local tensile stresses near the bar and then propagate until it reaches the surface. Equilibrium can then also be expressed with respect to the cross section of the crack and that located at the end of the transfer length: both sections must resist the same force. This condition leads to the formulation for the transfer length included in MC 1990[4-8] for stabilized cracking (see Eq. (4-11) and Fig. 4-7).

$$\left.\begin{aligned} &A_s \cdot \sigma_{s2} = A_s \cdot \sigma_{sE} + A_{c,ef} \cdot f_{ctm} \rightarrow \sigma_{s2} - \sigma_{sE} = \frac{\underbrace{\frac{A_{c,ef}}{A_s}}_{1/\rho_{ef}} f_{ctm}}{} \\ &l_s = \frac{\sigma_{s2} - \sigma_{sE}}{4\tau_{bms}}\phi \end{aligned}\right\} \rightarrow l_s = \frac{\phi}{\rho_{ef}}\frac{f_{ctm}}{4\tau_{bms}} \qquad (4\text{-}11)$$

This document is the intellectual property of the fib – International Federation for Structural Concrete. All rights reserved.
This PDF of fib Bulletin 92 is intended for use and/or distribution solely within fib National Member Groups.

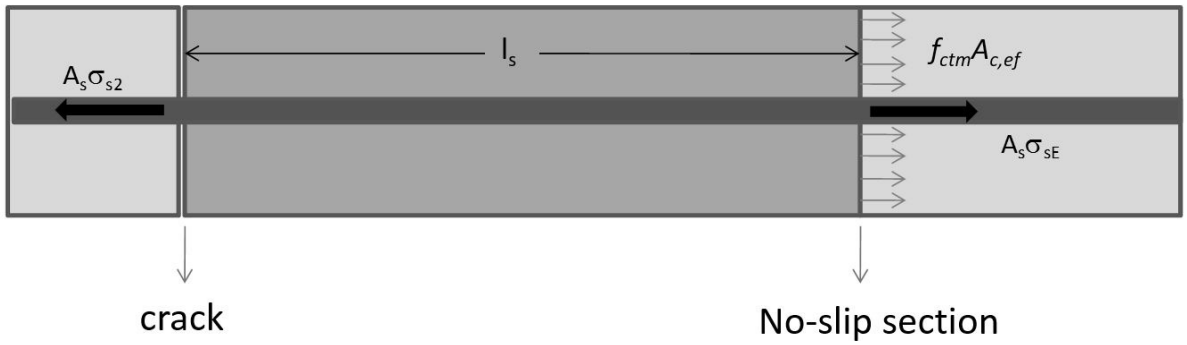


Fig. 4-7 Equilibrium between the section of the crack and the section of no-slip

Even though MC 1990[4-8] provides different expressions for single crack formation and stabilized cracking, the above formulation is actually applicable to both cases, the difference in formulation being only formal. MC 1990 introduces the fact that, for single crack formation σ_{sE} is equal to $\alpha_e \cdot f_{ctm}$. This way of presenting the model is unfortunate since it makes very similar problems look very different, and for this reason this approach has been abandoned in MC 2010[4-1]. Eq. (4-11) is therefore valid both for stabilized and single cracking. The expression of MC 1990 can be obtained from the same equations as follows:

$$\left.\begin{aligned} &\sigma_{s2} - \underbrace{\sigma_{sE}}_{\alpha_e \cdot f_{ctm}} = \frac{A_{c,ef}}{\underbrace{A_s}_{1/\rho_{ef}}} f_{ctm} \rightarrow \sigma_{s2} = \left(\frac{1+\alpha_e \cdot \rho_{ef}}{\rho_{ef}}\right) f_{ctm} \\ &l_s = \frac{\sigma_{s2} - \alpha_e \cdot f_{ctm}}{4\tau_{bms}}\phi \rightarrow l_s = \sigma_{s2}\left(1 - \frac{\alpha_e \cdot f_{ctm}}{\sigma_{s2}}\right)\frac{\phi}{4\tau_{bk}} = \sigma_{s2}\left(1 - \frac{\alpha_e \cdot \rho_{ef}}{1+\alpha_e \cdot \rho_{ef}}\right)\frac{\phi}{4\tau_{bms}} \\ &\rightarrow l_s = \frac{\sigma_{s2}}{4\tau_{bk}}\phi\frac{1}{1+\alpha_e \cdot \rho_{ef}} \end{aligned}\right\} \quad (4\text{-}12)$$

In MC1990 the effect of cover was not introduced explicitly, due to the lack of a theory which could provide its influence so clearly as the above expressions prove the influence of ϕ/ρ_{ef}.

The outcome of the discussions in the Project Team for EN 1992-1-1[4-9] was a compromise between those who did not want to include cover at all, arguing that cover was already taken into account in the definition of the effective tensile concrete area, and those, led by Andrew Beeby who argued, based mainly on empirical evidence, that cover was the only important variable affecting crack width and that ϕ/ρ_{ef} did not play a role at all. This point of view was expounded in a notorious article which fueled a heated debate after its publication in *fib*'s Journal *Structural Concrete*[4-11].

While studying the problem of cracking for EN 1992-1-1[4-9], the team lead by Hugo Corres, from the Structural Concrete Research Group of UPM, drafted a large data base including a large amount of experimental evidence[4-12] (later referred to as UPM data base), including tests from taken from several references[4-13, 4-14, 4-15, 4-16, 4-17, 4-18, 4-19, 4-20, 4-21]. When reviewing this evidence, it was hoped that some answers would be found which might settle the matter of cover vs. ϕ/ρ_{ef}.

This document is the intellectual property of the fib – International Federation for Structural Concrete. All rights reserved.
This PDF of fib Bulletin 92 is intended for use and/or distribution solely within fib National Member Groups.

4.2.1.2 The problem with data bases

Data bases are tricky to use, mainly due to lack of homogeneity in the measurement criteria used in different Laboratories and also because test reports are not always well detailed so that it is not easy to understand what the measuring procedure really was. In the case of crack measurement, subjective factors play a main role. It is seldom established exactly how cracks are measured. The truth is that cracks vary with the development of tests. They open and close and it is seldom easy to tell at which point the crack is largest. In many occasions cracks can subdivide or converge and follow rather crooked paths. Furthermore, optical means, used traditionally to measure crack width, put a great amount of stress in the eye of the person making the measurements, so much so, that it can be stated that the reliability of crack measurements can be questionable and errors in measurement can be large.

Looking first at crack spacing, it is clear that crack spacing evolves throughout a test, until crack stabilization is reached. It has even been argued that stabilization may be never attained. However, it is a fact that even though some cracks may appear at late stages, for members in which tension stiffening effects are limited (large reinforcement ratios and relatively large stresses – 250 to 300 MPa), the number of cracks is fairly stable up to failure, and the error in the mean crack spacing is not large even if a small percentage of cracks form at later stages.

Assuming this is so, actually measured values of mean crack spacing and values estimated from the measured crack widths should be approximately the same. The estimated (or inferred) value of the crack spacing is based on the definition of the crack width as shown in Eq. (4-13), where TS is used to denote tension stiffening effects.

$$w_m = \frac{\sigma_{s2}}{E_s} TS \cdot s_m \rightarrow s_m = \frac{w_m}{\sigma_{s2}} E_s \cdot \frac{1}{TS} \rightarrow s_m \geq \frac{w_m}{\sigma_{s2}} E_s \tag{4-13}$$

In Fig. 4-8, a comparison between the measured value of the mean spacing between cracks, measured at the end of the test s_m and the minimum value of $(w_m \cdot E_s)/(\sigma_s \cdot TS)$ is provided for tests measurements having a geometric reinforcement ratio greater than 1.5% and a tensile stress larger than 250 MPa, taken from the UPM data base. (From experience, a geometric reinforcement ratio of 1.5% is considered sufficiently large to attain stabilized cracking for a stress of 250 MPa.) In the evaluation of tension stiffening, the model proposed by Model Code 90[4-8] was used. As can be seen, if the tests conditions are properly restricted, acceptable results are obtained. Even so, scatter is still very wide and correlation is statistically significant but still rather low.

This document is the intellectual property of the fib – International Federation for Structural Concrete. All rights reserved.
This PDF of fib Bulletin 92 is intended for use and/or distribution solely within fib National Member Groups.

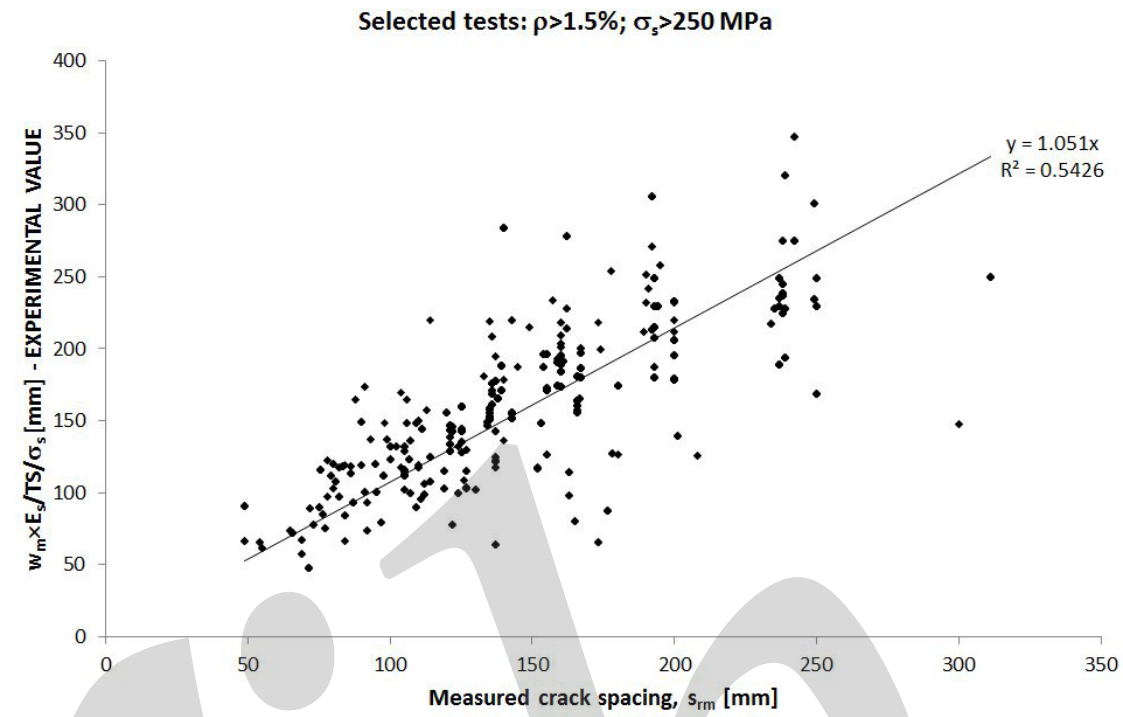


Fig. 4-8 Comparison of inferred and measured crack spacing for conditions restricted to cases in which tension stiffening effects are small[4-12]

When trying to estimate the effect of ϕ/ρ_{ef} on inferred crack spacing some tendency is observed, but the best word to describe this relationship would be scatter (see Fig. 4-9). Of course, one might think that this dispersion can be a consequence of the effect of cover, which is not explicit here and would affect the relationship.

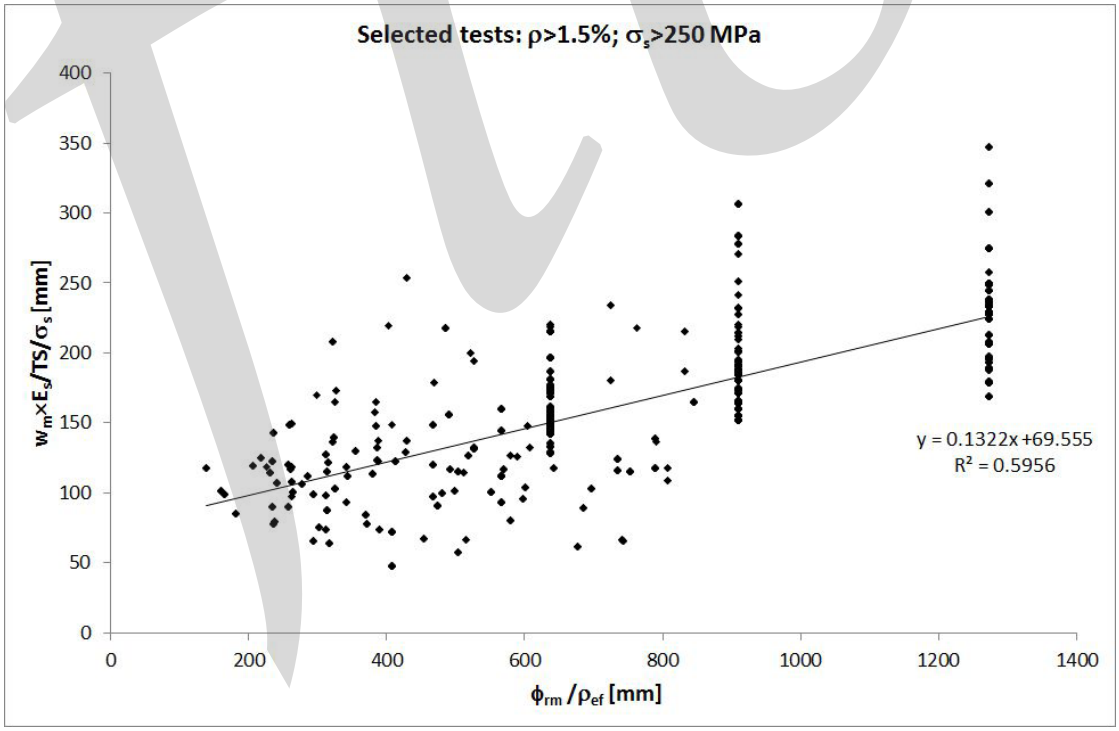


Fig. 4-9 Effect of ϕ/ρ_{ef} on inferred crack spacing for conditions restricted to cases in which tension stiffening effects are small[4-12]

This document is the intellectual property of the fib – International Federation for Structural Concrete. All rights reserved.
This PDF of fib Bulletin 92 is intended for use and/or distribution solely within fib National Member Groups.

One way to find out if the reason for the observed dispersion is or is not the effect of cover is to fragment this function into groups such that the variation of cover is very small in each group. As it turns out, this is not of much help in being able to conclude that ϕ/ρ_{ef} is really a significant factor (see Fig. 4-10).

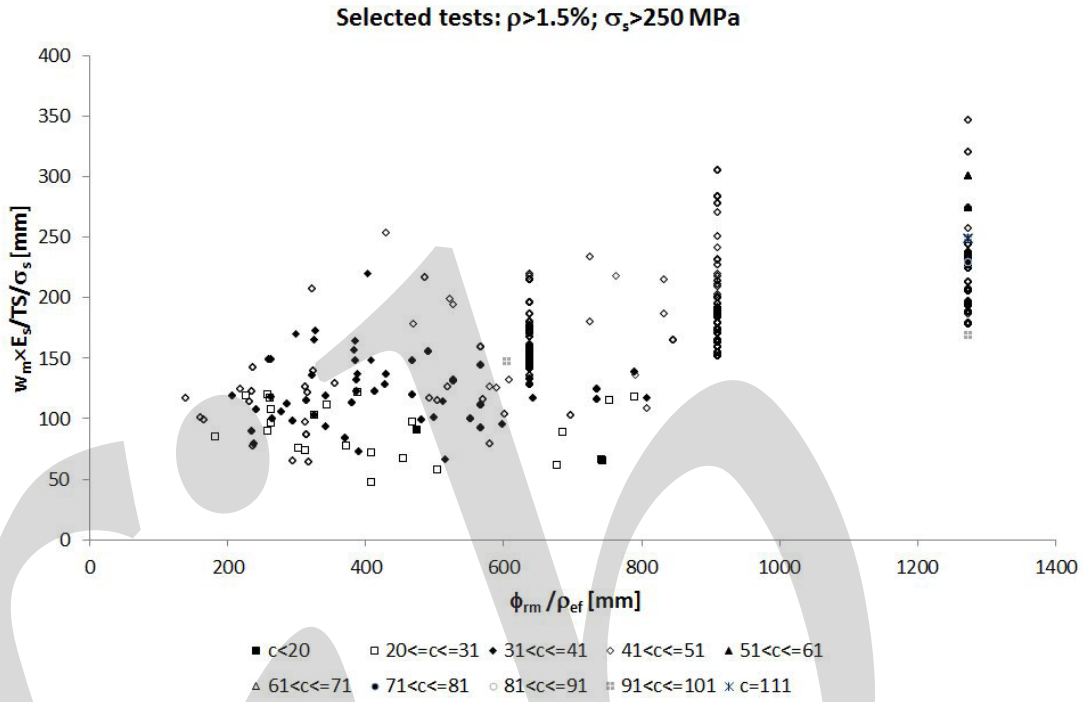


Fig. 4-10 Effect of ϕ/ρ_{ef} on inferred crack spacing for conditions restricted to cases in which tension stiffening effects are small[4-12] – Segmented by cover intervals

Given this experience, the conclusions of *fib* T 2.1 "Serviceability Models" Group regarding data bases considering cover influence were the following:

- Due to lack of homogeneity of data, no clear conclusions could be drawn from the lumping together of heterogeneous data
- No tests were found at the time of writing this document in which either cover was kept constant with a significant variation of ϕ/ρ_{ef} or ϕ/ρ_{ef} was kept constant with a significant variation of cover, this being difficult since ρ_{ef} depends on cover.

For these reasons an ad hoc experimental program was designed allowing to:

- Separate the effects of cover and ϕ/ρ_{ef}
- Ensure homogeneity in data and full information on how tests were performed
- Provide data regarding a seldom studied problem: the influence of stirrups. Should codes take them into account?
- Address the issue of flexure vs. tension

4.2.1.3 Ad hoc experimental program

Given the state of the matter as described in the previous paragraph in which the lack of homogeneity and the large scatter does not lead to experimentally prove or disprove that cover or ϕ/ρ_{ef} are both important parameters to be considered independently in crack

This document is the intellectual property of the fib – International Federation for Structural Concrete. All rights reserved.
This PDF of fib Bulletin 92 is intended for use and/or distribution solely within fib National Member Groups.

spacing models a specific, ad hoc, experimental program was undertaken at the Structure's Laboratory of the Civil Engineering school of the Polytechnic University of Madrid[4-22].

4.2.1.3.1 Test description

In order to cover the concerns described at the end of the paragraph 4.2.1.2, 12 beams were tested covering a wide range of practical situations:

- High (1.5%) and low (0.3%) reinforcement ratios
- Large (70mm) and small (20mm) covers
- No stirrups, high stirrup spacing (30 cm) and low stirrup spacing (10 cm)

The tests involved 1:1 scale beams ($b \cdot h$=0.35 · 0.45) with a long constant bending zone using the setup shown in Fig. 4-11.

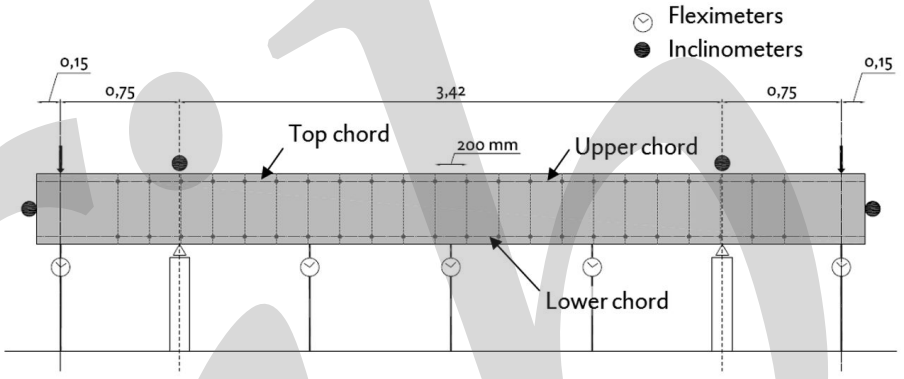


Fig. 4-11 Test setup

The main design parameters from the point of view of cracking are shown in Table 4-5. These parameters cover a wide range of practical situations. The beam cross sections are shown in Fig. 4-12.

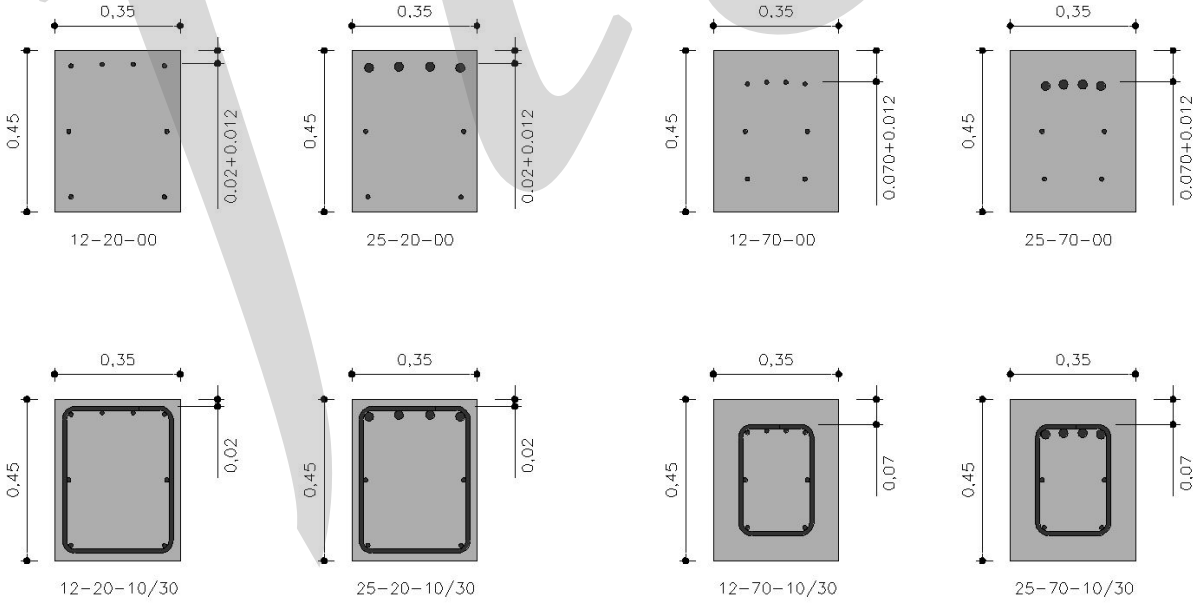


Fig. 4-12 Beam cross-sections

This document is the intellectual property of the fib – International Federation for Structural Concrete. All rights reserved.
This PDF of fib Bulletin 92 is intended for use and/or distribution solely within fib National Member Groups.

The specimens were coded as XX-YY-ZZ with XX referring to the bar diameter (12 or 25), YY referring to cover (20 or 70) and ZZ referring to stirrup spacing (00 for no stirrups, 10 and 30, for 10 cm spacing and 30 cm spacing, respectively).

Table 4-5 Main design parameters of the tested beams (* $h_{ef} \leq (h\text{-}x)/3$).

ID	ϕ [mm]	c [mm]	ϕ/ρ_{eff} [mm]	s_t [mm]
25-20-00	25	20	460	-
25-20-10	25	20	460	100
25-20-30	25	20	460	300
12-20-00	12	20	882	-
12-20-10	12	20	882	100
12-20-30	12	20	882	300
25-70-00	25	70	473(*)	-
25-70-10	25	70	473(*)	100
25-70-30	25	70	473(*)	300
12-70-00	12	70	1172	-
12-70-10	12	70	1172	100
12-70-30	12	70	1172	300

4.2.1.3.2 Test results

Test results regarding crack spacing are shown in Table 4-6.

Table 4-6 Test results. Mean (s_m) and maximum (s_{max}) crack spacing

Beam ID	ϕ [mm]	c[mm]	ϕ/ρ_{eff} [mm]	s_t [mm]	s_m [mm]	s_{max} [mm]
25-20-00	25	20	460	-	130.5	234
25-20-10	25	20	460	100	114	230
25-20-30	25	20	460	300	152	258
12-20-00	12	20	882	-	173	269
12-20-10	12	20	882	100	182	320
12-20-30	12	20	882	300	274	358
25-70-00	25	70	473	-	227	423
25-70-10	25	70	473	100	188.5	460
25-70-30	25	70	473	300	200	442
12-70-00	12	70	1172	-	235.5	412
12-70-10	12	70	882	100	259.5	381
12-70-30	12	70	1172	300	280.5	383

Influence of concrete cover

From the results of Table 4-6, some of the questions raised before could be answered. It can be observed that the specimens 25-20-ZZ and 25-70-ZZ have practically the same ϕ/ρ_{ef} ratio, but very different covers. They can therefore be used to investigate whether or not cover should be considered as a parameter independently from ϕ/ρ_{ef}. The answer to this question is given in Fig. 4-13: a larger cover provides a much larger crack widths for the same stress.

This document is the intellectual property of the fib – International Federation for Structural Concrete. All rights reserved.
This PDF of fib Bulletin 92 is intended for use and/or distribution solely within fib National Member Groups.

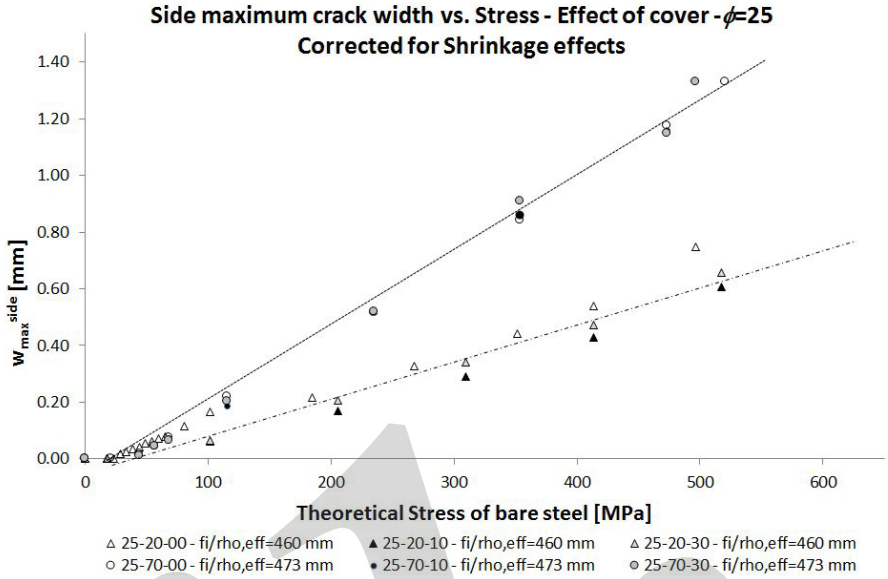


Fig. 4-13 Effect of cover on crack width. A very clear pattern is observed on specimens with nearly the same effective concrete area. (Results have been corrected by subtracting the increase in crack opening due to shrinkage using the formulation of MC 2010[4-1] for all models)

The explanation of what is observed in Fig. 4-13 is very clear when looking at the crack patterns of these beams: increase in cover results in a clear increase in crack spacing (Fig. 4-14).

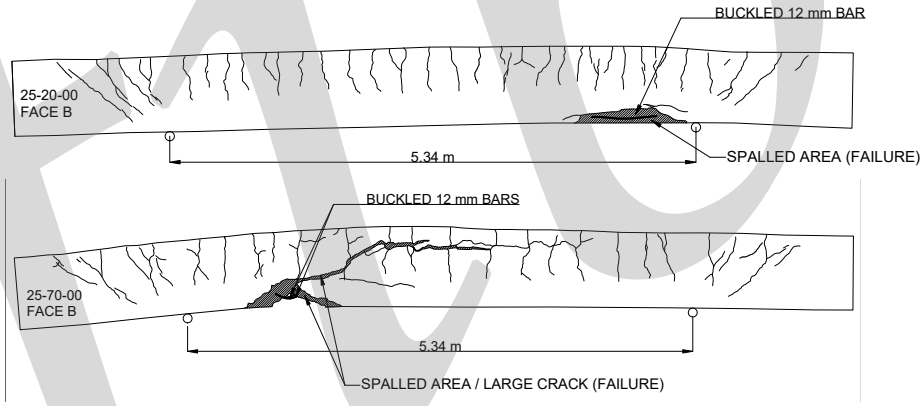


Fig. 4-14 Crack patterns of beams 25-20-00 and 25-70-00

Fig. 4-13 is also very interesting from the practical point of view. It shows that for the common serviceability range of stresses, between 200 and 300 MPa, while the maximum crack opening is acceptable for a small cover, it clearly exceeds the commonly accepted limits for the 70 mm cover (w_{max}>0.6 mm). Cover values of up to 70 mm are not uncommon since they are prescribed for elements concreted against the ground, such as piles or embedded walls. Such covers are prescribed to ensure adequate durability. However, as it turns out they also increase very much the crack width which is commonly regarded as pernicious for durability. Increasing the reinforcement in order to reduce the crack width does not seem like a good answer since, as can be seen, the cross section is already heavily reinforced and also, this does not seem reasonable from the point of view of economy and sustainability.

Regarding the physical explanation of why cover affects crack spacing and crack width, two effects can be considered. The first is the need to diffuse the tension stresses

This document is the intellectual property of the fib – International Federation for Structural Concrete. All rights reserved.
This PDF of fib Bulletin 92 is intended for use and/or distribution solely within fib National Member Groups.

transmitted by bond from the surface of the bar to the centre of the effective concrete area. This effect is shown in Fig. 4-15.

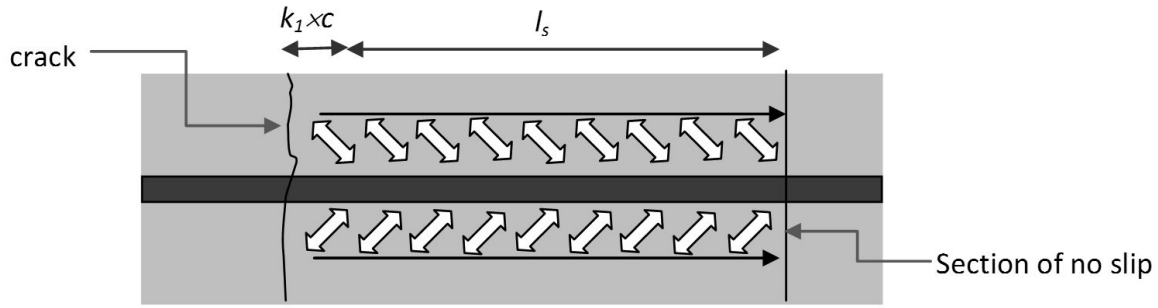


Fig. 4-15 Effect of cover explained as the need to transfer the tensile stresses from the bar surface to the centre of the effective concrete area in order to produce a new crack

The second explanation is based on experimental evidence which shows that the crack opens, non-linearly, from the bar surface, where it is minimum, to larger and larger values as the measurement is taken further away from the bar. Evidence of this is given in the two studies[4-23, 4-24]. This fact can be explained from another study[4-25], which, early on, showed that, at the level of reinforcement, a large number of secondary cracks form which do not make their way to the concrete surface. The implication is that at the bar surface the crack widths are small because the difference in strain between concrete and steel is distributed over a large number of closely spaced secondary and primary cracks. However, further from the bars, secondary cracks start to close and the difference in strain between concrete and steel concentrates in the passing cracks explaining the increase in their width. The practical consequence is that in order to control surface cracks to low limits it is necessary to provide closely spaced reinforcement and covers which are not very large[4-26].

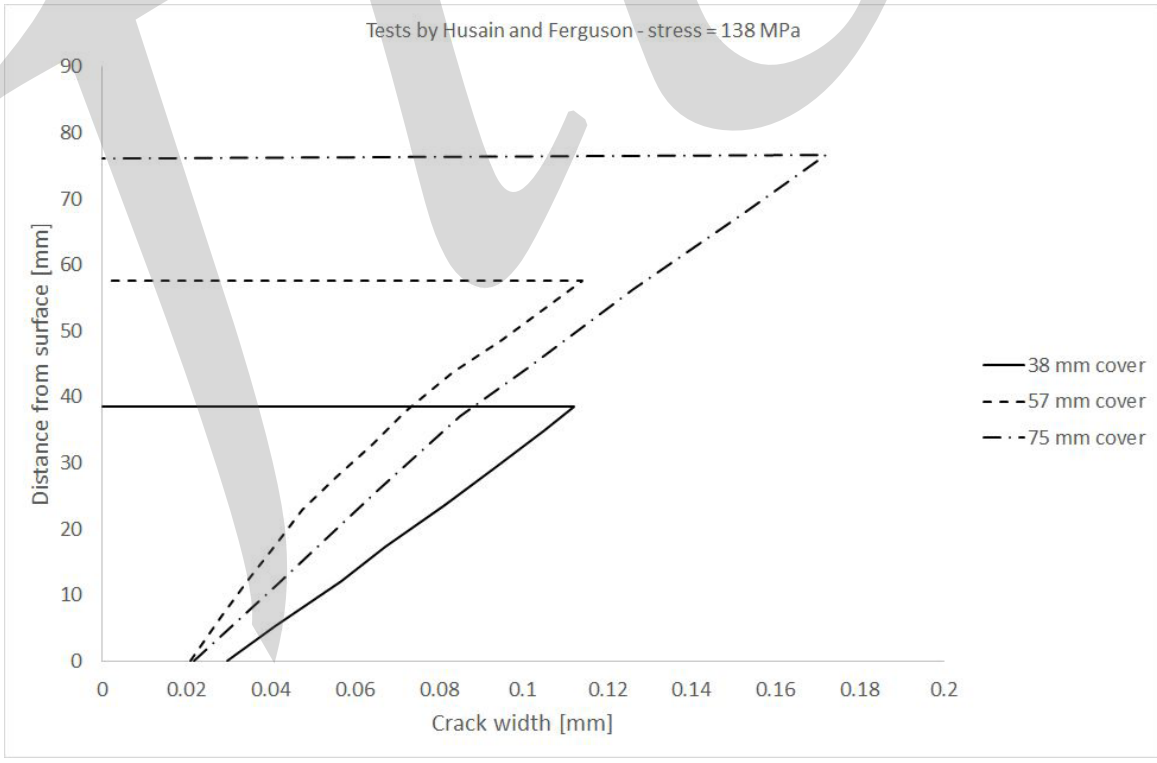


Fig. 4-16 Results showing the growth of cracks with distance from the bar surface[4-23]

This document is the intellectual property of the fib – International Federation for Structural Concrete. All rights reserved.
This PDF of fib Bulletin 92 is intended for use and/or distribution solely within fib National Member Groups.

Understanding why cracks increase in width when measured further away from the bar surface is useful to analyse the bearing of crack width on durability. Is a large crack necessarily a durability hazard, even when it is a consequence of having a large cover?

Fig. 4-17 is meant to help answer this question. As it can be seen, two elements are represented, one with a large cover (top) and one with a smaller cover (bottom). It can be seen that in the one with a large cover, secondary cracks close before reaching the surface. Therefore, on the surface, crack width and crack spacing in the specimen with the larger cover are doubled with respect to the one with the smaller cover. In the specimen with smaller cover, the secondary cracks in the beam with large cover actually become primary cracks and cracking would seem to be better controlled. This is certainly the case if crack width is being limited for aesthetic reasons. However, from a durability point of view, the crack opening at the level of the reinforcement would be the same and, if anything, the element with a large cover would be better protected.

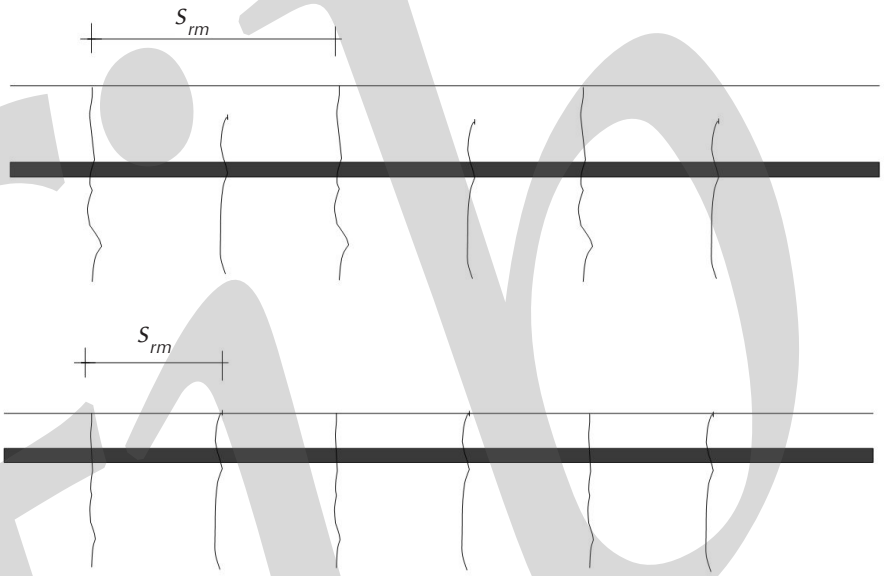


Fig. 4-17 As the cover becomes larger, a smaller number of secondary cracks make their way to the surface thereby increasing the observed crack spacing and surface crack width

This observation suggests that the allowable crack width cannot be independent of the cover. It seems that current crack width limits have been fixed considering normal covers, although no one is quite sure which ones. A reasonable guess can be 25 mm, as this was the implicit cover taken in the crack spacing formulation of ENV 1992-1-1[4-10]. One possible solution to this problem is to keep current crack width limits but make the calculation of the expected characteristic crack width using a nominal cover, c_0, not the real value, in the cases where the limiting condition is durability, not appearance, such as in piles or embedded retaining walls.

Influence of ϕ/ρ_{ef}

The influence of the ϕ/ρ_{ef} ratio on crack spacing is a direct consequence of the definition of the transfer length and can be easily derived from the equilibrium of the bar between a crack and the zero slip section and from the equilibrium of the two sections, as already shown in paragraph 4.2.1.1. The influence of this factor on crack spacing can easily be compared by counting the number of cracks in specimens having the same cover.

This document is the intellectual property of the fib – International Federation for Structural Concrete. All rights reserved.
This PDF of fib Bulletin 92 is intended for use and/or distribution solely within fib National Member Groups.

Fig. 4-18 shows this comparison. A clear influence can be seen with the crack spacing increasing with the value of ϕ/ρ_{ef}. These results seem to show a larger influence of this parameter for a smaller cover. This seems logical since crack spacing can be modelled as the sum of the effect of cover and the effect of ϕ/ρ_{ef}, as shown in Eq. (4.2.1-6) where k_1 and k_2 are calibration constants.

$$s_m = k_1 \cdot c + k_2 \frac{\phi}{\rho_{ef}} \tag{4-14}$$

As a cover becomes larger the relative importance of the second term in ϕ/ρ_{ef}, becomes smaller.

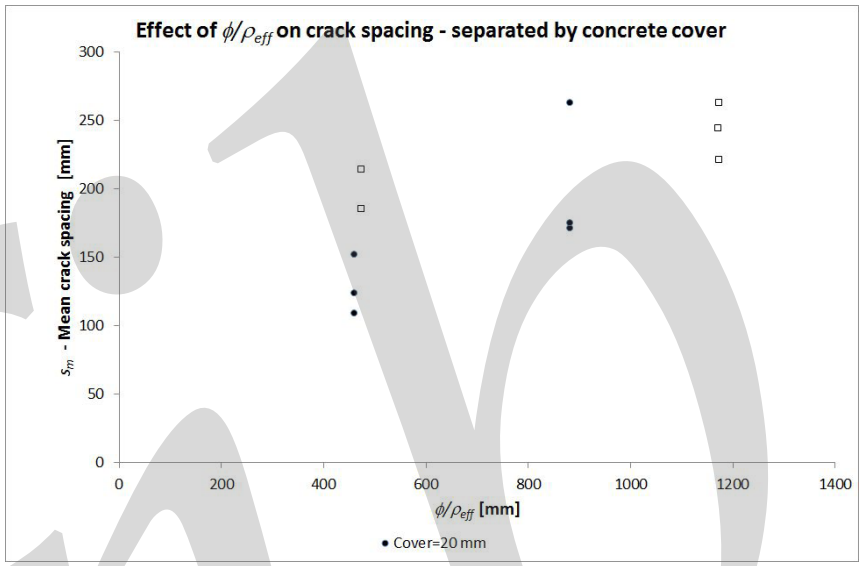


Fig. 4-18 Influence of ϕ/ρ_{ef} on mean crack spacing

It must be also noted, however, that for small amounts of reinforcement, which may coincide with small values of ϕ/ρ_{ef}, the effect of this parameter can be masked by tension stiffening effects, which will be larger for elements with smaller reinforcement ratios. Thus it can be seen that in some tests elements with larger ϕ/ρ_{ef} ratios and the same cover have smaller crack widths than element with smaller values of ϕ/ρ_{ef}. One such example is given in Fig. 4-19, where beams reinforced with 4ϕ25 and ϕ/ρ_{ef} ratio of about 460 have a larger crack width for a stress under 250 MPa than elements reinforced with 4ϕ12 and a ϕ/ρ_{ef} ratio of about 880. This fact is important in interpreting tests and also in comparing results from data bases, and can be an important source of scatter.

This document is the intellectual property of the fib – International Federation for Structural Concrete. All rights reserved.
This PDF of fib Bulletin 92 is intended for use and/or distribution solely within fib National Member Groups.

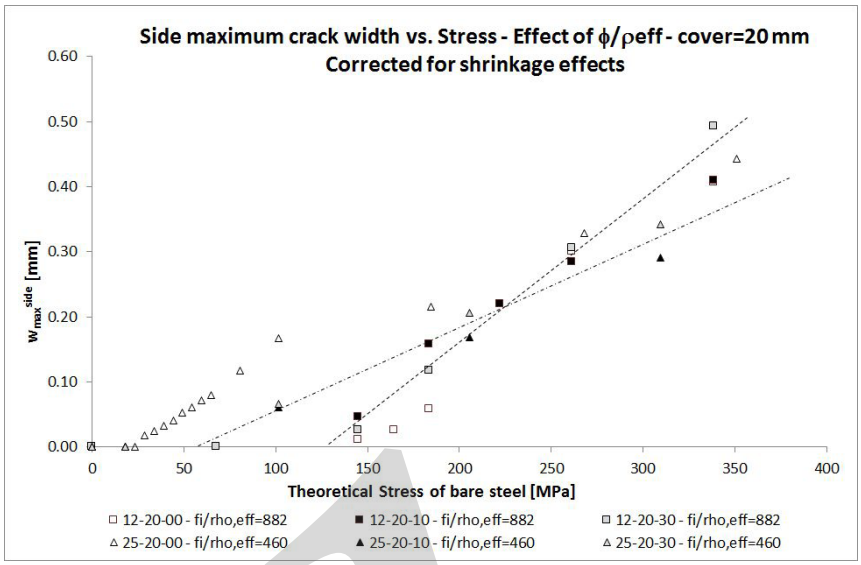


Fig. 4-19 How tension stiffening can mask the effect of ϕ/ρ_{ef} . Larger crack widths are observed for members with a ϕ/ρ_{ef} of 460 than for members with a ϕ/ρ_{ef} of 882. The reason is that tension stiffening effects are larger for members with lower reinforcement ratios. Results have been corrected by subtracting the increase in crack opening due to shrinkage using the formulation of MC 2010[4-1] for all models

Effect of the presence of stirrups

Most cracking tests which are carried out avoid the presence of stirrups, because they influence the cracking pattern. There are some examples of cracking tests in which the crack spacing closely mirrors the position of the stirrups[4-27]. This type of result has made the fact that cracking models included in codes do not consider the presence of stirrups rather puzzling for some. For this reason, the UPM tests studied this parameter.

The main conclusions from this study were the following:

- Stirrups can induce the formation of cracks. This effect is stronger with smaller covers. However, it is not correct to assimilate crack spacing and stirrup spacing. Cracks sometimes develop between stirrups and sometimes they do not develop at stirrup locations. Transfer length clearly still plays a role in crack formation.

- Although stirrup spacing has a significant effect on the mean crack spacing (and, thereby, on mean crack width), the test results show that their influence on the maximum crack spacing (and, thereby, on maximum crack opening) is much less. This is very clear in specimens with large covers.

- Since code are concerned with limiting the maximum crack width (not the mean crack width) and this value is not greatly influenced by the presence of the stirrups, it is logical that that code models do not consider stirrup spacing as a variable.

- The rather common belief that crack spacing and stirrup spacing are equal in beams with transverse reinforcement should be challenged. This experience seems to come from the older structures with very low concrete covers, which is not the case for contemporary structures.

Tension vs. flexure

EN 1992-1-1[4-9] considers that the transfer length in bending is half that in tension because the force needed to crack the same concrete area in tension is also half due to triangular force distribution. Analysis of the data base could not provide evidence to support this point of view.

This document is the intellectual property of the fib – International Federation for Structural Concrete. All rights reserved.
This PDF of fib Bulletin 92 is intended for use and/or distribution solely within fib National Member Groups.

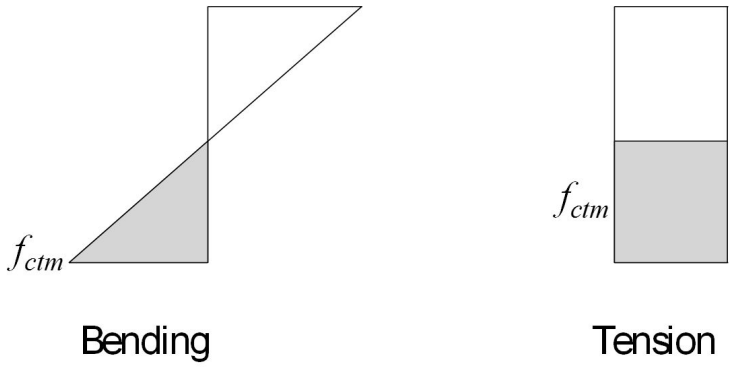


Fig. 4-20 Volume of tension stresses to be transferred from the cracked section to concrete in order to produce another crack, according to the formulation of EN 1992-1-1[4-9]

In EN 1992-1-1[4-9], this effect is considered by coefficient k_2 in the formula reproduced in Eq. (4-15), where k_3 and k_4 are calibration constants and k_1 accounts for the bond properties of reinforcement.

$$s_{r,\max} = k_3 \cdot c + k_1 \cdot k_2 \cdot k_4 \frac{\phi}{\rho_{ef}} \tag{4-15}$$

k_2 is taken 0.5 in bending and 1.0 in tension, thus implying that the transfer length for members in tension is double that of members in flexure.

MC 1990[4-8], on the other hand, takes a remarkably different approach and makes no difference between flexure and tension. The theory is formulated for a tie, and reinforcement in flexure is seen as a tie with a slightly variable tensile force, as shown in Fig. 4-21.

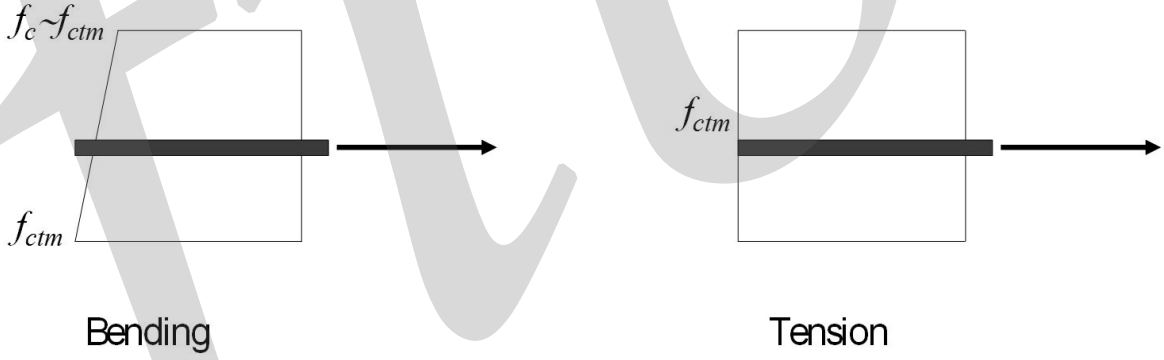


Fig. 4-21 In MC1990[4-8], flexure is seen as developing an equivalent tie around the reinforcement with slightly variable stress along the effective concrete tension area

In the UPM tests, cracks were measured both at the side of the beam and at the most tensioned face of the beam, always in correspondence with the tension reinforcement, as shown in Fig. 4-22. Since lateral and top covers were the same, if MC 1990[4-8] was correct, the same values of cracks and derived crack spacing would have been measured at both locations. This was not the case. Cracks were consistently larger when measured at the top of the beam than when measured at the side of the beam and the difference grew with the cover.

This document is the intellectual property of the fib – International Federation for Structural Concrete. All rights reserved.
This PDF of fib Bulletin 92 is intended for use and/or distribution solely within fib National Member Groups.

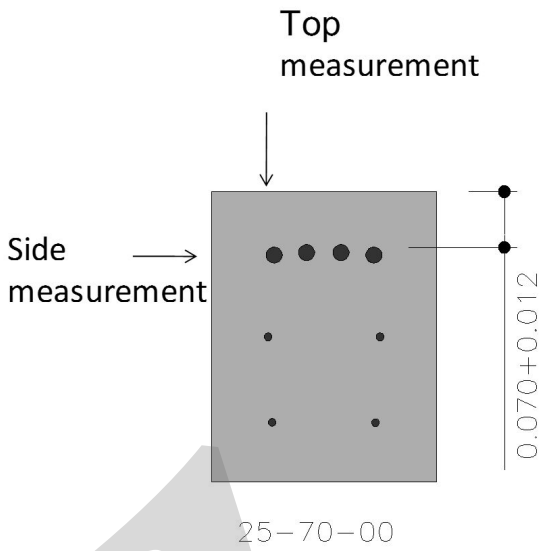


Fig. 4-22 Location where crack widths were measured

It was found that the difference could be virtually eliminated by multiplying the value measured at the side by $(h\text{-}x)/(d\text{-}x)$, as suggested by BS 5400, so that $w_{top} \sim w_{side} \times (h\text{-}x)/(d\text{-}x)$. This can be seen very clearly in Fig. 4-23. In order to avoid distortions due to differences in the placement of stirrups, the series are separated in three groups according to stirrup spacing. Within each series, with constant stirrup spacing, it can be seen that the correlation between $w_{m,top}/w_{m,side}$ and the factor $(h\text{-}x)/(d\text{-}x)$ is very high and the slope of the correlation lines is also close to one.

This result shows that there is a difference between bending and tension, since, in tension, the ratio $w_{m,top}/w_{m,side}$ would be expected to be equal to 1.00 from symmetry considerations.

It must also be noted that this effect, due to curvature, is unfavourable with respect to bending whereas the effect shown in Fig. 4-20 and considered in EN 1992-1-1[4-9], is favourable with respect to bending. Both effects are therefore opposed and tend to offset each other. This might be one of the reasons for which no clear effect regarding which is worse, bending or tension, can be seen from the results of the data base.

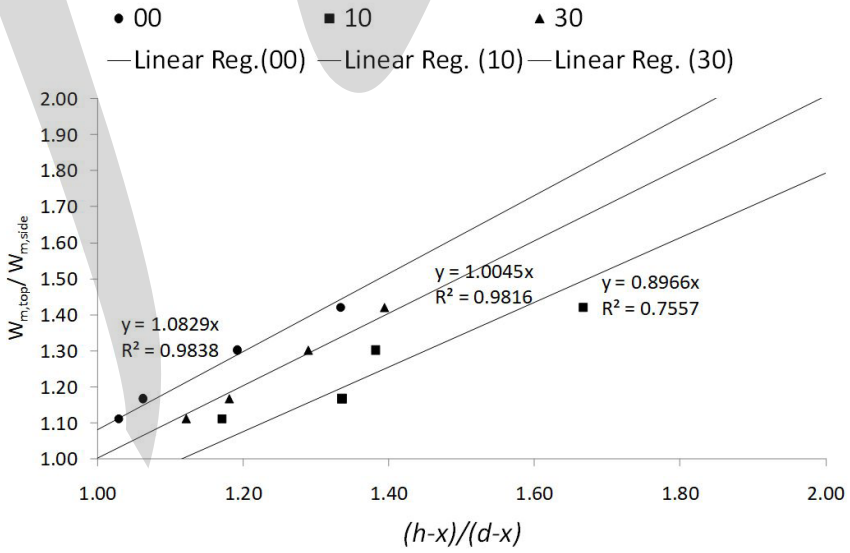


Fig. 4-23 Location where crack widths were measured

This document is the intellectual property of the fib – International Federation for Structural Concrete. All rights reserved.
This PDF of fib Bulletin 92 is intended for use and/or distribution solely within fib National Member Groups.

4.2.1.4 New model proposal and calibration

From the discussion above it seemed clear that the model for cracking to be included in MC 2010[4-1] had to include a term directly depending on cover. Furthermore, the large amount of scatter inherent to the phenomenon of cracking hinted at the difficulty in calibrating complex models. For these reasons, the simple additive model of Eq. (4-16) was chosen to be calibrated against a select subgroup of tests from the data base, where k is a calibration factor.

$$s_{\max} = 2\left(k \cdot c + \frac{1}{7.2}\frac{\phi}{\rho_{ef}} \right) \tag{4-16}$$

The second term is direct consequence of classical bond theory and coincides with the formulation of MC 1990[4-8]. The problem was therefore to calibrate the constant k.

Given the large scatter of data base results, and given that it was believed that a part of this scatter could be attributed to errors in the measurement of crack width, it was decided to use in this calibration only tests in which the actually measured mean crack spacing, and the inferred mean crack spacing, obtained by indirect means from the measured crack width were fairly similar. The condition established for this was to tolerate a 20% difference (see Eq. (4-17)), where TS is a factor accounting for tension-stiffening effects, determined according to Model Code 1990[4-8].

$$0.8 \le \frac{\dfrac{w_m \cdot E_s}{\sigma_2 \cdot TS}}{s_{m,measured}} \le 1.25 \tag{4-17}$$

Only 65 tests from the data base complied with this condition, including those of the following researchers:

- 8 out of 29[4-13],
- 14 out of 54[4-14],
- 5 out of 15[4-15],
- 3 out of 21[4-16],
- 22 out 116[4-20],
- 1 out of 7[4-21],
- and the 12 tests[4-28]

The relationship between measured and inferred crack spacing for these tests is represented in Fig. 4-24. A slope of the correlation line close to 1.00 can and a high value of R^2 be observed.

This document is the intellectual property of the fib – International Federation for Structural Concrete. All rights reserved.
This PDF of fib Bulletin 92 is intended for use and/or distribution solely within fib National Member Groups.

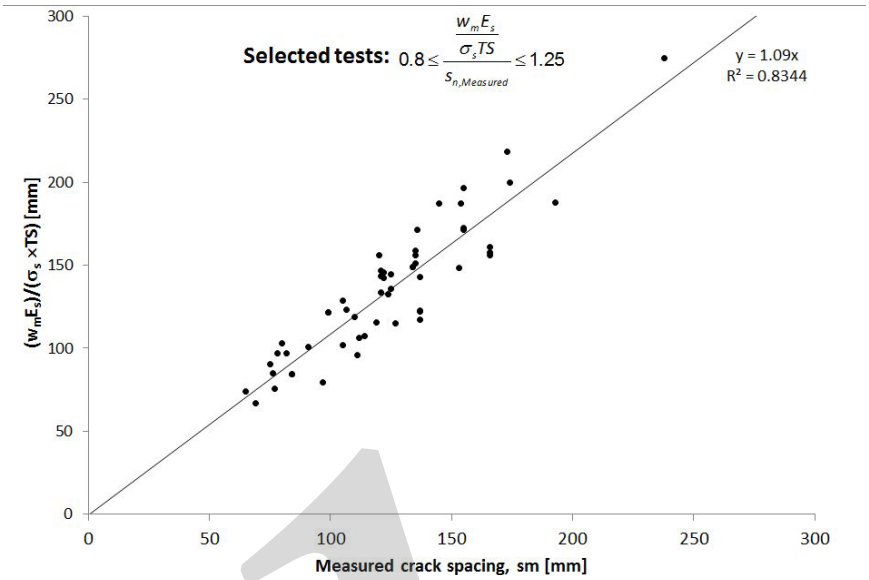


Fig. 4-24 Correlation between measured and inferred crack spacing in selected tests

Since the most reliable experimental values are mean values, these were the values which were used for calibration. However, Eq. (4-16) should really be interpreted as providing a value for the characteristic the crack spacing, even though it is formulated as a maximum crack with equal to twice the transfer length. For the purposes of calibration, this situation had to be addressed and an expression for the mean crack spacing was needed. If in MC 2010[4-1], s_{rmax} is really a characteristic value, then it is reasonable to assume that its value should be about 1.70 times the mean crack spacing[4-11]. Since s_{rmax} is formulated as twice the transfer length, s_m can be equated to about 1.17 times the transfer length (see Eq. (4-18).

$$s_{\max} = 2l_s \approx 1.7 s_m \rightarrow s_m \approx \frac{2}{1.7} l_s = 1.17 l_s \tag{4-18}$$

With this definition, the values of s_{rmax} and s_m can be formulated according to Eq. (4-19).

$$\begin{aligned} s_{rmax} &= 2\left(k \cdot c + \frac{1}{7.2}\frac{\phi}{\rho_{ef}} \right) \\ s_m &= 1.17\left(k \cdot c + \frac{1}{7.2}\frac{\phi}{\rho_{ef}} \right) \end{aligned} \tag{4-19}$$

Calibration of the model was performed in accordance with the bottom expression of Eq. (4-19).

With these premises, it was found that the best value for k was very close to 1.00. This being a round number, it was adopted for the code formulation.

This document is the intellectual property of the fib – International Federation for Structural Concrete. All rights reserved.
This PDF of fib Bulletin 92 is intended for use and/or distribution solely within fib National Member Groups.

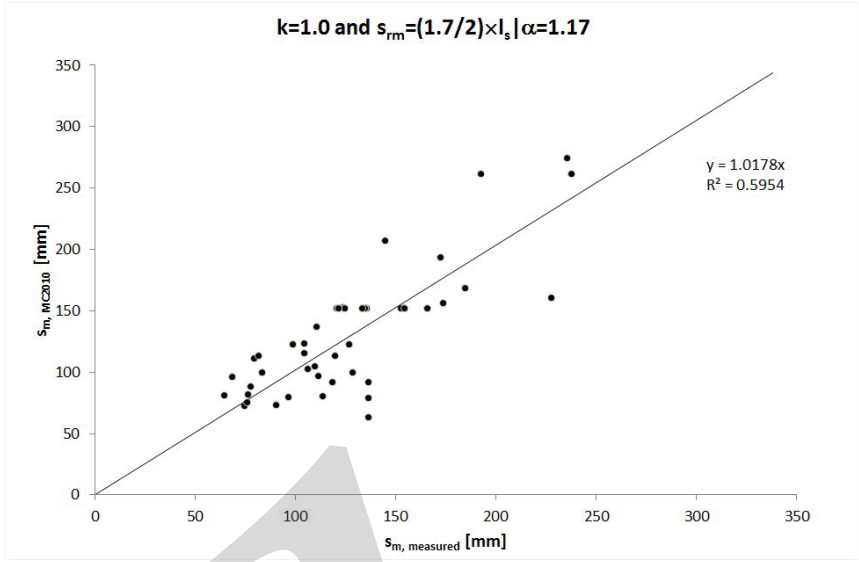


Fig. 4-25 Comparison of crack spacing estimated according to the calibrated model and measured for 65 selected tests

Fig. 4-25 shows the comparison between measured crack spacing and that estimated with the calibrated model of MC 2010 for the 65 selected tests. As can be seen the slope of the correlation line is closer to 1.00 and the coefficient of determination R^2 is decent.

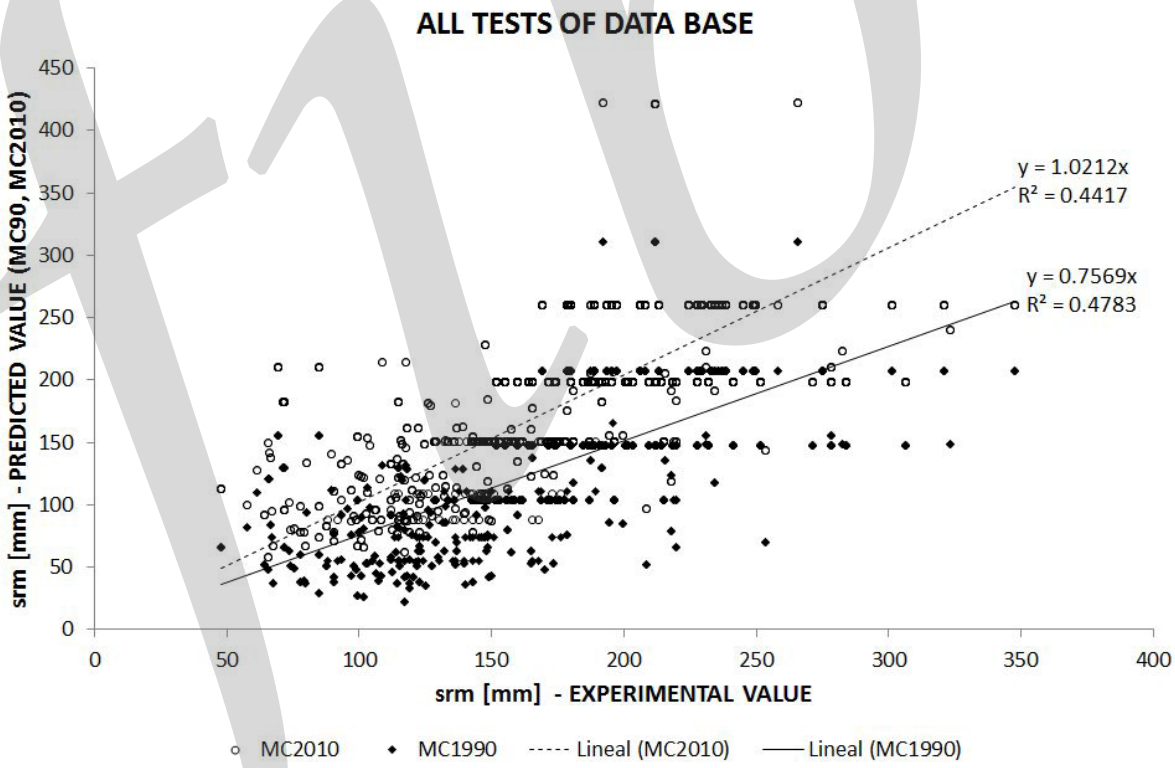


Fig. 4-26 Comparison of crack spacing estimated according to calibrated model and measured for all tests in data base, according to MC 1990 and MC 2010

Fig. 4-26 shows the same comparison for all the tests in the data base and compares the performance of MC 2010[4-1] to that of MC 1990[4-8]. As can be seen, MC 1990[4-8] underestimated the crack spacing, and this is the main correction introduced into MC 2010[4-1] by adding the term considering cover.

This document is the intellectual property of the fib – International Federation for Structural Concrete. All rights reserved.
This PDF of fib Bulletin 92 is intended for use and/or distribution solely within fib National Member Groups.

4.2.2 Shear cracks

4.2.2.1 Theory of shear crack appearance

The place of first crack initiation on concrete beam depends on the value of bending moment and shear force in the area. Where bending moment reaches significant values and shear force is very small, bending cracks occur when the axial stress in the external fibres of the cross section exceeds the tensile strength of concrete.

At the area where both the bending moment and shear force are relatively large, the resulting bending cracks develop and they change their slope, which explains the effort to resist shear force. For prestressed beams (in comparison with conventional reinforced beams) cracks are relatively low-inclined.

For thin walled concrete elements at the area with a small bending moment and relatively high shear force, it is possible to observe the formation of shear cracks. This is an area in the wall near the support, where the principal tensile stress exceeds the maximum tensile strength of concrete. Very often these cracks are observed earlier compared to the first bending cracks initiation at the midspan.

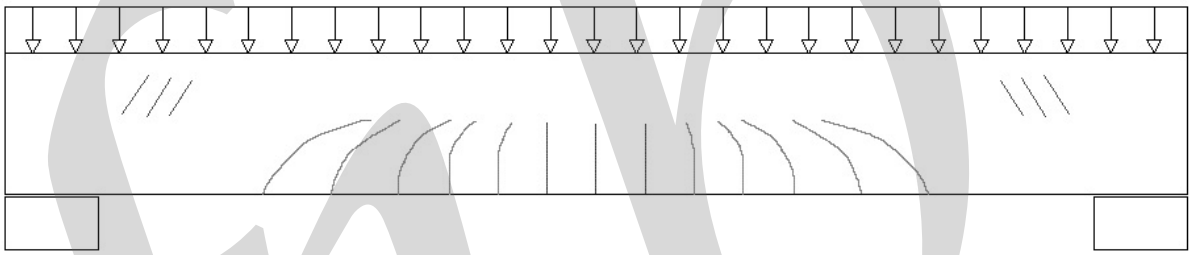


Fig. 4-27 The scheme of cracks of concrete element - cracks due to bending; shear cracks developed from bending cracks; cracks due to shear force at element walls

For prestressed concrete, additional compression stresses exist in the element. These additional compressive stresses cause later appearance of cracks in comparison with reinforced concrete elements. Generally, if the main tensile stress σ_1 reaches the value of concrete tensile strength, the concrete crack begins to form (and propagates in a direction perpendicular to the direction σ_1).

The effect of prestressing on the formation and direction of the crack could be described from the behaviour of small segment located in the central axis of the uncracked beam. By using Mohr's circle formulation, the direction of principal stresses could be found.

If a concrete element is not prestressed (element with no compressive force due to prestressing), the principal stress σ_1 is equal to shear stress and it has an inclination angle (related to beam axis) equal to 45° (Fig. 4-28). If this principal stress value exceeds the appropriate tensile strength of the concrete, then cracks appear. The crack direction is perpendicular to the principal tensile stress direction, i.e. at an angle of 45° to the beam axis.

This document is the intellectual property of the fib – International Federation for Structural Concrete. All rights reserved.
This PDF of fib Bulletin 92 is intended for use and/or distribution solely within fib National Member Groups.

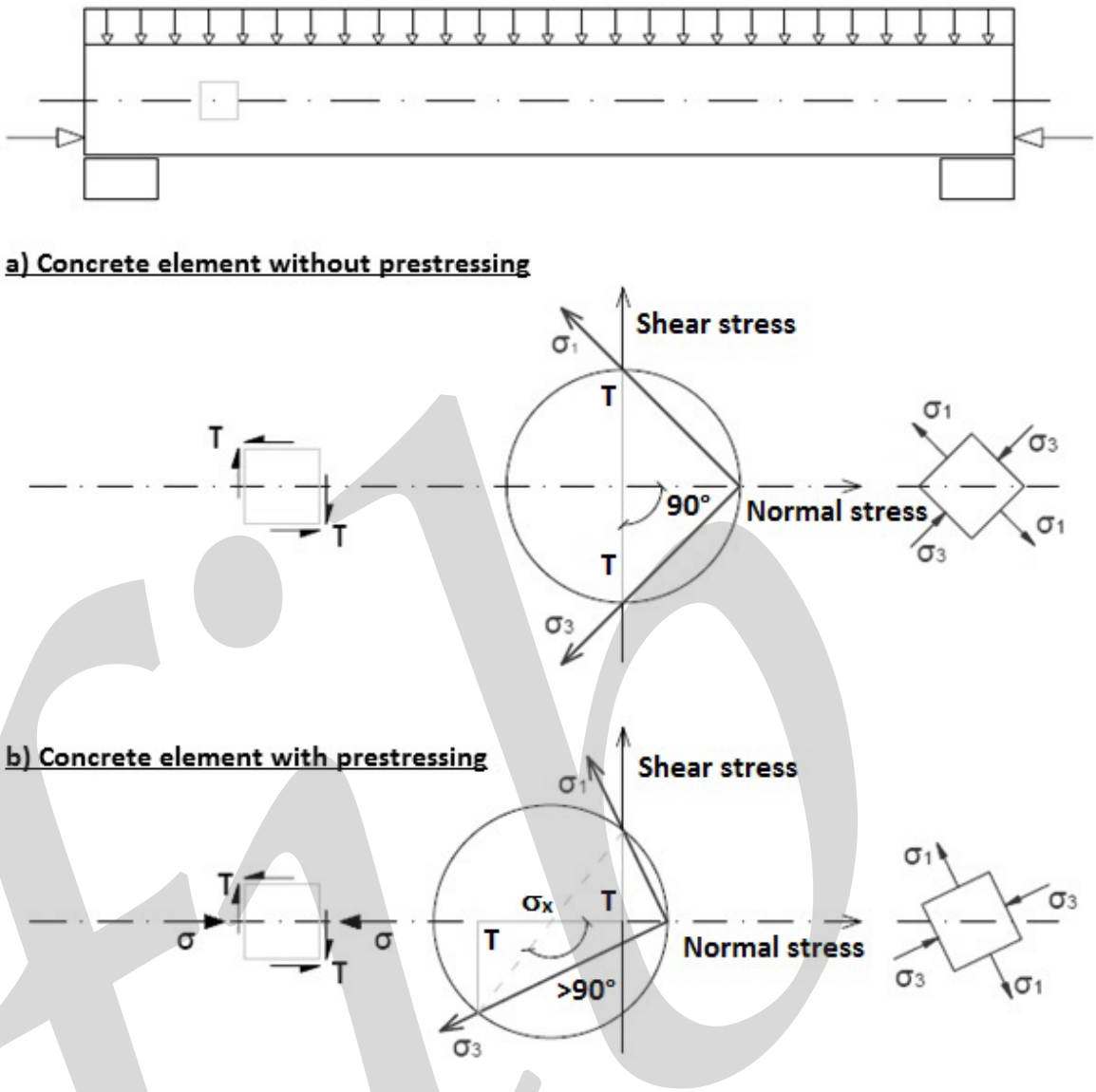


Fig. 4-28 Scheme of principal stresses for reinforced concrete and for prestressed concrete

Basic formulation for principal stress calculation (for 2 dimensional problems) is given by:

$$\sigma_{1,2} = \frac{\sigma_x}{2} \pm \sqrt{\frac{\sigma_x^2}{4} + \tau_{xz}^2} \tag{4-20}$$

For prestressed concrete elements the prestressing (compressive force) causes reduction of principal tensile stress σ_1. The angle between principal tensile stress direction and beam axis is increasing. That is why also the inclination of cracks is higher and reinforcement for shear force is more effective.

4.2.2.2 Serviceability limit states – shear cracks in accordance with standard design criteria

4.2.2.2.1 Assessment according to Eurocode

Eurocode 1992-2[4-29] for design of concrete bridges introduces the direction-dependent tensile strength f_{ctb} in the informative appendix QQ. This material characteristic reduces normal tensile strength f_{ctm} due to the acting principal compressive stress.

This document is the intellectual property of the fib – International Federation for Structural Concrete. All rights reserved.
This PDF of fib Bulletin 92 is intended for use and/or distribution solely within fib National Member Groups.

First, it is necessary to determine the direction-dependent tensile strength f_{ctb}:

$$f_{ctb} = \left(1 - 0.8\frac{\sigma_3}{f_{ck}}\right) f_{ctk;0.05} \tag{4-21}$$

where

f_{ctb} is tensile strength before crack creation at dual axis stress;

f_{ck} is compressive cylindrical concrete strength at age 28 days;

$f_{ctk;0,05}$ is 5% quantile of tensile concrete strength;

σ_3 principal stress in compression (positive value).

The requirement for crack creation is then described by the condition $\sigma_1 > f_{ctb}$ according to the EC. The tensile strength before crack creation at dual axis stress f_{ctb} is decreasing with increasing value of principal stress in compression σ_3.

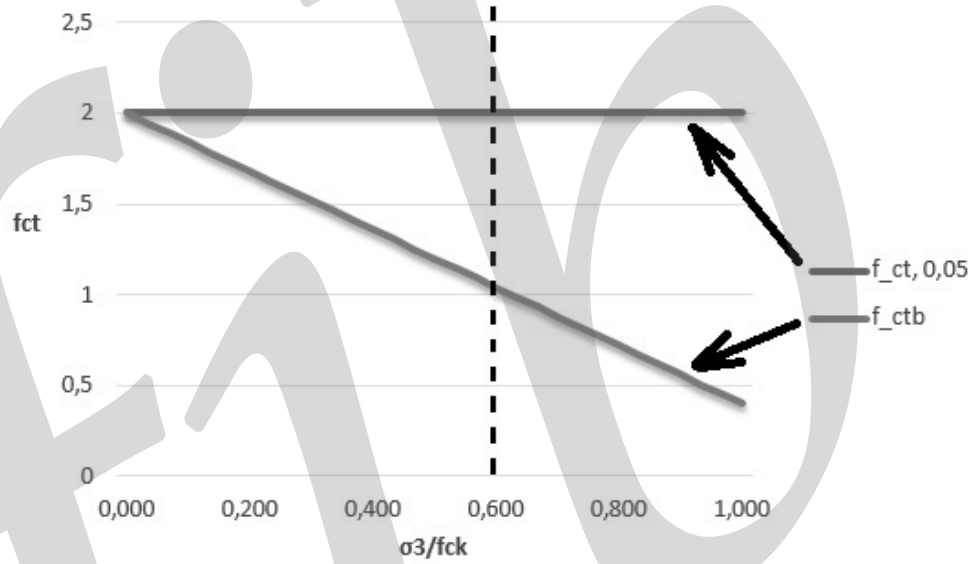


Fig. 4-29 The effect of principal compression stress value for tensile concrete strength at dual axis stress

4.2.2.2.2 Assessment according to the Model Code

There are no special requirements for computational method for shear cracks considering biaxial stress distribution. In the Model Code[4-1], the method is described for determination of the shear capacity of prestressed beams without bending cracks. These formulae are based on the design tensile strength of concrete. These formulae analyse only one cross-section located in distance $h/2$ from the face of the support. The assessment of the crack origin in an arbitrary point of the web is possible, but the MC2010[4-1] does not specify the direction-dependent tensile strength. It does not allow for the assessment of the crack origin in different points of the web along the length of the beam. Thus, the only alternative is to compare the principal tensile stress with the mean value of the tensile strength f_{ctm}. It is clear that cracks appear much later, when comparing calculations according to MC[4-1] with the EC.

$\sigma_1 > f_{ctm}$ condition for the crack origin according to MC

SLS checks in accordance with the MC 2010[4-1] requirements is also possible by a numerical simulation. It is not allowed to use principles based on one directional stress distribution for the assessment of a concrete element with shear force and bending

This document is the intellectual property of the fib – International Federation for Structural Concrete. All rights reserved.
This PDF of fib Bulletin 92 is intended for use and/or distribution solely within fib National Member Groups.

moment acting together. It is necessary to determinate conditions for biaxial stress and strain distribution and also conditions for biaxial failure.

The strength of material (concrete) for multi axial stress distribution is described by the surface of failures based on material strength in uniaxial stress distribution. MC2010[4-1] for example defines the failure condition as follows:

$$\alpha \frac{J_2}{f_{cmb}} + \lambda \frac{\sqrt{J_2}}{f_{cm}} + \beta \frac{I_1}{f_{cm}} - 1 = 0 \tag{4-22}$$

where

f_{cm} compressive strength of concrete – mean value;

f_{cmb} compressive strength of concrete for biaxial stress distribution – mean value;

I, J invariants of stress tensors;

f_{ctm} tensile strength of concrete - mean value;

α, β, λ coefficients.

This failure condition is helpful for using in numerical calculations. The formulation is given by one study[4-30].

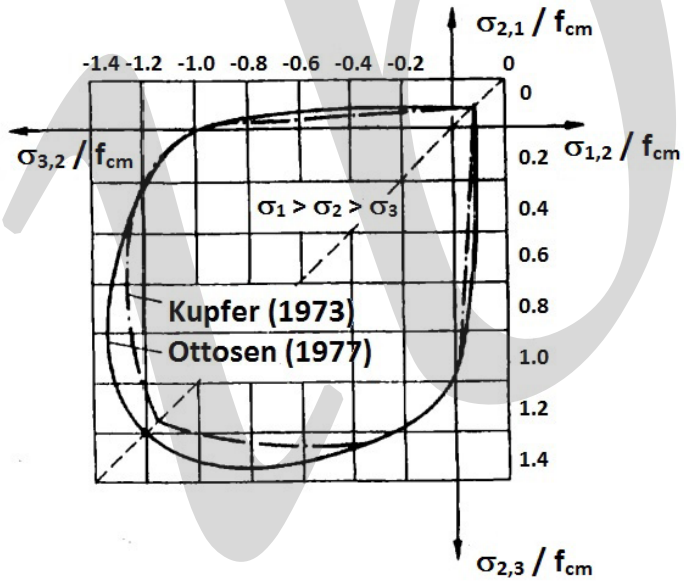


Fig. 4-30 Definition of failure surface[4-30]

The formulation for tensile strength in dual axis stress distribution is:

$$f_{ctmb} = \left(1 - 0.8 \frac{\sigma_2}{f_c}\right) f_{ctm} \tag{4-23}$$

where

f_{ctm} tensile strength of concrete – mean value;

f_{ctmb} tensile strength of concrete for biaxial stress distribution – mean value;

σ_2 principal stress in compression;

f_c compressive characteristic concrete strength.

This document is the intellectual property of the fib – International Federation for Structural Concrete. All rights reserved.
This PDF of fib Bulletin 92 is intended for use and/or distribution solely within fib National Member Groups.

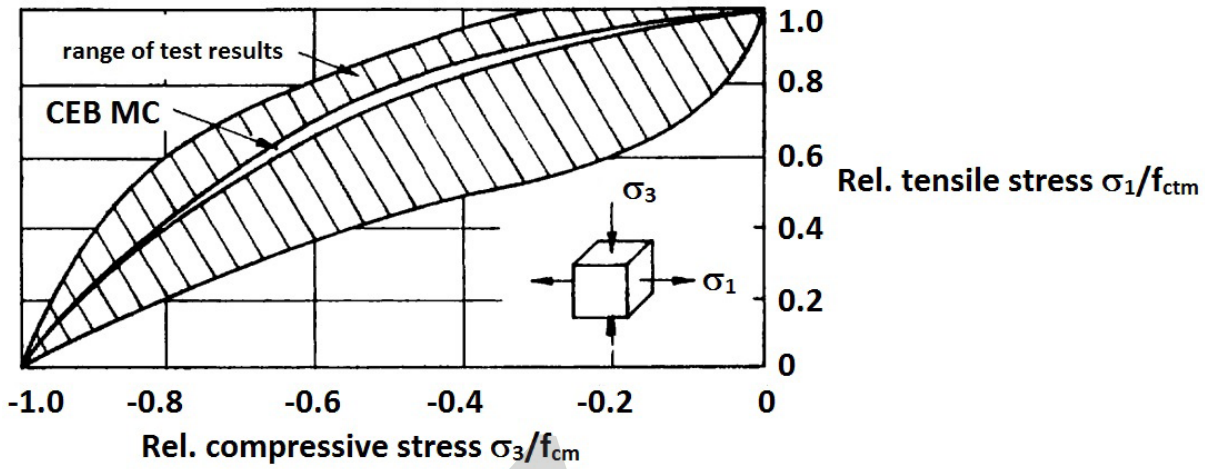


Fig. 4-31 Strength of concrete under biaxial stress state

4.2.3 Cracks induced by deformation restraint

Without action of loads, reinforced concrete members may crack due to e.g. shrinkage or temperature when their deformation is restrained. Cracking is capable of reducing the forces arising in such a case. In order to ensure the limitation of crack widths, the imposed deformations should be distributed across a sufficient number of cracks. Thus, additional cracks should appear after the formation of a first crack. This can be assured by sufficiently strong reinforcement that is capable of transfer by bond the tensile forces necessary to promote cracking at a different position within the structure or the structural member.

Under this condition, the basic behaviour of reinforced concrete elements as shown in Figs. 7.6-1 and 7.6-2 (in MC 2010[4-1]) can be used to assess the acting forces in the case of restrained deformation. Starting from the example of a prismatic reinforced concrete bar with imposed deformation or restraint of axial shortening (e.g. due to shrinkage, temperature decrease), it becomes evident that after onset of cracking new cracks will be formed. This enables distribution of the imposed deformation to a sufficient number of cracks. After formation of the first or a subsequent crack, the force drops down and rises again until formation of the next crack. As depicted in Fig. 7.6-1, the normal force at crack formation will increase only slightly until the end of the crack formation phase. While Figure 7.6-1 shows a certain increase of the normal force up to a maximum value of $N_r = A_c \cdot f_{ct,\max} \ (1+\alpha_E \cdot \rho_{s,ef}) \approx A_c \cdot f_{ct,\max}$, Fig. 7.6-2 uses a simplified approach assuming $N_r \approx A_c \cdot f_{ct,\max}$ =const.

The end of the crack formation phase marks the end of the plateau with (approximately) constant normal force acc. to Fig 7.6-2 and will be reached at a strain corresponding to $\varepsilon_{sm} = \frac{\Delta l}{l} = \left(1-\beta\right)\frac{\sigma_{sr}}{E_s}$.

Taking β = 0.6 as proposed by MC 2010[4-1] for short term loading, $\varepsilon_{sm} \approx 0.4\frac{\sigma_{sr}}{E_s}$ is obtained.

In order to be able to open new cracks after the first crack, the reinforcement must not be ruptured. Furthermore, in order to control crack widths effectively, the reinforcement shall not yield in any cracked section. Thus, assuming that the steel stress in the cracked sections shall not exceed the yield stress and assuming the characteristic yield stress f_{yk} to be around 500 MPa, the end of the crack formation phase can be expected at about

This document is the intellectual property of the fib – International Federation for Structural Concrete. All rights reserved.
This PDF of fib Bulletin 92 is intended for use and/or distribution solely within fib National Member Groups.

$\varepsilon_{sm} \approx 0.7...0.9\%$ $f_y = f_{yk} = 500$ MPa for practical cases. Except for large imposed deformations as e.g. due to high temperature changes, this value is high enough to justify the cracking force N_r to be considered as the relevant normal force for check of crack widths. This leads to the requirement of a minimal reinforcement of $\min A_s \geq f_{ct} \cdot A_c / f_y$. For limitation of the crack widths w to a specified value, lower steel stresses $\sigma_s(w) \leq f_y$ may also have to be ensured. Thus, for crack width limitation, $A_s(w) \geq f_{ct} \cdot A_c / \sigma_s(w)$ must be provided.

If imposed strains exceeding $\varepsilon_{sm} \approx 0.7...0.9\%$ have to be taken into account, a significant increase of normal force after the end of the crack formation phase can be expected which has to be considered e.g. by nonlinear structural analysis. In such a case, the minimum reinforcement as calculated above will not be sufficient.

On the contrary, there are also other exceptions from the "normal" case of considering the cracking force N_r as the decisive force for cases with restraint action:

1. free deformation is limited by other criteria, such as e.g. friction forces, forming a restraint. As an example for this, there are foundation mats with moderate length and/or relatively low friction between soil and concrete;

2. in addition to the reinforcement introducing tensile forces by bond action, other forces are being introduced into the structural member, e.g. by interaction with neighbouring elements (example: newly poured wall with shrinkage on already hardened foundation mat with older concrete having less shrinkage after time of pouring of wall);

3. thick R/C members with concentrated arrangement of reinforcement where primary cracking with a bundle of secondary cracks occur (see Fig. 4-32).

In addition to Figs. 7.6-1 and 7.6-2, Fig. 4-32 according to one study[4-31] shows the behaviour of a prismatic reinforced concrete bar subject to imposed elongation considering the effect of shrinkage of concrete. Since the rebars do not shrink, an internal restraint between concrete and steel exists. It leads to tensile stresses in the concrete even without external restraint or the action of external forces. Consequently, the first crack has to be expected at a smaller value of tensile normal force than for the (theoretical) case of zero shrinkage.

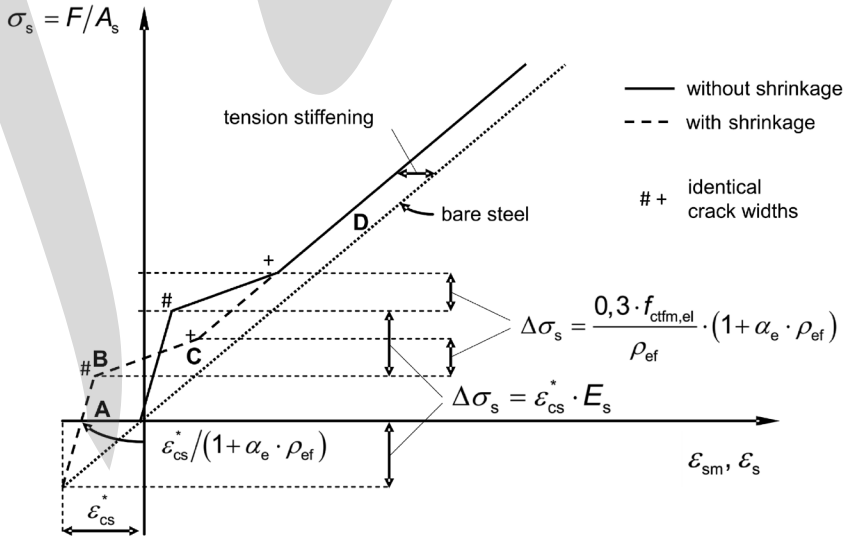


Fig. 4-32 Force - elongation relationship for prismatic reinforced concrete bar considering influence of shrinkage

This document is the intellectual property of the fib – International Federation for Structural Concrete. All rights reserved.
This PDF of fib Bulletin 92 is intended for use and/or distribution solely within fib National Member Groups.

Note that ε_{cs}^{*} denotes the shrinkage strain under consideration of the reduction due to creep / relaxation of concrete. Fig. 4-33 demonstrates the same effect for the case of shrinkage action in a R/C beam. Since the reinforcement in the bending tensile zone does not shrink as much as the concrete of the compression zone, a positive curvature exists even without a bending moment due to loading.

Fig. 4-34 shows examples of tests with thick reinforced concrete members where the formation of crack bundles has been observed in the region with concentrated reinforcement. Fig. 4-35 depicts the flow of forces inside a diaphragm element with concentrated reinforcement, which leads to the effect of crack bundles.

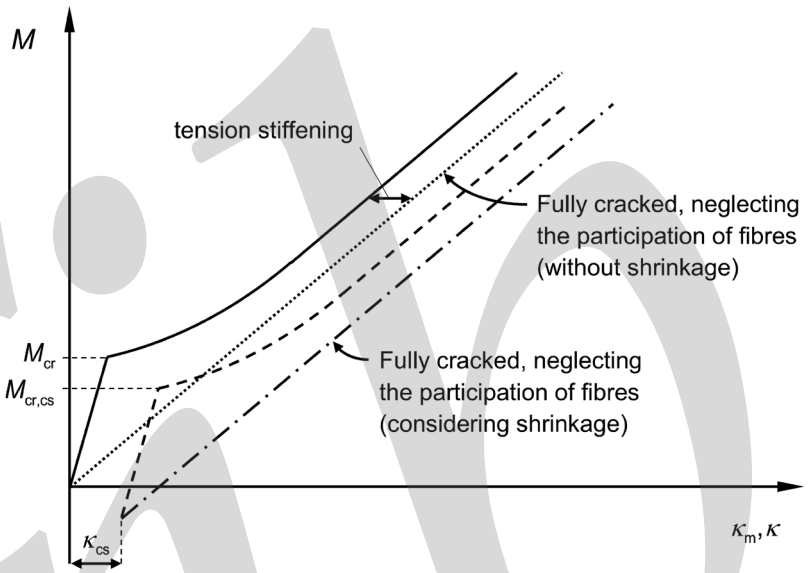


Fig. 4-33 Moment - curvature relationship for prismatic reinforced concrete beam considering influence of shrinkage on bending

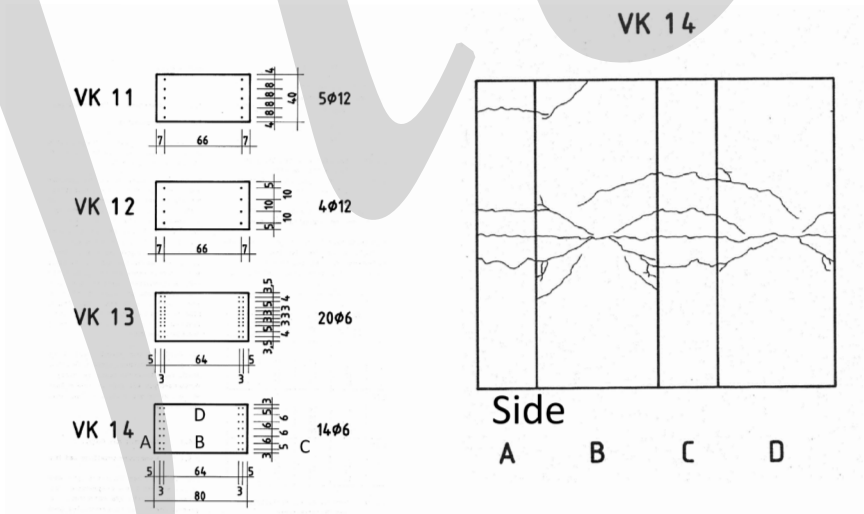


Fig. 4-34 Experimental results for thick R/C members with concentrated reinforcement

This document is the intellectual property of the fib – International Federation for Structural Concrete. All rights reserved.
This PDF of fib Bulletin 92 is intended for use and/or distribution solely within fib National Member Groups.

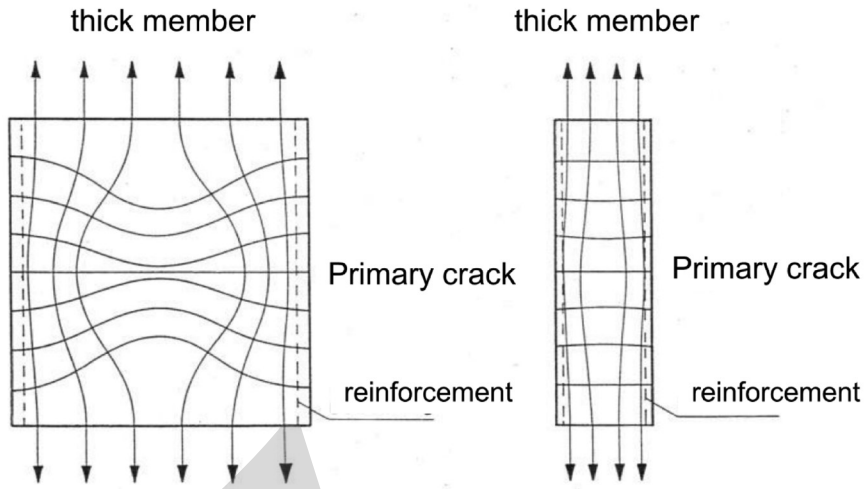


Fig. 4-35 Stress trajectories for thick R/C members with concentrated reinforcement

In order to capture the effect of crack bundles (see item 3 as mentioned in the list above) the bond force -being introduced by the concentrated reinforcement- necessary to form secondary cracks adjacent to a primary crack (throughout the whole cross section) must be known. In this regard, an effective concrete area may be defined. This area should be determined such that it represents that portion of the cross section that will have the same cracking load as the bond force being necessary to form a secondary crack.

As a result from nonlinear FE-models, one study[4-32] proposes to calculate the height of the effective tensile area as $m^*(h\text{-}d)$. The factor m can be obtained from Fig. 4-36.

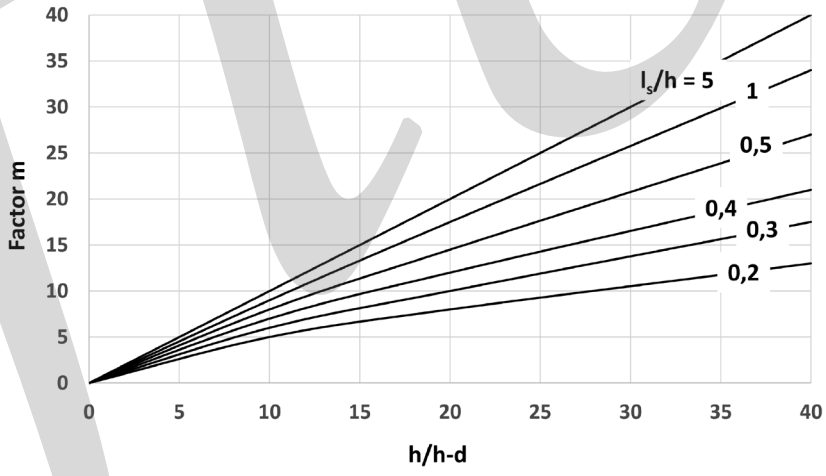


Fig. 4-36 Factor m as multiple of $(h\text{-}d)$ for calculation of height of effective tensile area $A_{ct,eff}$

This document is the intellectual property of the fib – International Federation for Structural Concrete. All rights reserved.
This PDF of fib Bulletin 92 is intended for use and/or distribution solely within fib National Member Groups.

For practical purposes, the effective height of the tensile area h_{eff} may be selected to be 2.5 times (*h-d*). For thick members with concentrated reinforcement, the transmission length may become small in relation to the member thickness. Relations depicted in Fig.4-37 may be proposed for the limit cases of pure axial tension and bending:

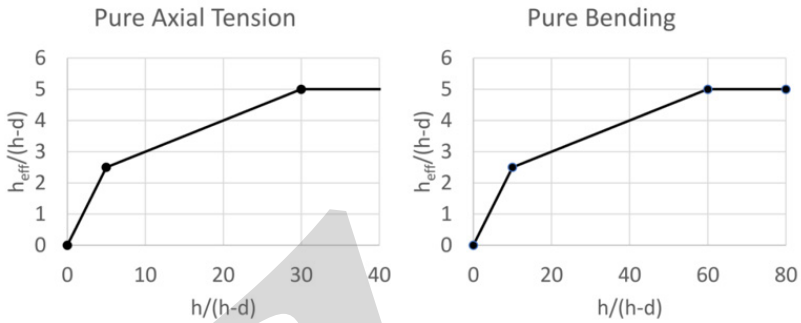


Fig. 4-37 Recommendation for selection of effective depth for axial tension and bending

4.2.4 Cracks in prestressed concrete structures

The main difference between cracking of reinforced concrete structures and prestressed concrete structures comes from the fact that bond properties of prestressing are weaker than those of reinforcing steel. In order to take into account this difference as well as that of the differing effective perimeters of both types of reinforcement in concrete elements containing both plain and prestressed reinforcement, MC 2010[4-1] proposes to determine an equivalent area of prestressing by multiplying the actual area A_p by the square of factor ξ_1, defined in Eq. (4-24).

$$\xi_1 = \sqrt{\frac{\tau_{bmp}}{\tau_{bms}} \frac{\phi_s}{\phi_{p,ef}}} \tag{4-24}$$

τ_{bmp}/τ_{bms} is the ratio of bond strength of prestressing and bond stress of plain reinforcement and is a factor which is typically less than 1.0. This value is given in Table 7.6-3 of MC 2010[4-1] as a function of the type of prestressing steel and reproduced here in Table 4-7.

Table 4-7 Bond factors τ_{bmp}/τ_{bms} for different types of prestressing steel

Surface condition	Pretensioned steel	Posttensioned steel	No bond
Smooth wire	0.40	0.20	0
Strand	0.60	0.40	0
Indented wire	0.80	0.60	0
Ribbed bar	-	1.00	0

With regard to equivalent diameter to be used for prestressing reinforcement, MC 2010[4-1] provides the formulation of Eq.(4-25).

$$\phi_{p,ef} = \frac{4A_p}{u_p} \tag{4-25}$$

A_p is the total area of prestressing and u_p is the total equivalent perimeter of prestressing steel (see Eq. (4-26)).

This document is the intellectual property of the fib – International Federation for Structural Concrete. All rights reserved.
This PDF of fib Bulletin 92 is intended for use and/or distribution solely within fib National Member Groups.

$$A_p = \sum A_{p,i}$$
$$u_p = \sum u_{p,i}$$
$$u_{p,i} = \begin{cases} 1.6\pi\sqrt{A_{p,i}} \text{ for bundles} \\ 1.75\pi\phi_{wire} \text{ for 7-wire strands} \\ 1.20\pi\phi_{wire} \text{ for 3-wire strands} \end{cases} \quad (4\text{-}26)$$

The value of the transfer length can be derived once again as in paragraph 4.2.1 for a section with a combination of plain and prestressing reinforcement, taking into account the different bond properties and equivalent perimeters of reinforcing and prestressing steel. It will be shown that the expressions obtained are equivalent to applying the same methodology outlined in 4.2.1 with the only modification of considering an area of reinforcement equal to the sum of A_s and $(\xi_1)^2 A_p$.

Referring now to Fig. 4-38, the equilibrium of the bar between the cracked section and the section of no slip – just before a new crack forms – is represented here for a tie having a combination of plain and prestressed reinforcement. The force in the prestressed reinforcement is that due to the deformation plane ($A_p\Delta\sigma_{p2}$ at the crack and $A_p\Delta\sigma_{pE}$ at the section of no slip) plus the force due to the prestressing of the reinforcement ($A_p \cdot E_p \cdot \varepsilon_0$, ε_0 being the pre-strain applied to the prestressing reinforcement at the time of calculation – that is normally subtracting prestressing losses).

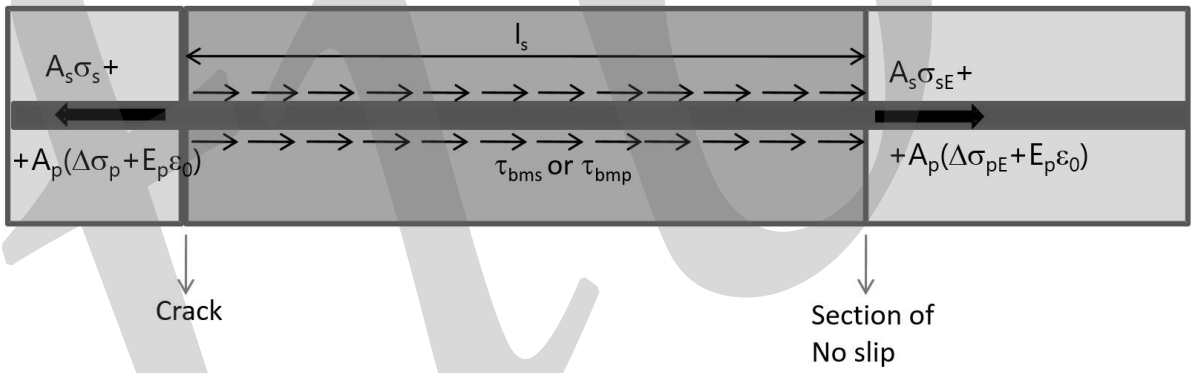


Fig. 4-38 Equilibrium of the bar between the cracked section and the section of no slip for a section combining plain and prestressed reinforcement

As in paragraph 4.2.1, parallel to Eq.(4-10), the equilibrium of the prestressing reinforcement can be written as given in Eq. (4-27), and the transfer length can be expressed in terms of the variation of stress in the prestressed reinforcement.

$$\left.\begin{aligned} & A_p\left(\Delta\sigma_{p2} + E_p \cdot \varepsilon_0\right) \\ & = A_p\left(\Delta\sigma_{pE} + E_p \cdot \varepsilon_0\right) + \tau_{bmp}\pi\phi_{p,ef} \cdot l_s \\ & A_p = \frac{\pi\phi_{p,ef}^2}{4} \end{aligned}\right\} \rightarrow l_s = \frac{\Delta\sigma_{p2} - \Delta\sigma_{pE}}{4\tau_{bmp}}\phi_{p,ef}$$
$$\rightarrow \Delta\sigma_{p2} - \Delta\sigma_{pE} = \frac{4l_s \cdot \tau_{bmp}}{\phi_{p,ef}} \quad (4\text{-}27)$$

This document is the intellectual property of the fib – International Federation for Structural Concrete. All rights reserved.
This PDF of fib Bulletin 92 is intended for use and/or distribution solely within fib National Member Groups.

The value of l_s, is of course the same when considering the equilibrium of the prestressed bar and that of the plain reinforcement bar present in the same element. It is the definition of l_s, that allows derivation of the equation of the equilibrium between axial forces at the section of the crack and at the section of zero slip right before the formation of a new crack, at which time the tensile stress of concrete in the effective concrete area is equal to the mean tensile strength of concrete (see Fig. 4-39 and Eq. (4-28)).

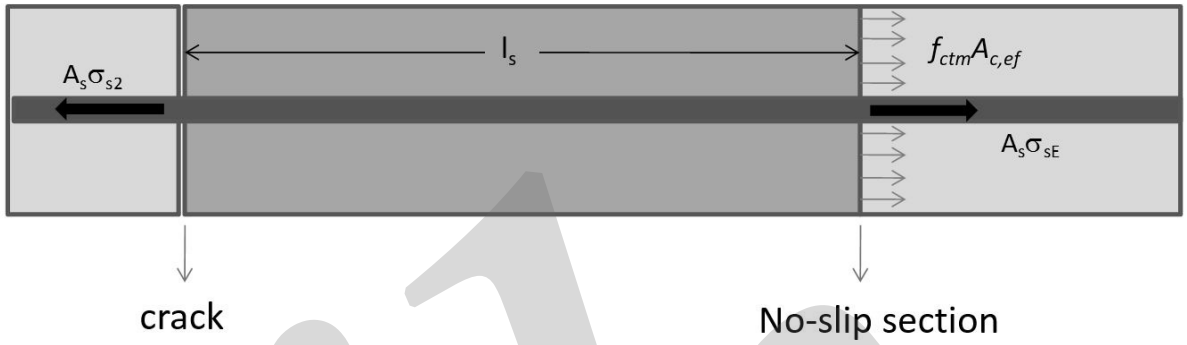


Fig. 4-39 Equilibrium between the section at the crack and the section of no slip just before the formation of a new crack

$$
\begin{aligned}
& A_s \cdot \sigma_{s2} + A_p \left(\Delta\sigma_{p2} + E_p \cdot \varepsilon_0 \right) = A_s \cdot \sigma_{sE} + A_p \left(\Delta\sigma_{pE} + E_p \cdot \varepsilon_0 \right) + f_{ctm} \cdot A_{c,ef} \\
& \rightarrow A_s \left(\sigma_{s2} - \sigma_{sE} \right) + A_p \left(\Delta\sigma_{p2} - \Delta\sigma_{pE} \right) = f_{ctm} \cdot A_{c,ef} \\
& \rightarrow A_s \frac{4 l_s \cdot \tau_{bms}}{\phi_s} + A_p \frac{4 l_s \cdot \tau_{bmp}}{\phi_{p,ef}} = f_{ctm} \cdot A_{c,ef} \\
& \rightarrow \frac{4 l_s \cdot \tau_{bms}}{\phi_s} \left(A_s + A_p \underbrace{\frac{\phi_s}{\phi_{p,ef}} \frac{\tau_{bmp}}{\tau_{bms}}}_{\xi_1^2} \right) = f_{ctm} \cdot A_{c,ef} \\
& \rightarrow l_s = \frac{f_{ctm}}{4\tau_{bms}} \frac{A_{c,ef} \cdot \phi_s}{\left(A_s + \xi_1^2 \cdot A_p \right)} = \frac{f_{ctm}}{4\tau_{bms}} \frac{\phi_s}{\rho_{s+p,ef}}
\end{aligned}
\tag{4-28}
$$

As can be seen, Eq. (4-28) is the same as that derived before for a reinforced concrete section changing only the definition of the steel ratio by considering the area of prestressing steel with a reduced value.

This is also true when calculating the value of the difference between the mean strain of reinforcement and the mean strain of concrete, ε_{sm}-ε_{cm}, as it will now be shown. For a reinforced concrete section, without prestressing, this difference can be evaluated as shown in Eq. (4-29), where β is an empirical factor. This equation is expressing the fact that the mean strain in steel along the transfer length is the stress at the crack minus a fraction β of the variation of the strain between the crack and the section of no slip, and that the mean strain in concrete along the transfer length is also a fraction β of the strain at the section of no slip (f_{ctm}/E_c), since the concrete strain at the crack is zero. In Eq. (4-29), α_e is the modular ratio equal to E_s/E_c.

This document is the intellectual property of the fib – International Federation for Structural Concrete. All rights reserved.
This PDF of fib Bulletin 92 is intended for use and/or distribution solely within fib National Member Groups.

By combining the first expression of ε_{sm}-ε_{cm} with the result derived from the equilibrium between the section of the crack and the section of no slip (see also Eq.(4-11)), the expression included in MC 2010 for reinforced concrete sections (Eq. 7.6-5 of MC 2010[4-1]) is obtained (albeit simplified since here, for the sake of simplicity, shrinkage has not been considered).

$$\left.\begin{aligned} \varepsilon_{sm}-\varepsilon_{cm} &= \frac{\sigma_{s2}-\beta\left(\sigma_{s2}-\sigma_{sE}\right)-\beta\cdot\alpha_e\cdot f_{ctm}}{E_s} \\ \sigma_{s2}-\sigma_{sE} &= \frac{f_{ctm}}{\rho_{ef}} \end{aligned}\right\} \rightarrow \varepsilon_{sm}-\varepsilon_{cm} = \frac{\sigma_{s2}-\beta\frac{f_{ctm}}{\rho_{ef}}\left(1+\alpha_e\cdot\rho_{ef}\right)}{E_s} \quad (4\text{-}29)$$

The same line of reasoning can be applied to sections with a combination of plain and prestressed reinforcements. As can be seen by Eq. (4-30), the correction of ρ_{ef} for $\rho_{s+p,ef}$ also is sufficient to correct the formula for mean differential strain in order for it to be applicable to sections combining both types of reinforcement.

$$\left.\begin{aligned} &\varepsilon_{sm}-\varepsilon_{cm} = \frac{\sigma_{s2}-\beta\left(\sigma_{s2}-\sigma_{sE}\right)-\beta\cdot\alpha_e\cdot f_{ctm}}{E_s} \\ &A_s\left(\sigma_{s2}-\sigma_{sE}\right)+A_p\left(\Delta\sigma_{p,2}-\Delta\sigma_{p,E}\right)=f_{ctm}\cdot A_{c,ef} \\ &\sigma_{s2}-\sigma_{sE} = \frac{4\tau_{bms}\cdot l_s}{\phi_s} \\ &\Delta\sigma_{p,2}-\Delta\sigma_{p,E} = \frac{4\tau_{bmp}\cdot l_s}{\phi_{p,ef}} = \left(\sigma_{s2}-\sigma_{sE}\right)\frac{\tau_{bmp}}{\tau_{bms}}\frac{\phi_s}{\phi_{p,ef}} \\ &\rightarrow\left(\sigma_{s2}-\sigma_{sE}\right)\underbrace{\left(A_s+\xi_1^2\cdot A_p\right)}_{A_{s+p,ef}}=f_{ctm}\cdot A_{c,ef} \\ &\rightarrow\left(\sigma_{s2}-\sigma_{sE}\right)=\frac{f_{ctm}}{\rho_{s+p,ef}} \end{aligned}\right\} \rightarrow \varepsilon_{sm}-\varepsilon_{cm} = \frac{\sigma_{s2}-\beta\frac{f_{ctm}}{\rho_{s+p,ef}}\left(1+\alpha_e\cdot\rho_{s+p,ef}\right)}{E_s} \quad (4\text{-}30)$$

Note that if no reinforcing steel is provided, Eq. (4-28) is modified as shown in Eq. (4-31), so that the general formulation can be applied with the condition $\phi_s=\phi_{p,ef}$.

$$\begin{aligned} &A_p\left(\Delta\sigma_{p2}-\Delta\sigma_{pE}\right)=f_{ctm}\cdot A_{c,ef} \\ &A_p\frac{4l_s\cdot\tau_{bmp}}{\phi_{p,ef}}=f_{ctm}\cdot A_{c,ef} \\ &\rightarrow l_s=\frac{f_{ctm}}{4\tau_{bmp}}\frac{A_{c,ef}\cdot\phi_{p,ef}}{\left(A_p\right)}=\frac{f_{ctm}}{4\tau_{bms}}\frac{A_{c,ef}\cdot\phi_{p,ef}}{\left(\frac{\tau_{bmp}}{\tau_{bms}}A_p\right)}=\frac{f_{ctm}}{4\tau_{bms}}\frac{A_{c,ef}\cdot\phi_{p,ef}}{\left(\xi_1^2\cdot A_p\right)} \end{aligned} \quad (4\text{-}31)$$

$$\Rightarrow\begin{cases}\xi_1=\sqrt{\dfrac{\tau_{bmp}}{\tau_{bms}}}\\ \phi_s=\phi_{p,ef}\end{cases}$$

This document is the intellectual property of the fib – International Federation for Structural Concrete. All rights reserved.
This PDF of fib Bulletin 92 is intended for use and/or distribution solely within fib National Member Groups.

4.2.5 Control of cracking without calculation

MC 2010[4-1] provides two tables which allow indirect verification of the SLS of cracking (w_d) by limiting the stress in reinforcement at the crack, σ_{s2}, and either the maximum diameter (Table 7.6-4 of MC2010) or the maximum spacing between bars (Table 7.6-5 of MC 2010): fulfilling one condition implies the fulfilment of the other. These tables are derived for reinforced concrete elements of rectangular cross section subjected to bending, although their application is also generalized in MC 2010 to prestressed elements.

The tables have been derived from the cracking model, already described above, by assuming a value for the crack width opening $w_d = w_{\text{lim}}$, and solving the equation giving the crack width opening for ϕ_s (see Eq. (4-32)).

$$w_d = \underbrace{\frac{\sigma_{s2} - \beta \frac{f_{ctm}}{\rho_{ef}}\left(1+\alpha_e \cdot \rho_{ef}\right)}{E_s}}_{\varepsilon_{sm}-\varepsilon_{cm}} \underbrace{2\left(c + \frac{1}{7.2}\frac{\phi_s}{\rho_{ef}}\right)}_{2l_{s,\max}} = w_{\text{lim}} \Leftrightarrow$$

$$\phi_{s,\max} = \left(\frac{1}{2} \frac{w_{\text{lim}} \cdot E_s}{\sigma_{s2} - \beta \frac{f_{ctm}}{\rho_{ef}}\left(1+\alpha_e \cdot \rho_{ef}\right)} - c \right) 7.2\rho_{ef} \tag{4-32}$$

In order to obtain values of $\phi_{s,\max}$ as a function of σ_{s2}, from this formula, some assumptions must be made regarding the rest of the variables involved. These assumptions are the following:

- $w_{\text{lim}} = 0.3$ mm
- The reinforcement provided is the minimum reinforcement necessary to obtain a stress in steel at the crack equal to σ_{s2} when the section cracks. This is equivalent to assuming $\sigma_{s2} = \sigma_{sr}$. This value of the reinforcement is given by Eq. (4-33).

$$\rho_{ef} = \rho_{ef,\min} = \frac{f_{ctm} \cdot k_c \cdot k}{\sigma_s} \frac{h_{cr}}{2.5\left(h-d\right)} \tag{4-33}$$

In Eq. (4-33), k_c is a factor taking into account the stress distribution, taken as 0.4 for bending, k is a factor taking into account the reduction of tensile strength due to self-equilibrating stresses, and is taken a 0.93 for an assumed depth of 400 mm, h_{cr} is the depth of the section with tensile stresses before cracking, and is taken as $h/2$ (bending, rectangular section), $2.5(h\text{-}d)$ is the height of the effective concrete section and $(h\text{-}d)$ is assumed to be approximately 0.10 h. The concrete strength is assumed to be 30 MPa and the mean tensile strength is therefore 2.9 MPa. With these assumptions, the expression of ρ_{ef} is that given in Eq. (4-34).

$$\rho_{ef} = \rho_{ef,\min} = \frac{2.9}{\sigma_s} 0.4 \cdot 0.93 \frac{\frac{h}{2}}{2.5 \cdot 0.1h} = \frac{2.16}{\sigma_s\left[\text{MPa}\right]} \tag{4-34}$$

This document is the intellectual property of the fib – International Federation for Structural Concrete. All rights reserved.
This PDF of fib Bulletin 92 is intended for use and/or distribution solely within fib National Member Groups.

- Cover is taken as 25 mm
- The value of maximum diameter is given for stabilized cracking in structures subjected to repeated loading (β = 0.4 and $\tau_{mbs} = 1.8 f_{ctm} \rightarrow 4\tau_{bms}/f_{ctm} = 7.2$)
- The modulus of elasticity of steel is taken as 200 GPa, and the modulus of concrete is that corresponding to a 30 MPa concrete, that is 33.6 GPa. Therefore, the modular ratio, α_e, is equal to 5.95.

With all these assumptions Eq. (4-32) is transformed into a direct relation between $\phi_{s,\max}$ and σ_{s2} only (see Eq. (4.2.5-4)).

$$\phi_{s,\max} = \left(\frac{1}{2} \frac{0.30 \cdot 200'000}{\sigma_{s2} - 0.4 \frac{2.9}{2.16} \sigma_{s2} \left(1 + 5.95 \frac{2.16}{\sigma_{s2}} \right)} - 25 \right) 7.2 \frac{2.16}{\sigma_{s2}} \rightarrow$$

$$\phi_{s,\max} = \frac{466'560}{\sigma_{s2}^2 \left(1 - 0.54 \left(1 + \frac{12.852}{\sigma_{s2}} \right) \right)} - \frac{388.8}{\sigma_{s2}} \qquad (4\text{-}35)$$

The values obtained from Eq. (4-35) have actually been rounded a bit on the unsafe side in Table 7.6-4 of MC 2010[4-1] as can be seen from Table 4-8 and Fig. 4-40.

Table 4-8 Comparison between table 7.6-4 of MC 2010[4-1] and Eq. (4-32)

		Formula	MC2010	
σ_{s2} [MPa]	$\rho_{ef,\min}$ valid	$\phi_{s,\max}$ [mm]	$\phi_{s,\max}$ [mm]	Ratio Form/Table
160	1.35%	40.93	40	1.023
200	1.08%	25.25	30	0.842
240	0.90%	17.01	20	0.851
280	0.77%	12.17	14	0.870
320	0.67%	9.10	10	0.910
360	0.60%	7.02	8	0.878
400	0.54%	5.56	6	0.927
450	0.48%	4.28	4	1.070

This document is the intellectual property of the fib – International Federation for Structural Concrete. All rights reserved.
This PDF of fib Bulletin 92 is intended for use and/or distribution solely within fib National Member Groups.

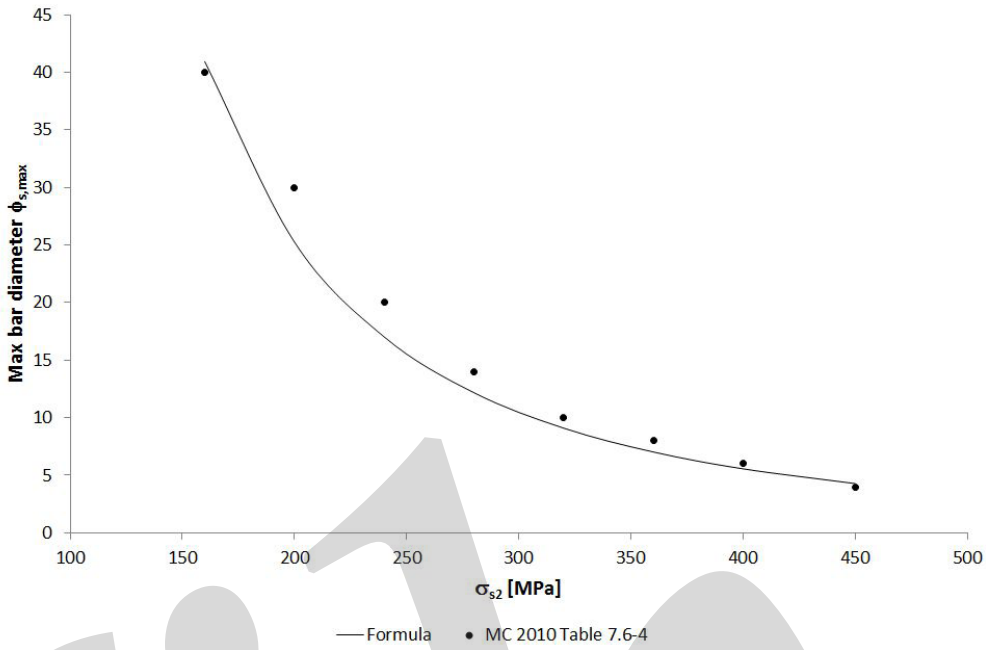


Fig. 4-40 Comparison between table 7.6-4 of MC 2010[4-1] and Eq. (4-35)

With regard to MC 2010[4-1] Table 7.6-5, it can be obtained from Table 7.6-4. Since each value of stress is related to an amount of reinforcement given by Eq. (4-34), given an assumed height of h = 400 mm, a certain spacing between bars implies a certain diameter, as shown in Eq. (4-36).

$$\rho_{ef} = \frac{\pi \frac{\phi_{s,\max}^2}{4} \frac{1}{s}}{2.5\underbrace{(h-d)}_{0.1h}} = \rho_{ef,\min} = \frac{2.16}{\sigma_s\left[\text{MPa}\right]} \rightarrow s_{\max} = \frac{\pi\phi_{s,\max}^2}{h\left[\text{mm}\right]} \frac{\sigma_s\left[\text{MPa}\right]}{2.16} \tag{4-36}$$

The values obtained from Eq. (4-36) fit very well with those of Table 7.6-5 of MC 2010[4-1], assuming the theoretical value of $\phi_{s,\max}$ (Eq.(4-35)) as can be seen from Table 4-9 and Fig. 4-41.

Table 4-9 Comparison between table 7.6-5 of MC 2010 and Eq. (4-36)

			Formula	MC2010
σ_{s2} [MPa]	$\rho_{ef,\min}$ valid	$\phi_{s,\max}$ [mm]	$\sigma_{s,\max}$ [mm]	$s_{\max}$ [mm]
160	1.35%	40.93	975	300
200	1.08%	25.25	464	300
240	0.90%	17.01	253	250
280	0.77%	12.17	151	150
320	0.67%	9.10	96	100
360	0.60%	7.02	65	60
400	0.54%	5.56	45	-
450	0.48%	4.28	30	-

This document is the intellectual property of the fib – International Federation for Structural Concrete. All rights reserved.
This PDF of fib Bulletin 92 is intended for use and/or distribution solely within fib National Member Groups.

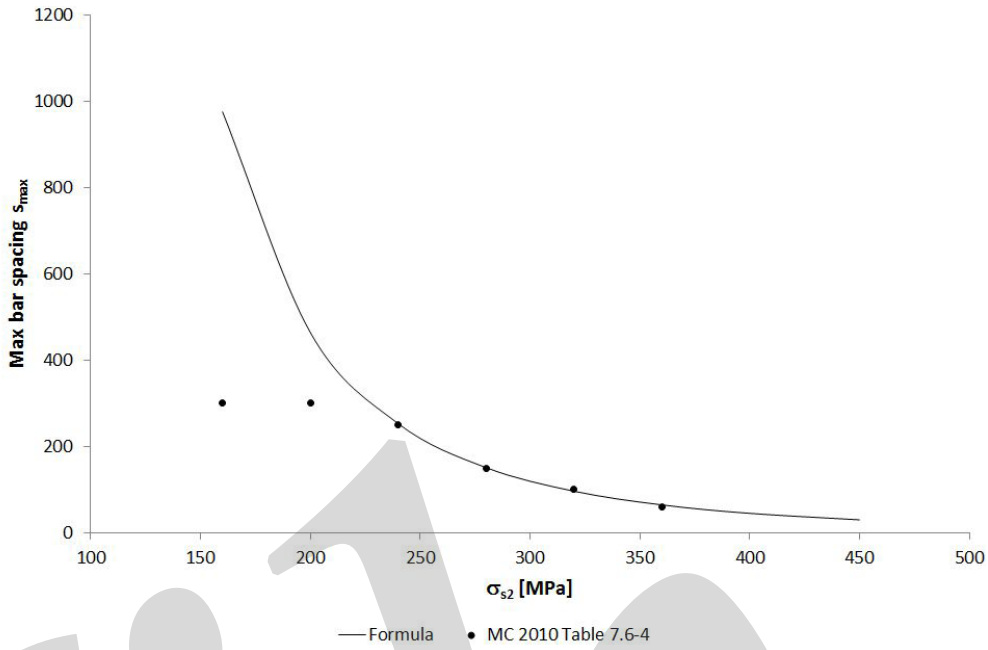


Fig. 4-41 Comparison between table 7.6-5 of MC 2010[4-1] and Eq. (4-36)

4.2.6 Cracks in orthogonally reinforced elements

This part is a contribution to the analysis of cracking (crack width, spacing and orientation) in elements reinforced in two orthogonal directions, with a crack pattern in a different direction. This particularly concerns reinforced concrete shear walls and thin webs, where only the membrane effects are considered.

4.2.6.1 Citation of the *fib* Model Code for Concrete Structures 2010

For this particular problem, the text of the *fib* Model Code 2010 is as follows:

Sect. 7.6.4.4.3 Orthogonal reinforcement directions

MAIN PROVISIONS

If the cracks in a member reinforced in two orthogonal directions are expected to form at an angle which differs substantially (> 15°) from the direction of the reinforcement, the approximation by Eq. (7.6-8) and (7.6-9) may be used to calculate $l_{s,\max}$ and w_d.

EXPLANATIONS

When a more refined model is not available, the following expression for $l_{s,\max}$ may be used: where:

$$l_{s,\max,\theta} = \left(\frac{\cos\theta}{l_{sx,k}} + \frac{\sin\theta}{l_{sy,k}} \right)^{-1} \qquad 7.6\text{-}8$$

θ denotes the angle between the reinforcement in the x-direction and the direction of the principal tensile stress.

$l_{x,k}$, $l_{y,k}$ denote the slip lengths in the two orthogonal directions, calculated according to Eq.(7.6-4)

The design crack width can then be calculated from:

$$w_d = 2 l_{s,\max,\theta} \left(\varepsilon_{\perp} - \varepsilon_{c,\perp} \right) \qquad 7.6\text{-}9$$

where:

$\varepsilon_{\perp}$ and $\varepsilon_{c,\perp}$ represent the total mean strain and the mean concrete strain, evaluated in the direction orthogonal to the crack (Figure 7.6-6).

This document is the intellectual property of the fib – International Federation for Structural Concrete. All rights reserved.
This PDF of fib Bulletin 92 is intended for use and/or distribution solely within fib National Member Groups.

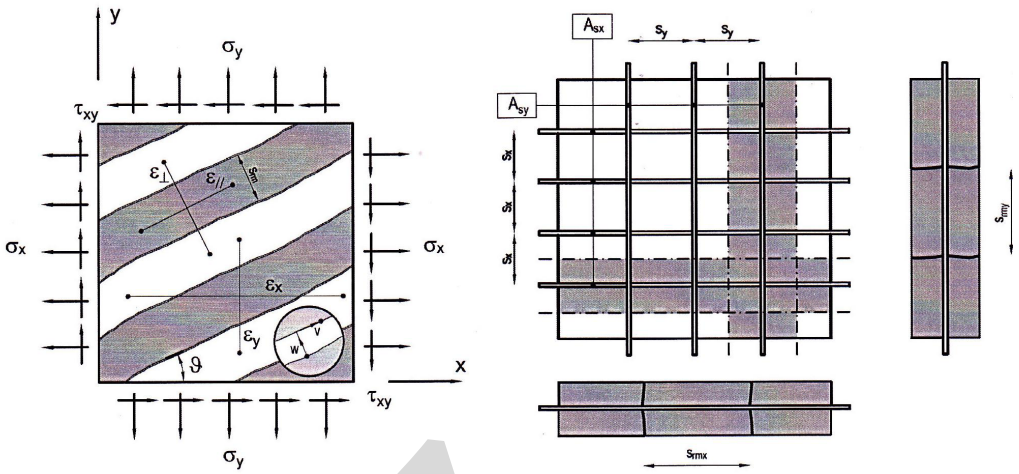


Fig. 4-42 Fig. 7.6-6 from MC2010[4-1] Basis for calculation of crack width for reinforcement deviating from the direction orthogonal to the crack

It is noted that in tie beams, the mean total deformation equals the mean deformation of the reinforcement. It will be shown below that this is not the case in the situation under consideration. It can be noted at this stage that, as there is no rebar in the orthogonal direction, $\varepsilon_{s,\perp}$ does not exist.

The situation considered in this paragraph is mainly that of a considerable influence of shear in a panel, where a "strut and ties" model is acceptable as indicated in Fig. 4-42. In this model, struts are limited by inclined cracks and tensile forces are balanced by orthogonal bars through the crack. It does not cover all the possible situations of stresses.

Alternate models have been developed in the recent years, for instance with different distributions of stresses in the struts; criticisms have also been brought to such models; some references are listed below. In spite of these reservations, for the sake of simplification, the code gives a general guidance to deduce cracks widths from this model; more detailed guidance is given below. This leads to reasonable results, comparable to experimental observation. However, as the subject is complex and not completely precise, further research is necessary for a better assessment of cracking in such situations.

4.2.6.2 Structural analysis

The first step in the assessment of cracking is to perform a structural analysis. In most cases, analytical models are not applicable and a FEM analysis should be performed.

It is necessary to have in each finite element a good evaluation of mean strains or stresses or both.

When the strain is imposed in the panel, e.g. due to shrinkage or temperature variation, or when the panel deformation is restrained by the rest of the structure, then Eq. (7.6-9) applies.

When the deformation of the panel is not restrained by the rest of the structure, then two cases may be considered:

- Where the structural analysis takes into account a realistic RC behaviour, it can be considered that the mean total deformation $\varepsilon_{\perp}$ obtained is representative of that of the reinforced concrete material; then the computed deformations can be used directly in Eq. (7.6-9) to calculate the crack width; $\varepsilon_{c,\perp}$ may be an output of the FEM analysis or can be evaluated using the method given below.

This document is the intellectual property of the fib – International Federation for Structural Concrete. All rights reserved.
This PDF of fib Bulletin 92 is intended for use and/or distribution solely within fib National Member Groups.

- Where the structural analysis is performed with a linear elastic model or more generally if the computed deformations are not realistic and if the calculated stresses may be accepted as a sufficient approximation, then 'realistic' deformations are calculated from these stresses. A simplified method is presented below.

In general, when a nonlinear behaviour is taken into account, the analysis allows proper assessment of the distribution of the stresses, as the variations of stiffness in the various structural components are included, together with the effects of the boundary conditions. But the quality of the local results for crack width is highly variable depending on the constitutive model used; this type of model is often not accurate enough locally to directly use the results in terms of local deformation, at the scale of crack spacing. This justifies using the stresses for cracking assessment.

Often, a linear elastic model gives acceptable results for the stress distribution, provided that the distribution of stiffness is properly assessed, which is sufficient for a good assessment of cracking according to the procedure below.

4.2.6.3 Validity of the strut and tie model

The condition for application of Sect. 7.6.4.4.3 of the *fib* Model Code 2010[4-1] is that the physical model shown in Fig. 7.6.6 (strut and ties) can actually develop. This supposes that cracks can actually exist and that struts can be drawn according to continuous and smooth lines, oriented to the compressive trajectories in the uncracked stage (based on the structural analysis). This also supposes that one of the principal stresses is tension and the other compression. The existence of cracks can be checked from the structural analysis either:

- locally, when the principal tensile stress is higher than f_{ct};
- globally, whenever the structural element under consideration can be assimilated to a linear element (beam or column); in that case, when the shear force applied to a section is lower than $V_{Rd,c}$ (Sect. 7.3.3 *fib* Model Code 2010[4-1]), cracking is not influenced by shear and may occur due to bending moments, generally applied to one of the main directions x or y.

It is clear that the existence of skew cracking depends mainly on the relative amplitude of shear to normal forces applied to planes perpendicular to x and y. So the application of the proposed method is limited to angles higher than 15° in the Model Code. When the model cannot apply, other models should be used (direct tension, bending…). This is particularly the case when both principal stresses are tensions, which may happen in some situations; then the strut and tie model cannot apply; these situations are not covered by the Model Code in Sect. 7.6.4.4.3.

4.2.6.4 Crack angle

According to the Model Code, the direction perpendicular to the principal direction of tensile stress gives an acceptable value for the crack angle θ. Note that it is an approximation, as the crack angle should in principle be obtained from the concrete intrinsic curve.

Generally, representative structural models provide the right order of magnitude of the angle of the cracks, compatible with the required accuracy.

Two families of models for cracked reinforced concrete exist: “fixed crack” or “rotating crack”. The method proposed below for crack width assessment is of the type “fixed

This document is the intellectual property of the fib – International Federation for Structural Concrete. All rights reserved.
This PDF of fib Bulletin 92 is intended for use and/or distribution solely within fib National Member Groups.

crack"; then, once the crack appears, its angle remains constant when the load increases. A consequence is that when the loads increase proportionally after cracking, the principal directions of stress do not change; on the contrary, principal directions of strains will change.

4.2.6.5 Slip lengths and cracks spacing

In the proposed physical model, the calculation of crack width according to formula (7.6-4), is based on a "virtual" slip length $l_{s,\max,\theta}$ in the direction perpendicular to θ, obtained from the slip lengths $l_{sx,k}$ and $l_{sy,k}$ of the bars in the x and y directions respectively, according to formula (7.6-8 of *fib* Model Code 2010) (Fig. 4-43). Cracks are randomly distributed; mean and characteristic values of crack spacing may be defined when cracking is stabilised.

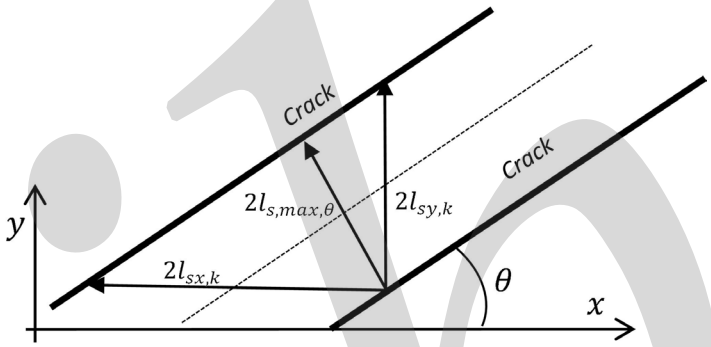


Fig. 4-43 Crack spacing

Indeed, there is a point between cracks where there is no slip between concrete and reinforcement; when the spacing between two cracks is lower than two times the slip length, then this point may be assumed to be on the centreline between the cracks, by symmetry, but this is a simplification. When cracking is stabilised and cracks regularly distributed, there is a random relationship between the mean spacing between cracks and the virtual slip length: $s_{rm} \approx 2l_{s,\max,\theta}/1.7$ (the Model Code assumes that the ratio between the maximal and the mean values of spacing is 1,7). Then the pattern of Fig. 4-43 applies, but with mean cracks spacing in lieu of slip length.

The geometrical projections $2l_{sx,k}$ and $2l_{sy,k}$ defined in Fig. 4-42 are linked to $2l_{s,\max,\theta}$ and the observed θ angle, by the equations:

$$l_{s,\max,\theta} = l_{sy,k}\cos\theta = l_{sx,k}\sin\theta \tag{4-37}$$

Formula (7.6-8) is a direct consequence of Eq. (4-37), assuming that $l_{sx,k}$ and $l_{sy,k}$ are the slip lengths along the bars in the *x* and *y* directions respectively; this is a strong physical hypothesis[4-33] which is consistent with the model when cracks are parallel and regularly distributed. However, it is clear that this relationship cannot apply when the angle is too close to 0° or 90°.

Slip lengths in the *x* and *y* directions are calculated using formula (7.6-4) for each layer of bars. In this formula, the first term is directly proportional to the cover and, in the second term, the cover may be involved in the term $\phi_s/\rho_{s,ef}$ in the case of thick elements. Taking the mean cover between each layer of rebars or the cover of each layer separately leads approximately to the same spacing $l_{s,\max,\theta'}$ so both hypotheses are acceptable.

With his Cracked Membrane Model, Kaufmann[4-34] demonstrated that formula (7.6-8) is an envelope of a more refined formula and gives a conservative value. However, formula

This document is the intellectual property of the fib – International Federation for Structural Concrete. All rights reserved.
This PDF of fib Bulletin 92 is intended for use and/or distribution solely within fib National Member Groups.

(7.6-8) is a good approximation for crack angles in the vicinity (≈ ± 20°) of the optimum angle θ_{opt} defined by $\frac{l_{sx,k}}{l_{sy,k}} = \cot g\theta_{opt}$. For angles outside this interval, Kaufmann's formula may be used for a better assessment.

From experimental results it can be deduced that $A_{c,eff}$ used to calculate $l_{sx,k}$ and $l_{sy,k}$ according to Figure 7.6-4 c may be too approximate in the case of thick elements; however, the value of $l_{s,\max,\theta}$ finally obtained by eq. 7.6-8 is an acceptable approximation, with the conditions given above.

4.2.6.6 Optimum design of reinforcement for cracking

In the frame of the model considered, it can be shown that, for the combination of actions which results in cracking in direction θ, when the two layers of bars in orthogonal directions are designed so that $\frac{l_{sx,k}}{l_{sy,k}} = \cot g\theta_{opt}$, then crack width is minimised and an error of assessment of the angle does not result in a significant error on the evaluation of crack spacing, or on crack width.

This conclusion does not necessarily apply to other combinations of actions, e.g. those which determine the sections of bars for resistance, if they are different.

4.2.6.7 Crack width

According to formula (7.6-9), the design crack width is determined as the product of two times the virtual slip length $l_{s,\max,\theta}$ with the difference between mean total strain $\varepsilon_{\perp}$ and mean concrete strain $\varepsilon_{c,\perp}$ in the direction perpendicular to the crack.

For the application of the formula, θ can be taken as the angle of the direction perpendicular to the principal direction of tension if the combination of loads considered corresponds to that which creates the crack (this situation is assumed below). For other combinations of loads, the angle and the crack pattern are already known and only the mean deformations should be calculated; in that case, the procedure given below should be adapted for considering the force tangential to the crack. In any case, it is necessary to determine first the combination of loads which defines the cracking pattern.

Once the angle of the crack is known, the mean stresses in bars and concrete may be obtained using the results of the FEM analysis. For instance, if the membrane tensor is calculated in the *x* and *y* axis, the force N_r applied on a unit length of crack is:

$$N_r = N_{xx}\sin^2\theta + N_{yy}\cos^2\theta - 2N_{xy}\sin\theta\cos\theta \qquad (4\text{-}38)$$

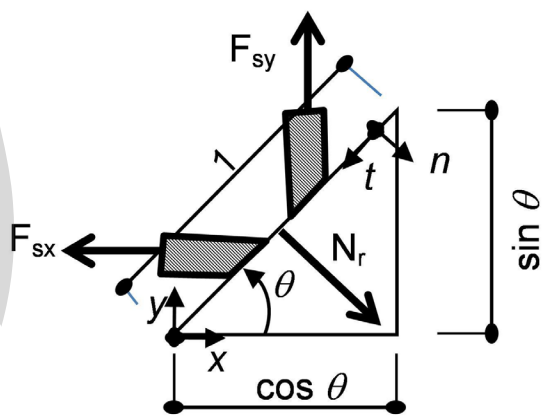


Fig. 4-44 Balance of forces in the crack

This document is the intellectual property of the fib – International Federation for Structural Concrete. All rights reserved.
This PDF of fib Bulletin 92 is intended for use and/or distribution solely within fib National Member Groups.

In the crack, this force is balanced by the tensions in the reinforcement (Fig. 4-44). In the usual hypothesis of a free crack, the total tangent force is 0 (principal direction). This allows the calculation of the forces in the reinforcement by unit length of crack:

$$\begin{cases} F_{sx} = N_r \sin\theta \\ F_{sy} = N_r \cos\theta \end{cases} \tag{4-39}$$

It is noted that if a tangent force exists (other combinations of loads), it can be easily added to these expressions. Also, aggregate interlock and dowel effect can be taken into account at this stage, but it leads to non-linear expressions.

The mean deformations $\varepsilon_{s,x}$ and $\varepsilon_{s,y}$ of the rebars are then obtained, taking into account the area of reinforcement crossing the unit length of crack and the force transferred to concrete by tension stiffening:

$$\varepsilon_{s,x} = \frac{N_r - 2\beta \cdot f_{ct} \cdot h_{eff}}{2h_{eff} \cdot \rho_{sx,eff}}; \varepsilon_{s,y} = \frac{N_r - 2\beta \cdot f_{ct} \cdot h_{eff}}{2h_{eff} \cdot \rho_{sy,eff}} \tag{4-40}$$

where h_{eff} is the effective thickness around each layer of bars, as defined in Fig. 7.6-4 c of the Model Code. Eq. (4.2.6-4) supposes that there are layers of bars on both surfaces of the wall; in that case $2h_{eff}$ cannot be higher than the total thickness of the wall t_c. The compression $N_{//}$ in the strut parallel to the crack is deducted from the FEM analysis:

$$N_{//} = N_{xx} \cos^2\theta + N_{yy} \sin^2\theta + 2N_{xy} \sin\theta \cos\theta \tag{4-41}$$

$N_{//}$ is negative in this model. The total mean deformation of concrete $\varepsilon_{c,\perp}$ in the direction perpendicular to the crack is due to the tension stiffening between cracks and to the Poisson effect due to the compression $N_{//}$ in the strut, but the latter may often be neglected:

$$\varepsilon_{c,\perp} = \frac{1}{t_c \cdot E_c}\left[2\beta \cdot f_{ct} \cdot h_{eff} - \nu \cdot N_{//}\right]; \varepsilon_{c,//} = \frac{1}{t_c \cdot E_c}\left[-2\nu \cdot \beta \cdot f_{ct} \cdot h_{eff} + N_{//}\right] \tag{4-42}$$

The distortion $\varepsilon_{c,nt}$ of concrete can be neglected, although it is not strictly zero.

However, a distortion exists through the crack as part of the total strain tensor. $\varepsilon_{\perp}$ should be evaluated taking into account this distortion. In fact the deformation of the bars is not linear, because of the distortion through the crack (Fig. 4-46).

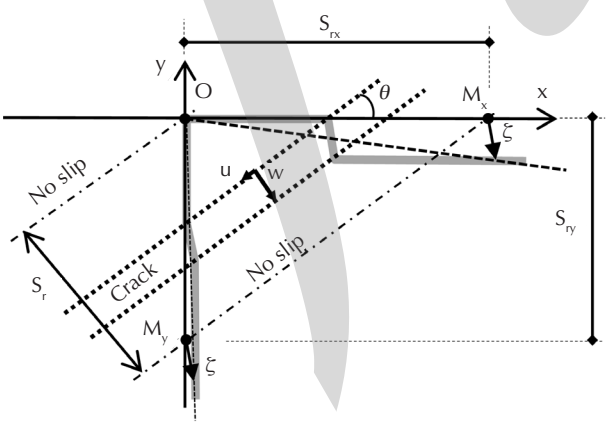


Fig. 4-45 Compatibility of deformations

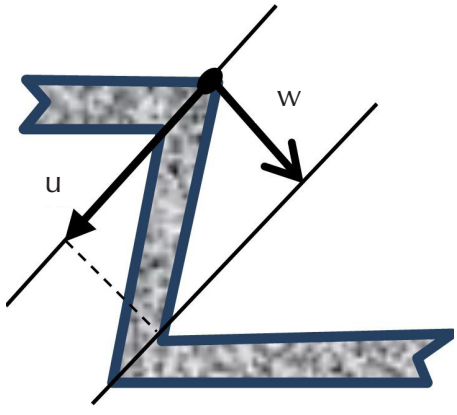


Fig. 4-46 Simplified (and exaggerated) distortion of the bar in the vicinity of the crack due to compatibility of deformation when the crack opens

This document is the intellectual property of the fib – International Federation for Structural Concrete. All rights reserved.
This PDF of fib Bulletin 92 is intended for use and/or distribution solely within fib National Member Groups.

In the physical model proposed by the *fib* Model Code 2010[4-1], when the crack pattern is stabilised, there is no slip between the bars and the concrete in points *O, M*$_x$ and *M*$_y$ (Fig. 4-45). Then, s_r is either the distance between cracks or 2 $l_{s,\max,\theta'}$ whichever is the lower.

The mean strain tensor ε_r due the opening of the crack (without consideration of the concrete deformation) may be calculated, considering a displacement at crack with a tangential component *u* and a normal component (the crack width) *w*:

$$\varepsilon_{r,xx} = -\frac{u}{s_{rx}}\cos\theta + \frac{w}{s_{rx}}\sin\theta = \left(-\frac{u}{s_r}\cos\theta + \frac{w}{s_r}\sin\theta\right)\sin\theta$$
$$\varepsilon_{r,yy} = \frac{u}{s_{ry}}\sin\theta + \frac{w}{s_{ry}}\cos\theta = \left(\frac{u}{s_r}\sin\theta + \frac{w}{s_r}\cos\theta\right)\cos\theta \qquad (4\text{-}43)$$
$$\varepsilon_{r,xy} = \frac{1}{2}\left(\frac{\varsigma_y}{s_{rx}} + \frac{\varsigma_x}{s_{ry}}\right) = \frac{u}{2s_r}\left(\cos^2\theta - \sin^2\theta\right) - \frac{w}{s_r}\sin\theta\cos\theta$$

where s_{rx} and s_{ry} are defined on the figure. $\varepsilon_{r,xx}$ is the elongation in straight line of the segment OM_x and is different from the elongation of the rebar $\varepsilon_{s,x}$ which includes a distortion (Fig. 4-46).

The deformation $\varepsilon_{r\perp}$ perpendicular to the crack is then obtained by the usual tensorial relationships:

$$\varepsilon_{r,\perp} = \varepsilon_{r,xx}\sin^2\theta + \varepsilon_{r,yy}\cos^2\theta - 2\varepsilon_{r,xy}\sin\theta\cos\theta = \frac{w}{s_r} \qquad (4\text{-}44)$$

The total mean deformation is obtained in adding the mean deformation of concrete, yielding formula (7.6-9) of the *fib* Model Code 2010[4-1].

But there is still no direct link with the deformations of the bars given by Eq. (4-40). When there is no tangential displacement u at the crack, the elongation of each bar is the crack width *w*. When there is a tangential displacement (Fig. 4-46), the elongation is $\sqrt{u^2 + w^2}$, which can be assimilated to *w* only when *u* is smaller. In that case, two conditions of kinematic compatibility are derived:

$$\left(\varepsilon_{c,//}\cos^2\theta + \varepsilon_{c,\perp}\sin^2\theta\right)s_{rx} + w = \varepsilon_{s,x}\cdot s_{rx}$$
$$\left(\varepsilon_{c,//}\sin^2\theta + \varepsilon_{c,\perp}\cos^2\theta\right)s_{ry} + w = \varepsilon_{s,y}\cdot s_{ry} \qquad (4\text{-}45)$$

These relations are compatible when the arrangement of bars is optimised as given above. Otherwise, *u* cannot be neglected and the complete nonlinear equations should be used. Assuming a linear approximation, this leads to an alternative – approximate – expression for the crack width:

$$w = s_r\left[\varepsilon_{s,x}\sin\theta + \varepsilon_{s,y}\cos\theta - \varepsilon_{c,//}\left(\cos\theta + \sin\theta\right)\sin\theta\cos\theta - \varepsilon_{c,\perp}\left(\sin^3\theta + \cos^3\theta\right)\right] \qquad (4\text{-}46)$$

where the mean strains in bars and concrete are given by Eq.(4-40) and Eq. (4-42). In this expression, the influence of the concrete deformation is small and can be neglected. It can be considered as a conservative evaluation (at least for low values of crack width), as aggregate interlock and dowel effects are not considered. Finally:

$$w \approx s_r\left(\varepsilon_{s,x}\sin\theta + \varepsilon_{s,y}\cos\theta\right) \qquad (4\text{-}47)$$

This document is the intellectual property of the fib – International Federation for Structural Concrete. All rights reserved.
This PDF of fib Bulletin 92 is intended for use and/or distribution solely within fib National Member Groups.

In addition, it is observed that the strain compatibility also imposes a variation of distortion along the crack: referring to Fig. 4-45, it is noted that the distance between M_x and M_y should remain constant when the concrete deformation is neglected. Adding the mean concrete deformation to $\varepsilon_{r,xy}$, this leads to the following relationship between the distortion and the crack width:

$$\alpha = 2\varepsilon_{xy} = \frac{u}{s_r}\left(\cos^2\theta - \sin^2\theta\right) - 2\left[\frac{w}{s_r} - \left(\varepsilon_{c,//} - \varepsilon_{c,\perp}\right)\right]\sin\theta\cos\theta \qquad (4\text{-}48)$$

that characterises the deformation of the wall. The compression in the strut (negative) increases the distortion.

4.3 Deflections of concrete structures

The importance of deflection control has progressively increased in the last decades due to changes introduced in the design methodology of flexural members, becoming in most cases a critical factor. Progressive refinement in the ultimate limit design of flexural members, reduction in overall safety factors, increase in strength of materials without significant increment of the stiffness, and generalization of the use of members working in flexure (in substitution of other structural configurations) have allowed a reduction in the stiffness that is often the cause of problems associated with deflections. Furthermore, design requirements related to architectural, aesthetics or functionality of buildings and infrastructure usually tend to increments of the span lengths and reduction of depths, leading to higher span-to-depth ratios, a factor directly related to deflection control. Also, increases in the construction speed may cause premature cracking as well as higher time-dependent deformations due to early permanent loading.

Deflections must be limited mainly to avoid detrimental effects on the following aspects:

- Appearance of the structure (aesthetics, confidence of users)
- Integrity of non-structural parts (brittle partitions or finishes)
- Proper functioning of the structure or equipment (machinery, doors, windows)
- Excessive vibrations (comfort, functionality of devices)

Several types of deflection can be considered for calculation purposes:

- Instantaneous (or immediate) deflections: Cracking of concrete as well as dead and live load are considered. Time-dependent effects such as creep and shrinkage of concrete and relaxation of prestressing steel are not taken into account.
- Long-term deflections: Time-dependent effects are considered. Only permanent (or quasi-permanent) affect this type of deflections. Cracking due to short-term load should be taken into account.
- Total deflections: Instantaneous plus long-term deflections.
- Deflection occurring after attachment of non-structural elements: Part of the total deflection that takes place after construction of elements that may be damaged by excessive deflections.

To avoid excessive deflections design codes and regulations limit their allowable design values as a fraction of the span of the element. For instance, a limit of span/250

This document is the intellectual property of the fib – International Federation for Structural Concrete. All rights reserved.
This PDF of fib Bulletin 92 is intended for use and/or distribution solely within fib National Member Groups.

is indicated in the *fib* Model Code 2010[4-1] for the deflection due to quasi-permanent loads to avoid impairing of appearance and general utility of the structure. Likewise a limit of span/500 for quasi-permanent loads is said to be appropriate for the deflection increment after the installation of parts susceptible to being damaged. Other limits may be considered, depending on the sensitivity of the adjacent parts.

It must be taken into account that actual deformations may differ considerably from calculated values. Some of the parameters involved in deflection calculation present high scatter, such as the tensile concrete strength, and this is especially important for loads close to the cracking moment. Other parameters may be difficult to assess due to the number of influencing factors, as is the case for creep and shrinkage of concrete.

Long-term deflections of reinforced concrete beams due to creep and shrinkage of concrete may be significant, especially for cracked beams, and can cause damage in structural and non-structural elements. Creep and shrinkage of concrete are influenced by the environmental conditions, the size of the element, the water/cement ratio, the type of cement, and on the curing conditions. Creep also depends on the level of applied stress, on the duration of the sustained load and on the age of concrete at the time of loading. In addition, deflections due to creep and shrinkage depend on the cracking level, on the amount of tensile and compressive steel, on the geometry and support conditions of the structure and on the construction sequence, among other factors. If deflection of a composite structure is computed, account shall be taken of curvatures resulting from differential shrinkage of precast and cast-in-situ components.

One of the most effective ways to limit excessive deflections is to provide sufficient stiffness of the beam. Such a minimum stiffness is related to the span/effective depth ratio, *l*/*d*, to the reinforcement ratio and to the support conditions, as will be shown later in this document.

For deflection calculations the CEB-FIP Model Code 1990[4-8] included a simplified method that corresponded to the formulation of the so-called "Method of global coefficients", proposed in the CEB Design Manual Cracking and Deformations[4-5] that was derived from the CEB bilinear method, after several simplifications and parametric studies. The method provided the following expressions to estimate the long-term deflections in RC flexural members:

$$a = a_c\left(1+\varphi\right) \text{ for } M < M_{cr} \tag{4-49}$$

$$a = a_c\left(\frac{h}{d}\right)^3 \eta\left(1-20\rho'_m\right) \text{ for } M \geq M_{cr} \tag{4-50}$$

where M is the bending moment at mid span of a beam or slab and at the fixed end of a cantilever, under the frequent combination of actions; a is the long-term deflection; a_c is the instantaneous elastic deflection, calculated with the rigidity $E_c \cdot I_c$ of the gross section, neglecting the reinforcement; φ is the creep coefficient; h is the total depth of the beam; d is the effective depth of the beam; ρ'_m is the geometrical mean percentage of compressive reinforcement, along the beam length; h is a factor taking into account the effects of cracking and creep that depend on the geometrical mean percentage of tensile reinforcement along the beam length ρ_m.

This method sacrificed accuracy in favour of simplicity, since it did not explicitly include the creep coefficient and shrinkage strain and, therefore, the effects of concrete strength (high strength concrete has usually less creep and shrinkage than conventional

This document is the intellectual property of the fib – International Federation for Structural Concrete. All rights reserved.
This PDF of fib Bulletin 92 is intended for use and/or distribution solely within fib National Member Groups.

concrete), the environmental conditions or the age at loading. In addition, it cannot be used to evaluate deflections at any instant of the service life of the structure, but only at long-term, nor to evaluate deflections under the effect of loads applied at different times. These considerations are important, for example, when evaluating deflections in high-strength concrete elements, or when estimating the deflections after installation of the non-structural elements susceptible to being damaged.

The formulation introduced in the *fib* Model Code 2010[4-1] is based on that of Eurocode 2[4-9]. It derives from the interpolation procedure in the CEB Manual on Cracking and Deformation[4-5] for calculation of mean curvatures also included in the MC90[4-8], taking into account tension-stiffening. Long-term effects due to creep can be calculated using the Age-Adjusted Modulus Method[4-4, 4-35], although for deflections an effective modulus is used, while effects of shrinkage are estimated at the section level.

Although also a simplification, this methodology allows taking into account main material properties and also considering the effects of environmental and loading conditions.

4.3.1 Calculation of deflections due to bending

4.3.1.1 General Method

Deflections due to bending can be estimated by double integration of flexural curvatures along the member axis, taking into account the support conditions and the stiffness at each section, which depends on the internal forces (N,M), the amount of longitudinal reinforcement and the state of cracking at each section. For statically determinate structures, the internal forces at each section are known, since reactions are obtained directly from equilibrium with external loads. However, for statically indeterminate structures, the distributions of internal forces are not known a priori, since reactions depend on the deformation of the structure and consequently on the distribution of stiffness along the members, which is a function of the force's distribution. Therefore, an iterative procedure is necessary in order to correctly obtain a distribution of forces along the element which fulfil equilibrium, compatibility and materials constitutive equations and to accurately calculate the deflections. Thus, non-linear analysis methods, taking into account the effects of cracking, non-linear stress-strain relationships, second order effects in axially loaded slender members and other non-linear effects must be performed. In order to trace the complete load-displacement curve through the elastic, cracked and ultimate load ranges, incremental procedures are necessary together with iterative methods

In addition, the time-dependent effects of creep, shrinkage and relaxation, must be considered in order to estimate the delayed deflections, either by a time step analysis or by using the ageing coefficient concept. In structures where the construction process requires an accurate estimation of deflections, a step by step analysis should be performed including the sequence of loading and possible changes in geometry, structural scheme, support conditions and the evolution of material properties with time.

In statically indeterminate structures, for usual reinforcement ratios and distributions, the cracked stiffness of the hogging and sagging zones, which depend on the amount of longitudinal reinforcement, are not very different. Therefore, the distribution of bending moments obtained elastically is similar to the actual one, and can be used in a nonlinear sectional analysis to obtain the curvature and, by double integration, the deflections.

This document is the intellectual property of the fib – International Federation for Structural Concrete. All rights reserved.
This PDF of fib Bulletin 92 is intended for use and/or distribution solely within fib National Member Groups.

4.3.1.2 Structural analysis

In general, the Finite Element Method (FEM) is the more versatile method to analyse any kind of structure, by adopting the most suitable type of element for the problem studied. Beam-columns, straight or curved, with constant or variable cross section dimensions, can be used for analysing planar or spatial beams, columns, arches, frames or structures similar to them; planar 2D elements can be used for analysing plane stress or plane strain problems, either walls, beams, joints or other D regions; plate and shell elements can be used for analysing slabs and shells subjected to membrane and out-of-plane forces, and solid elements can be used for massive structures or regions such as slab-column connections where stresses in the three dimensions are comparable.

The displacement formulation is the most common because its suitability for numerical analyses. In such formulation, the displacement field inside the element is obtained by interpolating the nodal displacements using shape functions. The accuracy of the solution will strongly depend on the accuracy of the shape functions to reproduce the actual displacement field inside the element. This aspect is not obvious, since cracking, yielding or other non-linear effects can take place only in some parts of the element. In such cases, a refinement of the finite element mesh is necessary in certain parts (for example near the cracking points or near the plastic hinge zones). However, in the case of frame structures, since once the element end forces are known, the distribution of internal forces can be accurately known, since it depends only on equilibrium and geometrical aspects. Therefore the use of flexibility-based beam-columns finite elements[4-36], in which forces are interpolated "exactly" from the end forces, are specially suitable for analysing such types of structures. In such cases a small number of larger elements can be used, although more time is required for integration along the element length.

Since most typical structures can be assimilated to frames, either planar or spatial, in the following a description of the most important aspects of a general model for the analysis of 2D and 3D concrete frames is provided. The general methodology is illustrated following the framework of a numerical model that takes into account the material and geometric non-linearity's, the time-dependent effects, the phased construction and their interaction[4-37, 4-38, 4-39]. Such a model, which has been experimentally verified with tests results[4-40], will be used in the examples of the next sections to compare the results of simplified models with those of the general model.

The model is applicable to three-dimensional reinforced and prestressed concrete frames subjected to any load, imposed movements and temperature histories under dominant flexure. Each member can be subjected to biaxial bending, axial load, torsion and skew shear forces. For this purpose, one-dimensional beam-column finite elements with a constant cross section of arbitrary shape are used. In order to properly evaluate the section mechanical properties at any instant and at any load level, the cross section is divided into a discrete number of concrete, steel or FRP filaments[4-41] made of their respective materials (see Fig. 4-47a). It is assumed that perfect bond exists between all the materials in a section. The filaments are considered to be subjected to a uniaxial state of normal stresses and the deformations due to shearing strains are neglected.

This document is the intellectual property of the fib – International Federation for Structural Concrete. All rights reserved.
This PDF of fib Bulletin 92 is intended for use and/or distribution solely within fib National Member Groups.

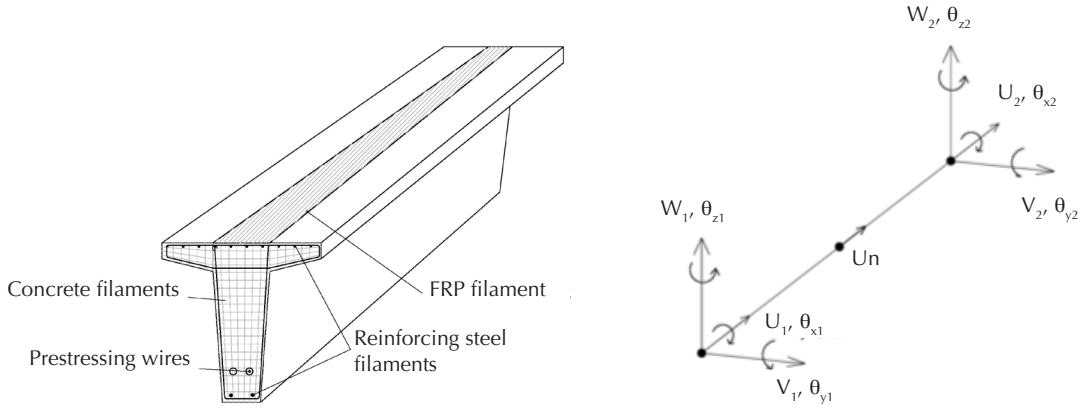


Fig. 4-47 a) Filament beam element b) External and internal degrees of freedom

Uniaxial constitutive equations are used for concrete and steel and FRP laminates. A parabolic stress-strain relationship with a descending post-peak linear branch, unloading parallel to the initial modulus of deformation and crushing is considered for concrete in compression Fig. 4-48a. Cracking and tension stiffening with a hyperbolic descending branch after cracking are considered in tension. Unloading in tension occurs with a degraded stiffness back to the residual strain. An elastic-plastic model with strain hardening is assumed for reinforcing steel. Unloading and reloading take place parallel to the initial branch and following a kinematic hardening rule as shown in Fig. 4-48b. The FRP laminate is considered elastic up to its rupture (see Fig.4-48c).

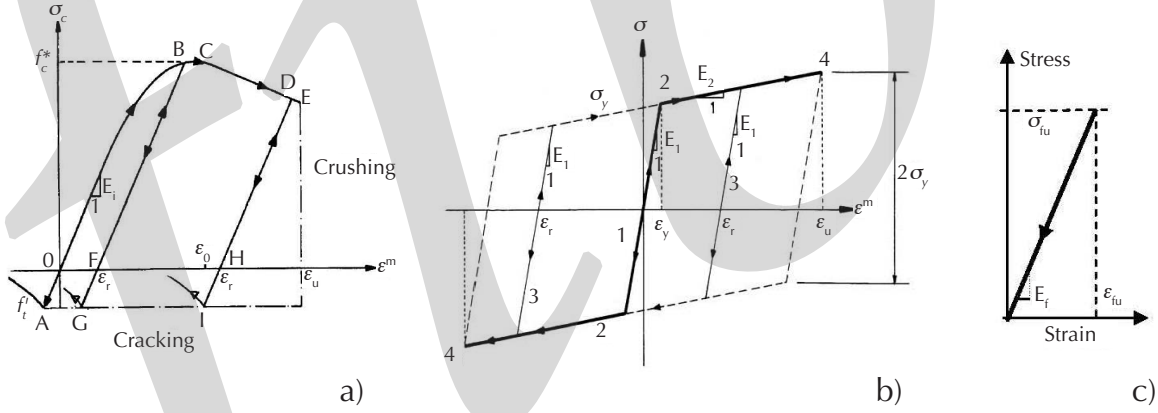


Fig. 4-48 Constitutive models for the structural materials: a) Concrete b) Steel c) FRP laminate

The total strain at a given time and point in the structure $\varepsilon(t)$, is taken as the direct sum of mechanical strain $\varepsilon_m(t)$, and non-mechanical strain $\varepsilon_{nm}(t)$, consisting of creep strain $\varepsilon^c(t)$, shrinkage strain $\varepsilon^s(t)$, ageing strain $\varepsilon^a(t)$, and thermal strain $\varepsilon^T(t)$.

$$\varepsilon(t) = \varepsilon^m(t) + \varepsilon^{nm}(t) \tag{4-51}$$

$$\varepsilon^{nm}(t) = \varepsilon^c(t) + \varepsilon^s(t) + \varepsilon^a(t) + \varepsilon^T(t) \tag{4-52}$$

Creep strain of concrete, $\varepsilon^c(t)$, is evaluated by an age-dependent integral formulation based on the principle of superposition.

$$\varepsilon^c(t) = \int_o^t C\left(\tau, t-\tau\right)\frac{\partial\sigma\left(\tau\right)}{\partial\tau}d\tau \tag{4-53}$$

This document is the intellectual property of the fib – International Federation for Structural Concrete. All rights reserved.
This PDF of fib Bulletin 92 is intended for use and/or distribution solely within fib National Member Groups.

where $c(\tau,t\text{-}\tau)$ is the specific creep function, dependent on the age at loading τ, and $\sigma(t)$ is the stress applied at instant τ. The integral in Eq. (4-53) can then be approximated by a finite sum involving incremental stress changes over the time steps. The adopted form for the specific creep function $c(\tau,t\text{-}\tau)$ is a Dirichlet series[4-42].

$$c\left(\tau,t-\tau\right)=\sum_{i=1}^{m}a_i\left(\tau\right)\left[1-e^{-\lambda_i\left(t-\tau\right)}\right] \tag{4-54}$$

in which the values of m, λ_i and $a_i(t)$ are coefficients to be determined through adjustment of experimental or empirical creep formulae. It is considered that sufficient accuracy is obtained using three terms of the series (m = 3), and adopting $\lambda_i = 10^{-i}$. The creep and shrinkage models used are those provided by the CEB-FIP Model Code 1990[4-8]. The use of a Dirichlet series enables obtaining the creep strain increment at a given instant by a recurrent expression that only requires to store the stress and an internal variable of the last time step, thus avoiding the need to store the entire stress history.

The Hermitian 13 degrees of freedom finite (DOF) element beam is used, having three displacements and three rotations at each end and an axial displacement associated to an internal node placed at the element mid length (see Fig. 4-47b) This incompatible axial displacement degree of freedom u_n, that is eliminated by static condensation, is necessary for the correct modelling of the bending stiffness and to take into account the shifting of the neutral axis due to cracking and other material non-linearity in a reinforced concrete beam. The displacement fields of the beam element on its local x-axis are cubic polynomials for the end transverse displacements and rotations, linear functions for the end axial displacements and rotations, and quadratic for the intermediate axial DOF.

There is a discrete number of pre-stressing steel tendons in the frame, each of which has a given profile and constant sectional area along its length. A pre-stressing tendon is modelled by a discrete number of pre-stressing segments, each of which is straight and spans a frame element. The location of the two end points of a pre-stressing steel segment in a frame element is defined by the local eccentricities e_y and e_z at each end, as shown in Fig. 4-49.

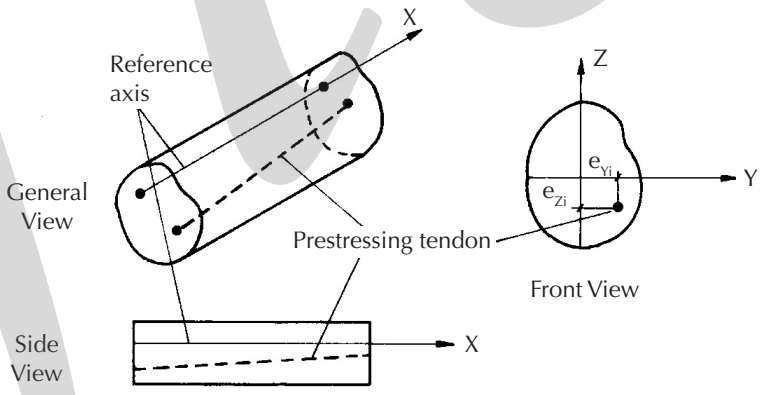


Fig. 4-49 Prestressed beam element

The axial strain ε_x at any point within the beam element can be obtained by assuming the Navier's plain section hypothesis. The elastic stiffness of a beam element is then obtained by the following known expression:

$$K_e=\int\int\int_V B^T\cdot E\cdot B\cdot dV \tag{4-55}$$

This document is the intellectual property of the fib – International Federation for Structural Concrete. All rights reserved.
This PDF of fib Bulletin 92 is intended for use and/or distribution solely within fib National Member Groups.

where E represents the material tangent modulus associated with either flexural or torsional degrees of freedom, and B is the matrix relating nodal displacements and strains at the Gauss points. The beam geometric stiffness obtained by considering the second order terms in the strain-displacement relationship is added to the elastic one, to get a better approach of the element stiffness in those cases where second order effects may be relevant.

The element internal resisting load vector due to stress in the concrete and steel filaments, can be evaluated by:

$$R^i = \int\int\int_V B^T \cdot \sigma \cdot d \cdot V + \int_L B_\vartheta \cdot T_x \cdot dx \tag{4-56}$$

in which T_x is the torque in the beam and B_θ is the component of the B matrix associated with the torsional degree of freedom. The equivalent load vector due to non-mechanical strain ε^{nm}, is calculated by the equation:

$$R^{nm} = \int\int\int_V B^T \cdot E \cdot \varepsilon^{nm} d \cdot V \tag{4-57}$$

The material properties of the concrete and the reinforcement at any time and load level depend on the non-linear stress-strain relationship, cracking, yielding and crushing of the concrete and yielding of the steel. The element stiffness matrix and the internal forces at any time are evaluated by integrating, over the volume of the element, the contribution of each concrete and reinforcement filaments over the sectional area and of each pre-stressing steel segment within the element. Numerical integration is performed by Gaussian quadrature using two Gauss points.

In order to incorporate the non-linear and time-dependent behaviour of a concrete structure, the time domain is divided in time intervals and a step forward integration is performed in which increments of displacements and strains are successively added to the previous total as time progresses.

A number of construction steps are defined along the time domain. A construction step is a situation of the structure in which any change to its geometry, loading or boundary conditions takes place. For each construction step, the pre-stressing, external joint loads, temperature distributions, short time stress-strain curves, time-dependent materials properties and structure scheme are given.

The time elapsed from one construction step to the next is subdivided into time intervals, separated by time steps. At each time step the material properties, the stiffness matrix and the load vector are updated. Increments of non-mechanical strains $\Delta\varepsilon^{nm}$ are evaluated, due to creep and shrinkage of the concrete, relaxation in the prestressing steel and temperature changes which occurred during the time interval from t_{n-1} to t_n. The equivalent joint load increments ΔR^{nm} at time t_n, summed for the concrete, reinforcing steel, prestressing steel and FRP reinforcement, are then calculated from their respective non-mechanical strain increments $\Delta\varepsilon^{nm}$. Thus, at a time t_n , the load increment ΔR_n to be applied to the structure is obtained by adding the external joint load increment ΔR_n^i and the unbalanced load R_{n-1}^u left over from time t_{n-1} to the equivalent joint load increments ΔR^{nm} due to non-mechanical strains:

$$\Delta R_n = \Delta R_n^i + \Delta R_n^{nm} + R_{n-i}^u \tag{4-58}$$

The total load obtained at each time step is divided into load increments, so that the load-displacement curve can be traced along the elastic, cracking, inelastic and ultimate

This document is the intellectual property of the fib – International Federation for Structural Concrete. All rights reserved.
This PDF of fib Bulletin 92 is intended for use and/or distribution solely within fib National Member Groups.

ranges. At each load step, the load vector is updated and a direct stiffness finite element method based on the displacement formulation is used, in which the resulting equilibrium equations will be non-linear for the current state of material properties and geometry. An iterative procedure is used in which tangential equilibrium equations are solved for global displacement increments at each iteration. At the beginning of any iteration, all the joint displacements, total strains, total non-mechanical strains and stresses at every point in the structure are known.

The increments of strain at any concrete, steel or FRP filament are obtained by first transforming the increment of global displacements to element local coordinates and, then, by means of the incremental form of the strain-displacements equations. Total strains are obtained by adding the increment of strain to the previous total. Mechanical strain is calculated by subtracting non-mechanical strain from total strain, and stress is calculated by the stress-strain curve. The internal resisting load vector is obtained from Eq. (4-56), and the unbalanced load vector is obtained by subtracting it from the current total external load vector.

A tri-linear model is used to represent the torsional response of a reinforced or pre-stressed concrete beam in terms of torque-twist relationship, as suggested by one study[4-43]. Torsion and bending are considered uncoupled.

To account for geometric nonlinearity, an updated Lagrangian formulation is used, in which the direction of the local reference system is continuously updated as the structure deforms. The continuously changing displacement transformation matrix for each element takes into account the effect of geometric nonlinearity along with the nonlinear form of the strain displacement relationship.

The effect of pre-stressing is introduced in the structure as an equivalent load vector obtained by equilibrating the forces of the pre-stressing tendons. The pre-stressing forces at each point along the tendon have taken into account the pre-stressing losses due to friction and anchorage slip. The increment of strain $\Delta\varepsilon_p$ at any segment, which varies as the structure deforms, is obtained from compatibility considerations. Then the corresponding stress σ_p is obtained by the stress-strain relationship of pre-stressing steel and the stress relaxation is subtracted. Relaxation under variable stress is taken into account by the fictitious stress method, proposed by one study[4-44]. Once the pre-stressing segment force P is known, consistent loads and moments at the two end nodes are evaluated. Pre-tensioned and post-tensioned structures can be analysed by adequately considering the instants of stressing, transfer and bond to account for the stresses in the steel and in the concrete and to add the stiffness of the tendons to the member stiffness after bond exists.

The present model has been designed to simulate most of the structural changes that take place during the construction process and along the entire service life of structures. At each construction step, changes in the longitudinal or transverse geometry of the structure can be accounted for by adding or removing elements or filaments of the cross section. Prestressing tendons and stays can be stressed, unstressed or removed at any time. External supports and connections between elements can be modified at any time.

The model has been implemented into a computer program called CONS, written in FORTRAN language, which can be run on personal computers. The general scheme of the program is schematically presented in Fig. 4-50, in which the general input data (1) includes geometry of the structure, finite element mesh, support conditions, materials properties, reinforcement, pre-stressing layout, construction steps, environmental conditions,

This document is the intellectual property of the fib – International Federation for Structural Concrete. All rights reserved.
This PDF of fib Bulletin 92 is intended for use and/or distribution solely within fib National Member Groups.

convergence criteria and output control information. At each construction step input data (2) includes variations on the geometry, boundary conditions, loading, and pre-stressing, as well as the number of time intervals between construction steps and load factors for load steps.

Many other models have been developed for the non-linear, time-dependent and segmental analysis, including or not their interaction effects. Among them, several are worth mentioning[4-45, 4-46, 4-47, 4-48]. General methods are also described in other studies[4-5, 4-49].

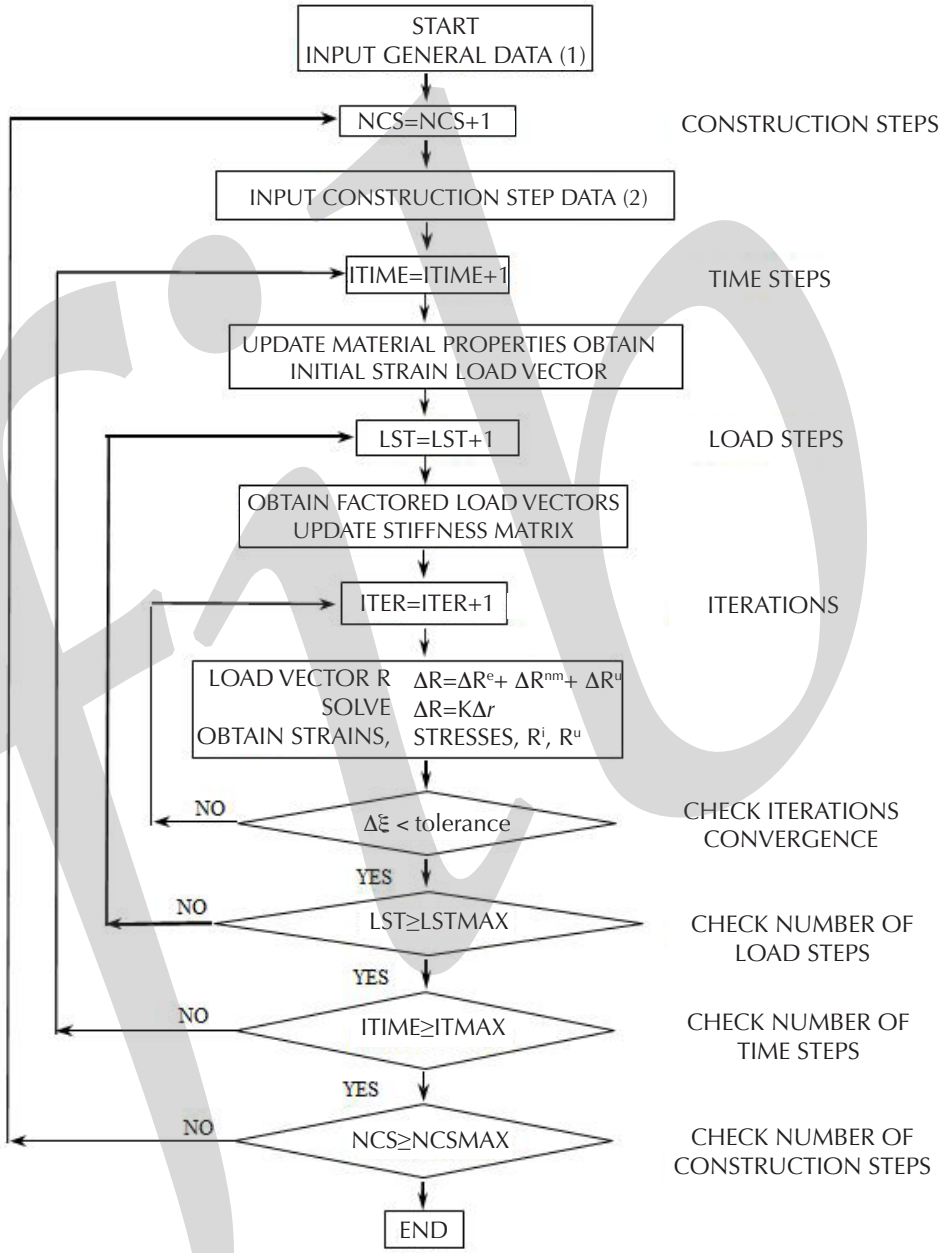


Fig. 4-50 Flow chart of the nonlinear structural analysis model CONS

This document is the intellectual property of the fib – International Federation for Structural Concrete. All rights reserved.
This PDF of fib Bulletin 92 is intended for use and/or distribution solely within fib National Member Groups.

4.3.1.3 Deformations at sectional level

4.3.1.3.1 Assumptions and equations

Given the sectional forces (axial forces and bending moments) referred to a reference system, the sectional deformations (axial strain and curvature) with respect to the same system of reference are to be obtained. The problem can be solved using the most general numerical procedures developed in the previous section. Nevertheless analytical methods have been proved to be a suitable and powerful methodology for the serviceability analysis of concrete structures with the assumption of some generally accepted simplifications[4-50, 4-51]. Once the sectional deformations are obtained, appropriate integration along the member allows obtaining member displacements.

Applying principles of structural analysis of equilibrium and compatibility at a member level, these methodologies can be implemented for the analysis of concrete frames using matrix stiffness of finite element methods[4-47, 4-52].

The assumption of plane sections hypothesis is accepted, the effects of cracking of concrete are taken into account, and the principles of linearity between instantaneous and creep strains and superposition of strains at any instant produced by stresses applied at different ages are accepted to evaluate the long-term sectional deformations. For cracked sections non-linear behaviour must be taken into account and equations must be solved using a proper procedure, usually based on non-linear iterative and/or incremental sectional analysis.

Although the procedure can be implemented for the more general case of sections of any shape with forces acting at any point[4-53], for the sake of simplicity the particular case of a section subjected to a normal force and a moment acting at an axis of symmetry, caused by applied loads, prestressing, creep, shrinkage and relaxation is described.

The method can apply to cracked or uncracked reinforced or prestressed concrete elements with steel or FRP reinforcement. The strain distribution $\varepsilon(y)$ over the cross section, having a vertical principal axis, under axial load N applied at the reference axis O and bending moment M, is defined by the axial strain, ε_o, at O and the curvature, ψ (Fig. 4-51, Eq. 4-59).

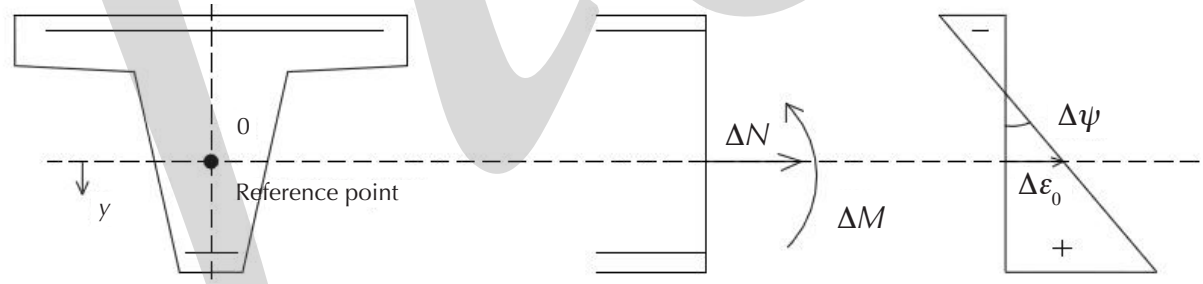


Fig. 4-51 Sectional forces and deformations

Materials (concrete and reinforcement) are assumed to behave linearly in compression and tension, although concrete in tension is ignored in the fully cracked state (Eq. 4-60). The increments of deformations and stresses are given by:

$$\Delta\varepsilon(y) = \Delta\varepsilon_0 + y\Delta\psi \tag{4-59}$$

$$\Delta\sigma(y) = E \cdot \Delta\varepsilon(y) \tag{4-60}$$

This document is the intellectual property of the fib – International Federation for Structural Concrete. All rights reserved.
This PDF of fib Bulletin 92 is intended for use and/or distribution solely within fib National Member Groups.

The principles of linear viscoelasticity are accepted even though concrete fibres near the neutral axis can become cracked with time, since their contribution to the sectional response is very small.

The total strain at any concrete point at age t, loaded at age t_0 with an instantaneous stress $\sigma(t_0)$, subject to continuous monotonic variation, can be calculated by:

$$\Delta\varepsilon(t) = \varepsilon_{cs}(t,t_0) + \sigma(t_0)J(t,t_0) + \left[\sigma(t) - \sigma(t_0)\right]\left[\frac{1}{E_c(t_0)} + \frac{\chi(t,t_0)\phi(t,t_0)}{E_{c,28}}\right] \tag{4-61}$$

where $\varepsilon_{cs}(t, t_0)$ is the free shrinkage of the concrete in the time $t - t_0$; $\sigma_c(t_0)$ is the concrete stress applied at age t_0; $J(t, t_0)$ is the creep function; $E_c(t_0)$ and $E_{c,28}$ are the modulus of elasticity of concrete at time t_0 and 28 days, respectively; $\varphi(t, t_0)$ is the creep coefficient at time t, when the load is applied at t_0; and $\chi(t,t_0)$ is the ageing coefficient, which can be assumed equal to 0.8.

From Eq. (4-61) an age-adjusted effective modulus of concrete $\overline{E}_c(t, t_0)$ can be defined to obtain the strain increment between t and t_0 due to the increment of stresses $\sigma(t)$ - $\sigma(t_0)$, given by:

$$\overline{E}_c = \frac{E_c(t_0)}{1 + \frac{E_c(t_0)}{E_{c,28}}\chi(t,t_0)\phi(t,t_0)} \tag{4-62}$$

Values for relaxation of tensile stress in prestressing steel at constant strain and temperature are given by the intrinsic relaxation, $\Delta\sigma_p$. For non-constant strain, a simplified procedure can be used based on a reduced relaxation value $\Delta\sigma_{pr} = \chi_r \cdot \Delta\sigma_p$, where χ_r can be assumed equal to 0.8.

From sectional equilibrium the resultant forces are given by:

$$\Delta N = \int \Delta\sigma d \cdot A \tag{4-63}$$

$$\Delta M = \int \Delta\sigma y d \cdot A \tag{4-64}$$

and substituting Eq. (4-60) into (4-63) and (4-64), and taking also into account time-dependent effects due to creep, shrinkage and relaxation, leads to:

$$\begin{bmatrix}\Delta N \\ \Delta M\end{bmatrix} = \begin{bmatrix}\int Ed \cdot A & \int Eyd \cdot A \\ \int Eyd \cdot A & \int Ey^2 d \cdot A\end{bmatrix}\begin{bmatrix}\Delta\varepsilon_0 \\ \Delta\psi\end{bmatrix} - \begin{bmatrix}\Delta N^0 \\ \Delta M^0\end{bmatrix} \tag{4-65}$$

where ΔN^0 and ΔM^0 are equivalent (restraining) forces required to prevent the free development of the aforementioned time-dependent effects.

Taking into account the definition of first, B, and second moment, I, of a section about an axis through the point O:

$$A = \int d \cdot A \qquad B = \int yd \cdot A \qquad I = \int y^2 d \cdot A \tag{4-66}$$

Eq. (4-65) may be rewritten as:

$$\begin{bmatrix}\Delta N \\ \Delta M\end{bmatrix} = E_{ref}\begin{bmatrix}A & B \\ B & I\end{bmatrix}\begin{bmatrix}\Delta\varepsilon_0 \\ \Delta\psi\end{bmatrix} - \begin{bmatrix}\Delta N^0 \\ \Delta M^0\end{bmatrix} \tag{4-67}$$

This document is the intellectual property of the fib – International Federation for Structural Concrete. All rights reserved.
This PDF of fib Bulletin 92 is intended for use and/or distribution solely within fib National Member Groups.

in which A, S and I are, respectively, the cross-sectional area of the transformed section and its first and second moments about a horizontal axis through O. For reinforced concrete members E_{ref} is usually taken as the modulus of elasticity of concrete (or one of the concretes in case of composite section), E_c, and the properties of the transformed section are calculated using the area of each material multiplied by the ratio of its modulus of elasticity to that of the reference concrete. For cracked sections only the area of concrete in compression is included in the transformed section.

4.3.1.3.2 Instantaneous and long-term deformations

Calculation of instantaneous deformations is performed assuming a zero value for ΔN^0 and ΔM^0 in Eq. (4-67), leading to:

$$\begin{bmatrix} \Delta\varepsilon_0 \\ \Delta\psi \end{bmatrix} = \frac{1}{E_c\left(A \cdot I - B^2\right)} \begin{bmatrix} I & -B \\ -B & A \end{bmatrix} \begin{bmatrix} \Delta N \\ \Delta M \end{bmatrix} \tag{4-68}$$

in which E_{ref} has been adopted as E_c. From previous equations it can be seen that when the reference point O coincides with the centroid of the transformed section ($B = 0$) the system is uncoupled, $\Delta\varepsilon_o$ only depends on ΔN and $\Delta\psi$ depends on ΔM. Likewise, when the reference point O coincides with the neutral axis ($\Delta\varepsilon_o = 0$) curvature only depends on ΔM.

From Eq.(4.3-20), strain and curvature is obtained by:

$$\Delta\varepsilon_0 = \frac{I\Delta N - B\Delta M}{E_c\left(A \cdot I - B^2\right)} \tag{4-69}$$

$$\Delta\psi = \frac{B\Delta N + A\Delta M}{E_c\left(A \cdot I - B^2\right)} \tag{4-70}$$

The strain and stress at any point and material at a vertical distance y from the horizontal reference axis can be obtained using Eqs. (4-59) and (4-60).

The increment of axial strain $\Delta\varepsilon_O$ and curvature $\Delta\psi$ with time, due to creep, shrinkage and relaxation of prestressing steel, can be calculated by:

$$\Delta\varepsilon_0 = \frac{\overline{I}\,\Delta N^0 - \overline{B}\Delta M^0}{\overline{E}_c\left(\overline{A} \cdot \overline{I} - \overline{B}^2\right)} \tag{4-71}$$

$$\Delta\psi = \frac{-\overline{B}\Delta N^0 + \overline{A}\Delta M^0}{\overline{E}_c\left(\overline{A} \cdot \overline{I} - \overline{B}^2\right)} \tag{4-72}$$

where $\overline{A}$, $\overline{S}$ and $\overline{I}$ are, respectively, the cross-sectional area of the age-adjusted transformed section and its first and second moments about a horizontal axis through O. These properties have to be calculated using the age-adjusted effective modulus of concrete $\overline{E}_c$.

ΔN^0 and ΔM^0 may be calculated as follows:

$$\Delta N^0 = \overline{E}_c \cdot \varphi\left(A_c \cdot \varepsilon_0 + B_c\psi\right) + \overline{E}_c \cdot \varepsilon_{sh} \cdot A_c - A_{ps} \cdot \Delta\sigma_{pr} \tag{4-73}$$

$$\Delta M^0 = \overline{E}_c \cdot \varphi\left(B_c \cdot \varepsilon_0 + I_c\psi\right) + \overline{E}_c \cdot \varepsilon_{sh} \cdot B_c - A_{ps} \cdot y_{ps} \cdot \Delta\sigma_{pr} \tag{4-74}$$

where A_c, I_c and B_c are referred to the concrete section, A_{ps} is the total area of prestressing steel and y_{ps} is the vertical distance from the horizontal reference axis to the position of

This document is the intellectual property of the fib – International Federation for Structural Concrete. All rights reserved.
This PDF of fib Bulletin 92 is intended for use and/or distribution solely within fib National Member Groups.

the equivalent prestressing tendon and ε_0 and y are the instantaneous axial strain and curvature obtained as described above. $\Delta\sigma_{pr}$ is the absolute value of the loss of tensile stress in the prestressing steel due to relaxation (reduced relaxation).

For any prestressed or non-prestressed section the mean curvature (instantaneous or long-term) can be obtained from interpolation between the values of deformation of the uncracked section and the fully cracked section applying the procedure described in Section 4.3.1.4.2.1.

4.3.1.4 Simplified methods

4.3.1.4.1 Introduction

Although the general method is the most accurate for calculation of deflections, it does not represent an efficient tool during the design phase, because is time-consuming and involves a lot of work for input data and for interpretation of results. During the design phase, simplified expressions are required based on the mechanics of the problem, which include the most important parameters governing the structural behaviour, in order to achieve a good approximation of the instantaneous and delayed deflection value, using few calculations.

Some of the most well-known simplified formulations are based on interpolation of the results obtained assuming the member totally uncracked (state I) or fully cracked (State II). In this way the fact that along the member there are sections which are cracked and other which are uncracked is taken into account.

The method of interpolation of deflections[4-5], and the expression proposed by one study[4-54] for interpolation of the stiffness are the most representative. Equivalent stiffness methods are another simplified methodology for obtaining instantaneous deflections. Empirical correlations based on experimental campaigns like the ACI time-dependent expression for delayed deflection is also known worldwide.

In the following, the interpolation method, valid for the calculation of instantaneous and long-term deflections, adopted in the Eurocode EC2[4-9, 4-29] and incorporated to the *fib* Model Code 2010[4-1], will be briefly explained. In addition, a simplified method for the long-term deflections proposed by one study[4-55], based on an assumption of the time-dependent sectional behaviour in accordance with experimental observations will be presented.

4.3.1.4.2 Instantaneous deflections

Cracking of concrete takes place at relatively low load levels, so that in most cases beams are cracked in service conditions. Cracking produces a significant change in the sectional response, reducing dramatically the stiffness and incrementing the curvature with respect to un-cracked sections. In order to satisfy equilibrium between forces (N,M) and internal stresses, and compatibility of deformations (plane sections, perfect bond), the neutral axis depth decreases and the stresses both in concrete and in the reinforcement increase.

In the case of beams free from cracks, the most important factors governing the instantaneous deflections are the elastic modulus of concrete, the inertia of the cross sections, the element span length and the support conditions. The amount of steel, for usual ratios, does not have much affect on the inertia.

However, in a cracked element the amount of longitudinal tensile reinforcement plays an important role in the stiffness of the section because a) the neutral axis depth depends on n and ρ, $n = E_s/E_c$ is the modular ratio between steel and concrete and $\rho = A_s/b \cdot d$ is the reinforcement ratio), and b) because the direct contribution of the steel to the inertia

This document is the intellectual property of the fib – International Federation for Structural Concrete. All rights reserved.
This PDF of fib Bulletin 92 is intended for use and/or distribution solely within fib National Member Groups.

is much more important than in un-cracked sections related to the concrete contribution. In addition, bond characteristics also affect the stiffness of a cracked beam, since stresses are transferred to concrete in tension between cracks, thus contributing to the stiffness of the element (tension stiffening).This fact is especially relevant for load levels slightly higher than the cracking load, since the contribution of tension stiffening is comparable to that of the steel.

Since the cracking moment of a section depends on the tensile strength of concrete, which is a parameter with a large scatter, errors in the estimation of deflections in lightly loaded beams, but cracked, can be considerable. In addition, when using a limited number of representative sections of the element to calculate deflections, (usually the sections subjected to maximum positive and negative moments) the error made can be significant. Moreover, the concrete tensile strength can be affected by early age stresses resulting from the restraint to the volume changes that develop during the hydration process of cement, or from non-uniform distributions of early age shrinkage, increasing the uncertainty in the calculation of deflections.

4.3.1.4.2.1 Interpolation method

The deflection interpolation method is based on an extrapolation of the mean curvature concept of cracked element, which takes into account the tension stiffening, to obtain deflection.

The mean curvature (ψ) can be approximated by interpolating the curvatures in the fully cracked (ψ_{II}) and uncracked (ψ_{I}) sections:

$$\psi = \psi_{II} \cdot \zeta + \left(1-\zeta\right)\psi_{I} \tag{4-75}$$

The curvature at an uncracked or a cracked section can be expressed in terms of the bending moment and flexural rigidity or in terms of strains. Fig. 4-52 represents the mean behaviour of a cracked reinforced concrete flexural member.

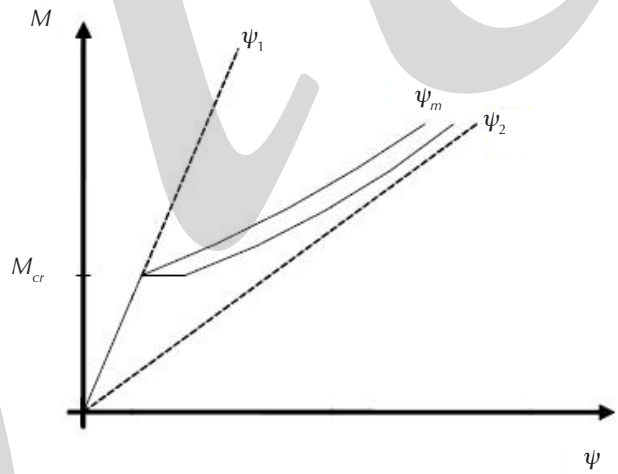


Fig. 4-52 Moment versus curvature in a reinforced concrete member in flexure

Since the deflection is very sensitive to the curvature of the determinant section, the interpolation of curvatures can be approximately extended to interpolation of deflections as follows:

$$y_{inst} = y_{II} \cdot \zeta + \left(1-\zeta\right)y_{I} \tag{4-76}$$

This document is the intellectual property of the fib – International Federation for Structural Concrete. All rights reserved.
This PDF of fib Bulletin 92 is intended for use and/or distribution solely within fib National Member Groups.

where y_{inst} is the instantaneous deflection and y_I and y_{II} are both the deflections calculated using the un-cracked (gross or homogeneous) and the cracked section properties, respectively. Factor ζ is the interpolation factor, which takes into account the tension stiffening contribution to the stiffness of the element. Factor β is a coefficient accounting for the influence of the duration and repetition of loading on the degradation of tension-stiffening. The value of β is 1 for first loading and 0.5 for sustained loads or multiple cycles of repeated loading. In general, the expression for the interpolation factor is:

$$\zeta = 1 - \beta \left(\frac{\sigma_{sr}}{\sigma_{s2}} \right)^2 \tag{4-77}$$

where σ_{sr} and σ_{s2} are the stresses at the tensile reinforcement calculated in state II, under the cracking moment, M_{cr}, and under the maximum moment, M, applied at the section, respectively.

In the case of beams without axial load, Eq.(4-77) can be replaced by

$$\zeta = 1 - \beta \left(\frac{M_{cr}}{M} \right)^2 \tag{4-78}$$

When bending moments are close to cracking moment the interpolation factor is similar to (1 - β) while for high levels of loading, the interpolation factor approaches the value ζ = 1, which means that tension stiffening hardly contributes to the stiffness.

Introduction of compression axial load, Fig. 4-53, reduces the difference between uncracked and fully cracked behaviour, and therefore the tension stiffening effect reduces [4-56]. Furthermore axial force affects the cracking load, which increases for the case of compression force (and reduces for tensile). Additionally the interpolation coefficient in Eq. (4-78) is slightly lower than for the case of pure bending, tending to be similar with increasing flexural moments.

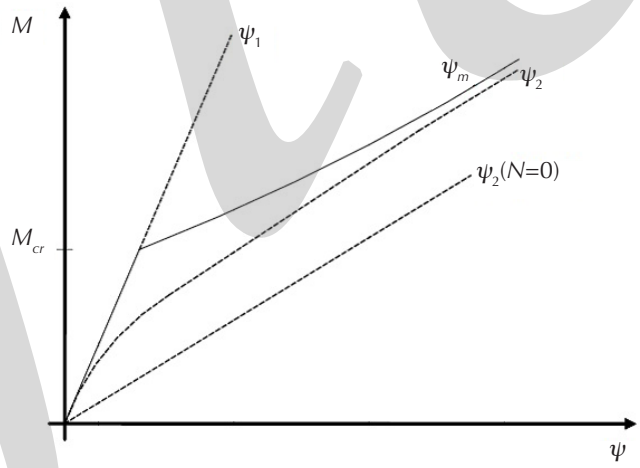


Fig. 4-53 Moment versus curvatures in a section with bending plus axial force

According to one study[4-51] when the bending moment is combined with axial force, the interpolation coefficient ζ may be expressed in terms of concrete stresses:

$$\zeta = 1 - \beta \left(\frac{f_{ct}}{\sigma_{1max}} \right)^2 \tag{4-79}$$

This document is the intellectual property of the fib – International Federation for Structural Concrete. All rights reserved.
This PDF of fib Bulletin 92 is intended for use and/or distribution solely within fib National Member Groups.

where σ_{1max} is the value of the tensile stress at the extreme fibre which would occur due to the applied *N* and *M*, assuming no cracking. The value f_{ct} is the tensile concrete strength.

The simplification of the interpolation method lies in the fact that the element deflection is obtained using the properties of one single critical section instead of integrating curvatures along the whole element. The reason for that simplification is that sections governing deflections are sections that present maximum curvatures having a big contribution in the integration process. This argument is adequate for simply supported beams where the stiffness of the central section has a large influence in the deflections. However, in continuous members both the stiffness and the length of the positive and the negative bending moment zones have influence on the value of the deflection.

The interpolation method is included in the final *fib* MC2010 version[4-1] and also in EC2[4-9, 4-29]. In those Codes no rules are given to obtain the deflection when designing continuous elements with different reinforcement ratios along its axis.

4.3.1.4.2.2 Effective stiffness method

An alternative approach for estimation of instantaneous deflections of a cracked reinforced concrete member is based on the calculation of an "Effective moment of inertia", J_{eff}, to be assumed constant over the full length of the member. Branson's equation is perhaps the best known[4-54].

Another possibility is to use an equivalent moment of inertia derived by imposing that the deflection obtained is equal to that calculated by the interpolation method, as described next. After reaching the cracking load, the instantaneous deflection of any element can be obtained using the standard formula for elastic deflection, considering an effective (or equivalent) stiffness, I_{eff}, representative of the mean behaviour of the cracked element:

$$y_{inst} = k\frac{M \cdot l^2}{E_c \cdot I_{eff}} \tag{4-80}$$

where *k* takes into account the support condition and the loading type.

The effective stiffness of a cracked element is directly obtained from the mean curvature formulation:

$$\psi = \psi_{II} \cdot \zeta + \left(1-\zeta\right)\psi_{I}, \quad \psi = \frac{M}{E \cdot I} \tag{4-81}$$

$$I_{eff} = \frac{I_I \cdot I_{II}}{\zeta \cdot I_I + \left(1-\zeta\right)I_{II}} \tag{4-82}$$

where I_I and I_{II} are the second moment of inertia of the un-cracked and fully cracked sections, respectively. The interpolation factor ζ is the interpolation coefficient defined in section 4.3.1.4.2.1.

Reinforced concrete elements are generally designed by adjusting the reinforcement ratios according to the bending moment diagram. As a consequence, the homogeneous and the cracked neutral axis depth varies along the element. In order to take into account the different distribution of reinforcement in to the equivalent stiffness of the whole beam, a mean reinforcement ratio (ρ_m, ρ'_m) may be used, as that proposed[4-5] which can be expressed by:

This document is the intellectual property of the fib – International Federation for Structural Concrete. All rights reserved.
This PDF of fib Bulletin 92 is intended for use and/or distribution solely within fib National Member Groups.

$$\rho_m = \rho_A \frac{l_A}{l} + \rho_B \frac{l_B}{l} + \rho_C \frac{l_C}{l} \tag{4-83}$$

$$\rho'_m = \rho'_A \frac{l_A}{l} + \rho'_B \frac{l_B}{l} + \rho'_C \frac{l_C}{l} \tag{4-84}$$

where:

ρ_A, ρ'_A, Amounts of tensile and compressive reinforcement at the end support *A*.

l_A Length of the beam subjected to negative bending moment near support *A*.

ρ_B, ρ'_B Amounts of tensile and compressive reinforcement at the end support *B*.

l_B Length of the beam subjected to negative bending moment near support *B*.

ρ_C, ρ'_C Amounts of tensile and compressive reinforcement at mid-span.

l_C Length of the beam subjected to positive bending moment.

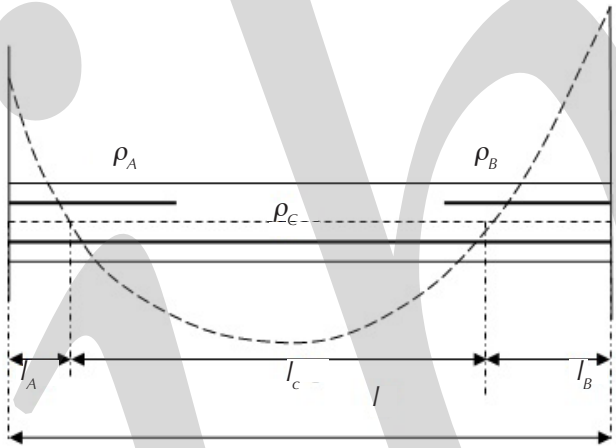


Fig. 4-54 Bending moment diagram for defining ρ_A, ρ_B, ρ_C, l_A, l_B and l_c

It should be verified that $l = l_A + l_B + l_C$

In general, to obtain the average reinforcement amounts ρ_m and ρ'_m approximate values of l_A , l_B and l_C provide satisfactory results. The following default values can be adopted:

- For members supported at one end and fixed at the other, and for end spans of continuous beams, $l_A / l = 0.25$ and $l_B / l = 0.75$
- For members with both ends fixed, $l_A / l = l_B / l = 0.20$, and $l_C / l = 0.60$
- For interior spans of continuous beams, $l_A / l = l_B / l = 0.15$, and $l_C / l = 0.70$

Once the mean reinforcement ratio (ρ_m, ρ'_m) is obtained, the cracked and un-cracked inertias are calculated. For the uncracked state inertia of the transformed section is preferable when high reinforcement ratios are considered, in other cases the gross inertia provides good agreement.

The cracked inertia of a rectangular section can be calculated as follows:

$$I_{II} = n \cdot b \cdot d \left[\rho_m \left(d - x\right)\left(d - \frac{x}{3}\right) + \rho'_m \left(x - d'\right)\left(\frac{x}{3} - d'\right) \right] \tag{4-85}$$

This document is the intellectual property of the fib – International Federation for Structural Concrete. All rights reserved.
This PDF of fib Bulletin 92 is intended for use and/or distribution solely within fib National Member Groups.

Where x is the neutral axis depth obtained by assuming zero tensile strength of concrete and linear concrete stress in compression. Its value, is given by:

$$x = n \cdot \rho \cdot d\left(1+\frac{\rho'}{\rho}\right)\left(-1+\sqrt{1+\frac{2\left(1+\frac{\rho'}{\rho}\frac{d'}{d}\right)}{n\rho\left(1+\frac{\rho'}{\rho}\right)^2}}\right) \tag{4-86}$$

In the case of sections with only tensile reinforcement, x is expressed by:

$$x = n \cdot \rho \cdot d\left(-1+\sqrt{1+\frac{2}{n \cdot \rho}}\right) \tag{4-87}$$

Furthermore, for practical applications, the next simplified expression represents a good approach to obtain the neutral axis depth for rectangular sections:

$$\frac{x}{d} = \frac{0.18+1.8n \cdot \rho_m}{1+\frac{\rho'_m}{\rho_m}\frac{d'}{d}} \tag{4-88}$$

Similarly, the following simplified expression of the fully cracked stiffness can be used for rectangular sections, as a simpler alternative to Eq. (4-85):

$$I_{II} = I_I\left(\frac{d}{h}\right)^3\left[0.12+5.4n \cdot \rho_m\left(1+\frac{\rho'_m}{\rho_m}\frac{d'}{d}\right)\right] \tag{4-89}$$

For the case of statically indeterminate elements, again an aspect open to consideration is the value of the bending moment to use when determining the interpolation coefficient. After several numerical simulations, it is proposed to calculate the equivalent stiffness with the interpolation parameter ζ corresponding to the section with the maximum bending moment in the element instead of a mean bending moment value. As an example, in a double fixed end beam, the bending moment considered is the negative one, at the supports.

Finally the equivalent inertia, I_{eff}, is obtained using Eq. (4-82).

4.3.1.4.3 Long-term deflections

Long-term deflections in RC elements take place basically due to creep and shrinkage. While creep of concrete is proportional to the instantaneous stress caused by sustained loads, shrinkage does not depend on the stress state, but on hygrometric, thermal and geometric conditions. The presence of reinforcement affects the delayed sectional behaviour, since reinforcement constrains the free concrete strain.

Before reaching the cracking load, creep is the most important parameter affecting the delayed curvature. For normal amounts of reinforcement ratios, un-cracked sections increase their instantaneous curvature by a rotation over the neutral axis. Constraint generated by the reinforcement due to deformation of the concrete and the shrinkage effects are not considered because of their small influence in the uncracked state. Thus the following equation can be applied for the calculation of time-dependent deflections in the un-cracked state:

$$y_{tot} = y_{inst}\left[1+\varphi\left(t,t_0\right)\right] \tag{4-90}$$

This document is the intellectual property of the fib – International Federation for Structural Concrete. All rights reserved.
This PDF of fib Bulletin 92 is intended for use and/or distribution solely within fib National Member Groups.

After cracking, time-dependent behaviour of sections changes drastically because of the neutral axis shift. When cracking occurs, time-dependent strains and stresses in the cracked section change significantly from the un-cracked state. Due to creep and shrinkage of concrete, the section curvature will increase with time and reinforcement strains will be equal to those of the surrounding concrete. However, since neither creep nor shrinkage takes place in the steel, the reinforcement partially constrains free deformation of concrete. Any increment of strain in the steel will produce an increment of stress and redistributions of stresses between concrete and steel, necessary to maintain equilibrium of normal forces at any time. In addition, a shift of the neutral axis depth will take place over time, in order to equilibrate the constant applied bending moment. Therefore, the final state of stresses, strains and curvature will be a result of the equilibrium and compatibility, accounting for the instantaneous and time-dependent behaviour of the materials.

Shrinkage of the uncracked zone of the section cannot be neglected in the cracked state.

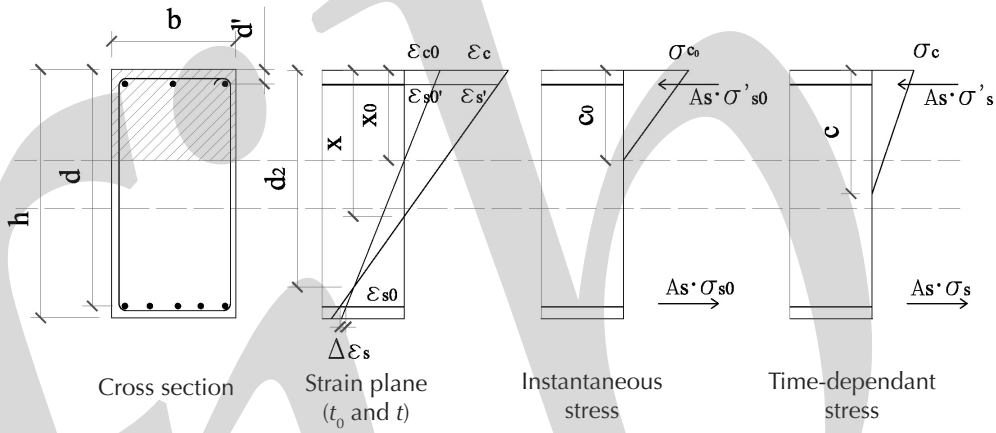


Fig. 4-55 Instantaneous and time-dependent strains and stresses of a cracked section

In Fig. 4-55 the instantaneous and time-dependent behaviour of a section is described, where ε_{c0}, ε'_{s0}, ε_{s0}, ε_{c}, ε'_{s}, es correspond to the instantaneous and long term deformations of concrete top fibre, compression reinforcement and tension reinforcement. It can be observed how due to creep and shrinkage initial stresses (σ_{c0}, σ'_{s0}, σ_{s0}) changes with time. As a result of internal stresses redistribution, new stresses values are obtained (σ_{c}, σ'_{s}, σ_{s}) and a shift of the instantaneous neutral axis (x_0) can be observed.

Many authors have worked on trying to find a simplified formulation to overcome the time-dependent analysis. Some codes provide empirical formulations like ACI-318-14[4-57], MC90[4-8] or EHE-08[4-58], while others propose analytical models as Eurocode 2[4-9, 4-29] and *fib* Model Code 2010[4-1].

4.3.1.4.3.1Interpolation method

Total deflection including creep can be determined using the method by considering an effective modulus of concrete, $E_{c,eff}$, to take into account creep effects:

$$E_{c,eff} = \frac{E_c\left(t_0\right)}{1+\varphi\left(t,t_0\right)} \tag{4-91}$$

$$y_{inst+\varphi} = y_{II}\cdot\zeta\left(1-\zeta\right)y_I \tag{4-92}$$

This document is the intellectual property of the fib – International Federation for Structural Concrete. All rights reserved.
This PDF of fib Bulletin 92 is intended for use and/or distribution solely within fib National Member Groups.

Using the effective modulus, new mechanical properties of the critical sections must be determined both for the uncracked section, where the modular ratio $E_s/E_{c,eff}$ changes, and for the cracked sections, in which a reduction of the concrete stress and a deeper neutral axis position takes place.

Under permanent loads the beta factor (β) of the interpolation coefficient must be taken equal to 0.5.

Shrinkage deflection is not included in Eq. (4-92) and must be obtained separately. The *fib* MC2010 provides the following expression for the shrinkage curvature in both un-cracked and fully cracked states:

$$\psi_{sh} = \varepsilon_{sh} \cdot n \frac{S}{I} = \varepsilon_{sh} \cdot n_{eff} \frac{As\left(x-d\right) - A's\left(x-d'\right)}{I} \tag{4-93}$$

in which ψ_{sh} is the shrinkage curvature; ε_{sh} is the shrinkage strain; $n_{eff} = E_s/E_{c,eff}$ is the effective modular ratio; and S and I are the first moment of area of the reinforcement and the moment of inertia about the centroid of the section, respectively, calculated using values of the effective transformed section.

Deflections due to shrinkage, both in the un-cracked and in the fully cracked states, are obtained by double integration of the shrinkage curvature. Mean shrinkage deflection is obtained by interpolation between the deflections calculated in both states Eq. (4-92).

4.3.1.4.3.2 Approximate method based on sectional kinematics

The time-dependent behaviour of a cracked section has been studied by several authors[4-47, 4-50, 4-51, 4-59]. Fig. 4-55 describes the actual time-dependent stresses and strains in a cracked RC section.

A parametric study was carried out[4-55] using the general method over a huge number of virtual fully cracked RC sections, considering different values of reinforcement ratios and different environmental conditions. According to the results of the previous parametric study, the increment of the strain at the longitudinal tensile reinforcement is very small in cracked sections. Such increment is smaller as the reinforcement ratio increases. Therefore it seems reasonable to assume that the strain and stress at the tensile reinforcement are constant over time and equal to the instantaneous ones produced by the sustained load ($\Delta\varepsilon_s = 0$).

Based on this assumption, and considering equilibrium of forces with the stress resultants, the compatibility of deformations at any time, and the time-dependent concrete constitutive equation using the ageing coefficient, χ, the following general analytical expression was derived for the delayed increment of curvature:

$$\Delta\psi = \frac{\varepsilon_{c0}\left(\varphi - \varphi\cdot\chi - 1 + \frac{C_0}{C}\left(1+\chi\cdot\varphi\right)\right) + \varepsilon_{sh}}{d\left(1 + n\cdot\rho' \frac{2\left(1+\chi\cdot\varphi\right)\left(1-\frac{d'}{d}\right)}{\left(\frac{x}{x_0}\right)\left(\frac{x_0}{d}\right)}\right)} \tag{4-94}$$

This document is the intellectual property of the fib – International Federation for Structural Concrete. All rights reserved.
This PDF of fib Bulletin 92 is intended for use and/or distribution solely within fib National Member Groups.

where:

ε_{c0} is the instantaneous concrete strain due to sustained loading, at $t = t_0$.

φ is the creep coefficient at time $t \geq t_0$.

ε_{sh} is the shrinkage strain at time $t \geq t_0$.

χ is the ageing coefficient at time $t \geq t_0$ taken as $\chi = 0.8$ in this work.

x_0 is the neutral axis depth at $t = t_0$

x is the neutral axis depth at $t > t_0$

$\rho' = A_s'/bd$ is the geometric ratio of compressive reinforcement.

$n = E_s/E_{c0}$ is the ratio between the modulus of elasticity of concrete and steel.

Eq. (4-94) can be simplified adopting a value for the ratio between the final and the initial depths of the concrete stress block $x/x_0 = 1.25$, according to the results of the previous parametric study. In addition, conservative values for other parameters affecting the second term of the denominator, which slightly influence the value of the increment of curvature, $\Delta\psi$, are adopted for the sake of simplicity. These values are:

- initial relative neutral axis depth, $x_0/d = 0.3$.
- ageing coefficient $\chi = 0.8$.
- ratio between covers of compressive and tensile reinforcements $d'/d = 0.1$.
- creep coefficient $\varphi = 2.0$, which is considered an average value for normal and high strength concrete.

Thus, substituting the above values in Eq. (4-94), and after further operations, the following approximate expression is obtained for the increment of curvature in fully cracked sections:

$$\Delta\psi = \Delta\psi_{creep} + \Delta\psi_{sh} = \psi_0 \frac{x_0}{d} \frac{0.84\varphi\left(t,t_0\right) - 0.2}{1 + 12n \cdot \rho'} + \frac{\varepsilon_{sh}}{d} \frac{1}{1 + 12n \cdot \rho'} \tag{4-95}$$

where:

χ_0 is the instantaneous curvature

x_0 is the neutral axis at $t = t_0$

d is the effective depth

ρ' is the compressive reinforcement ratio

Integrating the curvatures along the element length and taking into account the boundary conditions, the following expression is obtained for the delayed deflection:

$$\Delta y = \Delta y_{cr} + \Delta y_{sh} = y_{inst} \frac{x_0}{d} \frac{0.84\varphi - 0.20}{1 + 12n \cdot \rho_m'} + \frac{\varepsilon_{sh}}{d} \frac{1}{1 + 12n \cdot \rho_m'} k_{sh} \frac{l^2}{8} \tag{4-96}$$

where

y_{inst} is the instantaneous deflection

x_0 is the neutral axis at $t = t_0$ considering ρ_m and ρ'_m

d is the effective depth

This document is the intellectual property of the fib – International Federation for Structural Concrete. All rights reserved.
This PDF of fib Bulletin 92 is intended for use and/or distribution solely within fib National Member Groups.

ρ_m' is the mean compressive reinforcement ratio

k_{sh} is a constant that considers support conditions. For cantilever $k_{sh} = 0.4$, for pinned elements $k_{sh} = 1$, for pinned-fixed elements $k_{sh} = 0.7$ and for fixed beams $k_{sh} = 0.5$.

As it can be observed, the method assumes that time-dependent deflection is controlled by fully cracked sections. The accuracy of the sectional kinematic method depends on the ratio between the cracking moment and the maximum bending moment that ever acts on the element, M_{cr}/M (that can be the characteristic moment and not the maximum moment due to sustained loading).

Optimized designs of RC elements subjected to bending moments provides M_{cr}/M ratios greater than 2.5 due to the presence of live load. For those cases, the effective moment of inertia (I_{eff}) is similar to the fully cracked moment of inertia and the assumption made provides quite good results[4-55].

4.3.1.5 Deflections of composite structures

In members composed of parts made of different concretes the following aspects should be taken into account when calculating the deflections:

1. The different moduli of elasticity of each concrete
2. The curvatures resulting from the differential shrinkage of precast and cast-in-situ components.
3. The construction sequence, including the existence or not of propping, to take into account which part of the section contributes to the strength and the stiffness along the construction process.
4. When a cast in place concrete is poured over a precast-pretensioned member, the camber of the second one must be calculated previously.

4.3.2 Deflection due to shear

Deflections in concrete structures are induced by bending as well as by shear. If appropriate numerical methods are used, the general stiffness matrix covers both phenomena; even the effect of axial forces should be automatically included. If simplified methods are used then the effect of shear forces on deflections is usually neglected. *fib* MC2010[4-1] does not specifically describe the shear effects on deformations. Additional information is provided in the section 6.2.

In typical reinforced concrete structures the effects of shear strain on the overall deflection are rather small, in the order of unit percentages. There is a small inaccuracy if this effect is neglected, since the inaccuracy of the simplified analysis of the cracked concrete section may be of a similar order to the effect of shear strains.

In deep beams, the effect of shear strains on deflection is more important and it should be taken into account. If shear cracks are not indicated (in SLS) the assumption of elasticity may be used and the deflection due to shear force can be relatively easily calculated using the general rules of structural mechanics.

The shear strains become more important in prestressed structures. The deflection of the prestressed structure is the difference between the deflection induced by load and the reverse deflection induced by prestressing. Although the individual deflection components

This document is the intellectual property of the fib – International Federation for Structural Concrete. All rights reserved.
This PDF of fib Bulletin 92 is intended for use and/or distribution solely within fib National Member Groups.

may be relatively large the final deflection should be small (in order to satisfy the deflection criteria). If a small error exists in the calculated deflection due to load or due to prestressing the consequence may be rather significant.

In a girder subjected to bending, the load almost always induces bending moments and shear forces. The girder deflects due to both loadings (bending and shear). The prestressing may be designed in different ways. If curved tendons are used, they also produce bending moment and shear force. Both deflections may be partly balanced. If pretensioning is used, then the prestressing is normally made by straight elements which develop only bending moments but no shear force. The bending is balanced by prestressing and the shear is not balanced at all. This is one of example where the deflection due to shear forces can influence the final deflection more significantly. The effect of shear is very important in structures which are wide and the span is not too long, where the shear lag effects also contribute to the shear deformations.

It is recommended to check the possible effect of shear forces on deflections under short-term as well as long-term load and finally to use an appropriate computational tool for correct analysis taking into consideration all the phenomena important for the structure. In the SLS most prestressed structures can be analysed under the assumption of elasticity, which need not require any exceptional effort to also take into account the shear effects on deflections.

This document is the intellectual property of the fib – International Federation for Structural Concrete. All rights reserved.
This PDF of fib Bulletin 92 is intended for use and/or distribution solely within fib National Member Groups.

5. Examples

5.1 Stress and deflection analysis of a prestressed concrete beam

5.1.1 Stress analysis

A simply supported post-tensioned beam has a span 25 m. The dimensions of the cross-section are constant along the entire beam and they are indicated in Fig. 5-1 and in Tables 5-1 to 5-3.

Table 5-1 Dimensions and reinforcement of the beam

		Comment
Span [m]	25	
Depth [m]	1.2	
Width of the top flange [m]	1.0	
Depth of the top flange [m]	0.25	
Thickness of the web [m]	0.3	
Prestressed tendon 19 x 15.7 mm [m^2]	2.85 E-3	
Area of the duct profile 104 mm [m^2]	8.5 E-3	
Mild reinforcement 4 x 16 mm [m^2]	0.804 E-3	

Table 5-2 Material parameters

		Comment
Concrete C35/45 f_{ck} [MPa]	35	
f_{ctm} [MPa]	3.2	
E_c [MPa]	33'300	
Creep coefficient φ	2.0	
Shrinkage strain ε_{sh} [mm/m]	-0.2	
Reinforcing steel f_{yk} [MPa]	450	
E_s [MPa]	200'000	
Prestressing steel f_{pk} [MPa]	1'860	
E_p [MPa]	190'000	
Jacking stress [MPa]	1'150	
Prestress loss due to stress relaxation [MPa]	97.65	Infinite time

Table 5-3 Loading of the beam

		Comment
Self weight [kN/m]	13.38	
Additional dead load [kN/m]	12.75	
Applied load [kN/m]	11.25	
Total permanent load [kN/m]	26.13	
Total load [kN/m]	37.38	Characteristic comb.
Coefficient ψ_2	0.3	
Long-term load [kN/m]	29.51	Quasi-permanent comb.
Long term excl. self weight [kN/m]	16.13	Quasi-perm. c. excl. self weight

This chapter was mainly authored by Burns, Caldentey, Duarte, Fehling, Mari Bernat, Torres, Vítek and Vrablik.

doi.org/10.35789/fib.BULL.0092.Ch05

This document is the intellectual property of the fib – International Federation for Structural Concrete. All rights reserved.
This PDF of fib Bulletin 92 is intended for use and/or distribution solely within fib National Member Groups.

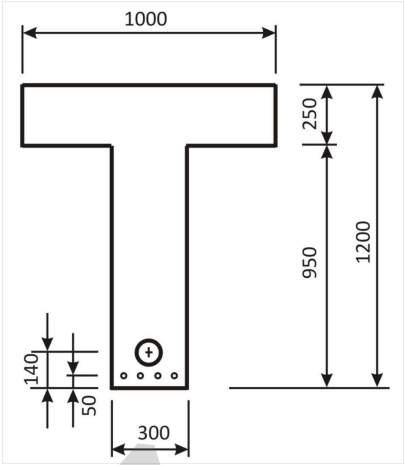


Fig. 5-1 Cross-section of the beam – dimensions and position of the reinforcement

The prestressing force is applied at one end of the beam. Due to the initial prestress losses (friction of the tendon in the duct) and anchor slip at the left end of the beam the stress in the prestressing tendon after anchorage varies along the length of the beam. The prestressing at the midspan is 1'074.4 MPa.

An approximate analysis will be applied. The analysis assumes elastic performance of the beam. The effects of the long term load resulting in prestress loss due to creep and shrinkage of concrete and due to stress relaxation in steel are taken into account in a simplified manner using an age-adjusted effective modulus method. Therefore the stresses from the analysis may slightly differ from those calculated by a more precise method based on incremental numerical analysis. It should be noted that the approximate method is intended for simplified preliminary analyses. The detailed analysis will be carried out using numerical methods which are incorporated in computer codes. The individual loading stages may be calculated separately and the results are taken as a sum of the partial loading stages. The stress is calculated at the midspan section.

The stress in concrete and steel due to individual loadings is calculated using the following steps.

1. The prestressing applied at time t_1 activates the self-weight and the duct is not grouted yet. The loading acts on the section, which consists of concrete and mild steel. The stress at the midspan is calculated using the parameters of the cross section (A_{eff}, I_{eff}) without prestressing steel and the area of the cross section is reduced by the area of the duct. At the midspan the results are in the Table 5-4.

Table 5-4 Values at the midspan – tendons not grouted.

		Comment
Area of the cross-section A_{eff} [m^2]	0.5313	
Distance of the centroid from the top fibres y_{eff} [m]	0.4412	
Second moment of inertia I_{eff} [m^4]	0.06986	
Prestressing force [MN]	3.062	
Bending moment self weight [MNm]	1.045	
Stress in the top fibres [MPa]	-0.398	
Stress in bottom fibres [MPa]	-14.990	
Stress in mild steel [MPa]	-86.380	
Stress in prestressed steel [MPa]	1'074.4	

This document is the intellectual property of the fib – International Federation for Structural Concrete. All rights reserved.
This PDF of fib Bulletin 92 is intended for use and/or distribution solely within fib National Member Groups.

2. The duct is grouted and additional dead load is applied. The loads now work on the complete effective cross-section composed of concrete, mild steel and prestressing steel. The duct is now filled, it is considered as a part of the cross-section. The parameters of the cross-section and the stresses induced by additional dead load are summarised in the Table 5-5.

Table 5-5 Values at the midspan – tendons are grouted.

	Stress increment	Total stress
Area of the cross-section A_{eff} [m^2]	0.5532	
Distance of the centroid from the top fibres y_{eff} [m]	0.466	
Second moment of inertia I_{eff} [m^4]	0.07792	
Bending moment (add.dead load) [MNm]	0.9961	
Stress in the top fibres [MPa]	-5.954	-6.351
Stress in bottom fibres [MPa]	9.387	-5.603
Stress in mild steel [MPa]	52.541	-33.838
Stress in prestressed steel [MPa]	43.349	1'117.75

3. Until the final time t_2 (end of the service life) the prestressing changes due to the long term prestress losses (effect of creep, shrinkage and stress relaxation in steel). The long-term prestress losses may be calculated using Eq. 5-1.

$$\Delta\sigma_{p,c+s+r} = \frac{\varepsilon_{cs}\cdot E_p + \sigma_{cp}\left(t_1\right)\dfrac{E_p\cdot\varphi\left(t_2,t_1\right)}{E_c} + \Delta\sigma_{rel}\left(t_2,t_1\right)}{1+\dfrac{E_p}{E_c}\dfrac{A_p}{A_c}\left(1+\dfrac{A_c}{I_c}z_{cp}^2\right)\left[1+\chi\cdot\varphi\left(t_2,t_1\right)\right]} \tag{5-1}$$

where $\sigma_c(t_1)$ is the stress in concrete in the level of prestressing steel. Prestress loss due to the stress relaxation in steel is assumed as follows. The final stress relaxation loss is assumed to be 3 times the value measured at 1000 h Table 5.3-2 in MC2010[5-1], 2.5% from 0.7 times ultimate tensile strength of the strands. The stress relaxation is estimated here as 0.7 · 1860 · 0.025 = 32.55 MPa at the time of 1000h. The ultimate prestress loss is taken as 3 times 32.55 MPa, which is 97.65 MPa. The prestress loss develops for a long time, therefore 80% of the final value is assumed to be used in Eq. 5-1, which is $\Delta\sigma_{rel}$ = 78 MPa. The prestress loss calculated from Eq. 5-1 is also approximate, since the effect of the mild reinforcement is not included.

The prestress loss induced during the permanent load (self-weight + additional dead load, $\sigma_{cp}(t_1)$ = -5.69 MPa) is 126.70 MPa. If the quasi permanent load (self-weight + add. dead load + $\psi 2$ · applied load, $\sigma_{cp}(t_1)$ = -3.68 MPa) was active, the prestress loss would be 95.93 MPa.

Up to the end of the service life the prestressing force will be reduced and the stresses at time t_2 are calculated as a sum of the stresses at time t_1 and stress increments induced by the drop of the prestressing force due to the long term prestress loss ΔN_p.

$$\begin{aligned}\Delta N_p &= \Delta\sigma_{p,c+s+r}\cdot A_p\\ \Delta M_p &= \Delta N_p\cdot e_p\end{aligned} \tag{5-2}$$

where, e_p is the eccentricity of the prestressing force. The internal forces ΔN_p and ΔM_p work on the section composed of concrete and mild steel without the effect of prestressing

This document is the intellectual property of the fib – International Federation for Structural Concrete. All rights reserved.
This PDF of fib Bulletin 92 is intended for use and/or distribution solely within fib National Member Groups.

steel. The principle of superposition is applied in order to obtain the final stresses at the time t_2. The individual stresses are summarised in the Table 5-6.

Table 5-6 Stresses in individual stages of construction [MPa].

	$\sigma_{c,\,top}$	$\sigma_{c,bot}$	σ_s	σ_p	σ_{cp}
Self weight + prestressing (t_1)	-0.40	-14.99	-86.38	1074.40	-13.29
Add. dead load	-5.95	9.39	52.54	43.35	7.60
Self w. + prestr. + add.dead l. (t_1)	-6.35	-5.60	-33.84	1'117.75	-5.69
Self w. + prestr. + add.d.l + ψ_2 ap.l. (t_1)	-7.93	-3.12	-19.93	1'129.22	-3.68
Self w.+prestr.+add.d.l.+ applied l. (t_1)	-11.60	2.68	12.52	1'156.00	1.01
Drop of prestressing due to long term prestress losses from t_1 to t_2*	-0.55	2.35	13.40	-95.93	2.01
Self w. + prestr. + add.d.l + ψ_2 ap.l. (t_2)	-8.48	-0.77	-6.53	1'033.29	-1.67
Self w.+prestr.+add.d.l.+ applied l. (t_1)	-12.15	5.03	25.92	1'060.07	3.02

* Assuming the quasi-permanent load when calculating the prestress losses in Eq. 5-1, i.e. $\Delta\sigma_{p,\,c+s+r} = 95.93$ MPa.

The stresses are also plotted in Fig. 5-2. The stresses show that the midspan section of the beam will be completely in compression when the quasi permanent load combination is assumed at time t_1. The stress at bottom fibres is -3.12 MPa. If the applied load becomes active, the tension 2.68 MPa appears at the bottom fibres. Since the concrete strength in tension is $f_{ctm} = 3.2$ MPa, cracks should not originate due to the assumed loading. However, during time the prestressing drops by about 100 MPa (95.93 MPa), the stress reserve at the bottom fibres reduces, but the bottom part of the section will be under compression in the quasi permanent load combination ($\sigma_{c,bot}$ = -0.77 MPa). If the entire applied load becomes active, the tensile stress at the bottom fibres will be 5.03 MPa, which is more than the tensile strength of concrete and cracks may be observed. However, the stress in mild steel is only about 26 MPa, therefore a very small crack width may be expected. Although the beam is not fully prestressed, the effect of prestressing is favourable for limitation of cracks and deflections.

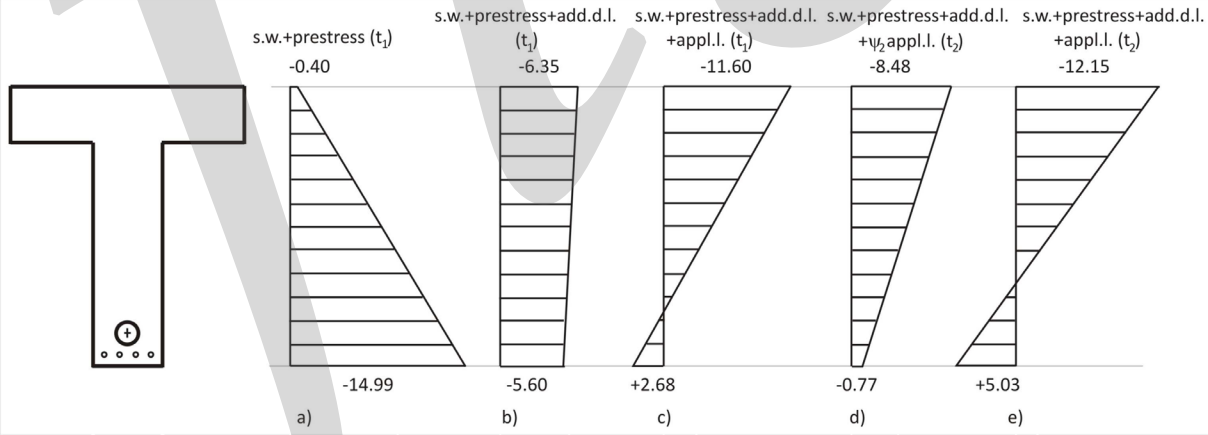


Fig. 5-2 Stress at the midspan in individual loading stages, b) permanent load, c) and e) characteristic load and d) quasi-permanent load

5.1.2 Deflection analysis

The deflection of the beam will be analysed again in a simplified way. The curvature of individual sections may be calculated from the strains in top and bottom fibres. The

This document is the intellectual property of the fib – International Federation for Structural Concrete. All rights reserved.
This PDF of fib Bulletin 92 is intended for use and/or distribution solely within fib National Member Groups.

strains depend on the stress directly using Hook's law if a short term load is assumed. If a long term deflection is analysed the creep and shrinkage is taken into account using age adjusted modulus method. The strain at time t_2 may be calculated using Eq. 5-3,

$$\varepsilon_c(t_2) = \varepsilon_{cs}(t_2,t_1) + \sigma_c(t_1)\frac{1+\varphi(t_2,t_1)}{E_c} + \frac{\sigma_c(t_2)-\sigma_c(t_1)}{E_c}\left[1+\chi\cdot\varphi(t_2,t_1)\right] \tag{5-3}$$

where χ is an ageing coefficient, approximately $\chi = 0.8$. The stresses σ_c at the times t_1 and t_2 are taken from the previous stress analysis. The curvature of the section at the midspan (the most loaded section) is governing for the deflection of the beam. The curvature 1/r (t_2) may be calculated using Eq.5-4 from the top and bottom strains at the section obtained from Eq. 5-3.

$$\frac{1}{r}(t_2) = \frac{\varepsilon_{c,bot}(t_2)-\varepsilon_{c,top}(t_2)}{h} \tag{5-4}$$

The curvature may also be calculated in other sections, in order to obtain more precise deflection of the beam. The procedure is exactly the same as shown for the midspan section. The parameters of the individual sections are given in the Table 5-7 and in Fig. 5-3.

Table 5-7 Section parameters of the beam

Section	*x*- coordinate [m]	d_p [m]*	$\sigma_{p,0}$ [MPa]**	Comment
1	0	0.550	1'027.5	Support
2	6.25	0.905	1'050.9	
3	12.5	1.060	1'074.4	Midspan
4	18.75	0.905	1'079.6	
5	25	0.550	1'056.1	Support

* Distance of the prestressing tendon from the top surface of the section
** Stress in prestressed steel after the prestress losses due to friction and anchor slip

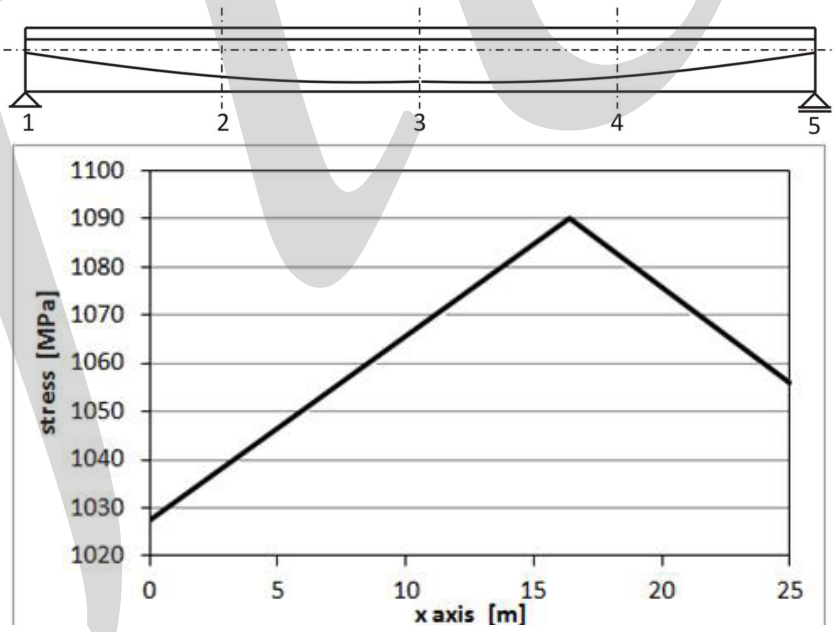


Fig. 5-3 Longitudinal section and diagram of the prestressing force

The calculated stresses and strains in the individual sections under the quasi permanent load at time t_2 are summarised in the Table 5-8.

This document is the intellectual property of the fib – International Federation for Structural Concrete. All rights reserved.
This PDF of fib Bulletin 92 is intended for use and/or distribution solely within fib National Member Groups.

Table 5-8 Stresses and strains along the beam at the time t_2

Section	1	2	3	4	5
$\sigma_{c,top}$ [MPa]	-4.96	-7.95	-8.48	-7.88	-5.11
$\sigma_{c,bot}$ [MPa]	-4.92	-0.88	-0.77	-1.41	-5.07
$\varepsilon_{c,top}$	$-6.54.10^{-4}$	$-9.13.10^{-4}$	$-9.57.10^{-4}$	$-9.06.10^{-4}$	$-6.68.10^{-4}$
$\varepsilon_{c,bot}$	$-6.50.10^{-4}$	$-3.03.10^{-4}$	$-2.97.10^{-4}$	$-3.50.10^{-4}$	$-6.64.10^{-4}$
1/r (t_2)	$3.135.10^{-6}$	$5.089.10^{-4}$	$5.502.10^{-4}$	$4.635.10^{-4}$	$3.229.10^{-6}$

The deflection of the beam at midspan may be calculated by the method of virtual works. The vertical unit force applied at the midspan results in bending moments M_1. The deflection is then given by Eq. 5-5.

$$f\left(t_2\right)=\int_0^l M_1 \frac{1}{r}\left(t_2\right),\ dx \tag{5-5}$$

The integral in Eq. 5-5 may be solved by different methods, e.g. using a Simpson rule.

$$f\left(t_2\right)=\frac{12.5}{6}\left(4\frac{l}{8}5.089\cdot10^{-4}+\frac{l}{4}5.502\cdot10^{-4}\right)+$$

$$\frac{12.5}{6}\left(\frac{l}{4}5.502\cdot10^{-4}+4\frac{l}{8}4.635\cdot10^{-4}\right)=39.6\text{mm}$$

In reinforced concrete structures even simpler analysis may be used, when the stiffness of the beam is calculated from the curvature at the midspan section, provided it is the section with the extreme bending moment. The stiffness is then assumed to be constant along the beam. Such an assumption is conservative, since the midspan section is cracked, while the other sections are not. The assumed constant stiffness is lower than the real stiffness of the beam which is variable and increasing towards the supports. If such approach was used here, the constant bending stiffness B would be calculated from Eq. 5-6.

$$B=\frac{M_{qp}}{\frac{1}{r}\left(t_2\right)} \tag{5-6}$$

where, M_{qp} is a bending moment induced by the quasi-permanent load combination (incl. self-weight). Then the deflection will be determined from the well known formula of structural mechanics.

$$f\left(t_2\right)=\frac{5}{48}\frac{M_{qp}l^2}{B},\quad B=\frac{2.305}{5.502\cdot10^{-4}}=4'189.8MNm^2$$

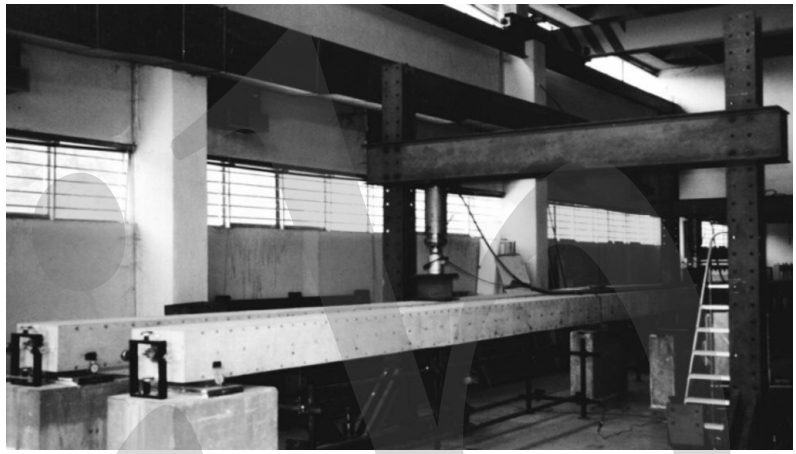
$$f\left(t_2\right)=\frac{5}{48}\frac{2.305\cdot25^2}{4'189.8}=35.8mm$$

The value obtained is smaller than that obtained by a numerical integration. In the investigated structure the section at midspan may not be the most loaded section, since the effects of loading and prestressing interact. Additionally the effect of shrinkage is not constant along the beam because of the different position of the prestressing steel along the beam. This example shows that the practice which is usual for RC beams may not be suitable for prestressed beams. The deflection therefore should be calculated as shown before, i.e. by the analysis of the entire beam.

This document is the intellectual property of the fib – International Federation for Structural Concrete. All rights reserved.
This PDF of fib Bulletin 92 is intended for use and/or distribution solely within fib National Member Groups.

5.2 Partially prestressed beam – cracking

A two span (8+8 m) partially prestressed beam tested at the structures laboratory of the Civil Engineering School of the Polytechnic University of Madrid is considered (Fig. 5-4). The beam is post- tensioned with a prestressing layout formed by tangent parabolas. The cross section is 400 mm wide by 300 mm high and is made of C35/45 grade concrete. The prestressing is formed by 3 strands of 13 mm of Y1860 prestressing steel, having a section of 300 mm^2 and is located 63 mm from the top of the section at the central support. The modulus of elasticity of concrete is taken as 34 077 N/mm^2 and that of steel as 200'000 N/mm^2.



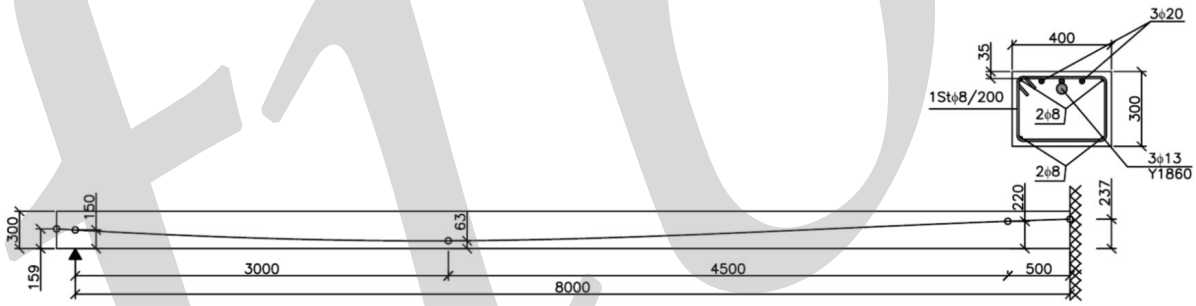


Fig. 5-4 Geometry and reinforcement of the prestressed beam

The section at the central support of the beam is reinforced at the upper face by 2Ø8+3Ø20 mm rebars (clear cover is 35 mm) with a yield stress of 500 N/mm^2 and is subjected to an SLS bending moment of -108.6 kNm due to its self-weight (3.0 kN/m), a dead load of 7.2 kN/m, and a live point load of 18 kN, situated 3.0 m from the outer supports. The long-term component of prestressing is considered by a pre-strain of 5.6‰, providing an axial force of $5.6 / 1000 \cdot 2 \cdot 10^8 \cdot 3 \cdot 10^{-4} = 336$ kN. The undetermined prestressing moment is about 9.0 kNm.

From these values the stress in the reinforcement can be obtained by sectional analysis of the cross section for a bending moment of -108.6+9=-99.6 kNm applied on a prestressed cross section having a pre-strain in the prestressing reinforcement of 5.6‰. This analysis is given in Fig. 15. The stress in the reinforcement (considering no tensile strength of concrete) for this load level and the depth of the neutral axis are:

σ_s = 68 N/mm^2, x = 157.4 mm.

This document is the intellectual property of the fib – International Federation for Structural Concrete. All rights reserved.
This PDF of fib Bulletin 92 is intended for use and/or distribution solely within fib National Member Groups.

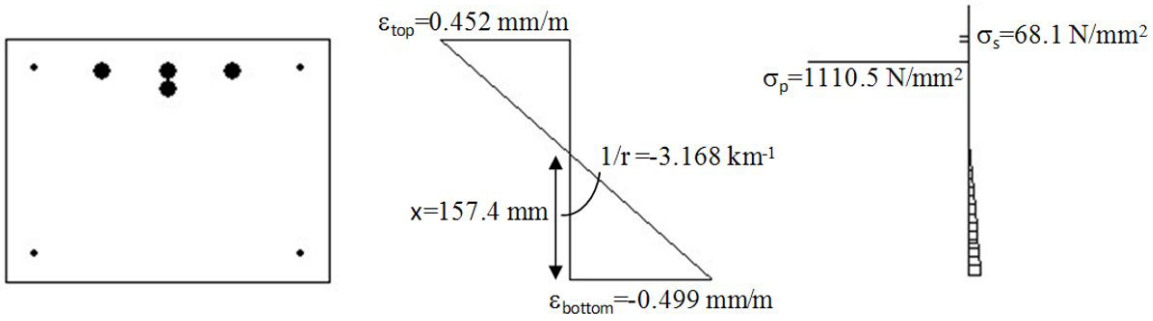


Fig. 5-5 Sectional analysis of prestressed section

The equivalent diameter for reinforcement is given by:

$$\phi_{eq} = \frac{n_1 \cdot \phi_1^2 + n_2 \cdot \phi_2^2}{n_1 \cdot \phi_1 + n_2 \cdot \phi_2} = \frac{2 \cdot 8^2 + 3 \cdot 20^2}{2 \cdot 8 + 3 \cdot 20} = 17.47 \text{ mm} \tag{5-7}$$

The effective area of concrete is determined as follows:

$$A_{c,ef} = b \cdot \min\left(\frac{h}{2}; \frac{(h-x)}{3}; 2.5(h-d)\right) = 400 \cdot \min\left(150; \frac{(300-157)}{3}; 2.5(45)\right) = \tag{5-8}$$

$$400 \cdot 4.8 = 19200 \text{ mm}^2$$

$$d \approx 255 \text{ mm}$$

The bond stress of prestressing is taken as 0.4 times the bond stress of passive reinforcement according to Table 7.6-3 of MC 2010 considering a post-tensioned strand, and the equivalent perimeter of the bundle is taken as u_p=1.6×π×3000.5 = 87 mm. Therefore the effective reinforcement ratio can be determined as:

$$\phi_{p,ef} = 4\frac{A_p}{u_p} = 4\frac{300}{87} = 13.8 \text{ mm} \tag{5-9}$$

$$\xi_1 = \sqrt{\frac{\tau_{bmp}}{\tau_{bms}}\frac{\phi_{eq}}{\phi_{p,ef}}} = \sqrt{0.4\frac{17.47}{13.8}} = 0.711 \tag{5-10}$$

$$\rho_{s+p,ef} = \frac{A_s + \xi_1^2 \cdot A_p}{A_{c,ef}} = \frac{2 \cdot 0.503 + 3 \cdot 3.14 + 0.711^2 \cdot 3}{192} = 0.062 \tag{5-11}$$

With these values, the maximum transfer length may be estimated for long-term, stabilized cracking as:

$$l_{s,\max} = kc + \frac{1}{4}\frac{f_{ctm}}{\tau_{bms}}\frac{\phi_{eq}}{\rho_{s+p,ef}} = 1.0 \cdot 35 + \frac{1}{4} \cdot \frac{1}{1.8} \cdot \frac{17.47}{0.062} = 74.1 \text{ mm} \tag{5-12}$$

Assuming a free shrinkage strain of 0.35 mm/m, the mean relative strain between concrete and steel can be determined from:

This document is the intellectual property of the fib – International Federation for Structural Concrete. All rights reserved.
This PDF of fib Bulletin 92 is intended for use and/or distribution solely within fib National Member Groups.

$$\varepsilon_{sm} - \varepsilon_{cm} - \eta_r \cdot \varepsilon_{sh} = \frac{\sigma_s - \beta \frac{f_{ctm}}{\rho_{s+p,ef}}\left(1+\alpha_e \cdot \rho_{s+p,ef}\right)}{E_s} - \eta_r \cdot \varepsilon_{sh} = \tag{5-13}$$

$$\frac{68 - 0.4\frac{3.21}{0.062}\left(1+\frac{200}{34.077}0.062\right)}{20'000} + 0.00035 = 0.55 \text{ mm/m}$$

$$f_{ctm} = 0.30\sqrt[3]{f_{ck}^2} = 0.30\sqrt[3]{35^2} = 3.21 \text{ N/mm}^2$$

Finally, the resulting maximum crack width would be:

$$w_d = 2l_{s,\max}\left(\varepsilon_{sm} - \varepsilon_{cm} - \eta_r \cdot \varepsilon_{sh}\right) = 2 \cdot 74.1 \cdot 0.55 \cdot 10^{-3} = 0.08 \text{ mm} < w_{\lim} \quad \text{O.K.} \tag{5-14}$$

5.3 Cracking due to shear

5.3.1 Experiment - Description of the structure

5.3.1.1 Geometry

The beam is 7.7 m long, 0.6 m high and the width of the flange is 0.4 m. It has an "I" shaped cross section. The thickness of the flanges is 80 mm, and thickness of the web is only 25 mm. The ends of the beam are stiffened by the 0.2 m thick cross beams. The positions where forces are applied are stiffened by the cross thin walls. Their thickness is 40 mm. The weight of one beam is 1.6 tons.

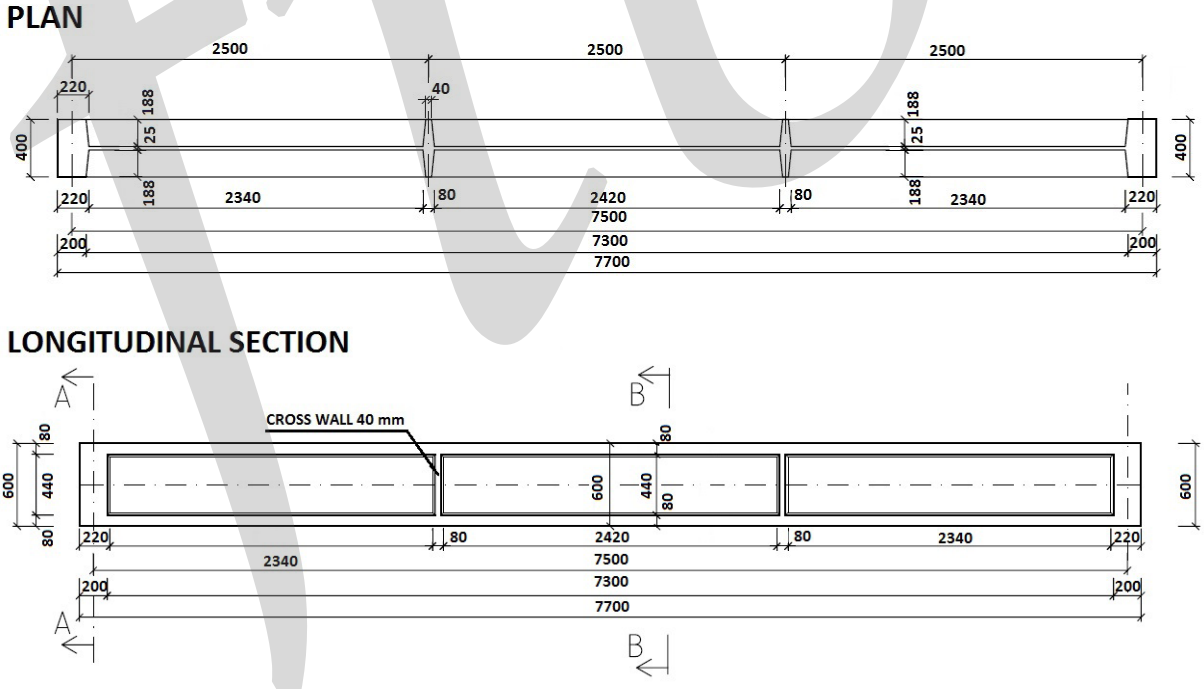


Fig. 5-6 Geometry of the element

This document is the intellectual property of the fib – International Federation for Structural Concrete. All rights reserved.
This PDF of fib Bulletin 92 is intended for use and/or distribution solely within fib National Member Groups.

5.3.1.2 Prestressing

The beam is prestressed with four tendons, of diameter 15.7 mm. Two tendons are in the lower flange, the tensile stress is 1'083 MPa (force in lower flange is 325 kN). Two tendons are in the upper flange, the tensile stress is 500 MPa (force in the upper flange is 150 kN).

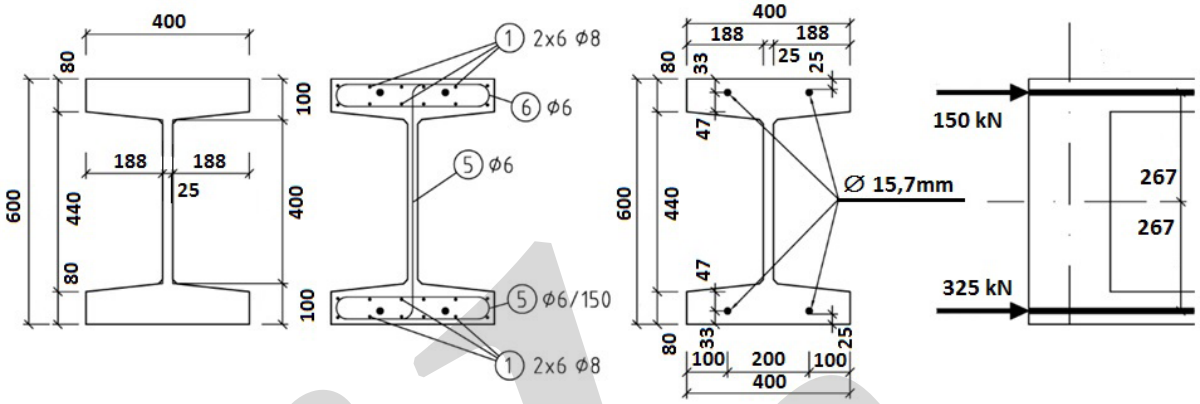


Fig. 5-7 Reinforcement and shape of cross section

5.3.1.3 Concrete

Concrete was made in the laboratory of CTU. There were several requirements for it:

- Strength class C 25/30 (or close to it);
- Good compaction of concrete or self-compacting concrete;
- Fast increase of strength over time.

All of these requirements were satisfied.

5.3.2 Numerical analysis of the formation of the first shear crack

It was necessary to determine the load level of the first shear crack appearing in the first stage of the calculation and whether the shear crack forms before the bending one. The results are compared according to EC, MC and the numerical calculation in ATENA 3D. Principal stresses have to be calculated in the web of the beam for the EC and MC assessment. These are a combination of the normal and shear stress. Analytical calculation of the principal stresses is based on the same formula for EC and MC:

$$\sigma_{1,2} = \frac{\sigma_x}{2} \pm \sqrt{\frac{\sigma_x^2}{4} + \tau_{xz}^2} \tag{5-15}$$

Computation of the principal stresses was done in the program EXCEL. The web is divided to elements 75 · 75 mm. Principal stresses are calculated in tension and compression in each node of the net.

5.3.2.1 Numerical analysis in the ATENA 3D FEM programme

The computation was carried out for the class of concrete C 25/30 according to the EC. The structure includes all of the real reinforcement. The beam was loaded with deformation increments of 1.5 mm until the formation of bending cracks. The computation was based on the mean values of the material strength and characteristic values of load.

This document is the intellectual property of the fib – International Federation for Structural Concrete. All rights reserved.
This PDF of fib Bulletin 92 is intended for use and/or distribution solely within fib National Member Groups.

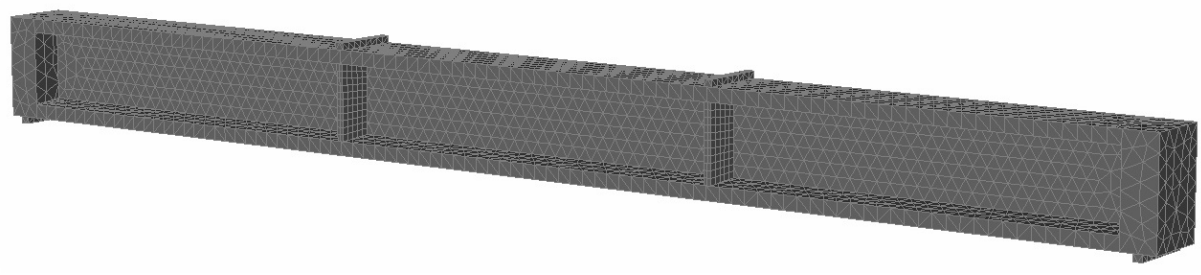


Fig. 5-8 Model of the structure in ATENA 3D

5.3.3 Comparison of numerical and experimental results

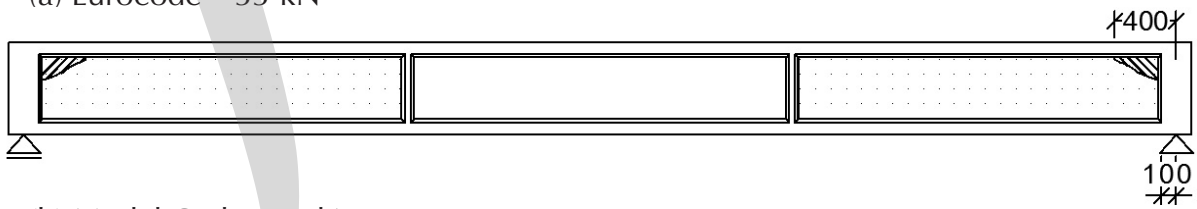
Table 5-9

Assessment		Force - first crack	Figure
EUROCODE 2 (2011)	$\sigma_1 > f_{ctb}$	33,0 kN	a)
MODEL CODE 2010	$\sigma_1 > f_{ctm}$	49,0 kN	b)
	$\sigma_1 > f_{ctm2}$	42,0 kN	c)
ATENA - NUMERICAL SIMULATION (2017)	$\sigma_1 > f_t^{'ef}$	41,0 kN	d)
	Sbeta material	40,6 kN	e)
EXPERIMENT		40,5 kN	f)

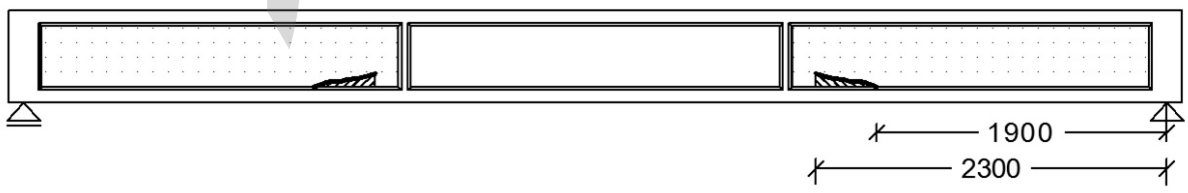
Table 5-10 Limit stress in tension

EUROCODE 2 (2011)	$f_{ctb} = \left(1 - 0.8\frac{\sigma_3}{f_{ck}}\right) f_{ctk;0.05}$
MODEL CODE 2010	f_{ctm}
	$f_{ctm2} = \left(1 - 0.8\frac{\sigma_2}{f_c}\right) f_{ctm}$
ATENA (2017)	$f_t^{'ef} = \left(1 - 0.95\frac{\sigma_{c2}}{f_c}\right) f_t'$

(a) Eurocode – 33 kN

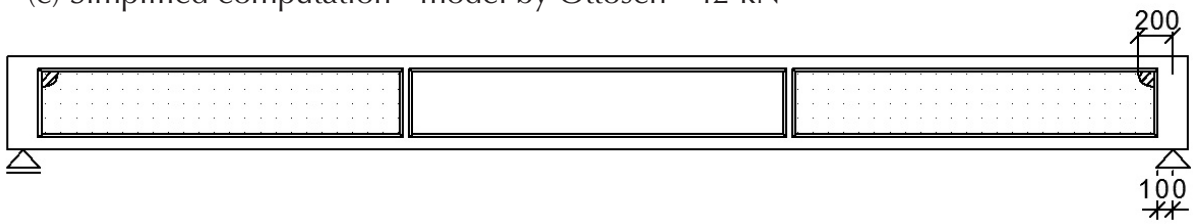


(b) Model Code - 49 kN



This document is the intellectual property of the fib – International Federation for Structural Concrete. All rights reserved.
This PDF of fib Bulletin 92 is intended for use and/or distribution solely within fib National Member Groups.

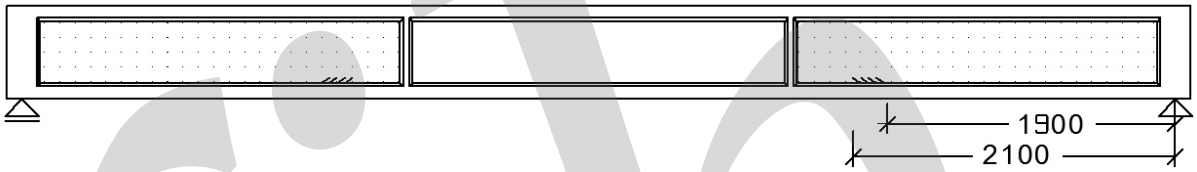
(c) Simplified computation - model by Ottosen - 42 kN



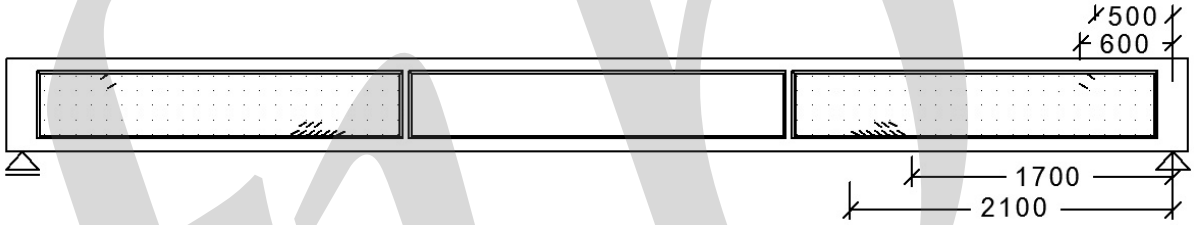
d) Simplified computation - model by Kupfer - 41 kN



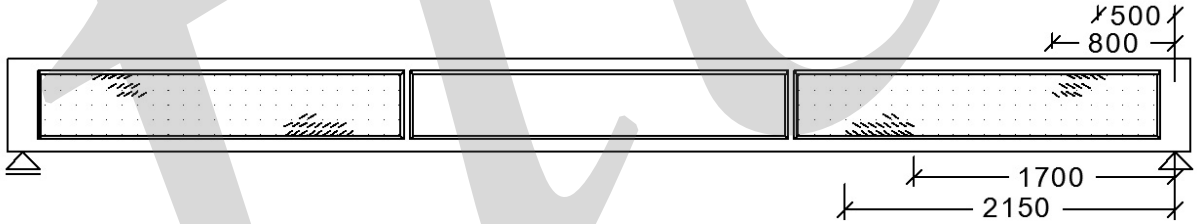
(e1) Atena - numerical simulation – 39,6 kN



(e2) Atena – 40,1 kN



(e3) Atena – 40,6 kN



(f) Experiment – 40,5 kN

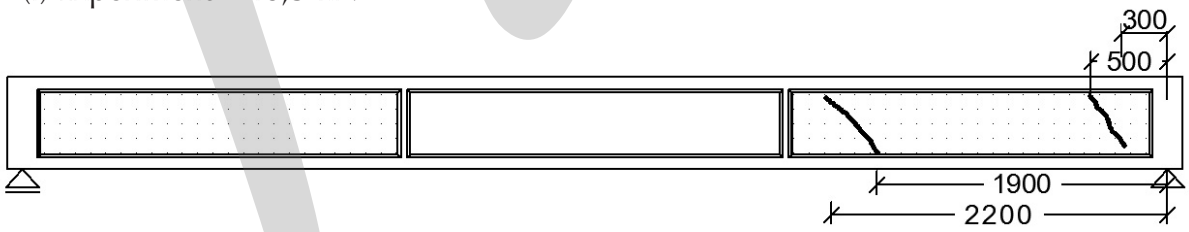


Fig. 5-9 First crack appearance

5.3.4 Conclusions

The example of a simple I – cross section beam with very thin section was studied. The task was to define minimal loading force, which would produce the first crack in the webs.

Real experimental results were compared with the numerical simulation. Numerical simulations were based on different material models of concrete, especially on the conditions defining a formation of the first shear crack.

This document is the intellectual property of the fib – International Federation for Structural Concrete. All rights reserved.
This PDF of fib Bulletin 92 is intended for use and/or distribution solely within fib National Member Groups.

The results show that it is important to use a lower tension stress limit for appearance of the first crack due to shear. The lower limit tension stress based on strength f_{ctm} and principal compression stress is very clear and the results compared well with the experiment. For detailed numerical simulation it is recommended to use material models based on failure condition as defined by one study[5-2].

5.4 Example for Combination of Restraint and Load Action

A simple rule to account for the combined action of restraint and load actions is to check whether load or restraint induced cracking alone requires more reinforcement for crack width limitation. Unless the stress in the reinforcement does not reach the yield strength, this simplified rule is stipulated in several codes (e.g. EN 1992-1[5-3], MC 2010[5-1]).

A frequent case for the combined action of restraint and load action is shrinkage of slabs or beams with restraint of longitudinal deformation at the ends. In order to compute the required reinforcement for crack width limitation for such a case, the fact that cracking may not occur everywhere across the whole length and cross section of the beam should be accounted for since this affects the deformation capacity. On the other hand, cracking in bending leads to positive strains at the centreline of a RC cross section which may help to compensate shortening of a beam or slab as induced by shrinkage or temperature change (see Fig. 5-10 and 5-11).

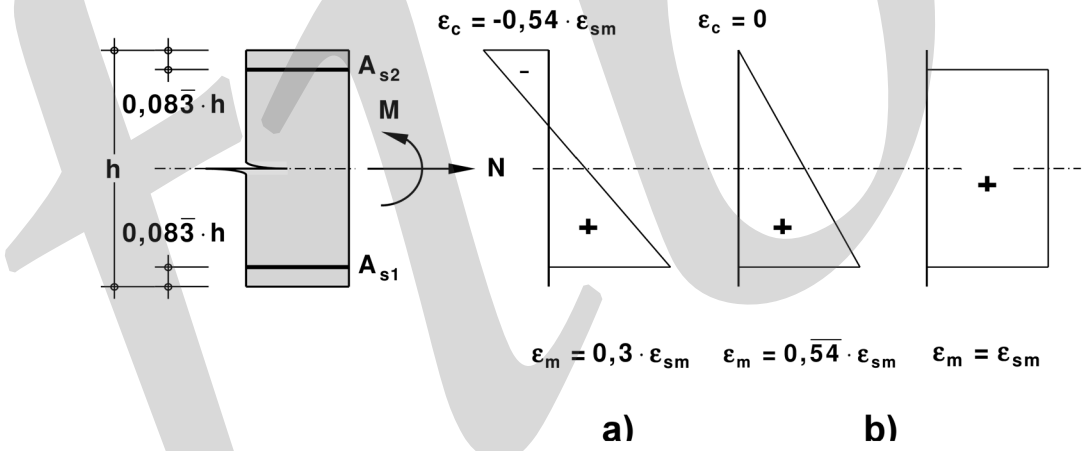


Fig. 5-10 Elongation at level of centreline due to bending induced cracking

Depending on the strain distribution the elongation at the centreline level can be taken from Fig.5-11 as compiled from on study[5-4], depending on the non-dimensional loading parameters ν_{ct} and μ_{ct}:

$$\upsilon_{ct}^{*} = \frac{N}{b \cdot h \cdot f_{ct,eff}} \qquad \mu_{ct}^{*} = \frac{M}{b \cdot h^2 \cdot f_{ct.eff}} \tag{5-16}$$

This document is the intellectual property of the fib – International Federation for Structural Concrete. All rights reserved.
This PDF of fib Bulletin 92 is intended for use and/or distribution solely within fib National Member Groups.

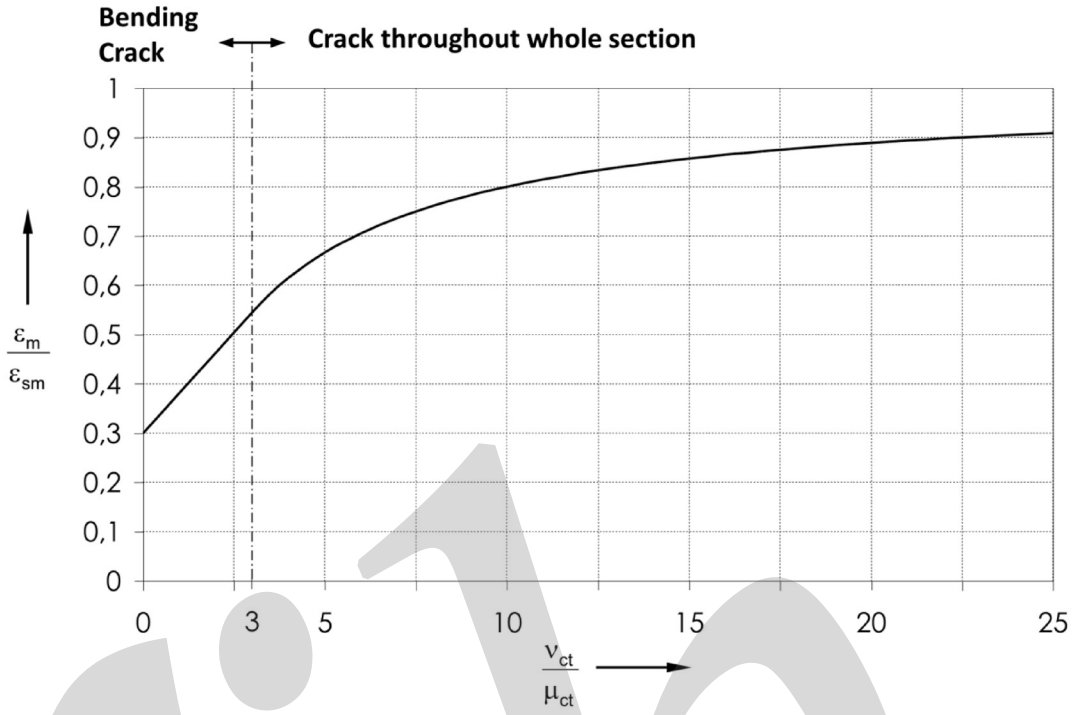


Fig. 5-11 Elongation at level of centerline

On this basis, different zones without cracks, with single cracks, and with stabilized cracking along the beam or slab can be distinguished (see Fig. 5-12).

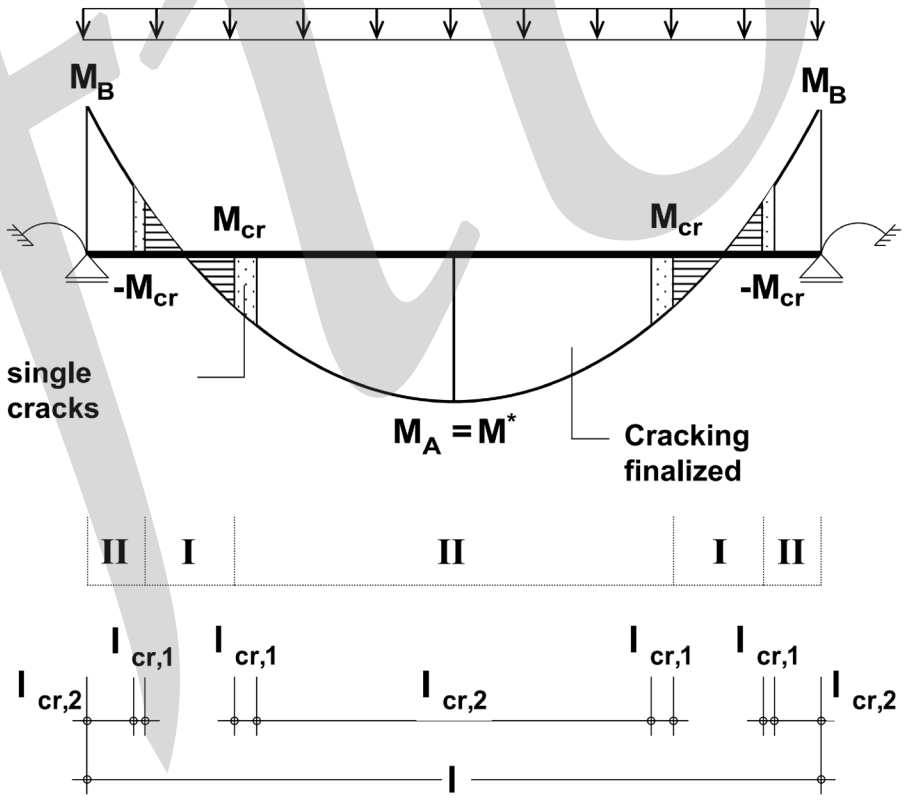


Fig. 5-12 Different cracking stages along a beam and calculation of average longitudinal strain ε_l

This document is the intellectual property of the fib – International Federation for Structural Concrete. All rights reserved.
This PDF of fib Bulletin 92 is intended for use and/or distribution solely within fib National Member Groups.

In one study[5-4], diagrams have been developed allowing determination of the normal force depending on the bending moments due to loading, the expected shortening ε_l (e.g. due to shrinkage and/or temperature) and the target value for crack width limitation. An example is shown in Fig. 5-13. The moment at midspan has to be taken as the decisive parameter for bending.

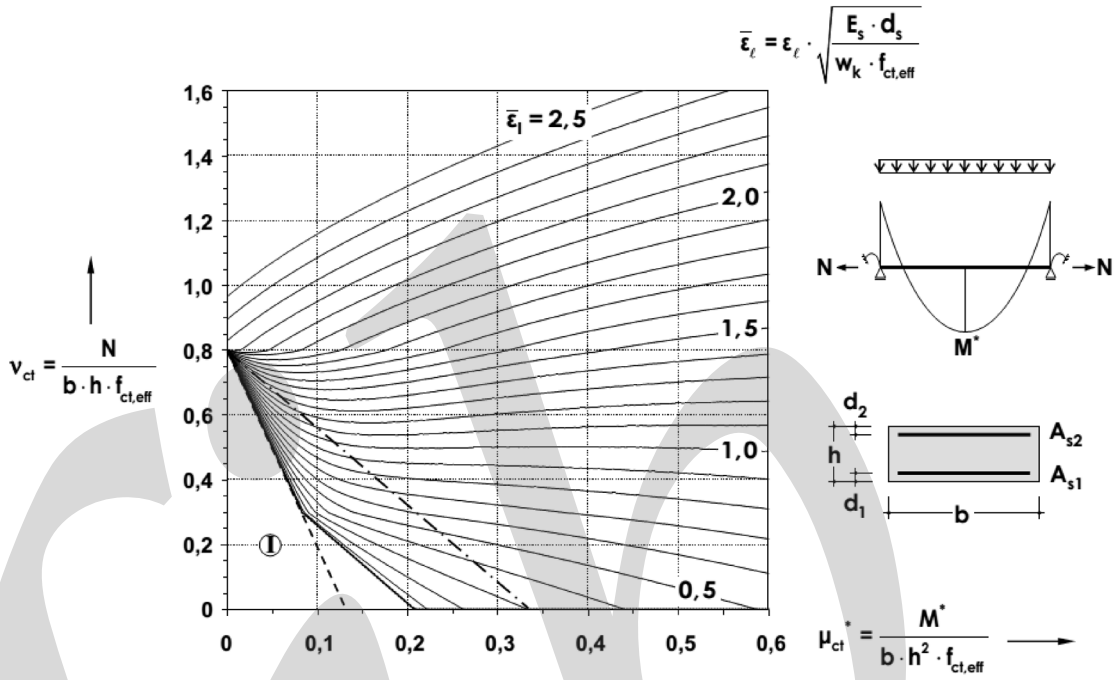


Fig. 5-12 Interaction of restraint and load induced bending

In order to show the application, a slab of a storage house (see Fig. 5-13) is taken as example.

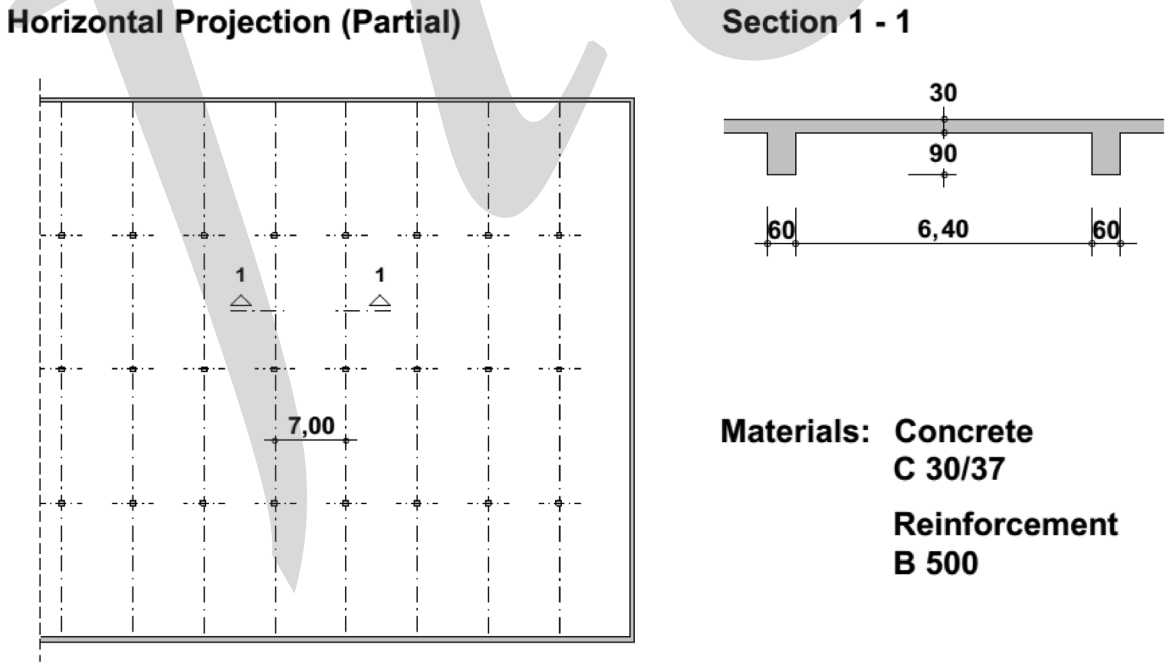


Fig. 5-13 Slab of storage house

This document is the intellectual property of the fib – International Federation for Structural Concrete. All rights reserved.
This PDF of fib Bulletin 92 is intended for use and/or distribution solely within fib National Member Groups.

The exposure class is XC. Hence, according to MC 2010[5-1] a crack width limit of $w_{lim} = 0.3$ mm applies. The shortening due to shrinkage and release of hydration heat shall be assumed to be 0.7 ‰. For this example, the effective concrete tensile strength is taken as $f_{ct} = 3{,}0$ MN/m². In order to account for the influence of self-equilibrating stresses from hydration heat, a reduction factor of $k = 0.8$ may be assumed for a structural member with 30 cm depth.

Since the restraint strain is below 0.8 ‰ and restraint and load act in combination, the steel stress should be limited to 0.8 fyk according to the provision given in section 7.6.3.4 of MC2010 for the characteristic combination of loads. In order to assess the effect of combined action, the diagram in Fig. 5.4-4 is applied. The bar diameter shall be 12 mm. Hence, the input parameters are:

$$\mu_{ct}^{*} = \frac{0.047}{1.0 \cdot 0.3^2 \cdot 3.0} = 0.174$$
$$\overline{\epsilon}_1 = \epsilon_1 \sqrt{\frac{E_s \cdot d_s}{w_{lim} \cdot f_{ct,eff}}} = 0.007 \sqrt{\frac{200'000 \cdot 12}{0.3 \cdot 3.0}} = 1.14 \qquad (5\text{-}17)$$

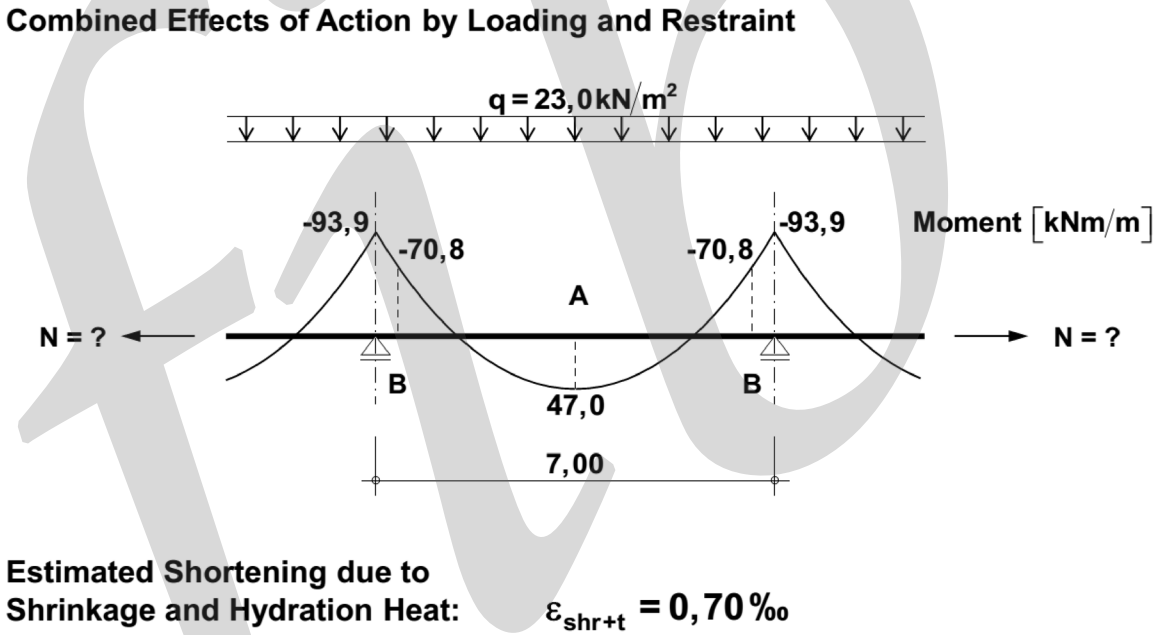


Fig. 5-14 Load and restraint induced forces for the slab of the example

From the diagram, a non-dimensional normal force of $n_{ct} \leq 0.6$ can be obtained. This leads to a normal force of

$$N = \nu_{ct} \cdot b \cdot h \cdot f_{ct,eff} \leq 0.6 \cdot 1.0 \text{ m} \cdot 0.3 \text{ m} \cdot 3.0 \ \frac{\text{MN}}{\text{m}^2} = 0.54 \text{ MN} \qquad (5\text{-}18)$$

For pure restraint without bending, the normal force would be higher:

$$N = \nu_{ct} \cdot b \cdot h \cdot f_{ct,eff} \leq 0.8 \cdot 1.0 \text{ m} \cdot 0.3 \text{ m} \cdot 3.0 \ \frac{\text{MN}}{\text{m}^2} = 0.72 \text{ MN} \qquad (5\text{-}19)$$

From this comparison it can be seen that the elongation at the level of the centreline as induced by bending decreases the normal force due to imposed deformation. However,

This document is the intellectual property of the fib – International Federation for Structural Concrete. All rights reserved.
This PDF of fib Bulletin 92 is intended for use and/or distribution solely within fib National Member Groups.

bending plus normal force both determine the force in the tensile reinforcement. Thus, where both bending and normal force lead to tensile force, more reinforcement will be required than by either load bending alone or by pure normal force due to restraint.

In one study[5-4], the same example has been used. It could be demonstrated that at the supports about 25 to 30 % more reinforcement is needed in comparison to the reinforcement required for pure restraint (in this case: normal force only). At the bottom, the increase in reinforcement amounts to about 10 % in the midspan region. However, at the upper side, much less reinforcement is required so that staggering is possible and rebar steel can be saved.

Fig. 5.4-7 shows the required reinforcement according to one study[5-4] which has been calculated according to DIN 1045-1[5-5] for w_{lim} = 0,4 mm. For MC 2010, the required absolute values are about 20 % higher altogether, since the crack width limitation is more stringent with w_{lim} = 0,3 mm.

The example is solved using the diagrams (Fig.5-15) calculated on the basis of the German code DIN 1045-1[5-5]. A similar diagram may be calculated using Model Code 2010[5-1]. It is intended to publish this in the next document focused especially on the effects of restrained deformations.

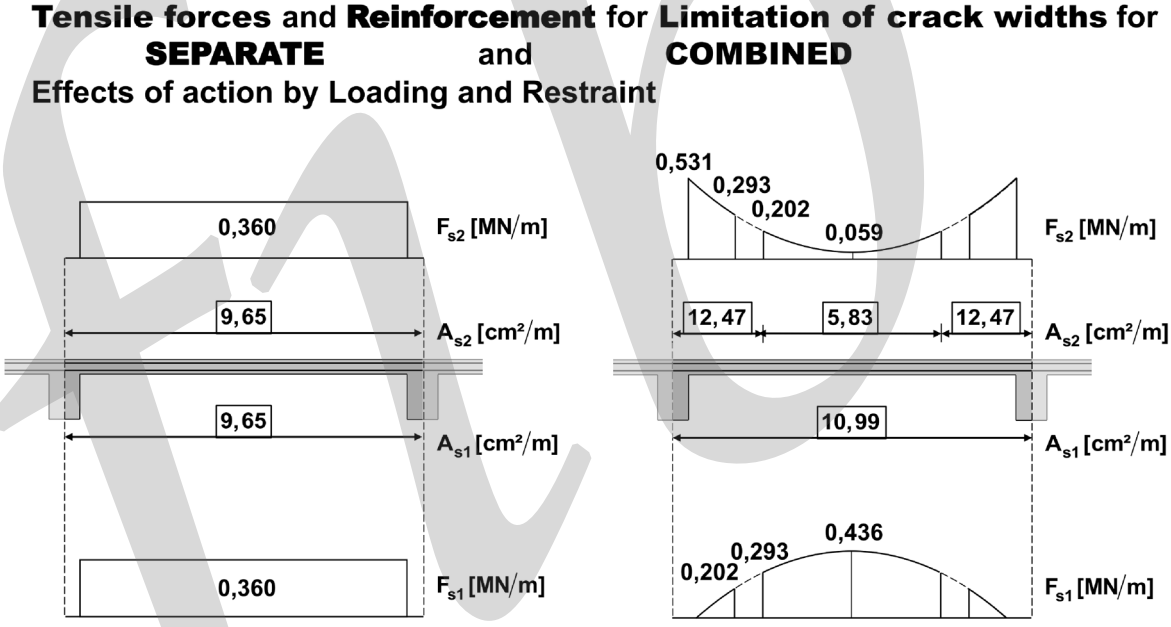


Fig. 5-15 Required reinforcement according to example with w_{lim} = 0,4 mm (compiled from this study[5-4]

5.5 Design of watertight wall

This example deals with the complex technology of watertight structures. There are many reasons for crack appearance in such structures, such as restrained deformations caused by temperature changes originating from heat of hydration, as well as by early shrinkage, autogenous and drying shrinkage, all of which are rather non-uniformly distributed along the thickness of the wall. The deformation of the wall is partially restrained. The degree of restraint is dependent on the boundary conditions given by the structural arrangement of the wall and location of the construction joints. Initially cracks originate and the structure is in the crack formation phase. During this phase the magnitude of the restrained deformation

This document is the intellectual property of the fib – International Federation for Structural Concrete. All rights reserved.
This PDF of fib Bulletin 92 is intended for use and/or distribution solely within fib National Member Groups.

is in fact not decisive and the concrete tensile strength is the most important criterion for the crack width. The magnitude of the restrained deformation (thermal contraction and shrinkage) becomes important once the crack formation phase is concluded. The following example is focused on the first case – the crack formation phase.

The 90 m long example wall shown in Fig. 5-16 is an external basement wall in an office building. The wall is located approximately 10 m below the groundwater level and has no external waterproofing ("weisse Wanne"). For ULS the vertical reinforcement of the wall is 20 mm bars spaced at 150 mm on the outer side (20/150) and 22 mm bars spaced at 150 mm on the inner side (22/150) (see Fig. 5.5-3a), as well as 10 and 12 mm stirrups spaced at 150 mm. The steel is B500B, the concrete is C30/37 and c_{nom} = 40 mm.

For the horizontal reinforcement the SLS is governing. The reinforcement options: 14/150, 16/150 and 18/150 are discussed in this example. All equations are calculated for all three options.

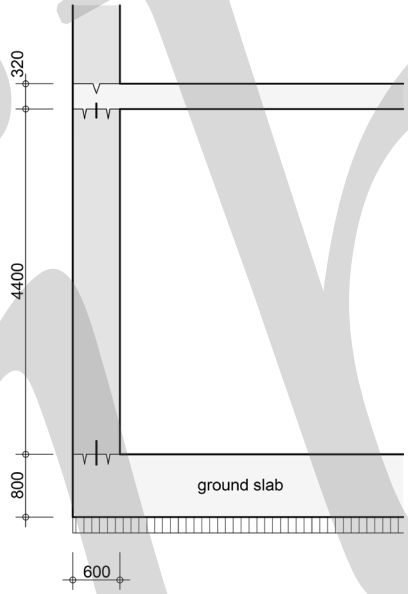


Fig. 5-16 Example wall, dimensions in mm

5.5.1 Assumptions

5.5.1.1 Cooling after hydration

Based on Table 4.5 in Lohmeyer and Ebeling (2009)[5-6], an average structure cooling ΔT = -15 K is assumed. This leads to cooling strains $\varepsilon_{\Delta T} = -15K\ 10^{-5}\ K^{-1} = -0.15‰$.

5.5.1.2 Shrinkage

Shrinkage strains equal to ε_{sh} = -0.35‰ are assumed.

5.5.1.3 Maximum crack width

According to 7.6.4.3 of MC2010 wlim for waterproof concrete is 0.2 mm.

5.5.1.4 Structural Model

The degree of restraint in uncracked base restrained walls varies over the height and width of the wall.

This document is the intellectual property of the fib – International Federation for Structural Concrete. All rights reserved.
This PDF of fib Bulletin 92 is intended for use and/or distribution solely within fib National Member Groups.

The regions around the top wall corners (see Fig. 5-17b) are hardly influenced by the base restraint and they do not crack unless the horizontal reinforcement ratio is large enough to cause closely spaced, fine cracks due to internal restraint.

The sections at the bottom of the wall are restrained by the ground slab. The fine base cracks, because closely spaced, only provide a local stress relief, so that they have no actual crack formation phase (theoretically for a constant concrete tensile strength they occur at the same time). The base cracks are not discussed within this example.

Not all of the base cracks extend up to the top of the wall; the ones that do are denominated as primary cracks. They occur in the wall regions outside the edge and base regions, which are restrained by the neighbouring wall sections. According to one study[5-7], their cracking behaviour can be modelled with end-restrained tension chords (see Fig. 5-17). Thus, the equations in 7.6.4.4 of Model Code 2010[5-1] apply to the primary cracks that occur in these wall regions. Their application is discussed in this example.

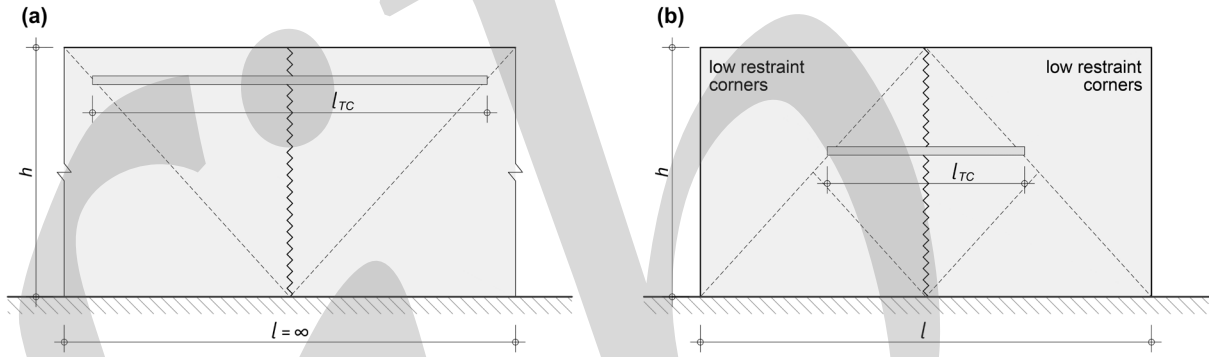


Fig. 5-17 Schematic illustration of tension chord lengths in base restrained walls: (a) Long wall ($l \rightarrow \infty$); (b) Short wall (or wall element between joints)[5-8]

5.5.2 SLS Design according to Model Code 2010 7.6.4.4[5-1]

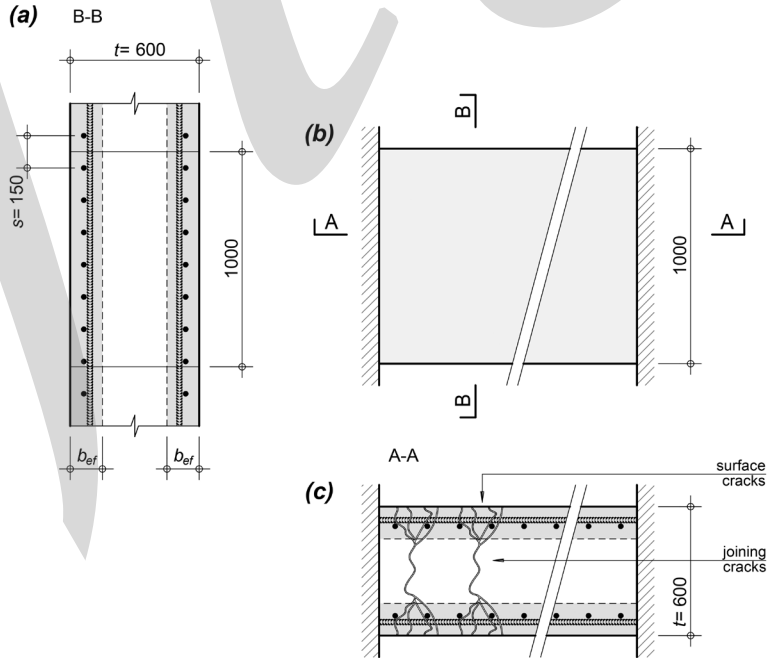


Fig. 5-18 Example wall (dimensions in mm): (a) Vertical Section B-B; (b) Elevation; (c) Cross-Section A-A

This document is the intellectual property of the fib – International Federation for Structural Concrete. All rights reserved.
This PDF of fib Bulletin 92 is intended for use and/or distribution solely within fib National Member Groups.

5.5.2.1 Effective reinforcement ratio

In thick walls ($t/2 > 2.5(c+ø/2)$), the surface cracks at the wall faces (see Fig. 5-18c) are distributed by the reinforcement and are finer than the joining cracks in the middle of the wall. If the surface cracks are small enough, they allow for self-healing, which prevents water from leaking through the joining cracks. The surface cracks tend to appear soon after casting, while the wall is cooling down after the heat release during hydration. Joining cracks are usually a result of restrained long term shrinkage strains. According to Fig. 7.6-4 (c) in Model Code 2010[5-1], the cracking behaviour of the surface cracks can be modelled assuming a tension chord with an effective area $A_{c,ef}$ with an effective width of:

$$\begin{aligned} t_{ef} &= 2.5\left(c+\frac{ø}{2}\right) < \frac{t}{2} \\ &= 2.5\left(40+\frac{14}{2}\right) = 118 \text{ mm} < 300 \text{ mm} \\ &= 2.5\left(40+\frac{16}{2}\right) = 120 \text{ mm} < 300 \text{ mm} \\ &= 2.5\left(40+\frac{18}{2}\right) = 123 \text{ mm} < 300 \text{ mm} \end{aligned} \tag{5-20}$$

With s = 150 mm this leads to an effective reinforcement ratio equal to:

$$\begin{aligned} \rho_{s,ef} &= \frac{A_s}{t_{ef}\cdot s} \\ &= \frac{154}{118\cdot 150} = 0.009 \\ &= \frac{201}{120\cdot 150} = 0.011 \\ &= \frac{254}{123\cdot 150} = 0.014 \end{aligned} \tag{5-21}$$

5.5.2.2 Max steel stress in surface crack during crack formation phase

During the crack formation phase, the maximum steel stress (in a crack) is defined by the cracking tensile force $N_r = A_{c,ef}\, f_{ctm}\, (1-\rho_{s,ef}+\alpha_e\cdot\rho_{s,ef})$ in the effective tension chord, as expressed (neglecting the term $\rho_{s,ef}$) by Eq. 7.6-6 of Model Code 2010[5-1]:

$$\begin{aligned} \sigma_{sr} &= \frac{f_{ctm}}{\rho_{s,ef}}\left(1+\alpha_e\cdot\rho_{s,ef}\right) \\ &= \frac{2.9}{0.009}\left(1+\frac{205}{30}0.009\right) = 342 \text{ N/mm}^2 \\ &= \frac{2.9}{0.011}\left(1+\frac{205}{30}0.011\right) = 283 \text{ N/mm}^2 \\ &= \frac{2.9}{0.014}\left(1+\frac{205}{30}0.014\right) = 227 \text{ N/mm}^2 \end{aligned} \tag{5-22}$$

All three horizontal reinforcement options (14/150, 16/150 and 18/150) meet the minimum reinforcement requirements, as the reinforcement does not yield upon cracking.

This document is the intellectual property of the fib – International Federation for Structural Concrete. All rights reserved.
This PDF of fib Bulletin 92 is intended for use and/or distribution solely within fib National Member Groups.

5.5.2.3 Transmission length of surface cracks

The transmission length (or transfer length) is the length on either side of a crack over which the perfect bond between the steel bars and the concrete is disturbed and slip occurs. It is the length necessary to build up the cracking tensile force in the net concrete section $N_{r,c} = A_{c,ef} \cdot f_{ctm}\,(1\text{-}\rho_{s,ef})$ with the bond stresses τ_{bms} acting at the interface between the steel bars and the concrete $N_{r,c} = l_{s,\max} \cdot \tau_{bms}\,\Sigma U$, where the circumference of the bars is $\Sigma U = 4A_s/\varnothing$. In addition the Model Code 2010[5-1] Eq. 7.6-4 (again neglecting the term $\rho_{s,ef}$) adds the empirical term k·c.

$$\begin{aligned} l_{s,\max} &= k \cdot c + \frac{1}{4}\frac{f_{ctm} \cdot \phi_s}{\tau_{bms} \cdot \rho_{s,ef}} \\ &= 40 + \frac{1}{4}\frac{2.9}{1.8 \cdot 2.9}\frac{14}{0.009} = 256 \text{ mm} \\ &= 40 + \frac{1}{4}\frac{2.9}{1.8 \cdot 2.9}\frac{16}{0.011} = 242 \text{ mm} \\ &= 40 + \frac{1}{4}\frac{2.9}{1.8 \cdot 2.9}\frac{18}{0.014} = 219 \text{ mm} \end{aligned} \tag{5-23}$$

to account for the influence of cover (as a simplification $k = 1$ can be assumed). Note that at the end of the crack formation phase the theoretical crack spacing varies between once and twice the transmission length.

5.5.2.4 Crack width of surface cracks during crack formation phase

Model Code 2010[5-1] Eq. 7.6-3 and Eq. 7.6-5 give the design crack width

$$\begin{aligned} w_d &= 2l_{s,\max}\left(\varepsilon_{sm} - \varepsilon_{cm} - \varepsilon_{cs}\right) = 2l_{s,\max}\left(\frac{\sigma_s - \beta \cdot \sigma_{sr}}{E_s} - \eta_r \cdot \varepsilon_{cs}\right) \\ &= 2 \cdot 256\left(\frac{342\left(1-0.6\right)}{205'000}\right) = 0.4 \text{ mm} \\ &= 2 \cdot 242\left(\frac{283\left(1-0.6\right)}{205'000}\right) = 0.3 \text{ mm} \\ &= 2 \cdot 219\left(\frac{227\left(1-0.6\right)}{205'000}\right) = 0.2 \text{ mm} \end{aligned} \tag{5-24}$$

During the crack formation phase $\sigma_s = \sigma_{sr}$. Parameters β and η_r are defined in Model Code 2010[5-1] Table 7.6.2.

5.5.2.5 End of crack formation phase

At the end of the crack formation phase there are $L/2_{ls,\max}$ cracks (assuming the maximum crack spacing) with widths according to Eq. (5-24), which (neglecting the concrete stresses) add up to the product of the imposed concrete strains and the wall length $|\varepsilon| \times L$. This leads to the imposed concrete strains necessary to conclude the crack formation phase, as expressed by Model Code 2010[5-1] Eq. 7.6-2

This document is the intellectual property of the fib – International Federation for Structural Concrete. All rights reserved.
This PDF of fib Bulletin 92 is intended for use and/or distribution solely within fib National Member Groups.

$$\left|\varepsilon\right| = \frac{\Delta L}{L} = \frac{\sigma_{sr}\left(1-\beta\right)}{E_s}$$
$$= \frac{342\left(1-0.6\right)}{205'000} = 0.67‰ > 0.15‰ + 0.35‰$$
$$= \frac{283\left(1-0.6\right)}{205'000} = 0.55‰ > 0.15‰ + 0.35‰ \qquad (5\text{-}25)$$
$$= \frac{227\left(1-0.6\right)}{205'000} = 0.44‰ > 0.15‰ + 0.35‰$$

For the options 14/150 and 16/150 the end of the crack formation phase is not reached, while for option 18/150 the assumed strains of -0.15 ‰ (cooling after hydration) plus -0.35‰ (shrinkage) complete the crack formation phase. This means evenly distributed cracks along the entire length of the wall.

5.5.3 Discussion

According to Eq. (5-24), which is based on the assumption of completely restrained shrinkage and hydration-induced strains in the effective tension chords, the basement wall requires a horizontal reinforcement of 18/150 (for the 1st and 4th layer) to ensure water tightness ($w_d < 0.2$ mm). This will result in approximately between 2 and 4 primary cracks max. 0.2 mm wide per meter at the top of the wall (see Fig. 5-19). At the bottom of the wall the base cracks will be significantly smaller than 0.2 mm because the base restraint contributes towards the distribution of the cracks.

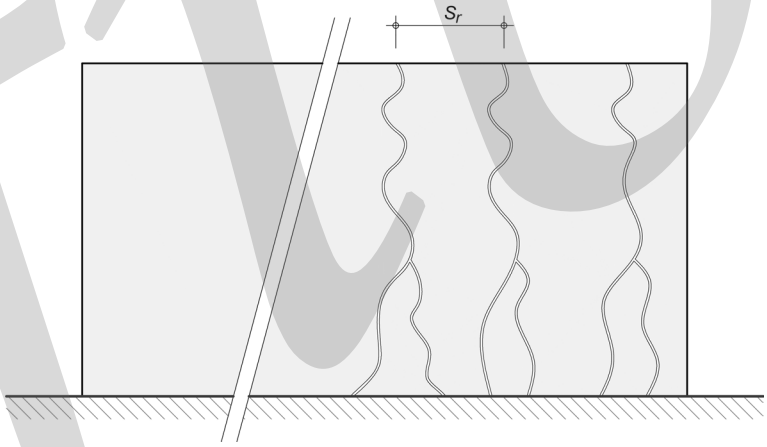


Fig. 5-19 Example wall showing crack spacing

5.5.4 Evenly spaced construction joints

A commonly used method for reducing the amount of horizontal reinforcement in long waterproof walls is the placement of construction joints with internal water stoppers at a prescribed spacing (e.g. approximately 2*h*). This method has three main advantages:

- Reduction of the degree of restraint for early-age cracking (due to early shrinkage and hydration-induced concrete strains) by gaining low restraint wall corners and thereby reducing the amount of (or in the best of cases eliminating) primary cracks with their widths defined by the reinforcement and not by the base restraint.

This document is the intellectual property of the fib – International Federation for Structural Concrete. All rights reserved.
This PDF of fib Bulletin 92 is intended for use and/or distribution solely within fib National Member Groups.

- Reduction of the residual concrete strains after joining at the construction joints, because early-age strains have already taken place.

- Facilitation of large (induced) cracks at the joints through smooth joints, blunt splices and section reducing joint bands to absorb the residual concrete strains after joining at the construction joints.

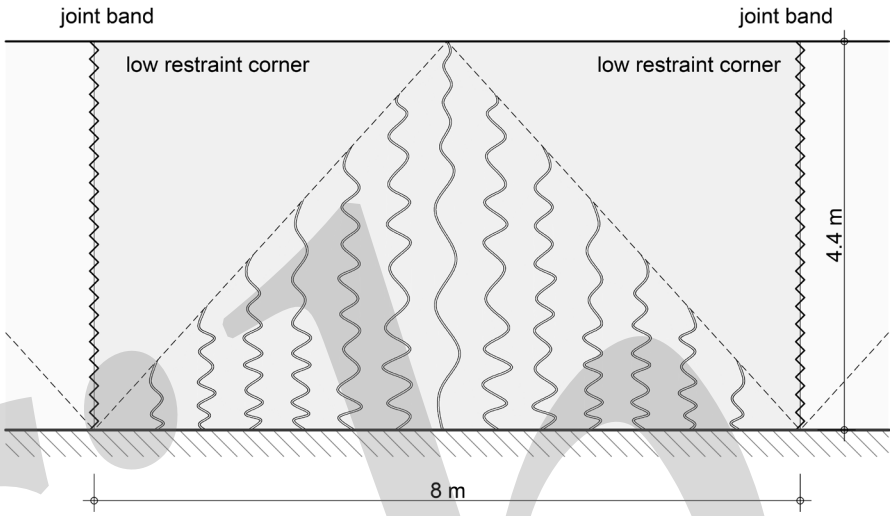


Fig. 5-20 Example wall with construction joints spaced at approximately 2*h*

In this case, one could consider choosing one of the solutions for reinforcement of 14/150 or 16/150, bearing in mind, that despite the above measures for reducing the number of primary cracks, there will be occasional cracks > 0.2 mm (up to 0.4 mm) which will need to be injected up to approximately 2 years after the wall is cast. This means that they must be accessible. With this strategy it is advisable to ensure that the concrete (tensile) strength does not excessively exceed the requested value, as in this case cracks larger than 0.4 mm may occur.

5.5.5 On-site experience

The example wall was built with a horizontal reinforcement of 14/150 with construction joints spaced at approximately 8 m. There were occasional leaking cracks that occurred up to one year after casting and had to be sealed.

5.6 Deflection analysis

5.6.1 Example of application of the general method

Consider a continuous one-way floor slab of 3 equal spans of 12 m, composed of precast pre-tensioned hollow core slabs of 250 mm total depth and 1200 mm width, and a 100 mm thick top cast-in-place reinforced concrete slab, as indicated by Fig. 5-21. The hollow core slab is pre-stressed at 7 days after casting, by means of 5 strands of A_{pi} = 140 mm^2 area each, providing a total pre-stressing force of 933 kN , after anchorage slip losses (σ_{p0} = 1'332 MPa). The eccentricity of the strands with respect to the centre of gravity of the slab is 75 mm.

This document is the intellectual property of the fib – International Federation for Structural Concrete. All rights reserved.
This PDF of fib Bulletin 92 is intended for use and/or distribution solely within fib National Member Groups.

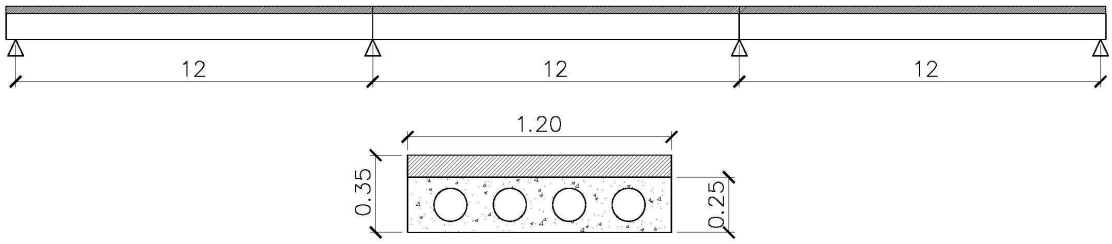


Fig. 5-21 Continuous floor slab layout and cross section

The precast elements are placed on site, working as simply supported beams with a span of 11.80 m. A top layer of mild reinforcement is placed on top at 50 mm of the upper face, consisting on a welded wire rod of 6 mm diameter bars spaced 100·100 mm along the whole structure length, plus additional 12 mm diameter bars at 100 mm spacing and extended longitudinally for 3 m on both sides of the two internal supports. At an age of 28 days the top concrete slab is poured, filling also the space between the hollow core slabs, creating a rigid joint of 1'200 × 350 mm rectangular section.

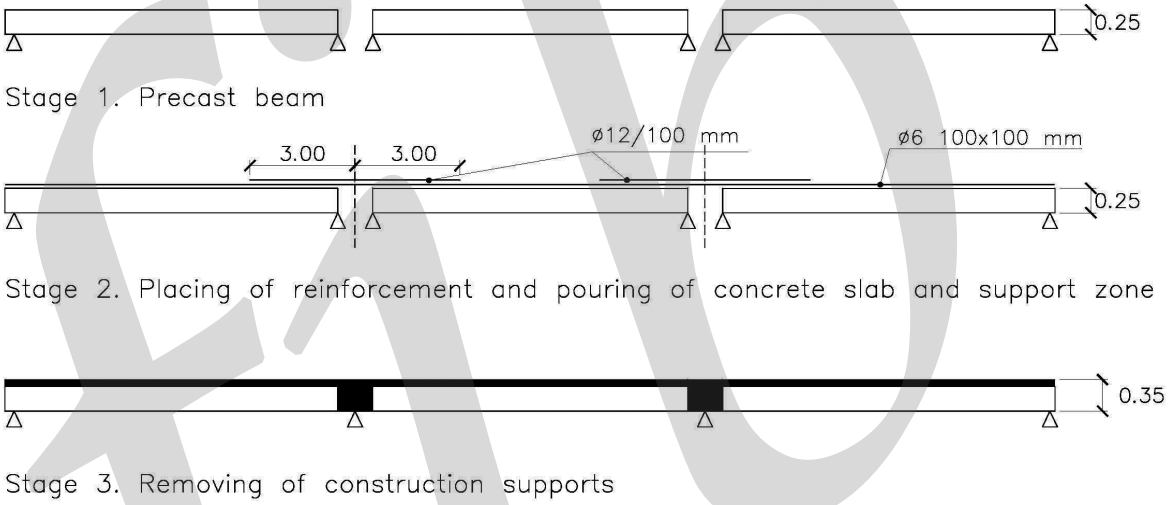


Fig. 5-22 Construction stages

As the top concrete slab hardens, continuity between the three simply supported members takes place, so that the negative moments over the supports, due to the live loads, will be resisted by the top mild reinforcement and by the bottom compression stresses in the concrete.

At the age of 56 days, the characteristic load is applied over the whole structure length, to pre-crack this top slab under negative moments. Afterwards, the quasi-permanent portion of the live load (0.2 Q) is applied over the lateral spans and maintained until 10000 days. Then the rest of the live load is applied again on the lateral spans, to obtain the characteristic load combination at long term. The load combination factors for service limit states are: $\psi_1 = 0.5$ and $\psi_2 = 0.2$ (for frequent and quasi-permanent loads, respectively)

The material characteristics are:

- Hollow core slabs: Concrete C40/45 $f_{c28} = 40$ MPa, $f_{ct,28} = 3.5$ MPa, $E_{c,28} = 32'826$ MPa
- Top slab concrete: C30/35 $f_{c28} = 30$ MPa, $f_{ct,28} = 2.9$ MPa, $E_{c,28} = 35'520$ MPa

This document is the intellectual property of the fib – International Federation for Structural Concrete. All rights reserved.
This PDF of fib Bulletin 92 is intended for use and/or distribution solely within fib National Member Groups.

- Prestressing strands: f_{pu} = 1'860 MPa, f_{pyk} = 1'670 MPa, E_p = 195'000 MPa, Final relaxation = 6%
- Mild reinforcement: f_y = 500 MPa, E_s = 200'000 MPa

The prestressing is designed so that at the construction stage, under the weight of the hollow core and the top slab, working as simply supported, no cracking takes place. In addition, at service, under the frequent load combination, the crack width is limited to 0.2 mm. On the other hand, the maximum deflection at long term under the characteristic load combination is limited to *l*/250.

A step by step non-linear and time-dependent analysis model has been used to analyse the structure, considering the construction phases, in order to check the stresses and deflections under service load conditions, implemented in the computer program CONS [5-9].

In Fig. 5.6-3 a number of representative results obtained with the model are presented and analysed. The origin of time considered is the casting of the precast member (t_0 = 0).

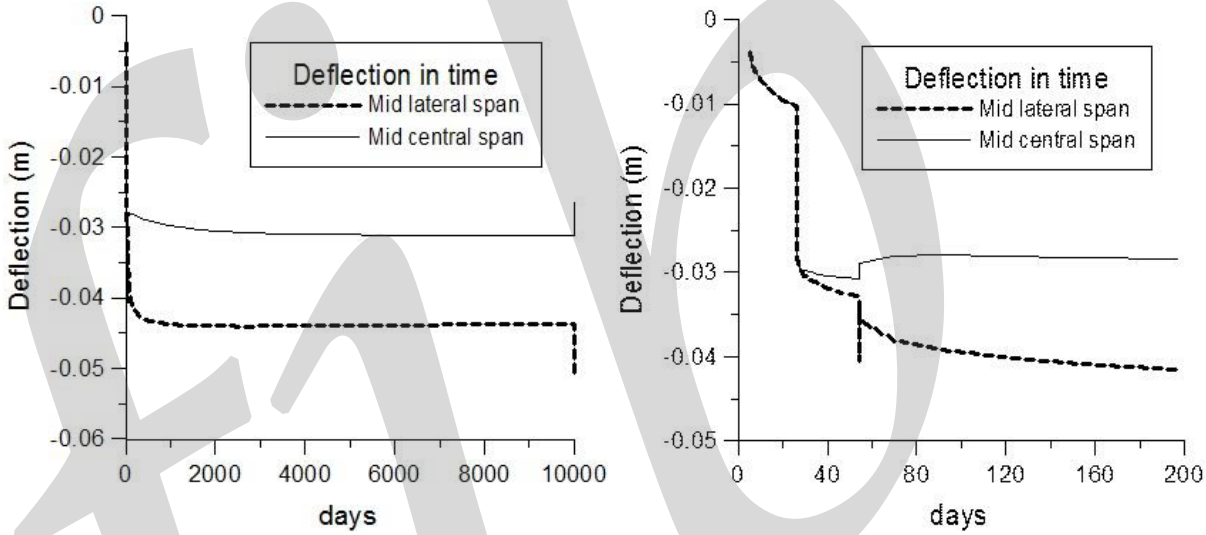


Fig. 5-23 Midspan and lateral span deflection in time a) until 10000 days b) 200 days

Fig. 5-23a shows the evolution over time of deflections at the centre of the lateral and central spans. Fig. 5-23b is a "zoom" of Fig. 5-23a, showing more clearly the deflections during the construction phase and short term at service. It can be seen that, according to the load distribution assumed, the deflection of the lateral spans is much higher than that of the central span. The total deflection in the long term, including the instantaneous and the time-dependent deflections due to the quasi-permanent loads, plus the instantaneous deflection due to the rest of live load applied at 10'000 days is around 45 mm. This value represents *l*/275, which is near the considered limit (*l*/250), usually established to avoid damage to non-structural elements.

This document is the intellectual property of the fib – International Federation for Structural Concrete. All rights reserved.
This PDF of fib Bulletin 92 is intended for use and/or distribution solely within fib National Member Groups.

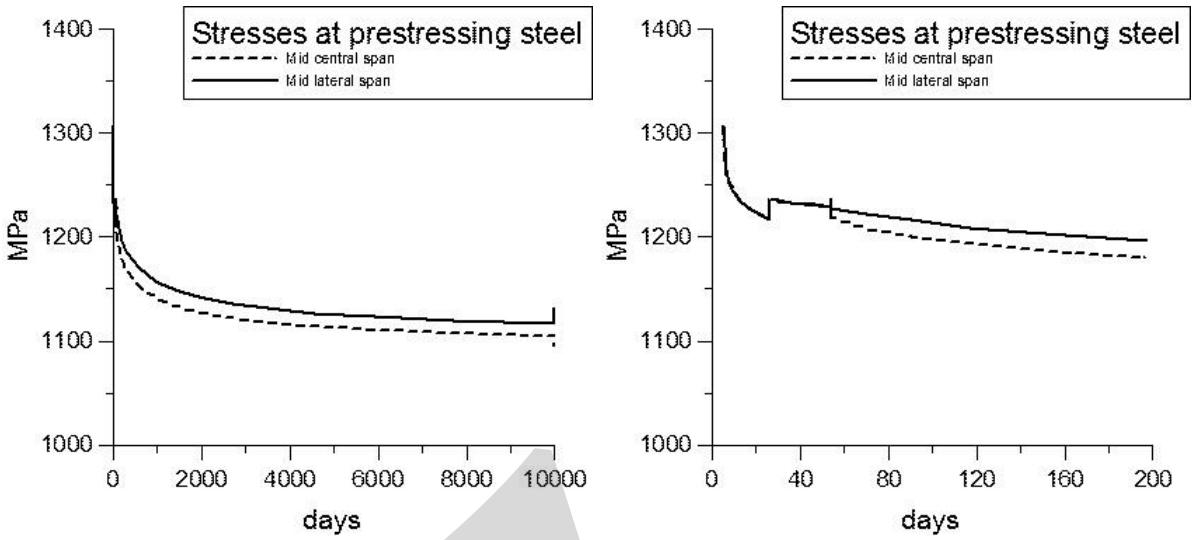


Fig. 5-24 Stresses at prestressing steel a) stresses until 10000 days b) 200 days

Fig. 5-24a shows the evolution along the time of the stresses at the pre-stressing tendons at the centre of the central and lateral spans. Fig. 5-24b is a "zoom" of Figure 5-24a, showing the stresses during the construction process. It is observed that instantaneous losses due to elastic shortening are $\Delta\sigma_{p,el}$ =1'332-1'240= 92 MPa (6,9% of $\sigma_{p,0}$), while the long-term losses $\Delta\sigma_{p,def}$, are: $\Delta\sigma_{p,def}$, = 1'240-1'120 = 120 MPa (9,0 % of $\sigma_{p,0}$), being the total losses (without including anchorage slip) $\Delta\sigma_p$ = 212 MPa (15.9%) at the centre of the lateral span.

Figs. 5-25a and b show the evolution with time of the bending moments at the centre of the lateral span and over the supports. During the construction process, no bending moments occur at the support, since the hollow core slabs work as simply supported. Negative moments appear under live load. Under the quasi-permanent load combination, a reduction of the negative moment and an increment of positive moments load takes place over time, to make the delayed deformations of the elements compatible with the constraints introduced by the construction process.

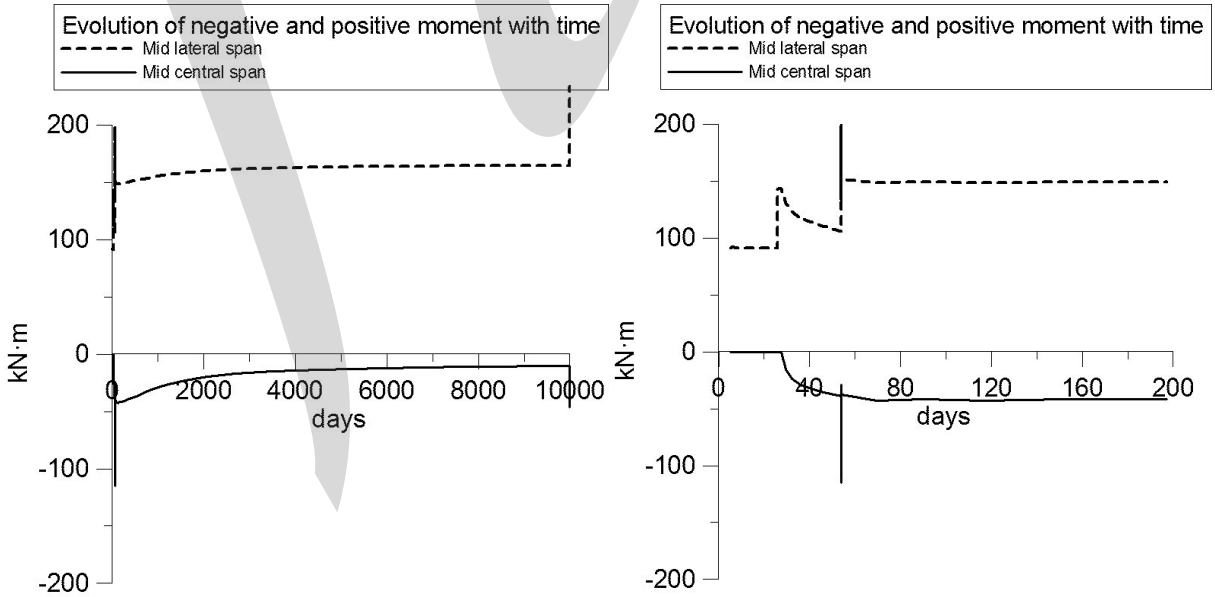


Fig. 5-25 Evolution of mid lateral span and central span moment a) until 10'000 days b) 200 days

This document is the intellectual property of the fib – International Federation for Structural Concrete. All rights reserved.
This PDF of fib Bulletin 92 is intended for use and/or distribution solely within fib National Member Groups.

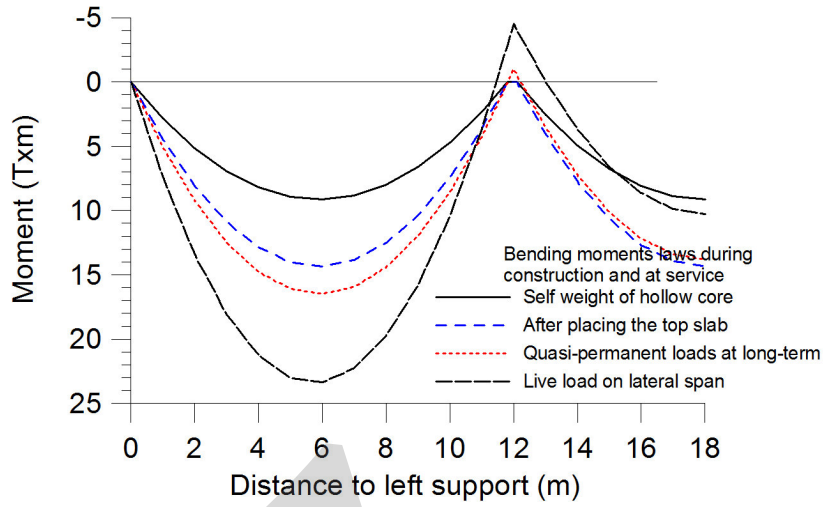


Fig. 5-26 Evolution of the bending moments law in different construction stages

Fig. 5-27 shows the crack patterns along the member at long-term under the characteristic load combination. It is observed that cracks appear both in the top slab, over the supports, and at the bottom of the hollow core slab at the centre of the lateral span.

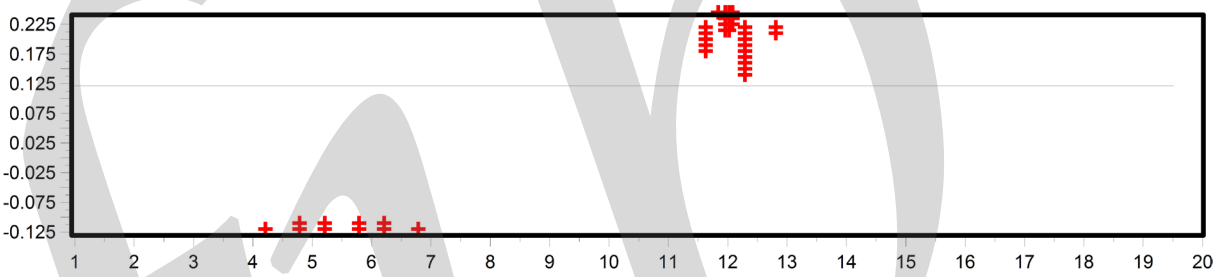


Fig. 5-27 Crack patterns at three instants of time and load levels

Fig. 5-28 shows the stresses in the top reinforcement, placed at mid-depth of the cast-in-place slab, over the support. It is observed that such reinforcement is under compression, even though is placed in the negative bending moment zone. The reason for that is twofold: on the one hand, shrinkage of concrete compresses the reinforcement; on the other, even though the live load produces tensile stresses in the steel (see Fig. 5-28b at long-term), the reduction of the negative bending moment with time increases the compression in the top slab and, thus, on the reinforcement.

This document is the intellectual property of the fib – International Federation for Structural Concrete. All rights reserved.
This PDF of fib Bulletin 92 is intended for use and/or distribution solely within fib National Member Groups.

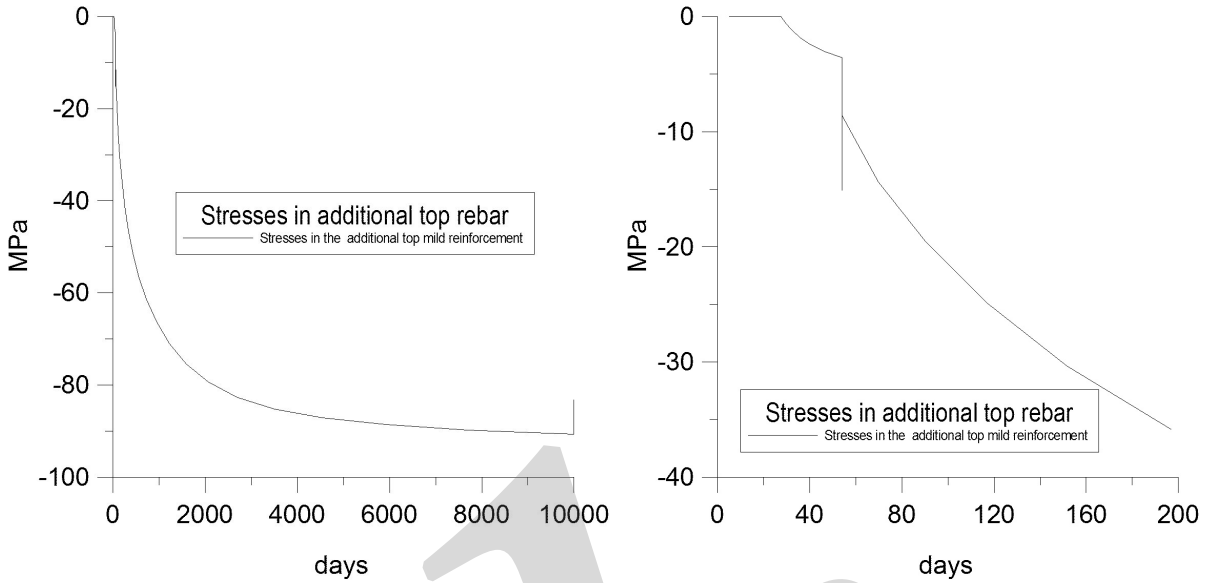


Fig. 5-28 Stresses in the additional top mild reinforcement: a) at 10000 days b) 200 days

Finally, Fig. 5-29 shows the stresses at the section of the lateral span with maximum bending moment (x ≅ 6.5 m). It can be observed that the hollow core slab is fully compressed initially. After pouring the cast in place concrete slab, the bottom of the hollow core slab is subject to tensile stresses, slightly lower than the tensile concrete strength, as required in the design. The redistribution of moments relaxes such tensile stresses over time.

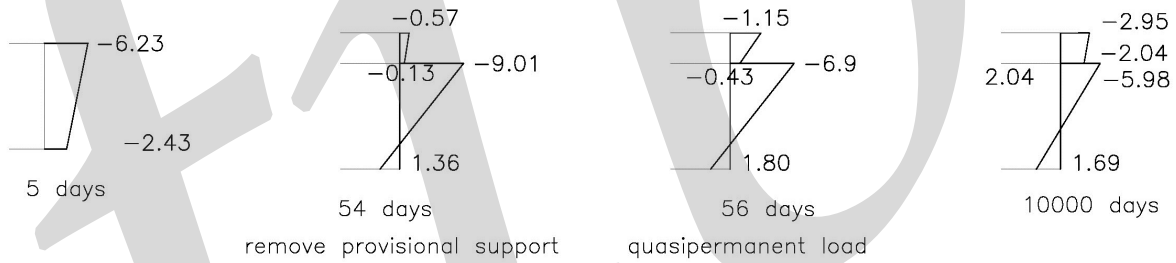


Fig. 5-29 Evolution of concrete stresses at the precast and cast in place concrete slabs

The above results show the capabilities of non-linear and time-dependent analysis models to capture the complex behaviour in service of segmentally constructed structures. The interaction between the effects of cracking, creep, shrinkage, prestressing and changes on the geometry and structural scheme would have been almost impossible to capture by simplified analysis models.

5.6.2 Example of application of simplified methods. Deflection control of a reinforced concrete slab

Consider a simply supported one-way slab of 6 m span, 300 mm total depth and effective depth d = 250 mm Fig. 5-30. The slab is subjected to a dead load g = 12 kN/m^2 and a live load q = 8 kN/m^{2,} both applied at 28 days after casting. A factor ψ_2 = 0.2 is used for the quasi-permanent load combination.

This document is the intellectual property of the fib – International Federation for Structural Concrete. All rights reserved.
This PDF of fib Bulletin 92 is intended for use and/or distribution solely within fib National Member Groups.

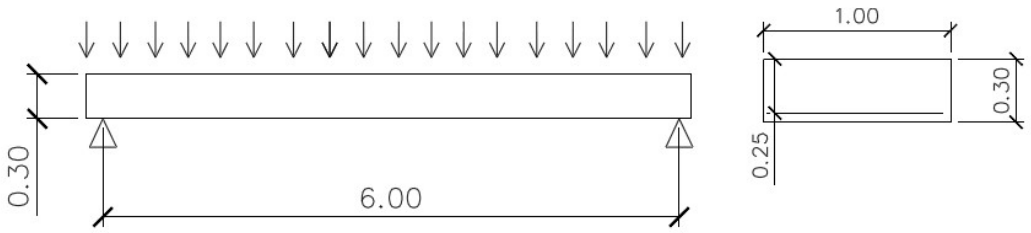


Fig. 5-30 Simply supported slab and cross section

The characteristic strength of concrete at 28 days is f_{ck} = 30 N/mm^2. The tensile reinforcement consists of bars of 20 mm diameter with 200 mm spacing (A_{sl} = 1'570 mm^2/m, ρ = 0.00628). Characteristic yield strength of reinforcement is f_{yk} = 500 N/mm^2. No compressive reinforcement is considered.

The instantaneous modulus of elasticity of concrete at 28 days is E_c = 32'836 N/mm^2, and the modulus of elasticity of steel is E_s = 200'000 N/mm^2, so the modular ratio is $\alpha_s = E_s/E_c$ = 6.09. The mean tensile strength of concrete is f_{ctm} = 2.89 N/mm^2. The value of creep coefficient considered is $\varphi(t, t_0) = 2$ and the shrinkage strain value ε_{sh} = 0.0003.

The actual slenderness ratio of the slab is l/d = 6/0.25=24. According to EC2 slenderness limits, the slenderness ratio should be less than l/d = 20, approximately, for a lightly stressed concrete element ($\rho \cong 0.5\%$). Therefore, in this case deflections should be checked by calculations.

The bending moment due to dead and live loads are M_g = 54 kNm and M_q = 36 kNm, respectively. The bending moment under the characteristic load combination is M_{Ed} = 90 kNm. The bending moment under the quasi-permanent load combination is M_{quasi} = 61.2 kNm.

5.6.2.1 Instantaneous deflection under the characteristic load combination

The instantaneous deflections in the uncracked and fully cracked states are calculated using the moments of inertia I_I =2.343·10^{-3} m^4 (moment of inertia of uncracked section) and I_{II} = 4.17·10^{-4} m^4 (moment of inertia of cracked section), respectively, according to the following expression:

$$a_{inst} = \frac{5(g+q)l^4}{384E_c \cdot I} \tag{5-26}$$

in uncracked elastic state (State I):

$a^I_{g,inst}$ = 2.63 mm, $a^I_{q,inst}$ = 1.75 mm and $a^I_{inst,tot}$ = 4.38 mm,

in cracked elastic state (State II):

$a^{II}_{g,inst}$ = 14.78 mm, $a^{II}_{q,inst}$ = 9.85 mm and $a^{II}_{inst,tot}$ = 24.63 mm

The curvature (and deflections) interpolation factor ζ is given by the following expression, with β factor equal to 0.5 (considering the load is applied repeatedly many times):

$$\zeta = 1 - \beta\left(\frac{M_{cr}}{M_a}\right)^2 = 1 - 0.5\left(\frac{46}{90}\right)^2 = 0.87 \tag{5-27}$$

This document is the intellectual property of the fib – International Federation for Structural Concrete. All rights reserved.
This PDF of fib Bulletin 92 is intended for use and/or distribution solely within fib National Member Groups.

Where M_{cr} = 46 kN·m is the cracking moment and M_a is the design value of bending moment acting at the critical cross section under the characteristic load combination. Then, the instantaneous deflection is calculated by:

$$a_{inst} = \zeta a_{inst}^{II} + \left(1-\zeta\right)a_{inst}^{I} = 0.87 \cdot 24.63 + \left(1-0.87\right)4.38 = 21.99 \text{ mm} \quad (5\text{-}28)$$

Alternatively, the instantaneous deflection of a member can be calculated using an effective moment of inertia for the element I_{eff} obtained as follows:

$$I_{eff} = \frac{I_I \cdot I_{II}}{\zeta I_I + \left(1-\zeta\right)I_{II}} = \frac{2.343 \cdot 10^{-3} \cdot 4.17 \cdot 10^{-4}}{0.87 \cdot 2.343 \cdot 10^{-3} + \left(1-0.87\right)4.17 \cdot 10^{-4}} = 4.667 \cdot 10^{-4} \text{ m}^4 \quad (5\text{-}29)$$

The instantaneous deflection a_{inst} in a simply supported beam due to the characteristic load is:

$$a_{inst} = \frac{5\left(g+q\right)l^4}{384E_c \cdot I_{eff}} = \frac{5\left(12+8\right)6^4}{384 \cdot 32'836'000 \cdot 4.667 \cdot 10^{-4}} = 22.00 \text{ mm} \quad (5\text{-}30)$$

As it can be seen both ways of determining the instantaneous deflections are equivalent.

Similarly, the instantaneous deflection due to the quasi-permanent load combination, taking into account the un-cracked and cracked inertia are 2.98 mm and 16.75 mm, respectively. The instantaneous deflection due to quasi-permanent load is 14.97 mm.

5.6.2.2 Long-term deflections

5.6.2.2.1 Long-term deflection due to creep

Sustained load produces creep of concrete, thus increasing the slab deflection with time. The long-term deflection is obtained for the quasi-permanent load combination, according to MC2010[5-1], sect. 7.6.5.1.2:

The instantaneous plus the creep deflection can be approximately calculated using an effective modulus of elasticity for concrete:

$$E_{ceff} = \frac{E_{cm}}{1+\varphi\left(t,t_0\right)} = \frac{32'836}{1+2} = 10'945 \text{ N/mm}^2 \quad (5\text{-}31)$$

The modular ratio for long-term loads is $n_{eff} = E_s/E_{c,ef}$ = 18.27 which can be used both for the calculation of the inertia in the uncracked and cracked elastic states. The new uncracked moment of inertia is $I_{I,ef} = 2.512 \cdot 10^{-3}$ m^4, and the instantaneous plus creep deflection, due to the quasi-permanent load, in State I can be obtained as follows:

$$a_{inst+\varphi}^{I} = \frac{5\left(g+0.2q\right)l^4}{384E_{ceff} \cdot I_{I,ef}} = 8.35 \text{ mm} \quad (5\text{-}32)$$

So the creep deflection in the uncracked state for the quasi-permanent combination will be:

$$a_{\varphi}^{I} = 8.35 - 2.98 = 5.37 \text{ mm} \quad (5\text{-}33)$$

The cracked moment of inertia calculated with n_{eff} = 18.27 results to be $I_{II} = 9.75 \cdot 10^{-4}$m^4. Then, the instantaneous plus the creep deflection in the cracked elastic state (State II) will be:

This document is the intellectual property of the fib – International Federation for Structural Concrete. All rights reserved.
This PDF of fib Bulletin 92 is intended for use and/or distribution solely within fib National Member Groups.

$$a_{inst+\varphi}^{II} = \frac{5\left(g+0.2q\right)l^4}{384E_{eff}\cdot I_{II,ef}} = \frac{5\left(12+0.2\cdot 8\right)6^4}{384\cdot 10'945'000\cdot 975\cdot 10^{-4}} = 0.0215 = 21.50 \text{ mm} \qquad (5\text{-}34)$$

Then, the creep deflection in the cracked state for the quasi-permanent combination will be:

$$a_{\varphi}^{II} = 21.50 - 16.75 = 4.75 \text{ mm} \qquad (5\text{-}35)$$

Where 16.75mm is the instantaneous deflection under the quasi-permanent loads, previously obtained. Therefore, the instantaneous plus creep deflection due to the quasi-permanent load will be (using interpolation factor $\zeta = 0.87$):

$$a_{inst+\varphi} = \zeta a_{inst+\varphi}^{II} + \left(1-\zeta\right)a_{inst+\varphi}^{I} = 0.87\cdot 21.50 + \left(1-0.87\right)8.35 = 19.79 \text{ mm} \qquad (5\text{-}36)$$

Thus the deflection caused by the creep in the simple supported beam is:

$$a_{\varphi} = 19.79 - 14.97 = 4.82 \text{ mm} \qquad (5\text{-}37)$$

5.6.2.2.2 Long-term deflection due to shrinkage

Shrinkage curvatures may be assessed by:

$$\frac{1}{r_{sh}} = \psi_{sh} = \varepsilon_{sh}\cdot n_{eff}\frac{S}{I} \qquad (5\text{-}38)$$

where:

ψ_{sh} is the curvature due to shrinkage

ε_{sh} is the free shrinkage strain

S is the first moment of area of the reinforcement about the centroid of the section

I is the second moment of area of the section

n_{eff} is the effective modular ratio = E_s/E_{eff}

S and I are calculated for the uncracked and the fully cracked condition, using an effective modulus of elasticity for concrete.

Their values are:

- in uncracked elastic state (State I) $S_I = 0.000144\,\text{m}^3$, $I_I = 0.002512\,\text{m}^4$
- in cracked elastic state (State II) $S_{II} = 0.0002442\,\text{m}^3$, $I_{II} = 0.0009746\,\text{m}^4$

The curvatures in the uncracked and cracked states are:

$$\frac{1}{r_{sh}} = \psi_{sh} = \varepsilon_{sh}\cdot n_{eff}\frac{S}{I} \qquad (5\text{-}39)$$

$$\left(\frac{1}{r}\right)_{sh}^{I} = 0.0003142 \quad ; \quad \left(\frac{1}{r}\right)_{sh}^{II} = 0.001373 \quad ; \qquad (5\text{-}40)$$

The deflections are calculated from the shrinkage curvatures, for a simply supported beam as:

$$a_{sh}^{I} = \left(\frac{1}{r}\right)_{sh}^{I}\frac{l^2}{8} = 1.41\,\text{mm}; \quad a_{sh}^{II} = \left(\frac{1}{r}\right)_{sh}^{II}\frac{l^2}{8} = 6.18 \text{ mm} \qquad (5\text{-}41)$$

This document is the intellectual property of the fib – International Federation for Structural Concrete. All rights reserved.
This PDF of fib Bulletin 92 is intended for use and/or distribution solely within fib National Member Groups.

And using the interpolation equation with $\zeta = 0.87$:

$$a_{sh} = \zeta a_{sh}^{II} + \left(1-\zeta\right)a_{sh}^{I} = 0.87 \cdot 6.18 + \left(1-0.87\right)1.41 = 5.56 \text{ mm} \tag{5-42}$$

The long-term deflection due to creep and shrinkage will be:

$$a_{\varphi+sh} = 4.82 + 5.56 = 10.38 \text{ mm} \tag{5-43}$$

and the total long-term deflection due to sustained loads is:

$$a_{total} = 14.97 + 10.38 = 25.33 \text{ mm} \tag{5-44}$$

which represents *l*/237.

5.6.2.3 Long-term deflections calculated by the simplified kinematics model

The long-term deflections under the quasi-permanent load will be calculated now using the simplified method described in section 2.2.3.2, which assumes constant stress and strain at the longitudinal tensile reinforcement along the time. To calculate the long-term deflection, the instantaneous deflection due to the quasi-permanent load, previously calculated by the interpolation method, will be used (14.97 mm.).

The long term deflection will be calculated by the following expression

$$\Delta y = \Delta y_{\varphi} + \Delta y_{sh} = y_{inst}\frac{x_0}{d}\frac{0.84\varphi - 0.20}{1+12n\cdot\rho_m^{'}} + \frac{\varepsilon_{sh}}{d}\frac{1}{1+12n\cdot\rho_m^{'}}k_{sh}\frac{l^2}{8} =$$

$$14.97 \cdot 0.241\left(0.84\cdot 2 - 0.20\right) + \frac{0.0003\cdot 6'000^2}{250\cdot 8} = 5.34 + 5.40 = 10.74 \text{ mm} \tag{5-45}$$

where

y_{inst} = 14.97 mm (instantaneous deflection due to quasi-permanent load)

$$\frac{x_0}{d} = n\cdot\rho\left(-1+\sqrt{1+\frac{2}{n\cdot\rho}}\right) = 0.241 \tag{5-46}$$

k_{sh} = 1, for a simply supported beam

5.6.3 Solution of the problem by the General Sectional Method

The same problem is solved using the methodology presented in 4.3.1.3.

Deformations in the midspan section are to be calculated. The reference point is fixed at the top of the section.

The applied forces are:

$$\Delta N = 0$$

$$\Delta M = \frac{\left(g+q\right)l^2}{8} = \frac{20\cdot 6^2}{8} = 90\text{kN}\cdot\text{m}$$

1. Instantaneous deformations in the uncracked state

$$\Delta\varepsilon_0 = \frac{I\Delta N - B\Delta M}{E_c\left(A\cdot I - B^2\right)} \tag{5-47}$$

This document is the intellectual property of the fib – International Federation for Structural Concrete. All rights reserved.
This PDF of fib Bulletin 92 is intended for use and/or distribution solely within fib National Member Groups.

$$\Delta\psi = \frac{B\Delta N + A\Delta M}{E_c\left(A \cdot I - B^2\right)} \tag{5-48}$$

The properties of the transformed section at time t_0:

$$\begin{aligned} A &= 1'000 \cdot 300 + \left(6.09 - 1\right)1'570 = 308 \cdot 10^3 \text{ mm}^2 \\ B &= 1'000 \cdot 300 \cdot 300 / 2 + \left(6.09 - 1\right)1'570 \cdot 250 = 47 \cdot 10^6 \text{ mm}^3 \\ I &= 1/3 \cdot 1'000 \cdot 300^3 + \left(6.09 - 1\right)1'570 \cdot 250^2 = 9'500 \cdot 10^6 \text{ mm}^4 \end{aligned} \tag{5-49}$$

Therefore the instantaneous curvature and the deformation at the reference point are:

$$\varepsilon^{I}_{0inst} = -179.7 \cdot 10^{-6};\ \psi^{I}_{0inst} = 1.177 \cdot 10^{-6} \text{ mm}^{-1} \tag{5-50}$$

Assuming parabolic distribution of curvatures[5-10]

$$a^{I}_{0inst} = \frac{L^2}{96} 10 \cdot \psi_{centre} \tag{5-51}$$

the instantaneous deflection due to total load (g+q) is 4.414 mm

2. Instantaneous deformations in the fully cracked state

Neutral axis depth is 60.20 mm.

Properties of the transformed section at time t_0 are:

$$\begin{aligned} A &= 1'000 \cdot 60.2 + \left(6.09\right)1'570 = 69.76 \cdot 10^3 \text{ mm}^2 \\ B &= 1'000 \cdot 60.2 \cdot 60.2 / 2 + \left(6.09\right)1'570 \cdot 250 = 4.202 \cdot 10^6 \text{ mm}^3 \\ I &= 1/3 \cdot 1'000 \cdot 60.2^3 + \left(6.09\right)1'570 \cdot 250^2 = 670.3 \cdot 10^6 \text{ mm}^4 \end{aligned} \tag{5-52}$$

$$\Delta N = 0; \quad \Delta M = 90 \text{kN} \cdot \text{m} \tag{5-53}$$

therefore

$$\varepsilon^{II}_{0inst} = -395.7 \cdot 10^{-6};\ \psi^{II}_{0inst} = 6.576 \cdot 10^{-6} \text{ mm}^{-1} \tag{5-54}$$

The instantaneous total deflection in the fully cracked state is 24.63 mm

3. Time-dependent deformations in the uncracked state

Considering $\varphi(t,t_0) = 2$, $\varepsilon_{sh} = -300 \cdot 10^{-6}$, $\chi = 0.8$

$$\begin{aligned} \overline{E}_c &= \frac{E_c}{1 + \chi \cdot \varphi} = \frac{32'836}{1 + 0.8 \cdot 2} = 12'629 \text{N/mm}^2 \\ \overline{\alpha} &= \frac{E_s}{E_c} = 15.84 \end{aligned} \tag{5-55}$$

Properties of the age-adjusted transformed section:

$$\begin{aligned} \overline{A} &= 1'000 \cdot 300 + \left(15.84 - 1\right)1'570 = 323.3 \cdot 10^3 \text{ mm}^2 \\ \overline{B} &= 1'000 \cdot 60.2 \cdot 60.2 / 2 + \left(15.84 - 1\right)1'570 \cdot 250 = 50.82 \cdot 10^6 \text{ mm}^3 \\ \overline{I} &= 1/3 \cdot 1'000 \cdot 300^3 + \left(15.84 - 1\right)1'570 \cdot 250^2 = 10'456 \cdot 10^6 \text{ mm}^4 \end{aligned} \tag{5-56}$$

This document is the intellectual property of the fib – International Federation for Structural Concrete. All rights reserved.
This PDF of fib Bulletin 92 is intended for use and/or distribution solely within fib National Member Groups.

Taking into account the instantaneous deformations due to quasi permanent load $(g + 0.2q)$ =13.6 kN/ml

$$\varepsilon^{I}_{0qp} = -179.7 \cdot 10^{-6}\left(\frac{13.60}{20}\right) = -122.2 \cdot 10^{-6}$$
$$\psi^{I}_{qp} = 1.177 \cdot 10^{-6}\left(\frac{13.60}{20}\right) = 0.800 \cdot 10^{-6}\ \text{mm}^{-1} \tag{5-57}$$

$$\Delta N^{0}_{creep} = \overline{E}_c \cdot \varphi\left(A_c \cdot \varepsilon_0 + B_c \cdot \psi\right)$$
$$\Delta N^{0}_{sh} = \overline{E}_c \cdot \varepsilon_{sh} \cdot A_c$$
$$\Delta M^{0}_{creep} = \overline{E}_c \cdot \varphi\left(B_c \cdot \varepsilon_0 + I_c \cdot \psi\right) \tag{5-58}$$
$$\Delta M^{0}_{sh} = \overline{E}_c \cdot \varepsilon_{sh} \cdot B_c$$

$$A_c = 1'000 \cdot 300 = 300 \cdot 10^3\ \text{mm}^2$$
$$B_c = 1'000 \cdot 300^2 / 2 = 45 \cdot 10^6\ \text{mm}^3 \tag{5-59}$$
$$I_c = 1/3 \cdot 1'000 \cdot 300^3 = 9'000 \cdot 10^6\ \text{mm}^4$$

therefore

$$\Delta N^{0}_{creep} = -16.67 \cdot 10^3 N;\ \Delta N^{0}_{sh} = 1137 \cdot 10^3 N$$
$$\Delta M^{0}_{creep} = 42.96 \cdot 10^6 N \cdot \text{mm}\ ;\ \Delta M^{0}_{sh} = -170.5 \cdot 10^6 N \cdot \text{mm}$$

$$\Delta\varepsilon^{I}_{creep} = -234 \cdot 10^{-6};\ \Delta\varepsilon^{I}_{sh} = -320 \cdot 10^{-6}$$
$$\Delta\psi^{I}_{creep} = 1.463 \cdot 10^{-6} \rightarrow a^{I}_{creep} = 5.49\ \text{mm} \tag{5-60}$$

Assuming constant distribution of shrinkage curvatures

$$a = \psi_{sh}\frac{L^2}{8}$$
$$\Delta\psi^{I}_{sh} = 0.264 \cdot 10^{-6} \rightarrow a^{I}_{sh} = 1.19\ \text{mm} \tag{5-61}$$

4. Time-dependent deformations in the fully cracked state:

$$\overline{A} = 1'000 \cdot 60.2 + 15.84 \cdot 1'570 = 85.07 \cdot 10^3\ \text{mm}^2$$
$$\overline{B} = 1'000 \cdot 60.2 \cdot 60.2 / 2 + 15.84 \cdot 1'570 \cdot 250 = 8.029 \cdot 10^6\ \text{mm}^3 \tag{5-62}$$
$$\overline{I} = 1/3 \cdot 1'000 \cdot 60.2^3 + 15.84 \cdot 1'570 \cdot 250^2 = 1627 \cdot 10^6\ \text{mm}^4$$

$$A_c = 1'000 \cdot 62.2 = 60.2 \cdot 10^3\ \text{mm}^2$$
$$B_c = 1'000 \cdot 62.2^2 / 2 = 1.812 \cdot 10^6\ \text{mm}^3 \tag{5-63}$$
$$I_c = 1/3 \cdot 1'000 \cdot 60.2^3 = 72.72 \cdot 10^6\ \text{mm}^4$$

$$\varepsilon^{II}_{0qp} = -269.1 \cdot 10^{-6};\ \psi^{II}_{0qp} = 4.468 \cdot 10^{-6}\ \text{mm}^{-1} \tag{5-64}$$

$$\Delta N^{0}_{creep} = -204.7 \cdot 10^3 N\ ;\ \Delta N^{0}_{sh} = -4.109 \cdot 10^3 N$$
$$\Delta M^{0}_{creep} = 228.1 \cdot 10^6 N \cdot \text{mm}\ ;\ \Delta M^{0}_{sh} = -6.864 \cdot 10^6 N \cdot \text{mm}$$

This document is the intellectual property of the fib – International Federation for Structural Concrete. All rights reserved.
This PDF of fib Bulletin 92 is intended for use and/or distribution solely within fib National Member Groups.

$$\Delta\varepsilon^{II}_{creep} = -321.3\cdot10^{-6}\ ;\ \Delta\varepsilon^{II}_{sh} = -338.4\cdot10^{-6}$$
$$\Delta\psi^{II}_{creep} = 1.386\cdot10^{-6} \rightarrow a^{II}_{creep} = 5.20\ \text{mm} \qquad (5\text{-}65)$$

$$a = \psi_{sh}\frac{L^2}{8}$$

$$\Delta\psi^{II}_{sh} = 1.336\cdot10^{-6} \rightarrow a^{II}_{sh} = 6.01\,\text{mm} \qquad (5\text{-}66)$$

5. Mean deflections

Using the interpolation method the mean curvatures can be calculated. Numerical integration of curvatures along the element allows obtaining deflections.

For the sake of simplicity in this case only the deformations at the midspan section have been calculated. For comparison purposes with the previous example the different parts of deflections have already been calculated with the simplifications of parabolic (external loads and creep effects) and constant distribution of curvatures (shrinkage). Therefore the mean deflection can be obtained by interpolation between values of deflection in the uncracked and fully cracked states.

$$a_m = \zeta\cdot a^{I} + \left(1-\zeta\right)a^{II}$$
$$\zeta = 1-\beta\left(\frac{M_{cr}}{M_a}\right)^2 = 1-0.5\left(\frac{46}{90}\right)^2 = 0.87$$

Final deflection values are a_{inst} = 22 mm, $a_{inst(qp)}$ = 14.96 mm and $a_{\varphi+sh}$ = 10.62 mm. The total long term deflection is 25.58 mm.

5.6.4 General Method and Comparison of results

Deflections obtained by the Simplified Method and the General Sectional Method are compared with those obtained by the General method, (Section 6.4 of [54]). The characteristic load is applied at 28 days, the live load is removed and the quasi-permanent load is applied until 10'000 days. The results provided by the General method are shown in Fig. 5-31.

The instantaneous deflections due to the dead, live, quasi-permanent and total loads are 12.30 mm, 7.80 mm, 13.81 mm and 20.10 mm, respectively. The delayed deflection due to creep plus shrinkage is 10.26 mm and the long-term deflection due to the sustained load is 24.07 mm. Creep and shrinkage deflections are not obtained separately in the General Method, because they interact.

The differences obtained are mainly due to the fact that the General Method integrates the curvatures along the whole span length, so it adequately considers the stiffness and the delayed behaviour of the parts of the beam which are uncracked ($M < M_{cr}$), while the simplified methods refer to the calculation of deflections only in the midspan section, which is cracked.

This document is the intellectual property of the fib – International Federation for Structural Concrete. All rights reserved.
This PDF of fib Bulletin 92 is intended for use and/or distribution solely within fib National Member Groups.

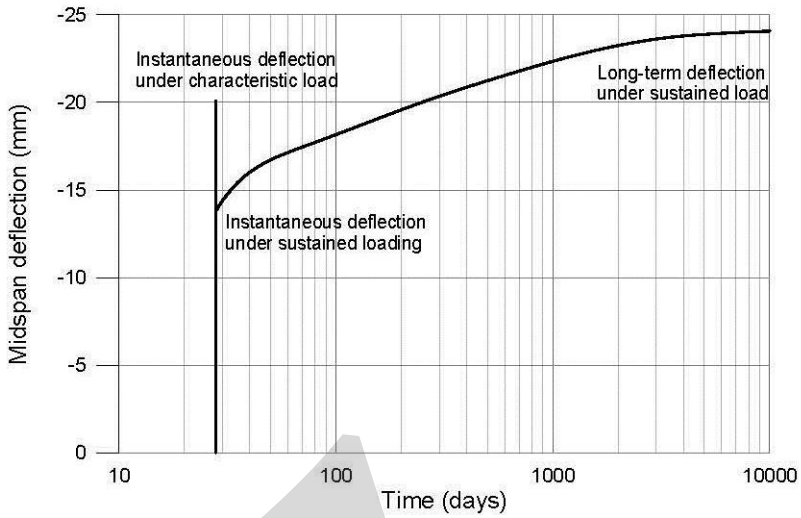


Fig. 5-31 Deflection vs. Time calculated using the General Method

Table 5-11 Summary of deflections in the example of reinforced concrete slab calculated according to MC2010.

	Instantaneous				Time-dependent			
Method	Dead load	Live load	Quasi-Perm. load	Dead + Live load	Creep*	Shrink.*	Total*	Long-term*
Interpolation	13.20	8.80	14.97	22.00	4.82	5.56	10.38	25.35
Simplified **	----	-----	14.97	-----	5.34	5.40	10.74	25.71
General section method	-----	-----	14.96	22.00	5.24	5.38	10.62	25.58
General	12.30	7.80	13.81	20.10	--------	--------	10.26	24.07

*Values obtained for the quasi-permanent load combination
** Simplified method for long-term deflections based on constant reinforcement stress $\Delta\sigma_s(t) = 0$

In addition, the General Method provides relevant information about the evolution of strains and stresses in steel and concrete as shown in Fig. 5-31 and in Fig. 5-32.

It can be observed that the steel strain practically remains constant with time, while the compressive concrete strain increases and its stress relaxes due to creep and shrinkage.

This document is the intellectual property of the fib – International Federation for Structural Concrete. All rights reserved.
This PDF of fib Bulletin 92 is intended for use and/or distribution solely within fib National Member Groups.

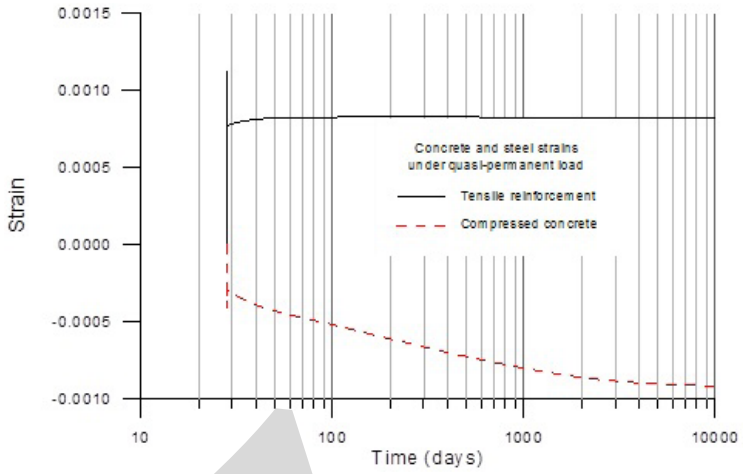


Fig. 5-32 Evolution of strains in concrete and steel with time

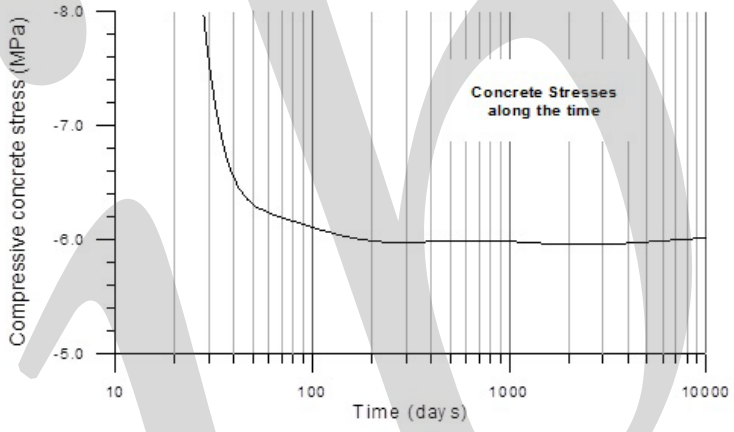


Fig. 5-33 Evolution of stresses in concrete with time

This document is the intellectual property of the fib – International Federation for Structural Concrete. All rights reserved.
This PDF of fib Bulletin 92 is intended for use and/or distribution solely within fib National Member Groups.

6. Outlook on serviceability limit states

Model code 2010[6-1] is a concise document which is not able to provide more detailed information due to its limited extent. Some closely related extensions were mentioned in previous chapters. This chapter provides results of studies and experiments and some additional knowledge associated closely with serviceability limit states. The reader can find some extended knowledge on partially prestressed structures, shear effects on deflections, slenderness limits and effect of concrete cover on crack width. The results mentioned illustrate different problems and show the variability of individual situations which cannot be completely included in the MC2010[6-1], but the designers and researchers should be aware of them.

6.1 Deflections of prestressed concrete beams

In the case of prestressed concrete beams the calculation of deflections is complex and uncertain not only because of the high scattering of the variables of influence (e.g. the variation of the loads over time and the stages of construction), as well as the complexity of the physical phenomena involved (creep, shrinkage and relaxation), but also for the effect of other variables such as the prestressing grade, the presence of ordinary steel and the different amounts of self-weight, superimposed dead load and live load that can act. On the other hand, according to international standards (Model Code 2010[6-1], Eurocode 2[6-2]) control of deflection has to be considered under the quasi-permanent load combination, for which all the sections of a PC beam have to remain uncracked. As seen in paragraph 4.1, this allows refined calculation of stresses due to long term loading to be performed in a closed form, which simplifies the problem.

The deflection can therefore be calculated integrating the curvatures along the beam under the quasi-permanent load combination. The curvature at time t is defined as:

$$\frac{1}{r}(t) = \frac{\varepsilon_{c,bottom}(t) - \varepsilon_{c,top}(t)}{h} \tag{6-1}$$

where $\varepsilon_{c,bottom}(t)$ and $\varepsilon_{c,top}(t)$ are the strains at time t in the bottom and top fibres of the cross section and h is the height of the section.

To calculate the strains at time t, the effect of self-weight, the initial prestress, other quasi-permanent actions and the stress variation due to creep, shrinkage and relaxation can be taken into account according to the following equation:

$$\varepsilon_c(t) = \varepsilon_{cs}(t,t_0) + \sigma_c(t_0)\frac{1+\varphi(t,t_0)}{E_{cm}} + \frac{\sigma_c(t) - \sigma_c(t_0)}{E_{cm}}\left[1+\chi\cdot\varphi(t,t_0)\right] \tag{6-2}$$

where $\sigma_c(t_0)$ is the concrete stress at the initial time t_0 due to prestress and load effects, $\sigma_c(t)$ is the concrete stress at time t that can be obtained applying the refined procedure, already discussed in paragraph 4.1, proposed by one study[6-3].

This chapter was mainly authored by Borosnyoi , Caldentey, Debernardi, Guiglia, Taliano and Windisch.

doi.org/10.35789/fib.BULL.0092.Ch06

This document is the intellectual property of the fib – International Federation for Structural Concrete. All rights reserved.
This PDF of fib Bulletin 92 is intended for use and/or distribution solely within fib National Member Groups.

6.1.1 Slenderness limits

In order to avoid the difficulties associated with direct calculation of deflections and, at the same time, to supply indications which are simple, though conservative, especially when a quick pre-design is needed, a simpler and useful tool that limits the slenderness of PC beams should be provided as in the case of RC structures. In this regard, neither Eurocode 2[6-2] nor Model Code 2010[6-1] introduces any limiting value. Moreover, the values of the span-to-depth ratio given for RC structures are too conservative for the design of prestressed structures. The designer can therefore assess a fundamental parameter, such as the height, for the dimensioning of PC beams.

In this context, a parametric analysis on PC structures was carried out[6-4] to discuss the influence of the variables that affect the phenomena and to analyse the span-to-height ratios that comply with the requirements both for total and active deflections (span / 250 and span / 500, respectively, under the quasi-permanent load combination). In the analysis the vibrations that may affect the serviceability of the structure are taken into account.

The analysis took into consideration fully and partially prestressed beams or slabs with a constant section along the axis which were designed to satisfy ULS verifications and stress limitations in service, according to Eurocode 2.

6.1.2 Basic assumptions for the parametric analysis

The structural systems considered in the parametric analysis are listed in Table 6-1.

Table 6-1 Characteristics of the considered members

Type of structure	Type of prestress	Type of restraints
T or I-section beam	Full	Simple supports
T or I-section beam	Partial	Simple supports
One-way solid slab	Full	Simple supports
		Fixed ends

The following uniformly distributed loads were taken into account:

- the self-weight of the structure G_{k0} which represents the minimum load that permanently acts on the structure from the time the prestress is introduced. The corresponding moment at the mid-span is indicated as M_0;
- the permanent load G_k that includes the self-weight of the structure;
- the variable load Q_k.

The load history considered three times:

- t_1 when the structure is prestressed and the self-weight is automatically applied to the structure;
- t_2 when the quasi-permanent load is applied to the structure;
- t_3 which is the final time for the evaluation of the time dependent effects.

The construction stages, until the application of the whole quasi-permanent load, are in fact often more complex. An exact analysis of the long term effects would be time

This document is the intellectual property of the fib – International Federation for Structural Concrete. All rights reserved.
This PDF of fib Bulletin 92 is intended for use and/or distribution solely within fib National Member Groups.

consuming and require iterative procedures that take into account the evolution of the state of stress over time for each element into which the section is divided. However, this analysis could be meaningless because of the high variability of the possible situations that can occur. For this reason, considering simplified conditions is more suitable and on the safe side.

The grouting process of the duct occurred at time t_1, which was 28 days from the casting of the element, and after the prestressing of the structure. This process allowed the tendon to be bonded to the concrete. As far as the variation of the strains is concerned, the hypothesis of plane sections becomes valid from this point. The remaining part of the load that was necessary to obtain the total quasi-permanent load was applied to the structure at time t_2, immediately after t_1.

Time t_3, which was considered in the calculations of the total and active deflections, was assumed for the analysis of the long term effects when the creep and shrinkage of the concrete and relaxation of the reinforcement were complete.

6.1.2.1 Dimensioning of structural members

The structures were designed according to Eurocode 2[6-2], assuming the following characteristic strengths: f_{ck} = 30, 40 and 50 N/mm^2 for concrete, f_{yk} = 500 N/mm^2 for ordinary steel, f_{pk} = 1860 N/mm^2 for prestressing steel. The design was performed respecting:

- at the serviceability limit state (SLS), the stress limitations on concrete to $0.45f_{ck}$ under the quasi-permanent load combination and $0.60f_{ck}$ under the characteristic load combination;
- the stress limitations on prestressing steel to $0.80f_{pk}$ at tensioning and $0.75f_{pk}$ in service conditions under the characteristic load combination;
- the ULS verifications for bending M_{Ed} at mid-span and for shear V_{Ed} in the zones close to the supports.

In order to obtain the appropriate values of the amounts of ordinary and prestressing steel and the concrete dimensions that were strictly necessary for the ULS and SLS verifications, an iterative procedure was carried out with successive corrections of the geometrical data.

The dimensioning was made for various values of the *L/h* ratio, considering the most critical section. The geometry was assumed constant along the beam. The soundness of the beam cross section was verified with varying degrees of prestress both at the early stage and for long-term loading , imposing the condition of uncracked section under the quasi-permanent load combination. Cracking occurs under the frequent load combination. The profile of the prestressing tendon was formed by parabolic segments with eccentricities in such a way that tensile stresses in the concrete were avoided at tensioning, when the dead load acted.

The tendon was tensioned at one end. The immediate losses of prestress that occurred during tensioning were determined, considering a coefficient of friction μ = 0.19, an unintentional angular displacement k = 0.01 rad/m and a wedge draw-in of the anchorage devices Δa = 5 mm.

The calculation of the strains and stresses was carried out at the SLS on the basis of Bernoulli's hypothesis and the linear elastic behaviour of materials. After tensioning, the tendon was bonded to the concrete by means of duct grouting, then the remaining

This document is the intellectual property of the fib – International Federation for Structural Concrete. All rights reserved.
This PDF of fib Bulletin 92 is intended for use and/or distribution solely within fib National Member Groups.

part of the quasi-permanent load was applied to the structure. The time dependent losses due to creep and shrinkage of concrete and relaxation of strands were then taken into account. A visco-linear elastic behaviour of the concrete was considered, assuming a creep coefficient $\varphi = 2.5$ and a shrinkage strain $\varepsilon_{cs} = -0.35$ mm/m. The long term (final) values of the relaxation losses were estimated as three times the relaxation losses at 1'000 hours, that means $3\rho_{1'000}$.

The strain of the concrete in time was assessed according to the Age Adjusted Effective Modulus Method[6-5, 6-6, 6-7] using Eq.6-2.

The traditional linearity of creep and superposition of effects assumptions were applied.

The structure was divided into 20 blocks and the curvatures in the different stages of the structural life were determined for these blocks. For this purpose the procedure described by this study[6-3] was applied.

The total deflection and the active deflection that occurs after construction were determined under the quasi-permanent load by integrating the long term curvatures along the axis of the structure.

6.1.3 Parametric analysis

The purpose of this analysis was to define appropriate limits of the span-to-height ratio, *L/h*, for prestressed members that comply with the control of deflection required by international standards (Model Code 2010[6-1], Eurocode 2[6-2]).

Many parameters affect the structural behaviour at serviceability, but taking into account all the possible variabilities could be very burdensome and also unnecessary. Therefore, the influence of the following parameters was considered:

- the variable-to-permanent load ratio Q_k/G_k;
- the permanent load G_k;
- the span L;
- the concrete strength f_{ck}.

6.1.3.1 Fully Prestressed Simply Supported T-Section Beams

The reference values for which the study was performed were:

- span-to-height ratios between 18 and 45 with steps equal to 1;
- spans of the beams: 20 m, 30 m and 40 m;
- permanent loads: 30 kN/m, 40 kN/m and 50 kN/m;
- variable-to-permanent load ratios of 0.25, 0.50 and 0.75.

Referring to ratios of Q_k/G_k equal to 0.25, 0.50 or 0.75 means referring to quasi-permanent-to-design load ratios equal to 0.46, 0.52 or 0.61, respectively, that is

$$\frac{q_{qp}}{q_d} = \frac{1+\psi_2 \frac{Q_k}{G_k}}{1.35+1.5\frac{Q_k}{G_k}} \tag{6-3}$$

This document is the intellectual property of the fib – International Federation for Structural Concrete. All rights reserved.
This PDF of fib Bulletin 92 is intended for use and/or distribution solely within fib National Member Groups.

where ψ_2 is the factor for the quasi-permanent value of variable actions (here, $\psi_2 = 0.2$ was assumed). It is worth noting that the parametric analysis, on which the basic span-to-depth ratios for RC members proposed by Eurocode 2[6-2] and Model Code 2010[6-1], are based, assumes a quasi-permanent load at 50% of the corresponding design load.

Each beam of this typology was dimensioned with a I-section, if a bottom flange was needed (Fig. 6-1), otherwise a T-section was chosen. In fact, a bottom flange with a height of $0.25h$ and a width b_i was introduced in order to avoid a greater concrete compressive stress than $0.6f_{ck}$ at the bottom of the section during tensioning. The height of the top flange was assumed to be $0.20h$, while the width b was obtained from the calculation at the ULS for bending. The width of the web b_w was determined from the ULS verification for shear, assuming $\theta = 45°$ and imposing that the maximum shear resistance $V_{Rd,\max}$ was equal to the shear V_{Ed} acting at the support. However, a lower value of the width of the web was assumed equal to 150 mm.

A parabolic profile of the tendon was considered with zero eccentricity, with respect to the centre-line of the structure, at the ends. The maximum eccentricity at mid-span was obtained, considering a distance from the bottom point of the central core equal to M_0/P_m, where P_m was the value of the prestressing force immediately after tensioning. The sectional area of the duct was assumed as twice the area of the tendon.

In order to be on the safe side, ordinary steel was not considered in this analysis.

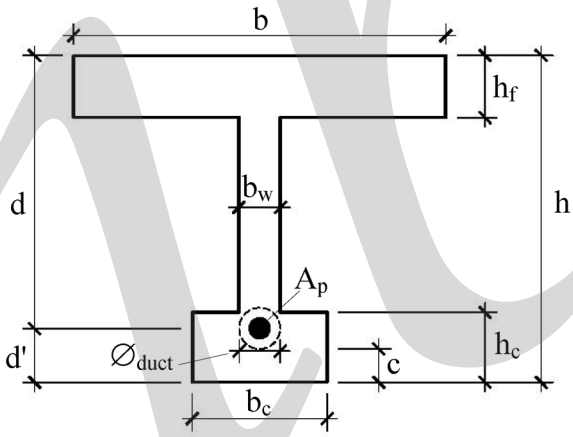


Fig. 6-1 Fully prestressed beams: transversal section

1. Influence of the Permanent Load

The three values of the permanent load G_k, associated to the three values of the ratio Q_k/G_k and the three values of the span L led to very different geometries of the transverse section and amounts of the prestressing steel. The results of the deflection-to-span ratios were quite similar on the same length L and the same variable-to-permanent load ratio Q_k/G_k. This means that the permanent load is not a significant parameter, as shown in Fig. 6-2, Fig. 6-3 and Fig. 6-4, which contain the diagrams of the total deflection-to-span ratio and the active deflection-to-span ratio as a function of the span-to-height ratio L/h of the beam. Fig. 6-2 and Fig. 6-3 refer to beams with the same variable-to-permanent load ratio, $Q_k/G_k = 0.75$, but different lengths (20 m and 40 m, respectively), while Fig. 6-3 and Fig. 6-4 refer to beams with the same length (40 m), but different Q_k/G_k ratios (0.75 and 0.25, respectively). The study was stopped at a span-to-height ratio of 45.

This document is the intellectual property of the fib – International Federation for Structural Concrete. All rights reserved.
This PDF of fib Bulletin 92 is intended for use and/or distribution solely within fib National Member Groups.

From Fig. 6-2 it appears that the maximum deflection-to-span ratio, $(L/h)_{max}$, consistent with the allowable total deflection (1/250*L*), is 42, while with reference to the limit on the active deflection (1/500*L*), it is 33. It was possible to obtain the maximum *L/h* ratios for the other situations in a similar way.

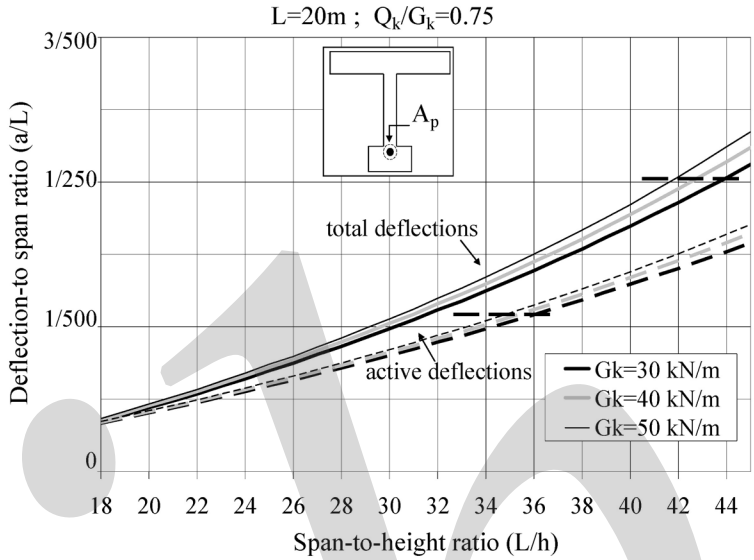


Fig. 6-2 Fully prestressed beams: total deflection-to-span (continuous lines) and active deflection-to-span (dotted lines) ratios as a function of the span-to-height ratio *L/h* (Data: *L* = 20 m, Q_k/G_k = 0.75; G_k = 30 kN/m, 40 kN/m and 50 kN/m)

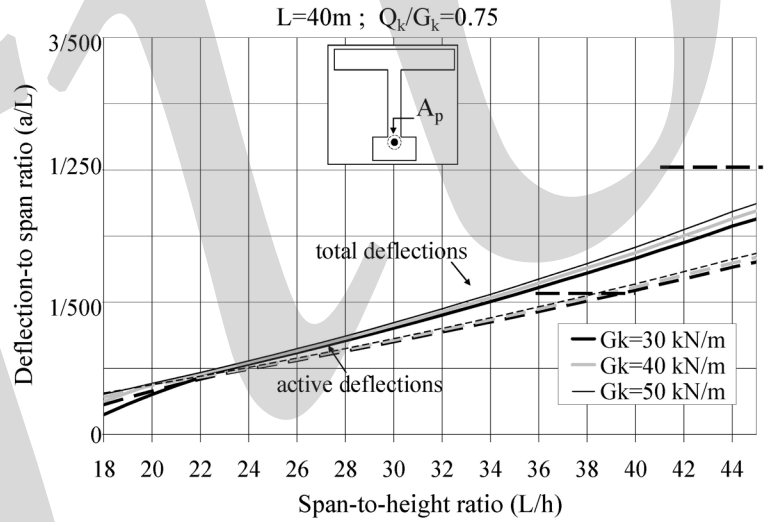


Fig. 6-3 Fully prestressed beams: total deflection-to-span (continuous lines) and active deflection-to-span (dotted lines) ratios as a function of the span-to-height ratio *L/h* (Data: *L* = 40 m, Q_k/G_k = 0.75; G_k = 30 kN/m, 40 kN/m and 50 kN/m)

This document is the intellectual property of the fib – International Federation for Structural Concrete. All rights reserved.
This PDF of fib Bulletin 92 is intended for use and/or distribution solely within fib National Member Groups.

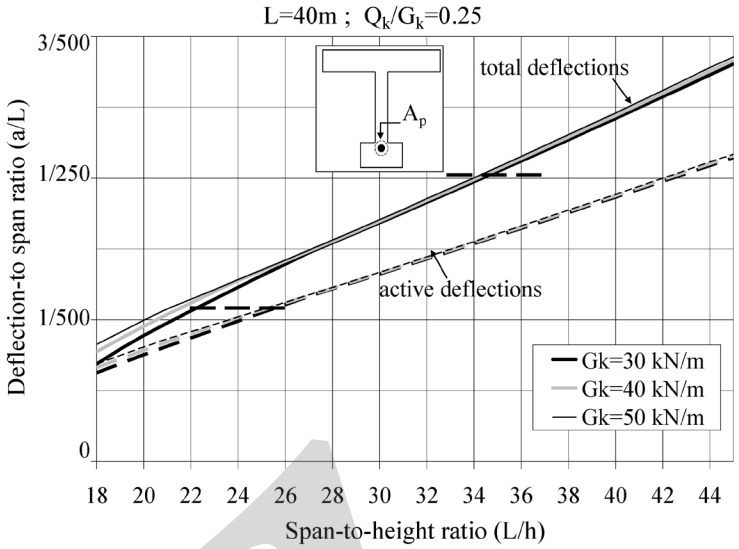


Fig. 6-4 Fully prestressed beams: total deflection-to-span (continuous lines) and active deflection-to-span (dotted lines) ratios as a function of the span-to-height ratio *L/h* (Data: L = 40 m, Q_k/G_k = 0.25; G_k = 30 kN/m, 40 kN/m and 50 kN/m)

The beams with length L = 40m and ratio Q_k/G_k = 0.75 (Fig. 6-3) presented lower total deflections in the considered range of *L/h* (from 18 to 45), but which still conformed with the limit on the total deflection. This is due to the high area of prestressing steel (A_p) that was calculated under the design load, in compliance with the ULS verification for bending. In other words, this is a case in which the ULS verification is stricter than the SLS verification. This situation changes completely when the variable load is reduced, as confirmed in Fig. 6-4 which refers to beams with the same length but lower variable load.

2. Influence of the Span

In order to study this effect, the values of the span-to-height ratio *L/h*, which corresponded to the limits on the active and total deflections of 1/250*L* and 1/500*L*, respectively, were searched for. The results are shown in Fig. 6-5 as a function of the length of the beams, for various values of the ratio Q_k/G_k. A permanent load G_k = 30 kN/m was assumed. Because of the sub-horizontal trend of the curves, it appears that the span has little influence on the span-to-height ratio *L/h*, for either the total or the active deflection.

As already mentioned above when discussing Fig. 6-3, the adopted design procedure of the beams subjected to relatively high variable load, that is with ratio Q_k/G_k = 0.75, led to small total deflections. For beams with lengths of 30 and 40 m, the limit on the total deflection could be achieved for span-to-height ratios greater than 45 which here, prudently, were not taken into account. In Fig. 6-5, this is reflected in the values that correspond to the ratio Q_k/G_k = 0.75 which are reduced to one point.

3. Influence of the Variable-to-Permanent Load Ratio Q_k/G_k

The same *L/h* values used in Fig. 6-5 are shown in Fig. 6-6 as a function of the ratio Q_k/G_k, for various beam spans. The ratio Q_k/G_k between variable and permanent loads has a great influence on the deflections in prestressed structures. In fact, on the same permanent load G_k, increasing the ratio Q_k/G_k, and therefore the design load, increases the dimensions of the beams and the area of the prestressing steel. On the other hand, the increase of the variable load does not affect to any great extent the quasi-permanent load, which is the reference load for the calculation of deflection.

This document is the intellectual property of the fib – International Federation for Structural Concrete. All rights reserved.
This PDF of fib Bulletin 92 is intended for use and/or distribution solely within fib National Member Groups.

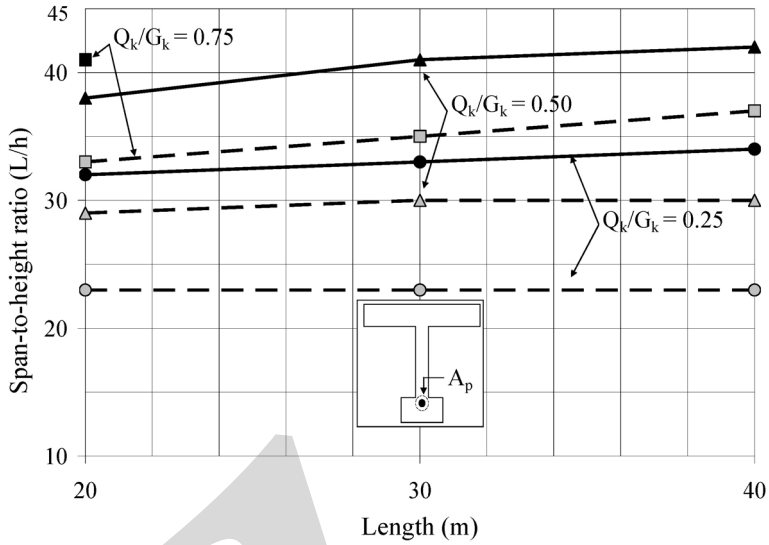


Fig. 6-5 Fully prestressed beams: allowable span-to-height ratios $(L/h)_{max}$ referred to the total (continuous lines) and active (dashed lines) deflections as a function of the span L (Data: G_k = 30 kN/m)

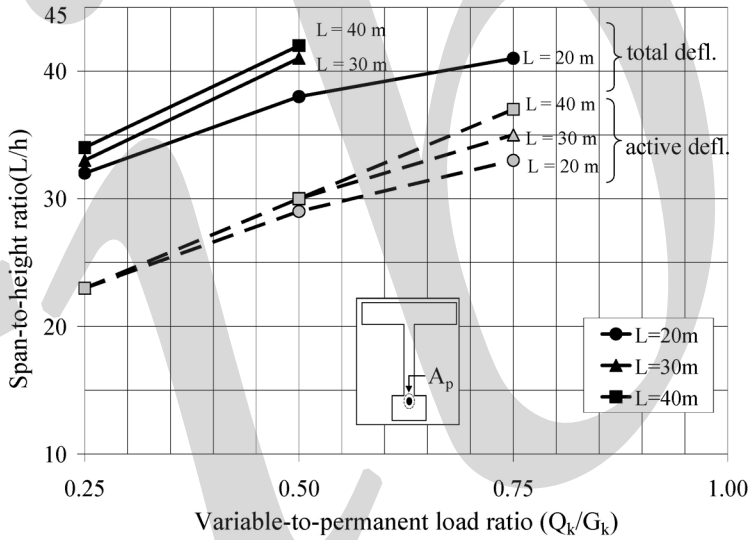


Fig. 6-6 Fully prestressed beams: allowable span-to-height ratios $(L/h)_{max}$ referred to the total (continuous lines) and active (dashed lines) deflections as a function of the variable-to-permanent load ratio Q_k/G_k (Data: G_k = 30 kN/m)

4. Influence of the Concrete Strength

Three strength classes of concrete were considered, C30/37, C40/50, C50/60. Fig. 6-7 shows the values of the total deflection-to-span and active deflection-to-span ratios as a function of the beam span-to-height ratio L/h, for 30 m length beams. The L/h values which corresponded to the attainment of the limits on the active and total deflections, decrease as the concrete strength increases. This unexpected result is a consequence of the hypotheses assumed to optimize the design. In fact, the design of the width of the sections was defined at the ULS in such a way that the compressive resultant on concrete balanced the tension resultant. Because of the constant values of the tension resultant, smaller widths of the section and, therefore, smaller stiffnesses, corresponded to higher strengths of concrete.

This document is the intellectual property of the fib – International Federation for Structural Concrete. All rights reserved.
This PDF of fib Bulletin 92 is intended for use and/or distribution solely within fib National Member Groups.

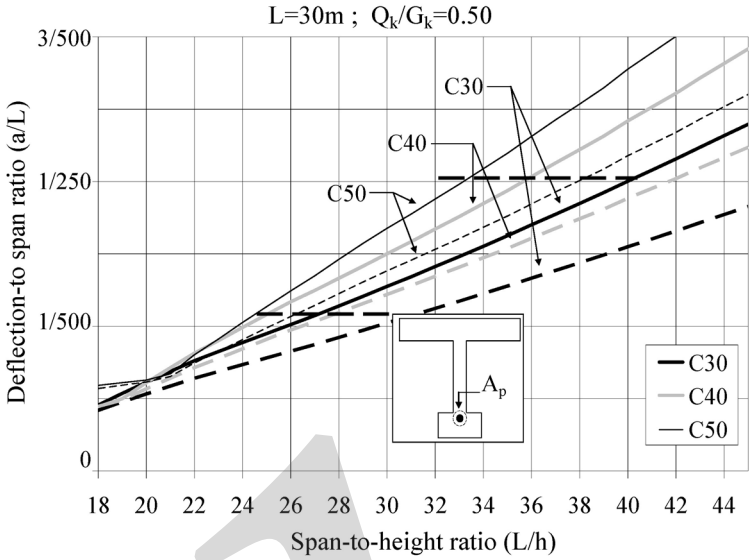


Fig. 6-7 Fully prestressed beams: total deflection-to-span (continuous lines) and active deflection-to-span (dotted lines) ratios as a function of the concrete strength (Data: L = 30 m, Q_k/G_k = 0.50; G_k = 30 kN/m)

6.1.3.2 Partially Prestressed Simply Supported T-Section Beams

The reference values for which the study was performed are:

- span-to-height L/h ratios between 18 and 28 with steps equal to 1;
- spans of the beams: 15 m, 20 m and 25 m;
- permanent loads: 30 kN/m, 40 kN/m and 50 kN/m;
- variable-to-permanent load ratios of 0.25, 0.50 and 0.75.

The geometrical properties of the flanges and web (Fig. 6-8) fulfilled the proportions used for fully prestressed beams. The bottom flange was often unnecessary because of the lower prestressing force. The tendon, which again had a parabolic profile, presented relatively large eccentricity at the mid-span in comparison to the fully prestressed beams since the ratio M_0/P_m was greater on the same permanent load, as the prestressing force P_m was lower.

In the design of the beams, it was assumed that the sections remained entirely compressed under the quasi-permanent load combination, and in particular the concrete stress at the bottom was null when the time-related phenomena were exhausted. This condition allowed the area and position of the prestressing steel to be determined. The ordinary reinforcement was situated on the bottom side of the beams, at a distance equal to 0.1h from the edge of the section. Its area was calculated in order to satisfy the ULS verification for bending. An iterative procedure was able to fulfill all these conditions.

This document is the intellectual property of the fib – International Federation for Structural Concrete. All rights reserved.
This PDF of fib Bulletin 92 is intended for use and/or distribution solely within fib National Member Groups.

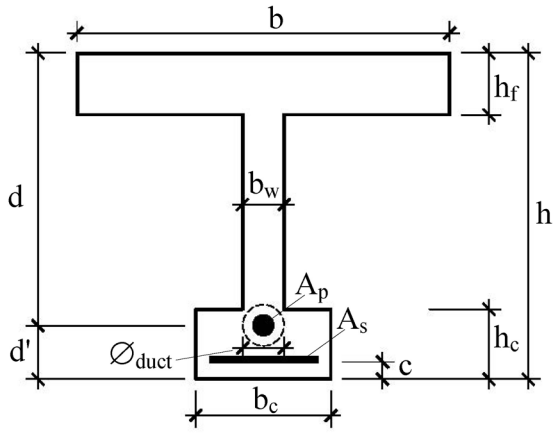


Fig. 6-8 Partially prestressed beams: transversal section

The values of the deflection-to-span ratio are shown in Fig. 6-9 and Fig. 6-10 as functions of the *L/h* ratio, for beams with 15 m and 25 m lengths, respectively, a ratio $Q_k/G_k = 0.50$ and three values of the permanent load. The influence of the permanent load G_k on the deflections is once again considered negligible.

A slight influence on the deflections is also given by the variable-to-permanent load ratio Q_k/G_k, for a fixed value of G_k. The allowable span-to-height ratios $(L/h)_{max}$ are in Fig. 6-11 which are basically the same for the same Q_k/G_k ratio, and remain constant as the span changes, on average equal to 27.5 for the case of total deflection and 23 for the active deflection. This result is different from fully prestressed beams because of the hypotheses assumed for the optimization of the design. In this context, some points need to be discussed. First, partially prestressed beams and fully prestressed beams with the same *L/h* ratio present similar values of the top width of the section, therefore this parameter is not responsible for the different behaviour. Moreover, both typologies show similar values of the resulting force in the tensile zone at the ULS for bending moment. For fully prestressed beams, this resultant is directly connected to the area A_p of the prestressing steel.

For partially prestressed beams, the design of the area of prestressing steel is not performed at ULS, but at SLS under the quasi-permanent load. The quasi-permanent load does not depend to any great extent on the variable load because of the combination factor ψ_2 in the term $\psi_2 \cdot Q_k$. As a consequence, for the same G_k, when the Q_k/G_k ratio varies, the area of prestressing steel and therefore the deflections do not vary to any great extent.

This document is the intellectual property of the fib – International Federation for Structural Concrete. All rights reserved.
This PDF of fib Bulletin 92 is intended for use and/or distribution solely within fib National Member Groups.

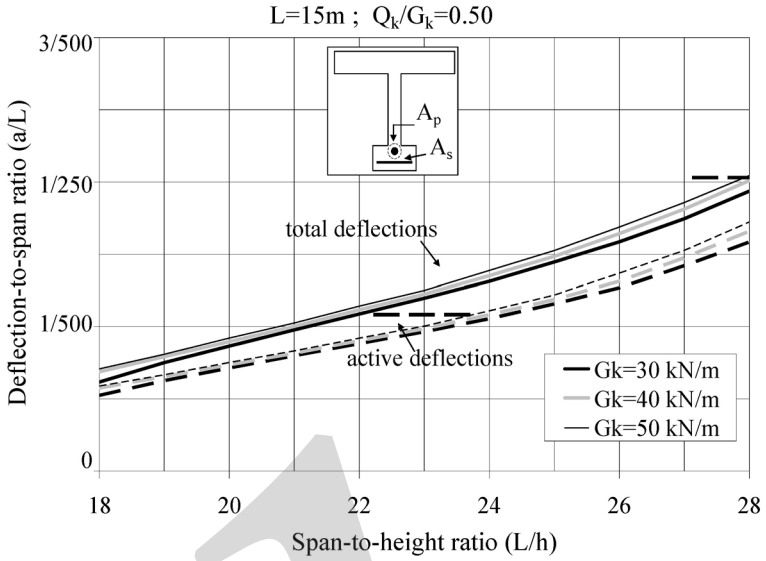


Fig. 6-9 Partially prestressed beams: total deflection-to-span (continuous lines) and active deflection-to-span (dotted lines) ratios as a function of the span-to-height ratio *L/h* (Data: L = 15 m, Q_k/G_k = 0.50; G_k = 30-40-50 kN/m)

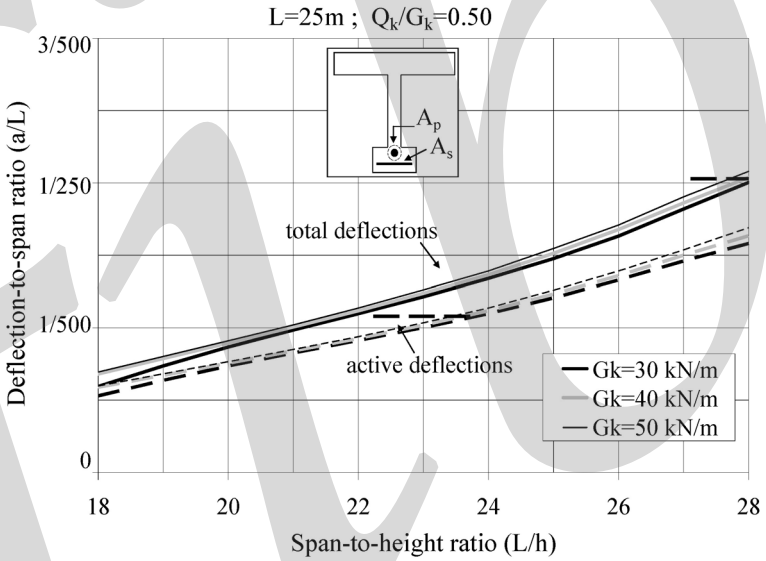


Fig. 6-10 Partially prestressed beams: total deflection-to-span (continuous lines) and active deflection-to-span (dotted lines) ratios as a function of the span-to-height ratio *L/h* (Data: L = 25 m, Q_k/G_k = 0.50; G_k = 30-40-50 kN/m)

This document is the intellectual property of the fib – International Federation for Structural Concrete. All rights reserved.
This PDF of fib Bulletin 92 is intended for use and/or distribution solely within fib National Member Groups.

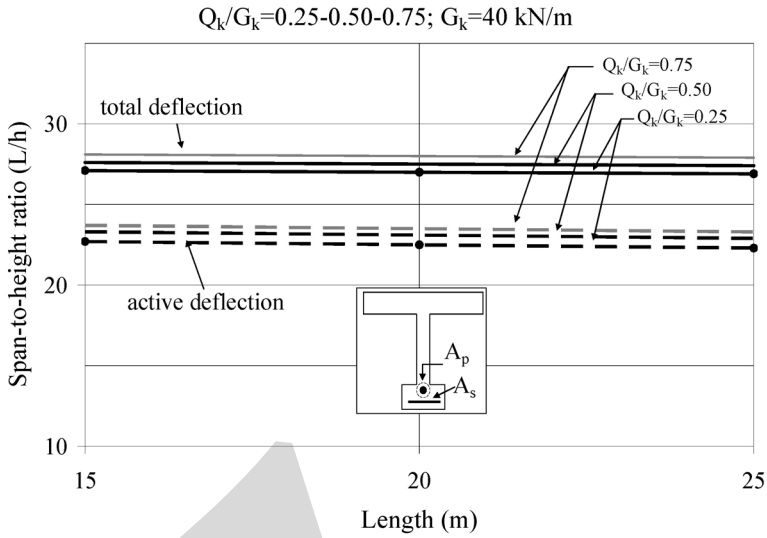


Fig. 6-11 Partially prestressed beams: influence of the length of the beam on the *L/h* ratios to which the attainment of the limits on the active and total deflections corresponds (Data: Q_k/G_k = 0.25-0.50-0.75; G_k = 40 kN/m)

6.1.3.3 One-Way Slabs

One-way slabs are bi-dimensional members with small thickness, supported on beams or walls, subjected to load-effects that mainly act on a plane perpendicular to their mid plane. For the sake of simplicity and to be on the safe side, they can be considered as spanning one-way. Here, the study concerned fully prestressed 1.0 m wide one-way solid slabs without any additional ordinary reinforcement. Two restraining conditions, that is, simply supported slab and fixed end slab, were considered.

1. Simply Supported Solid Slabs

The reference values for which the analysis was performed are:

- span-to-height ratio *L/h* between 18 and 40 with steps equal to 1;
- spans of the slabs: 10 m, 15 m and 20 m;
- permanent loads: dead load + 2.5 kN/m;
- variable-to-permanent load ratios of 0.25, 0.50 and 0.75.

The tendon, which again had a parabolic trend had, with respect to the centre-line of the structure, zero eccentricity at the ends and maximum eccentricity at the mid-span equal to M_0/P_m.

Fig. 6-12 shows the total deflection-to-span and active deflection-to-span ratios as functions of the span-to-height ratio, for beams with a Q_k/G_k ratio equal to 0.75, which is the most critical of the situations examined. From these diagrams the limit of 1/250*L* for the total deflection corresponds to a ratio *L/h* of 33.5, while the limit of 1/500*L* for the active deflection corresponds to a ratio *L/h* of 27.5.

The Q_k/G_k ratio did not affect these allowable limits appreciably. In fact, the highly non-linear trend of the curves, which was not observed for the T- or I-sections, is due to the fact that the dimensions, and in particular the width of the top flange, were assumed to be strictly necessary for the beams, while for slabs the width was assumed constant.

This document is the intellectual property of the fib – International Federation for Structural Concrete. All rights reserved.
This PDF of fib Bulletin 92 is intended for use and/or distribution solely within fib National Member Groups.

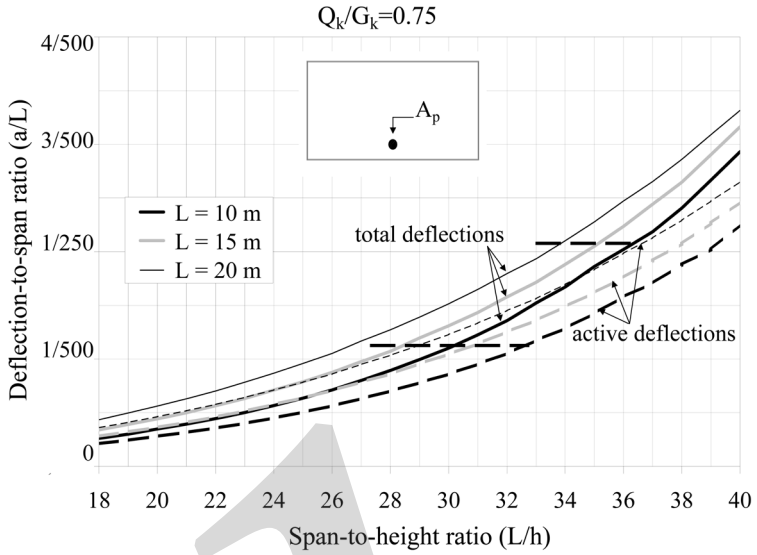


Fig. 6-12 Simply supported solid slabs: total deflection-to-span (continuous lines) and active deflection-to-span (dotted lines) ratios as a function of the span-to-height ratio *L/h* (Data: Q_k/G_k = 0.75; G_k = dead load + 2.5 kN/m)

2. Fixed End Solid Slabs

The profile of the tendon was formed by three parabolic segments with eccentricities e_1 at mid-span and e_2 at the two ends. The statically indeterminate moments due to the prestressing and the effects of the loads were calculated elastically and considered constant over time. The prestressing steel area and the eccentricities e_1 and e_2 were determined through an iterative procedure respecting two conditions: the complete utilization of the strength of the prestressing steel and the stress limitation of the concrete at the SLS.

The reference values for which the study was performed were the same as those considered before:

- span-to-height ratio *L/h* between 18 and 54 with steps equal to 1;
- spans of the slabs: 10 m, 15 m and 20 m;
- permanent loads: dead load + 2.5 kN/m;
- variable-to-permanent load ratios of 0.25, 0.50 and 0.75.

The total deflection-to-span and active deflection-to-span ratios are shown in Fig. 6-13 as functions of the span-to-height ratio *L/h*. From these curves the allowable span-to-height ratio $(L/h)_{max}$, corresponding to a total deflection of 1/250*L*, is equal to 46, but the limitation on the active deflection is once again determining with an allowable span-to-height ratio of 41.

This document is the intellectual property of the fib – International Federation for Structural Concrete. All rights reserved.
This PDF of fib Bulletin 92 is intended for use and/or distribution solely within fib National Member Groups.

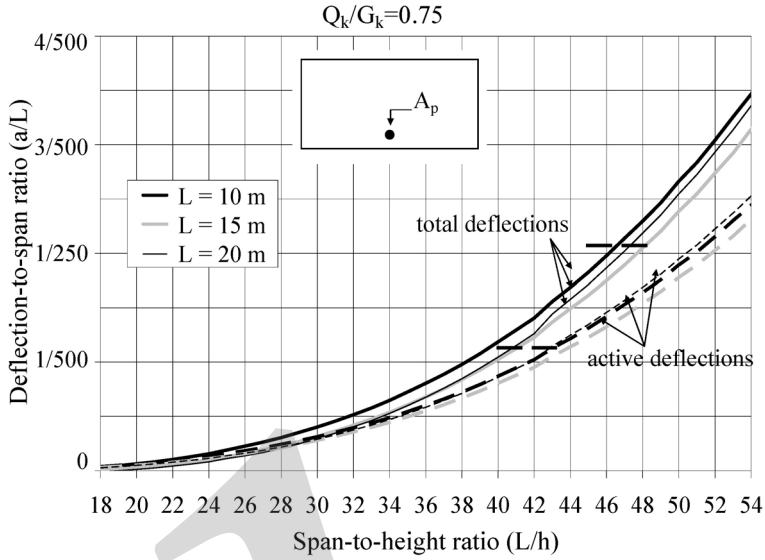


Fig. 6-13 Fixed ends solid slabs: total deflection-to-span (continuous lines) and active deflection-to-span (dotted lines) ratios as a function of the span-to-height ratio L/h (Data: Q_k/G_k = 0.75; G_k = dead load + 2.5 kN/m)

6.1.4 Conclusions

A parametric analysis has been performed in order to calculate the total and active deflections of prestressed concrete beams and slabs and to determine the span-to-height ratios to which the attainment of the limits on the deflections corresponds to: span / 250 under the quasi-permanent load combination (total deflection), span / 500 for the deflection after construction that could damage adjacent parts of the structure such as partitions and finishes (active deflection). Two typologies of simply supported beams have been considered, fully prestressed and partially prestressed. Two typologies of fully prestressed solid slabs have also been taken into account, namely, simply supported or fixed end slabs.

The design of the beams and slabs has been carried out to optimize the dimensions of the sections, with reference to ULS and SLS verifications.

The span-to-height ratios which correspond to the attainment of the limits for the active and total deflections are summarised in Table 6-2 for various variable-to-permanent load ratios and structural standard typologies. A simple, though conservative, tool is therefore provided which limits the slenderness of PC beams, particularly useful when a quick pre-design is needed. Referring to ratios of Q_k/G_k equal to 0.25, 0.50 and 0.75 means considering quasi-permanent load-to-design load ratios equal to 0.61, 0.52 and 0.46 (here, ψ_2 = 0.2).

Table 6-2 Allowable span-to-height ratios $(L/h)_{max}$ that comply with the limitations for the total (1/250L) and the active (1/500L) deflections, for various variable-to-permanent load ratios and structural standard typologies

	Simply Supported Beams				One-Way Fully Prestressed Solid Slabs			
	Fully Prestressed		Partially Prestressed		Simply supported		Fixed ends	
Q_k/G_k	1/250L	1/500L	1/250L	1/500L	1/250L	1/500L	1/250L	1/500L
0.25	32	23	28	23	34	28	46	41
0.50	38	29						
0.75	41	33						

This document is the intellectual property of the fib – International Federation for Structural Concrete. All rights reserved.
This PDF of fib Bulletin 92 is intended for use and/or distribution solely within fib National Member Groups.

The limits on the active deflection give the most restrictive values of the span-to-height ratio. In comparison with the values proposed in international standards for RC simply supported or fixed end beams and slabs, these values are obviously higher because of the favourable effects of prestress. Due to the design procedures adopted, the ratio Q_k/G_k influences the allowable span-to-height ratios to a great extent in the case of fully prestressed simply supported beams, where a linear interpolation for intermediate values may be used, while its influence is rather negligible in the remaining cases.

When the design is carried out without any optimization of the dimensions of the section, which means the stresses on the materials are less than the recommended limits, the maximum span-to-height ratios proposed can be considered conservative and higher values could be acceptable. On the other hand, high values of the slenderness may lead to unacceptable vibrations.

6.2 Shear effects on deflections

6.2.1 Introduction

In general, deflection should be calculated taking into account the contribution from bending and shear. International Standards (EN 1992-1-1[6-2], Model Code 1990[6-8]) allow the shear contribution to be ignored, when it is likely to be less than 10% of that due to bending. However, shear deformation in cracked sections, at service conditions, is often neglected because there are no suitable models for everyday applications, even though, as shown by experimental observations on RC beams with thin webs, the above limit could be already overcome for span-to-depth ratios lower than 12[6-9, 6-10] . The difficulty setting up a consistent model that is able to describe the behaviour of RC beams under shear and bending is due to the characteristics of the physical phenomenon, such as the complexity of the crack pattern and its evolution when the load increases[6-11, 6-12, 6-13]. Moreover, the cracked web of a reinforced concrete beam transmits shear in a relatively complex manner, through shear failure mechanisms, such as aggregate interlock and friction, dowel action of the longitudinal steel and shear carried across uncracked concrete[6-11, 6-14]. The dowel effect can be neglected for members with shear reinforcement, while the shear components transferred across the uncracked concrete and by friction play a significant role in reducing the amount of shear transferred by transverse reinforcement. According to the classification proposed by this study[6-15], the principal models that describe the shear transferred by concrete and the rotation of web struts in a detailed way can be divided into two different approaches: “truss models with crack friction” and “smeared models”. Truss models with crack friction consider cracking in a “discrete” form, and model the geometry (spacing and inclination θ_{cr}) of the crack, the friction connected to the slip and the consequent rotation of the θ-angle of the struts. In smeared approaches, the stress fields are modelled independently from the crack pattern, assuming that both the crack angle θ_{cr} and the strut angle θ are equal. In this case, the shear transferred by the concrete is considered by means of the tension fields acting in the cracked concrete.

This document is the intellectual property of the fib – International Federation for Structural Concrete. All rights reserved.
This PDF of fib Bulletin 92 is intended for use and/or distribution solely within fib National Member Groups.

6.2.2 Experimental background

6.2.2.1 Determination of the mean curvature and the mean shear strain of a beam block

The analysis of a beam block subjected to a bending moment is traditionally carried out referring to the parameter of the deformation constituted by the mean curvature $(1/r)_m$.

In an analogous way it is necessary to define an experimental procedure able to determine the mean deformation parameters (mean shear strain and mean curvature) in the case of shear and bending acting simultaneously.

An experimental setup to evaluate the mean curvature $(1/r)_m$, the mean shear strain γ_m and the mean inclination θ of the compressive web struts[6-16, 6-17] can be made by the measure of the deformations of the AB, BC, CD, DA and DB sides of the measuring lattice shown in Fig. 6-14.

With reference to the measuring lattice the mean curvature is obtained through the expression

$$\frac{1}{r} = \frac{\frac{\Delta_{BC}}{L_0} - \frac{\Delta_{AD}}{L_0}}{L_0} \qquad 6\text{-}4$$

where Δ_{AB}, Δ_{BC}, Δ_{CD}, Δ_{DA}, Δ_{DB} are the deformations of the measuring bases and L_o their initial lengths.

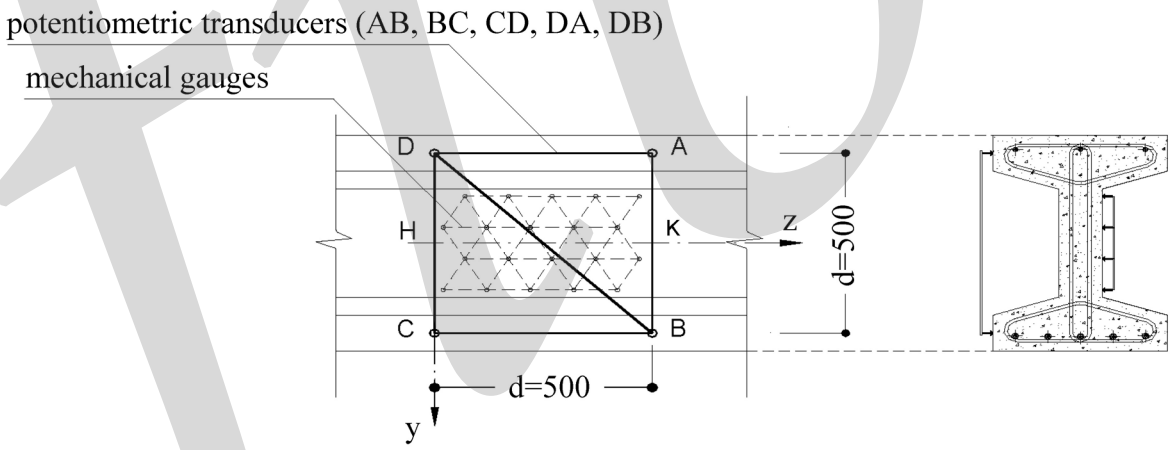


Fig. 6-14 Measuring lattice and the network of points at the initial non-deformed state

In order to determine the mean shear strain, a reference system of (z-y) axes is assumed with origin in H (at mid-point between points C and D), the y-axis that coincides with the CD direction and the z-axis that is orthogonal to y. The z-axis is therefore situated at the mid-height between the tension and compression chords. The vertical displacement v_k of point K (at mid-point between points A and B) in the y-direction can be divided into two parts, one, v_K', which represents the effect of the mean curvature, while the other one, v_K'', represents the effect of the mean shear strain (v_K' and v_K'' positive if on the same versus of y-axis in Fig. 6-14):

$$v_K = v_K' + v_K'' \qquad (6\text{-}5)$$

This document is the intellectual property of the fib – International Federation for Structural Concrete. All rights reserved.
This PDF of fib Bulletin 92 is intended for use and/or distribution solely within fib National Member Groups.

The contribution due to the mean curvature, v_K', is

$$v_K' = \frac{1}{r}\frac{L_0^2}{2} \tag{6-6}$$

The contribution due to the mean shear strain, v_K'', is determined by subtracting the displacement due to curvature from the total displacement which is obtained analytically from the measured deformations of the lattice. The mean shear strain results to be:

$$\gamma_m = \frac{v_K''}{L_0} \tag{6-7}$$

The mean shear strain can be determined in another way, considering the following experimental strains "smeared" on the web:

- the mean axial strain in the direction of the z-axis, which is obtained from the mean of the strains of the top and bottom chords:

$$\varepsilon_{z,G} = \frac{\Delta_{AD} + \Delta_{CB}}{2L_0} = \frac{\varepsilon_{sm} + \varepsilon_{cm}}{2} \tag{6-8}$$

- the mean axial strain in the y-direction:

$$\varepsilon_{y,G} = \frac{\Delta_{CD} + \Delta_{AB}}{2L_0} \tag{6-9}$$

- the mean axial strain along the diagonal DB which is inclined by 45° with reference to the horizontal axis:

$$\varepsilon_{\theta,G} = \frac{\Delta_{DB}}{L_{0,DB}} \tag{6-10}$$

If the mean strains along three directions passing through point G (fixed in the centre of the web, at the mid-height between the tension and compression chords) are known, the strain state around the point G is completely determined, which means, for the mean strain in the θ-direction,

$$\varepsilon_{\theta,G} = \varepsilon_{z,G} \cdot \cos^2\theta + \varepsilon_{y,G} \cdot \sin^2\theta + \gamma_{zy} \cdot \sin\theta \cdot \cos\theta \tag{6-11}$$

From Eq. 6-11, with reference to the case in which θ is equal to 45°, the expression for the determination of the mean shear strain γ_{zy} as a function of the experimental measures of the mean strains can be obtained:

$$\gamma_{zy} = 2\varepsilon_{45,G} - \varepsilon_{z,G} - \varepsilon_{y,G} \tag{6-12}$$

The comparison between the theoretical values of the mean shear strain obtained with Eq. 6-7 and 6-12 shows a very good correspondence, with differences of less than 1% in the examined cases.

The above mentioned methodology was applied, for example, to the tests on several reinforced concrete I-section beams with thin web, a height of 0.6 m and spans of 6.3 and 7.0 m[6-16, 6-18], longitudinally reinforced with a reinforcement ratio of $\rho_l = \frac{A_s}{b \cdot d} = 0.0045$ and $\rho_l = 0.008$ and transversally with a ratio of $\rho_w = \frac{A_{sw}}{b_w \cdot s} = 0.0051$, subjected to two symmetrical or non-symmetrical load.

This document is the intellectual property of the fib – International Federation for Structural Concrete. All rights reserved.
This PDF of fib Bulletin 92 is intended for use and/or distribution solely within fib National Member Groups.

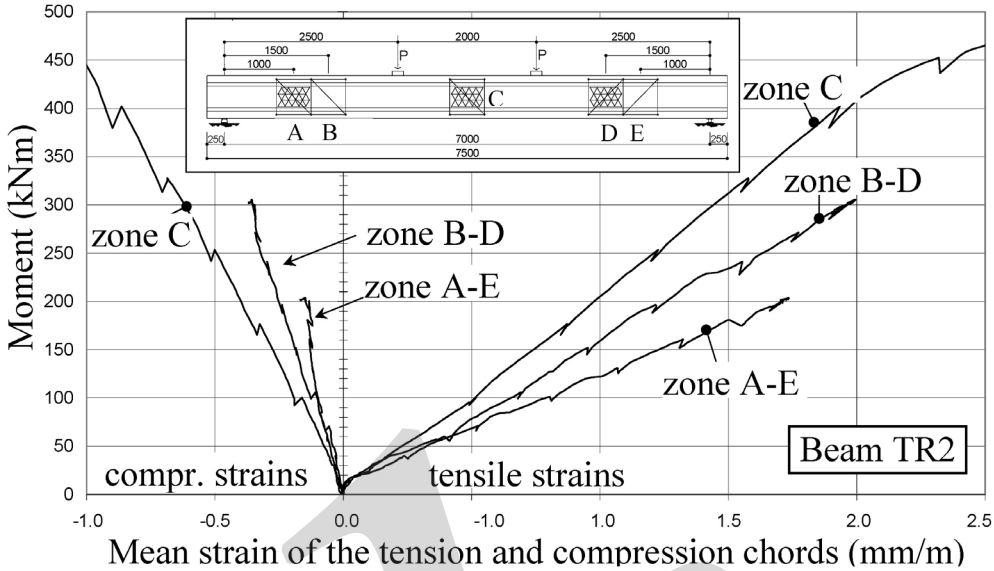


Fig. 6-15 TR2 beam, zones C, A-E, B-D: mean strains of the tension and compression chords as a function of the moment

Fig. 6-15 and Fig. 6-16, referring to a test with two symmetrical loads, show the influence of the shear on the mean strains of the tension and compression chords and the mean curvature, respectively. The tensile deformations are greater for zones A and E than for zones B and D, where the acting shear is smaller on the same moment. An analogous consideration can be made for the C-zone where the shear is nil. The mean shear strain is shown in Fig. 6-17 as a function of the shear.

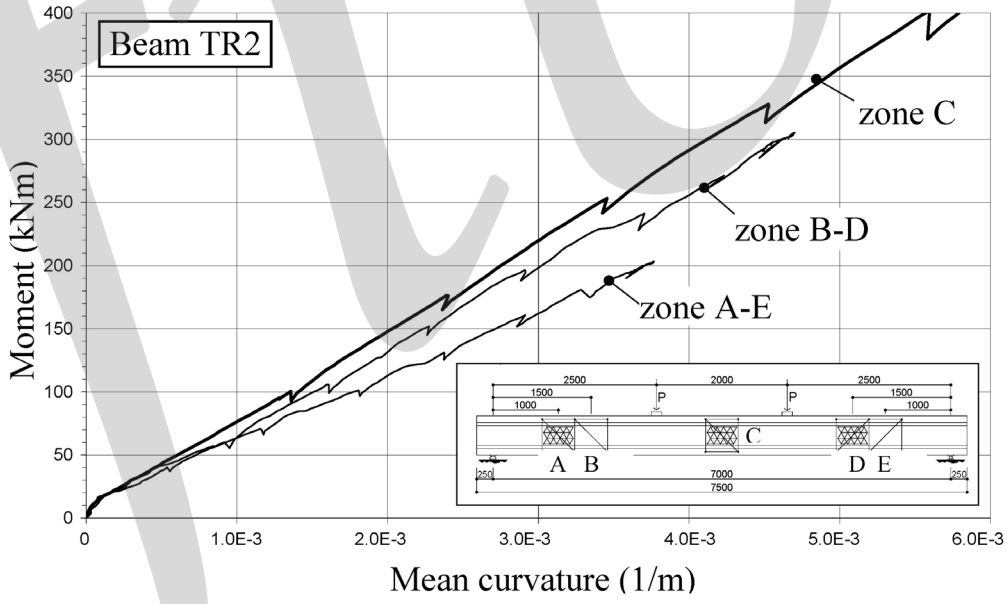


Fig. 6-16 TR2 beam, zones C, A-E, B-D: moment – mean curvature diagrams

This document is the intellectual property of the fib – International Federation for Structural Concrete. All rights reserved.
This PDF of fib Bulletin 92 is intended for use and/or distribution solely within fib National Member Groups.

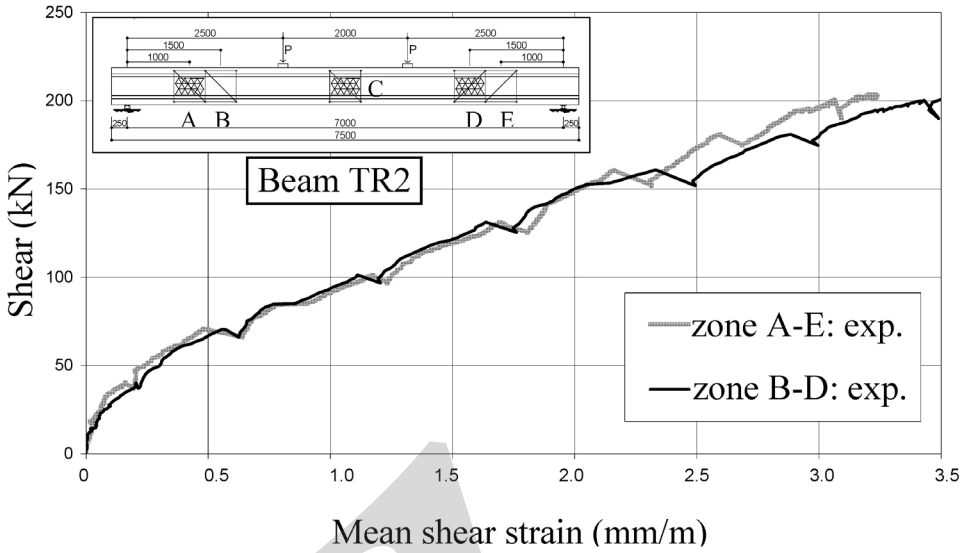


Fig. 6-17 TR2 beam, zones C, A-E, B-D: shear – mean shear strain diagrams

6.2.2.2 Determination of the contribution of shear on deflection

The experimental determination of the contribution of shear on deflection is not immediate; according to the previous analysis of the beam block, actually the shear firstly indirectly influences the deflection because of the variation of forces acting on the top and bottom chords with respect to the flexural behaviour (increase of the mean curvature), and secondly, directly because of the mean shear strain. The problem is how to separate the different contributions.

Two experimental procedures are suitable to this goal. A first method is to measure not only the total deflection (for example by means a potentiometric transducer at the mid span) but also the mean curvatures along the whole beam. It is thus possible to determine the 'curvature deflection', which is obtained through the integration of the experimental mean curvatures along the beam. This value takes into account the effects of the moment and the shear on the mean curvature. Therefore, the difference between the experimental values of the total deflection and the curvature deflection represents the experimental deflection attributable to the mean shear strain.

The second methodology require to perform a series of tests conducted on different beams which have the same values of height h, width b and longitudinal and transversal reinforcement, but different values of web thickness. The influence of mean shear strain on deflection can be evidenced by means of comparison between the experimental deflection values as a function of the b/b_w (width of section)/(web thickness) ratio for each series of beams. Moreover, in an approximate way, the experimental curvature deflection of each beam can be assumed equal to the value obtained with a reference beam with a rectangular section, since the effect of the mean shear strain on deflection is almost negligible in this case.

Fig. 6-18[6-16] shows the diagram of the maximum deflection as a function of the applied load obtained by applying the first method to a three-point bending test that were conducted on a *I*-beam characterised by a L/d ratio of 11 and a b/b_w (width of the section)/(web thickness) ratio of 4 (longitudinal reinforcement ratio $\rho_l = 0.008$). The contribution of shear deflection to the total deflection at service load (50% of ultimate load) in this case was greater than 25% while, in an analogous beam with a lower longitudinal reinforcement ratio, this contribution was greater than 30%.

This document is the intellectual property of the fib – International Federation for Structural Concrete. All rights reserved.
This PDF of fib Bulletin 92 is intended for use and/or distribution solely within fib National Member Groups.

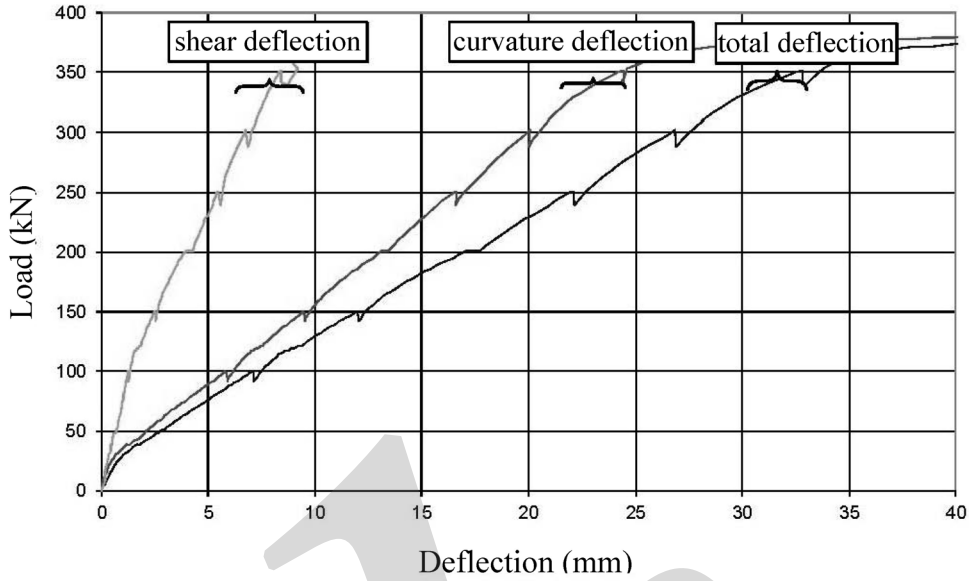
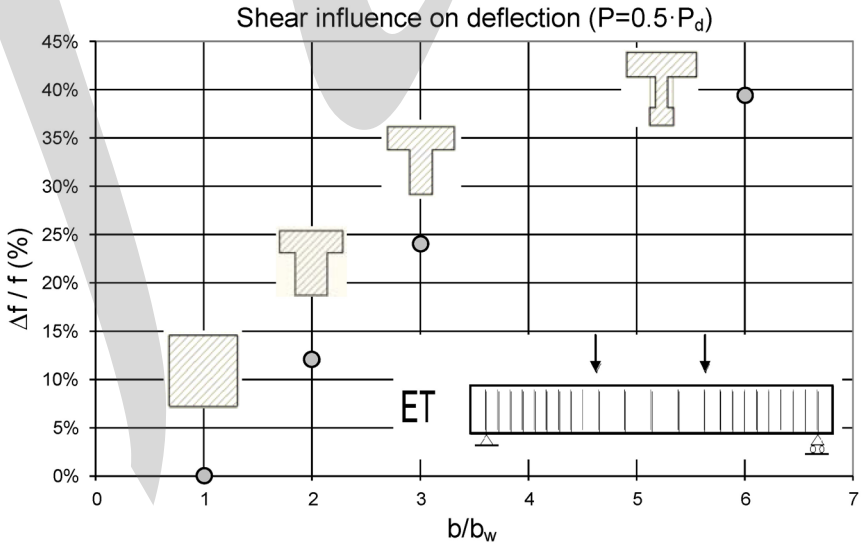


Fig. 6-18 Three-point bending test on an I-beam: diagram of the experimental maximum deflection as a function of the applied load

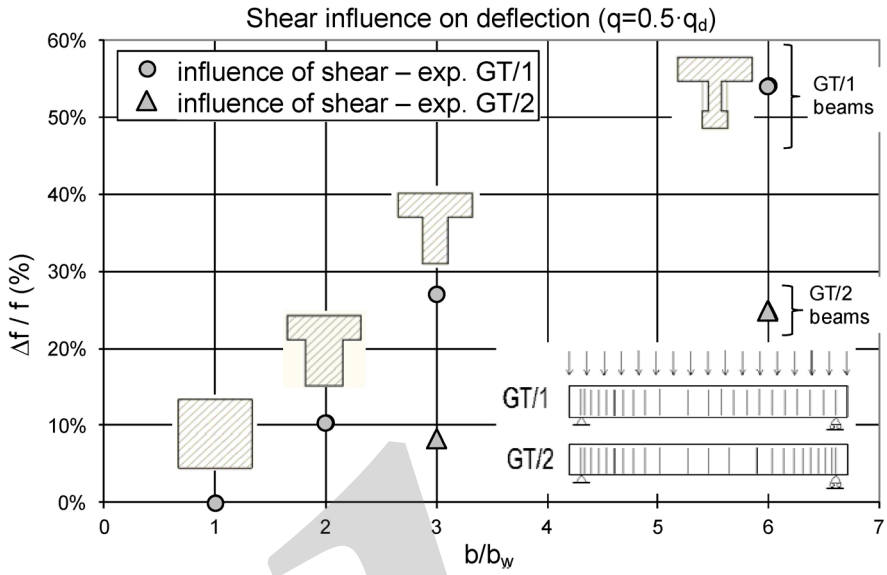
The second method is applicable to the well-known Leonhardt tests[6-10]. The tests involved ten RC T-section beams with thin web, 0.35 m high, a width of the flange of 0.3 m and spans of 3.0 m, an *L/d* value of 10, and longitudinally reinforced with a ratio of $\rho_l = A_s/b_d = 0.014$. Uniform load (GT series) and four-point bending (ET series) tests were considered. In the GT series, four beams (GT/1) had an asymmetric layout of stirrups, whereas two beams (GT/2) had a symmetric layout. Each series of tests was conducted on four beams which had the same values of height h, width b and longitudinal reinforcement, but different values of web thickness ($b/b_w = 1, 2, 3, 6$).

Fig. 6-19a and b show the experimental diagram of the (deflection due to shear strain)/(deflection due to curvature) ratio as a function of the b/b_w. A clear increase in deflection can be observed when the thickness of the web decreases.



a)

This document is the intellectual property of the fib – International Federation for Structural Concrete. All rights reserved.
This PDF of fib Bulletin 92 is intended for use and/or distribution solely within fib National Member Groups.



b)

Fig. 6-19 a) ET beams, b) GT beams: diagram of the (deflection due to shear)/(deflection due to bending) ratio as a function of the (width of section)/(web thickness) ratio

6.2.3 Review of theoretical models for the calculation of the deformation of a macro-element of the beam block due to bending and shear

6.2.3.1 Leonhardt model

The model, proposed by Leonhardt[6-10], considers the truss behaviour of the element as a lattice composed of a compression chord at the top of the beam, a tension chord at the bottom of the beam, a vertical (or inclined) tie representing stirrups and a compressed web strut rotated by the θ-angle on the horizontal axis (Fig. 6-20)

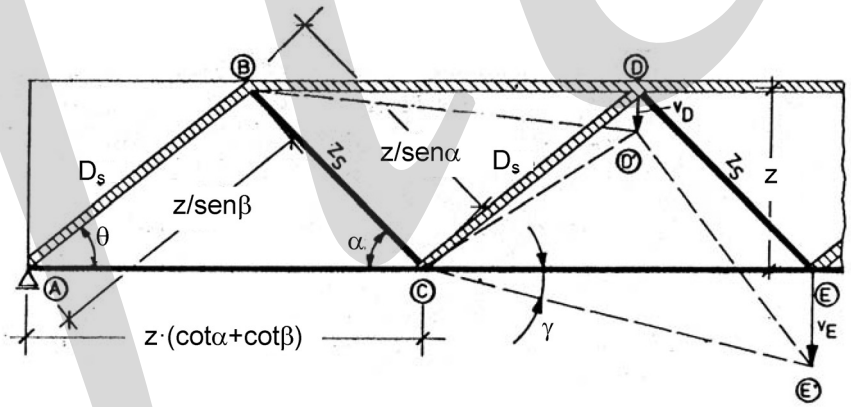


Fig. 6-20 Truss considered by Leonhardt

The mean deformation of a beam block is evaluated on the basis of the deformation of each element of the truss, assuming the hypothesis that the deformation of the top and the bottom chords is not influenced by the shear and, mutually, the deformation of the web struts and ties is not influenced by the bending moment.

The concrete contribution is considered in a simplified manner by means of a predetermined shear stress value τ_0 that reduces the acting design shear force. At the same time the θ-angle is considered constant and equal to 45°.

This document is the intellectual property of the fib – International Federation for Structural Concrete. All rights reserved.
This PDF of fib Bulletin 92 is intended for use and/or distribution solely within fib National Member Groups.

The problem is thus reduced to the calculation of the forces acting on the element of a statically determinate structure and of the corresponding mean strains.

The mean shear strain of the beam block can be evaluated on the basis of the vertical displacement v_e (Fig. 6-20):

$$\tan_{\gamma} \approx \gamma = \frac{v_E}{z\left(\cot g\alpha + \cot g\beta\right)} \tag{6-13}$$

6.2.3.2 Modified Compression Field Theory

This model, first proposed in a study[6-19] and then further developed by other authors, can be ascribed to the "smeared models": a reinforced concrete cracked element is actually considered as a new material whose strength and deformability properties are represented by the mean values.

This theory was developed and calibrated by observing the response of a large number of reinforced concrete elements loaded in pure shear or in shear combined with axial stress. The problem addressed by the model is thus to predict up to failure the relationships between the axial and shear stresses applied to a membrane element and the resulting axial and shear strains in the same element.

The central assumption of the theory is that the average direction of principal compressive stress in the cracked concrete corresponds to the average direction of principal compressive strain and that the critical cracks are also inclined in this direction. In addition to considering average stresses and average strains in the cracked concrete and the relationships between them, the theory considers how the stresses are transmitted across the critical cracks.

The model considers a set of equations representing the average stress relationships, the geometric compatibility conditions and the stress-strain relationships. The analytical procedure requires an iterative process for the solution of 15 simultaneous nonlinear equations.

The equilibrium equations, geometric conditions and stress-strain relationships used in the MCFT are summarized in Fig 6-21.

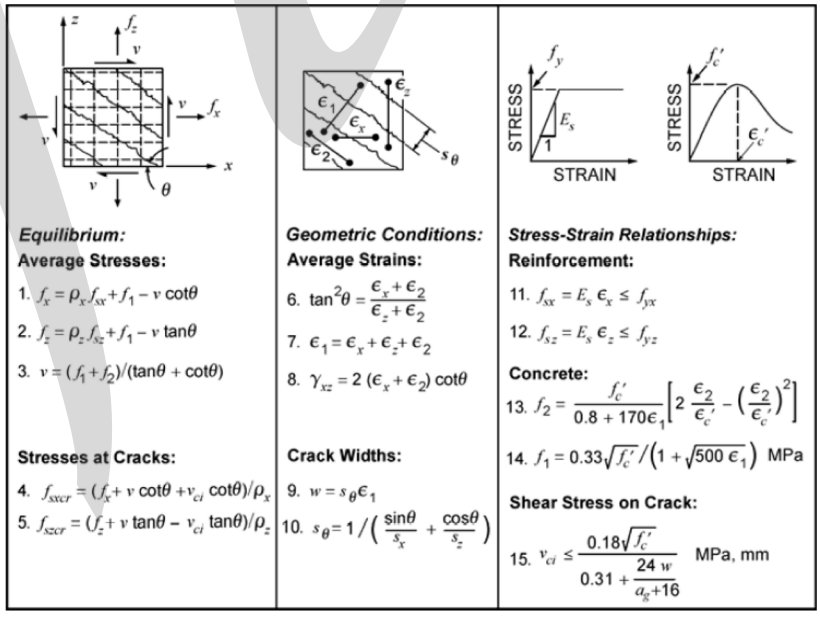


Fig. 6-21 Equilibrium equations, geometric conditions and stress-strain relationships used in the MCFT

This document is the intellectual property of the fib – International Federation for Structural Concrete. All rights reserved.
This PDF of fib Bulletin 92 is intended for use and/or distribution solely within fib National Member Groups.

It should be noted that smeared approaches, such as the Modified Compression Field Theory, have been defined and calibrated with reference to an extensive amount of experimental work that was carried out on RC panels reinforced with bars in two directions and subjected to shear and axial forces. However, the application of these models to RC beams is not easy, because of the coinciding presence of shear and bending moment. In fact, it is necessary to subdivide the section into horizontal strips, each of which is considered as a finite element that has to respect the equilibrium of forces and congruency of the strain conditions[6-19]. In this way the computational difficulties are not reduced but it is possible to consider the simultaneous presence of shear and bending moment.

The results of the analysis enables complete description of the equilibrium and strain conditions of each strip (each fibre over the height of the section): the shear strain, that varies over the height of the section, has thus to be intended as a local deformation parameter; it is possible, however, to determine the mean deformation of the section, for example referring to the local shear strain of the fibre set at the mid-height of the section.

This is the basis of program Response-2000, implemented by Bentz, which is capable of predicting the shear stress distribution over the height of the beam and the shear force-shear deformation relationship of the section.

6.2.3.3 Mixed model and simplified model

A synthesis between the two previous approaches can be found in two different theoretical models, called the mixed model and the simplified model, proposed in two studies[6-18, 6-20] for the calculation of shear strain in the service condition. These methods do not subdivide the cross section into different layers, but instead consider a unique element that coincides with a beam block, which is described by a mixed model that superimposes smeared behaviour of the web onto truss behaviour of the chords (adopting the same constitutive laws as MCFT for the concrete in tension and compression).

With the mixed model, which is more refined and which considers all the main parameters involved in a detailed way but requires an iterative calculation procedure, it has been possible to verify the correspondence of the theoretical formulation with experimental data and calibrate the simplified model. The latter is deduced from the refined procedure, introducing some simplifications related to the calculation of the shear component transferred across the uncracked and cracked concrete and the strut angle θ.

The so called "mixed" model for the analysis of shear strain in service conditions considers both a truss model and a smeared model:

- the lattice is composed of a compression chord at the top of the beam, a tension chord at the bottom of the beam, a vertical tie representing stirrups and a compressed web strut rotated by the θ-angle on the horizontal axis;
- the behaviour of the web is represented, in mean terms, by a field of stresses and strains referring to the mid-point of the lever arm: ε_{cz} the mean axial strain, ε_{c2} the mean strain of the concrete struts in θ direction, ε_{c1} the mean strain of the concrete in tension in the (90-θ) direction.

When the deformation of each element of the truss is known, the mean shear strain γ_{zy} can be obtained using:

This document is the intellectual property of the fib – International Federation for Structural Concrete. All rights reserved.
This PDF of fib Bulletin 92 is intended for use and/or distribution solely within fib National Member Groups.

$$\gamma = \frac{2\left(\varepsilon_{c,z} - \varepsilon_{c2}\right)}{\tan\left(\theta\right)} \tag{6-14}$$

Therefore, the problem then is how to calculate the θ angle of the compressed web struts and the strains $\varepsilon_{C,z}$ and ε_{C2}. The refined method refers to MCFT constitutive laws in order to describe the mean behaviour of the beam web for both stresses and strains. This method takes into consideration the mean strains of the chords, imposes overall equilibrium, according to the lattice-like scheme with variable strut inclinations, and it also takes into account the contribution of the mean tensile stresses that act on the cracked concrete.

It is assumed that, in state II, the principal compressive stress axis, the crack direction and the principal compressive strain axis coincide: $\theta_c = \theta_{cr} = \theta$. The constitutive laws of cracked concrete have been taken from the literature, in particular for concrete in tension and compression (relationships derived from those proposed in a study[6-19], for strains in the tension chord and the vertical tension ties (relationships that take into account the tension stiffening effect, according to Model Code 1990[6-8].

The calculation procedure, which starts from two tentative values of the main variables θ and V_c (vertical component of the tension stresses in the web) and contains two iterations based on the respect of the congruency and equilibrium conditions, is performed to determine ε_{cz}, ε_{cy}, ε_{c2} and θ. The main concepts of the mixed model are shown in the left side of Fig. 6.2-9. The complete procedure is described in a study[6-18].

Since the mixed model is a very time consuming procedure, a simplified model has been set up for use in practical applications[6-21], on the basis of theoretical data compared with experimental results.

The unknowns of the problem, such as the concrete contribution V_c and the q-angle, are determined in an approximate way to avoid any iterative procedure and obtain the solution in closed form. Thus, the structural analysis can be carried out in the simple form of a "truss model with concrete contribution", but taking into account the rotation of the struts with the increase in applied shear force and the interaction between bending moment and shear. Fig. 6-22 shows a comparison between the main aspects of the simplified and mixed models.

As far as the concrete contribution, V_c, is concerned, numerical results obtained by means of the mixed model show that it varies with the increase in applied shear; in the first loading phase (before the occurrence of diagonal cracks), and it completely balances the shear. Then, with the formation of inclined web cracks, the truss behaviour begins and both contributions, due to concrete V_c and to transverse reinforcements V_{ws}, balance the shear. In the second phase, the concrete contribution does not actually change to any great extent, while the shear increases[6-15, 6-16, 6-20]. For the sake of simplicity, the concrete contribution can therefore be assumed as a constant in this phase and equal to the value V_{cr} of the shear that causes shear cracking.

The term $V_{cr} = V_c$ has here been approximated, with a good accuracy, using the formula proposed in Model Code 1990[6-8]; the shear length a_v is assumed equal to the moment-to-shear ratio M/V (see Fig. 6-22).

The value of the θ-angle depends on the geometrical parameters of the section, the longitudinal and transverse reinforcement ratios ρ_l and ρ_w, the material properties and the acting moment and shear.

This document is the intellectual property of the fib – International Federation for Structural Concrete. All rights reserved.
This PDF of fib Bulletin 92 is intended for use and/or distribution solely within fib National Member Groups.

A parametric analysis based on the mixed model has shown that the variability of the θ-angle can be simplified by means of a function that refers to four principal parameters: $\varepsilon_{cz}\frac{\tau}{f_{ctm}}=\frac{V-V_c}{b_w\cdot d\cdot f_{ctm}}$; $\rho_{ws}=\frac{A_{sw}}{b_w\cdot s}$; f_{ck}. The deformation ε_{CZ} takes into account the influence of the longitudinal reinforcement ratios ρ_l and the bending moment on the θ-angle.

The assessment of the concrete contribution V_c and the θ-angle "a priori" allows the calculation to be carried out by means of the analysis of an isostatic truss and of the forces acting in the compressed chord, in the tension chord and in the web struts along the θ-direction. The non-iterative calculation procedure described in this study[6-20] leads to the determination of the corresponding mean deformations, such as the horizontal mean strains at the level of the resultant of the compressed chord ε_{cm} and at the level of the tension chord ε_{sm} and of the mean strain along the θ-direction at the mid-height level between the tension and compression chords respectively.

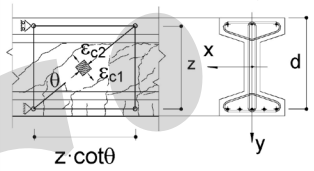
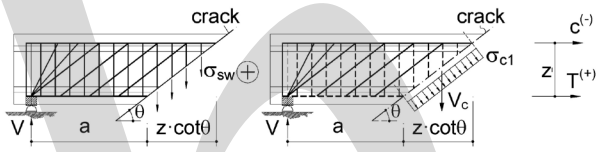
	MIXED MODEL	SIMPLIFIED MODEL
	 Smeared truss model	 Truss model with concrete contribution
θ-angle = inclination of web struts	$\theta_{cr}=\theta$ $\tan^2(\theta)=\frac{(\varepsilon_{c,z}-\varepsilon_{c2})}{(\varepsilon_{c1}-\varepsilon_{c,z})}$ θ changes with the applied shear force	$\theta_{cr}=\theta$ θ calculated "a priori" as: $\theta=k_1\cdot k_2\cdot\theta_0$ $\theta_0=a\left(\frac{\tau}{f_{ctm}}\right)^b$ $a=30+\rho_w\cdot 1150$ $b=5\cdot\rho_w-0{,}215$ $k_1=\left[1+0.1\cdot\left(\frac{f_{ck}-25}{25}\right)\right]$ $k_2=0.64+(960\cdot\varepsilon_{c,z})-(6\cdot 10^5\cdot\varepsilon_{c,z}{}^2)$ θ changes with the applied shear force
Concrete contribution V_C	Vertical component of the tension field; V_C changes with the applied shear force	V_c calculated "a priori" as: $V_c\cong C_c\cdot\left(\frac{3\cdot d}{M/V}\right)^{1/3}\cdot\left(1+\sqrt{\frac{200}{d}}\right)\cdot\left(\frac{100\cdot A_s}{b_w\cdot d}\cdot\lvert f_{ck}\rvert\right)^{1/3}\frac{b_w\cdot d}{1000}\le\frac{J_{x,I}\cdot b_w}{S_x}\cdot f_{ctm}$ V_C is constant with the applied shear force
Procedure	iterative	closed form

Fig. 6-22 Comparison of the mixed model and the simplified model

This document is the intellectual property of the fib – International Federation for Structural Concrete. All rights reserved.
This PDF of fib Bulletin 92 is intended for use and/or distribution solely within fib National Member Groups.

The mean curvature 1/*r* can therefore be thus determined as:

$$\frac{1}{r} = \frac{\varepsilon_{sm} - \varepsilon_{cm}}{0.9d} \tag{6-15}$$

and the mean shear strain g can be obtained applying Eq. 6-14.

Equations 6-14 and 6-15 allow the mean deformation parameters (mean shear strain and mean curvature) to be calculated for all the blocks into which the beam has been divided.

6.2.4 Calculation of the deflection of the beam due to bending and shear

The above mentioned models allow the mean deformation parameters (mean shear strain and mean curvature) to be calculated for all the blocks into which the beam has been divided. When these parameters have been obtained, the deflection can be determined through their integration, for example by means of application of the principle of virtual works.

From the conceptual point of view and according to the previous experimental analysis, the total deflection will be composed of three terms: the contribution due to the bending moment on the mean curvature, the contribution due to the increase of the mean curvature produced by the shear, and the direct contribution of the mean shear strain.

The shear, in fact, indirectly influences the deflection because of the variation of forces acting on the top and bottom chords with respect to the flexural behaviour, and also directly because of the mean shear strain.

The adoption of the MCFT applied to the beams or both the mixed models (refined or simplified) allows the influence of the shear on the curvature to be taken into account. In this case the integration of the mean curvature lead to the calculation of both the contribution of the bending moment on the deflection and the indirect effect of the shear. Mutually, the integration of the mean shear strain allows evaluation of the direct contribution of the shear.

6.2.5 Practical evaluation of the influence of shear on deflection

For practical purposes the calculation of the deflection, taking into account the shear contribution, is not immediate as it requires the mean deformations to be integrated; thus can be a useful support for the design, both defining the cases in which this contribution is significant and directly quantifying its amount. In this context, an extensive parametric analysis has been carried out to highlight the influence of shear on deflection as a function of the main parameters involved.

Four static schemes were considered: a simply supported beam, a beam with fixed ends, a beam with a fixed and a supported end and a cantilever. The influence of shear on the deflection was pointed out for each scheme, taking into account the significant parameters that affect the phenomena, by means of the "deflection due to shear / the deflection due to bending" ratio. In this case the deflection due to bending was evaluated by only referring to the curvature due to the bending moment, without any shear interaction. This ratio represents the percentage increase in the deflection due to bending, and can be used to obtain the total deflection.

This document is the intellectual property of the fib – International Federation for Structural Concrete. All rights reserved.
This PDF of fib Bulletin 92 is intended for use and/or distribution solely within fib National Member Groups.

In this way, the total deflection can be determined on the basis of the value of the deflection calculated for bending $f_{bending}$ with the relationship:

$$f_{total} = f_{bending}\left(1+\frac{f_{shear}}{f_{bending}}\right) \tag{6-16}$$

The shear contribution is determined for each scheme through a parametric analysis, based on the simplified model and considering the main parameters involved. The calculation refers to the quasi-permanent condition, assuming a uniform load of 50% of the ultimate design load.

6.2.5.1 Parametric analysis

The total deflection of a beam depends on several parameters, which can be listed in the following categories:

- geometrical parameters: L, d, B, b_w, h_f
- longitudinal and transversal reinforcement ratios: ρ_l, ρ_w
- material properties: f_{ck} , E_C and creep coefficient φ.

These parameters do not affect the $f_{shear}/f_{bending}$ ratio to the same extent. The results of the analysis show that the L/d ratio is considerably important while the value of span L and the creep coefficient φ, although very significant when referring to the total deflection, have a negligible influence on $f_{shear}/f_{bending}$, as has been demonstrated in the numerical analysis. Therefore, the study does not consider the variability of L and φ and assumes two fixed values for these parameters: L = 6 m and φ = 2, while two strength classes are considered: f_{ck} = 30 N/mm² and f_{ck} = 50 N/mm².

All the other parameters are taken into account by means of the following procedure.

The fixed pattern of longitudinal and transverse reinforcement shown in Fig. 6-23 is considered for each static scheme.

The longitudinal reinforcement amount is defined for the critical section (section subjected to the maximum bending moment) as the reinforcement that is strictly necessary for ULS verification. The amount of reinforcement in the other sections is a function of the reinforcement at the critical section, in accordance with the pattern shown in Fig. 6-23. Similarly, the transverse reinforcement amount is determined for the section subjected to maximum shear in order to optimize the ULS design, but is maintained constant along the element.

The geometry of the beam is determined via the following procedure (assuming a value of L = 6 m and h_f = 0,2d):

1. assume specific values of L/d, A_S and $\rho_l = \frac{A_s}{b \cdot d}$;
2. determine the consequent values of d, b;
3. calculate the resistant bending moment at ULS M_{Rd} in the critical section, assuming an inner lever arm $z = 0.9 \cdot d$.
4. calculate the design load q_d at ULS and the corresponding shear design value V_{Ed} at the critical section;
5. assume a specific value of $\frac{b}{b_w}$ and determine the consequent values of b_w;

This document is the intellectual property of the fib – International Federation for Structural Concrete. All rights reserved.
This PDF of fib Bulletin 92 is intended for use and/or distribution solely within fib National Member Groups.

6. calculate the transverse reinforcement A_{sw} and s_w; the calculation of the transverse reinforcement is based on the truss model proposed in EN1992-1-1[6-2], limiting the values for the θ angle of the inclined struts in the web to the $1 \leq \cot\theta \leq 2{,}5$ range (ultimate conditions). When possible, the optimum value of angle θ is determined by imposing the simultaneous collapse of the shear reinforcement and the concrete struts in the web ($V_{Rd,s} = V_{Rd,max}$).

7. calculate the service condition load corresponding at quasi permanent condition, $q_{ser} = 0{,}5q_d$;

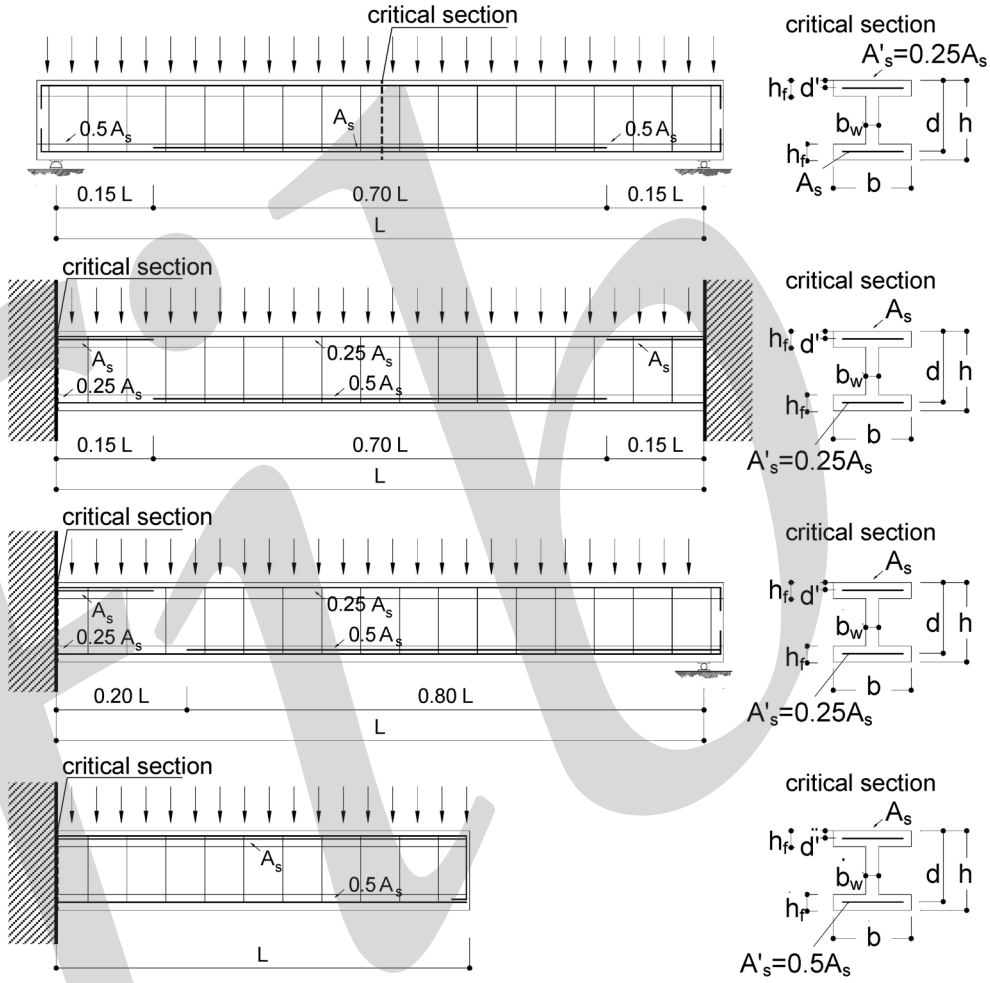


Fig. 6-23 Distribution of the longitudinal and transverse reinforcement along the beam for each schema of restraints – a) simply supported beam, b) beam with fixed ends, c) beam with fixed and support end, d) cantilever

The (deflection due to shear) - to - (deflection due to bending) ratio is calculated for each case and the shear contribution to deflection, as a function of variables L/d and b/b_w (Fig. 6-24, Fig. 6-25, Fig. 6-26, Fig. 6-27, Fig. 6-28, Fig. 6-29, Fig. 6-30, Fig. 6-31), is highlighted. The analysis is conducted separately for the four types of restraints and the three values of the longitudinal reinforcement ratios $\rho_l = 1{,}5\%$, $\rho_l = 1{,}0\%$, $\rho_l = 0{,}5\%$. The longitudinal reinforcement ratio is connected to the concrete compression stress in the compressive zone of the section and the adopted values can refer to highly stressed, medium stressed and lightly stressed concrete respectively (EN 1992-1-1[6-2]). The deflection is carried out by referring to mean values of the mechanical properties of materials.

This document is the intellectual property of the fib – International Federation for Structural Concrete. All rights reserved.
This PDF of fib Bulletin 92 is intended for use and/or distribution solely within fib National Member Groups.

The diagrams can be used for a direct evaluation of the influence of shear on the basis of the concrete strength f_{ck}, and the L/d and b/b_w ratio and, if necessary, using linear interpolation. The minimum value of the L/d ratio assumed in the diagrams refers to cases in which the effects of discontinuity regions become predominant and the model should no longer be considered valid. The end of each curve is related to the maximum web slenderness b/b_w that is allowed by the resistance of concrete struts at ULS: after this point a curve actually exists (service condition), but it refers to cases that have not been verified at ULS and are therefore not shown.

The diagrams show that the influence of shear appears significant (greater than 10%) for many common cases, even for not very low L/d ratios.

The influence of shear increases when the b/bw ratio increases and the slenderness L/d decreases. For the same value of b/b_w, a higher longitudinal reinforcement ratio ρ_l produces a greater influence of shear.

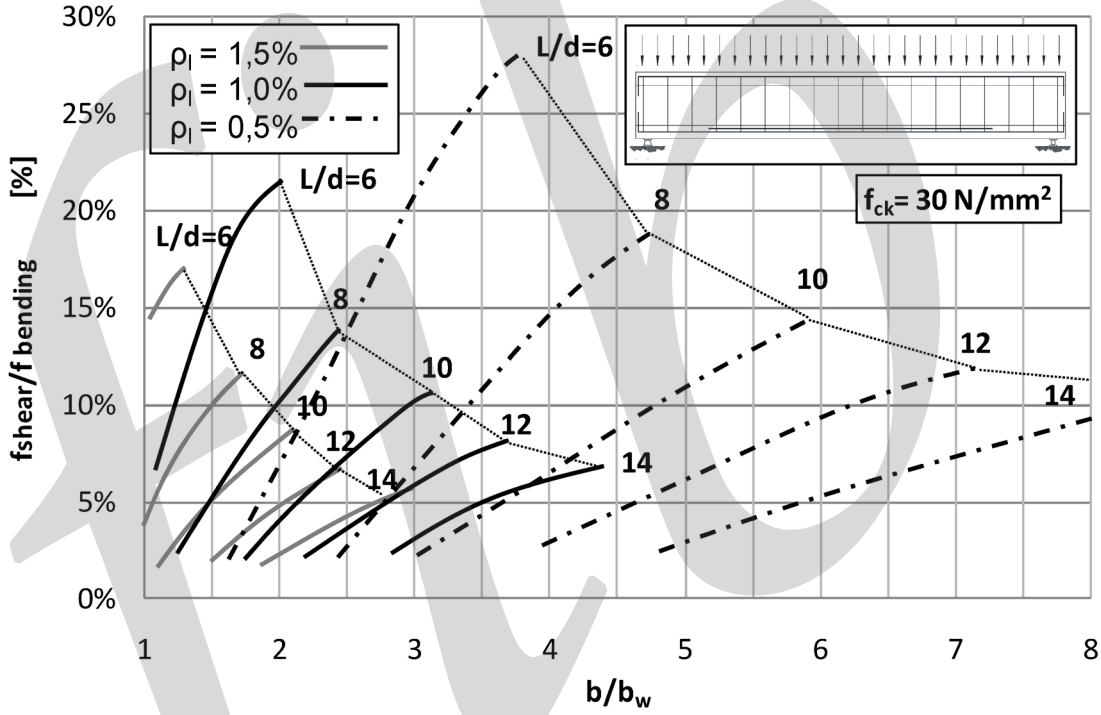


Fig. 6-24 Simply supported beam, f_{ck} = 30 N/mm², ρ_l = 0,5% (dot line), ρ_l = 1,0% (continuous line) and 1,5% (grey line): diagram of the (deflection due to shear) / (deflection due to bending) ratio as a function of the (width of section) / (web thickness) ratio

This document is the intellectual property of the fib – International Federation for Structural Concrete. All rights reserved.
This PDF of fib Bulletin 92 is intended for use and/or distribution solely within fib National Member Groups.

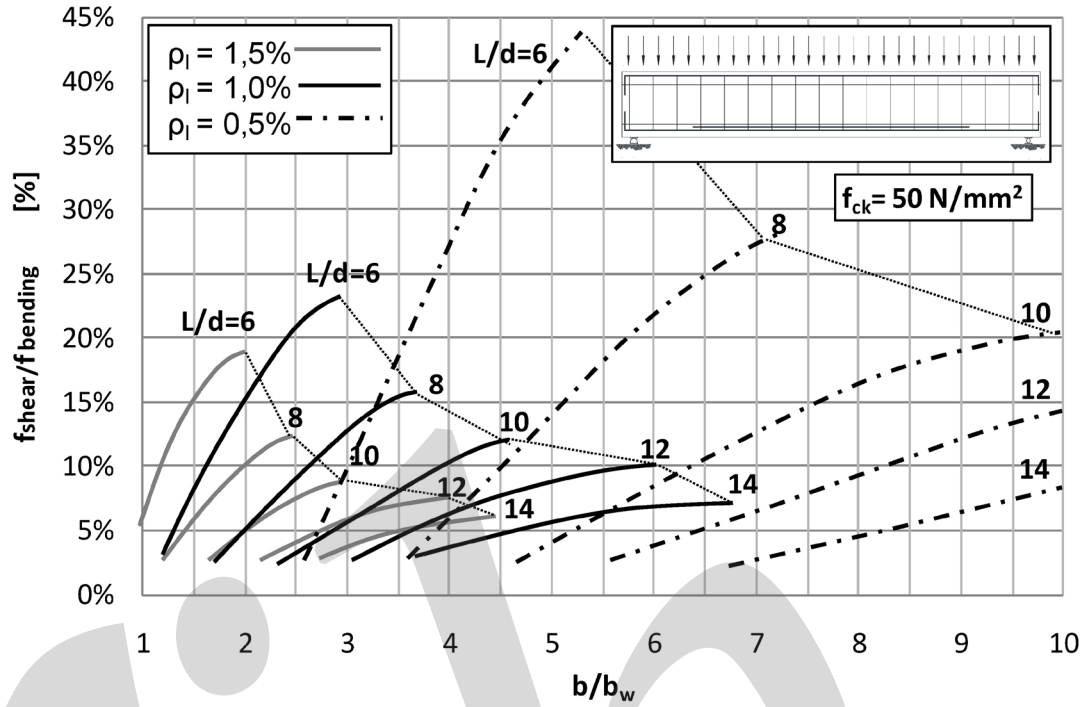


Fig. 6-25 Simply supported beam, f_{ck} = 50 N/mm², ρ_l = 0,5 % (dot line), ρ_l = 1,0 % (continuous line) and 1,5% (grey line): diagram of the (deflection due to shear) / (deflection due to bending) ratio as a function of the (width of section) / (web thickness) ratio

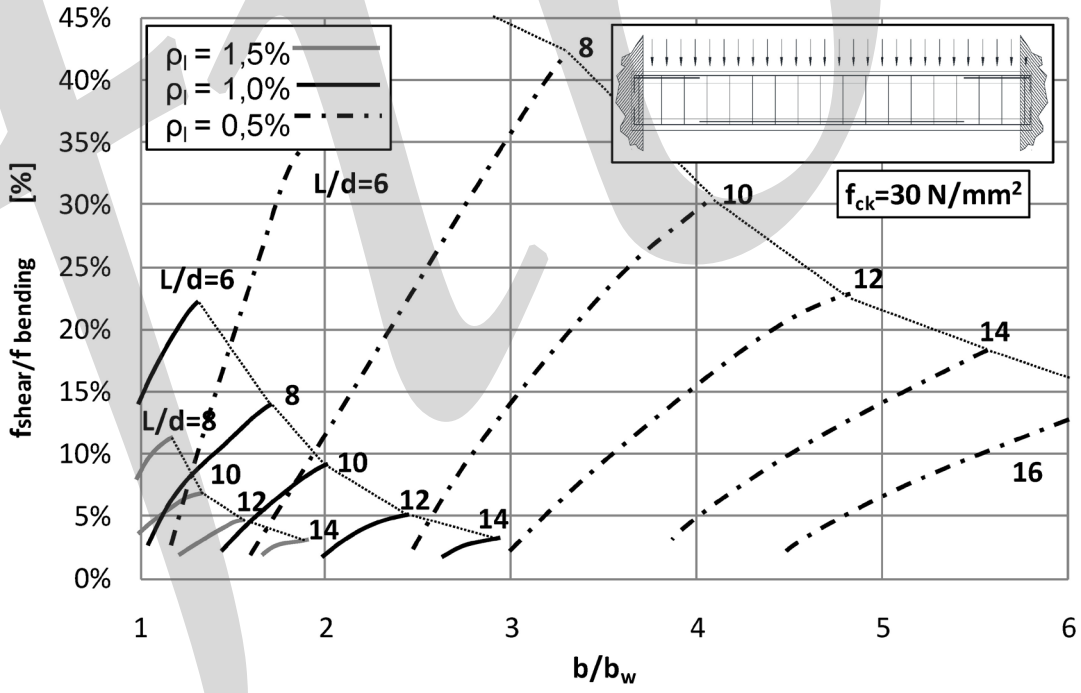


Fig. 6-26 Beam with fixed ends, f_{ck} = 30 N/mm², ρ_l = 0,5% (dot line), ρ_l = 1,0% (continuous line) and 1,5% (grey line): diagram of the (deflection due to shear) / (deflection due to bending) ratio as a function of the (width of section) / (web thickness) ratio

This document is the intellectual property of the fib – International Federation for Structural Concrete. All rights reserved.
This PDF of fib Bulletin 92 is intended for use and/or distribution solely within fib National Member Groups.

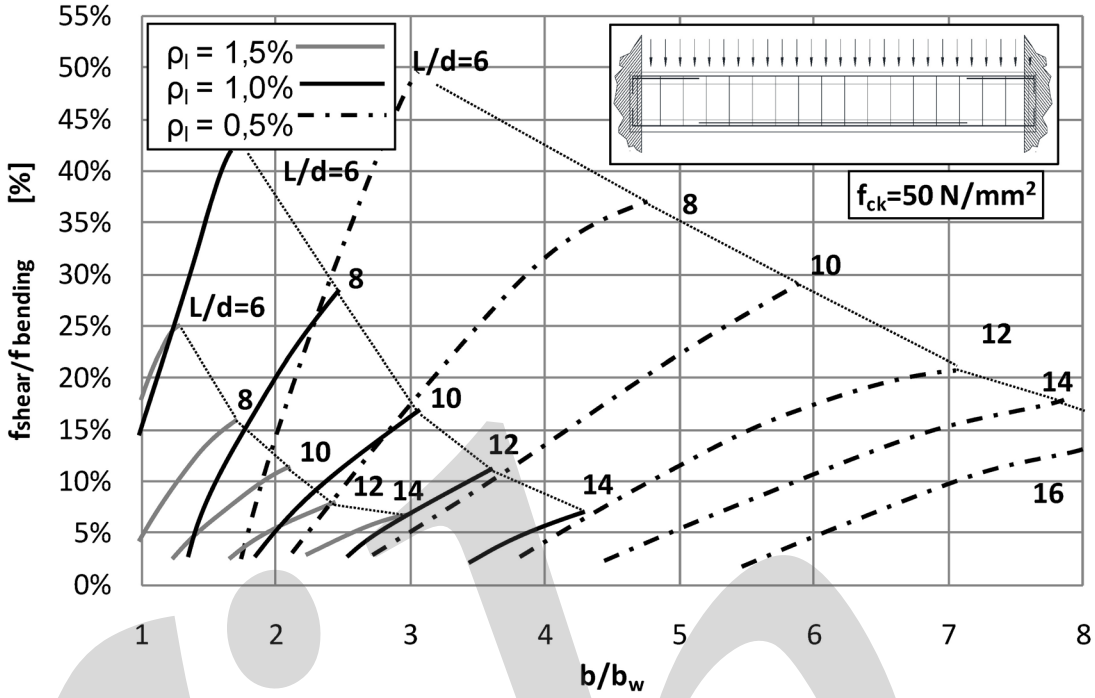


Fig. 6-27 Beam with fixed ends, f_{ck} = 50 N/mm², ρ_l = 0,5% (dot line), ρ_l = 1,0% (continuous line) and 1,5% (grey line): diagram of the (deflection due to shear) / (deflection due to bending) ratio as a function of the (width of section) / (web thickness) ratio

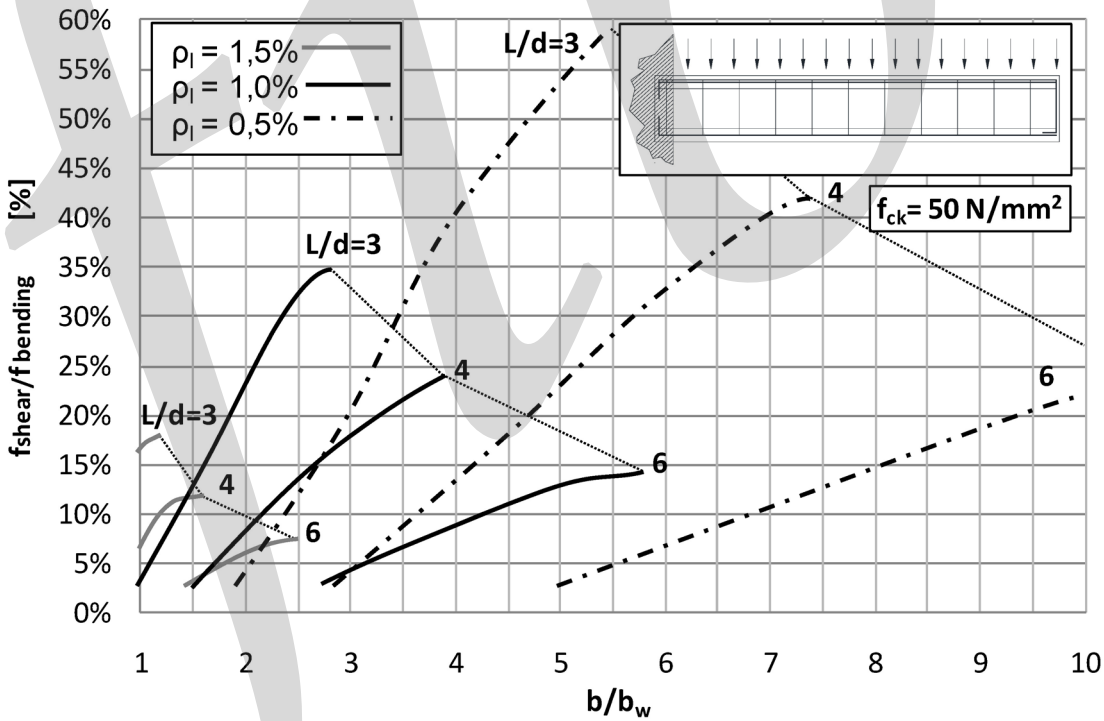


Fig. 6-28 Cantilever, f_{ck} = 50 N/mm², ρ_l = 0,5% (dot line), ρ_l = 1,0% (continuous line) and 1,5% (grey line): diagram of the (deflection due to shear) / (deflection due to bending) ratio as a function of the (width of section) / (web thickness) ratio

This document is the intellectual property of the fib – International Federation for Structural Concrete. All rights reserved.
This PDF of fib Bulletin 92 is intended for use and/or distribution solely within fib National Member Groups.

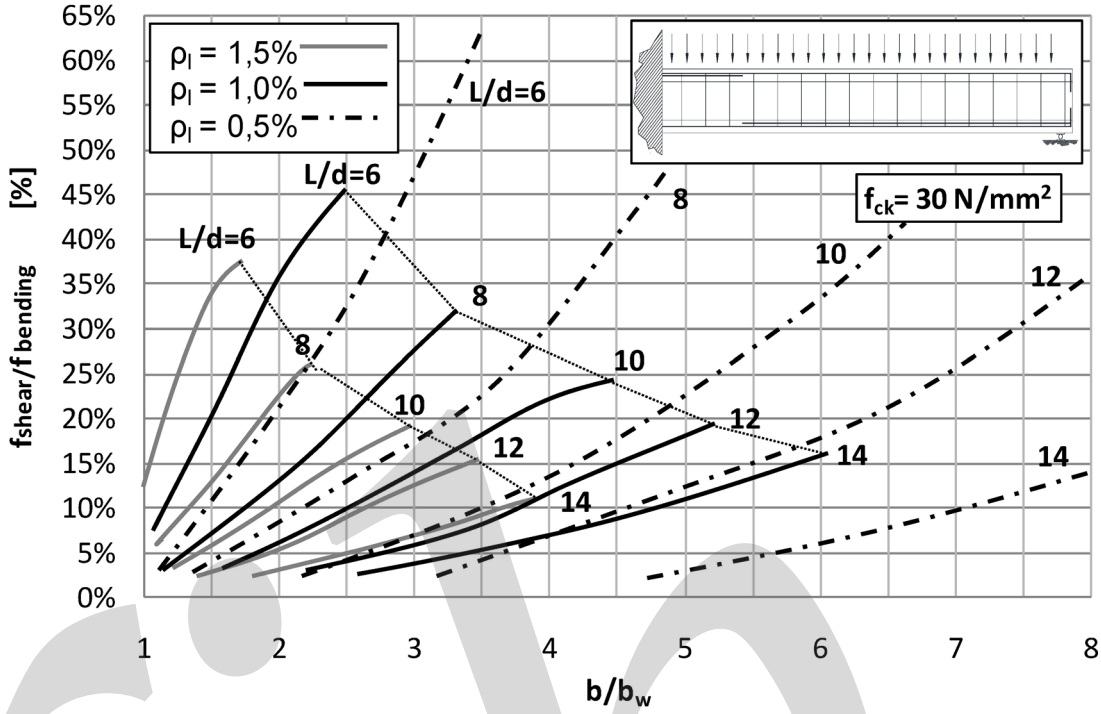


Fig. 6-29 Fixed and support end, f_{ck} = 30 N/mm², ρ_l = 0,5% (dot line), ρ_l = 1,0 % (continuous line) and 1,5% (grey line): diagram of the (deflection due to shear) / (deflection due to bending) ratio as a function of the (width of section) / (web thickness) ratio

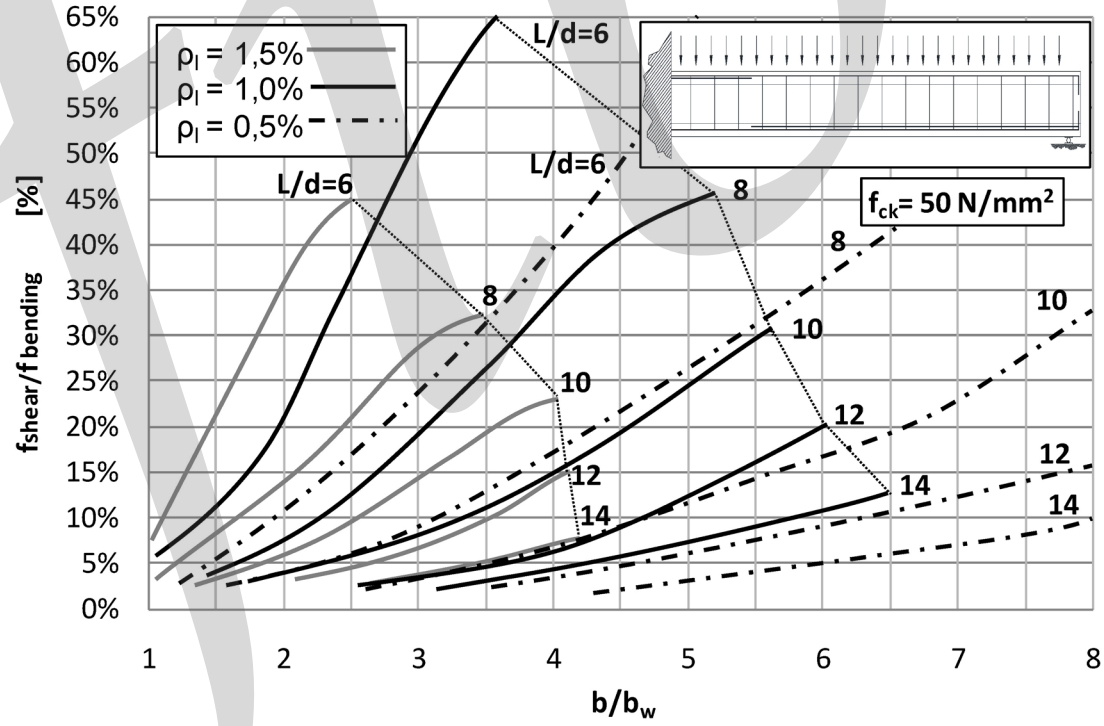


Fig. 6-30 Fixed and support end, f_{ck} = 50 N/mm², ρ_l = 0,5% (dot line), ρ_l = 1,0% (continuous line) and 1,5% (grey line): diagram of the (deflection due to shear) / (deflection due to bending) ratio as a function of the (width of section) / (web thickness) ratio

This document is the intellectual property of the fib – International Federation for Structural Concrete. All rights reserved.
This PDF of fib Bulletin 92 is intended for use and/or distribution solely within fib National Member Groups.

The procedure allows one to highlight the contribution of shear to deflection as a function of the variables L/d and b/b_w, considering different longitudinal reinforcement ratios and concrete strengths. Thus the results of this analysis allows one to identify the most common cases in which this influence becomes significant and they also constitute a tool for the direct evaluation of this contribution. In order to show the cases in which the contribution of shear is not negligible ($f_{shear} \geq 0{,}10\ f_{bending}$), the results can also be summarized, as in Fig. 6-31 (f_{ck} = 30 N/mm^2), where each quadrant refers to a particular static scheme. The same figure considers the three static schemes introduced above, but the case of a simply supported beam subjected to a concentrated load applied at mid-span has also been added. The curves, concerning two amounts of longitudinal reinforcement, are limited to cases in which the verification at ULS is satisfied (horizontal cutting of diagrams). A comparison between the different static schemes shows significant differences in the extent of the influence of shear, L/d and b/b_w ratios being equal. Moreover the figure highlights that the contribution of shear on deflection can be greater than 10% even for not very low span-to-depth ratios.

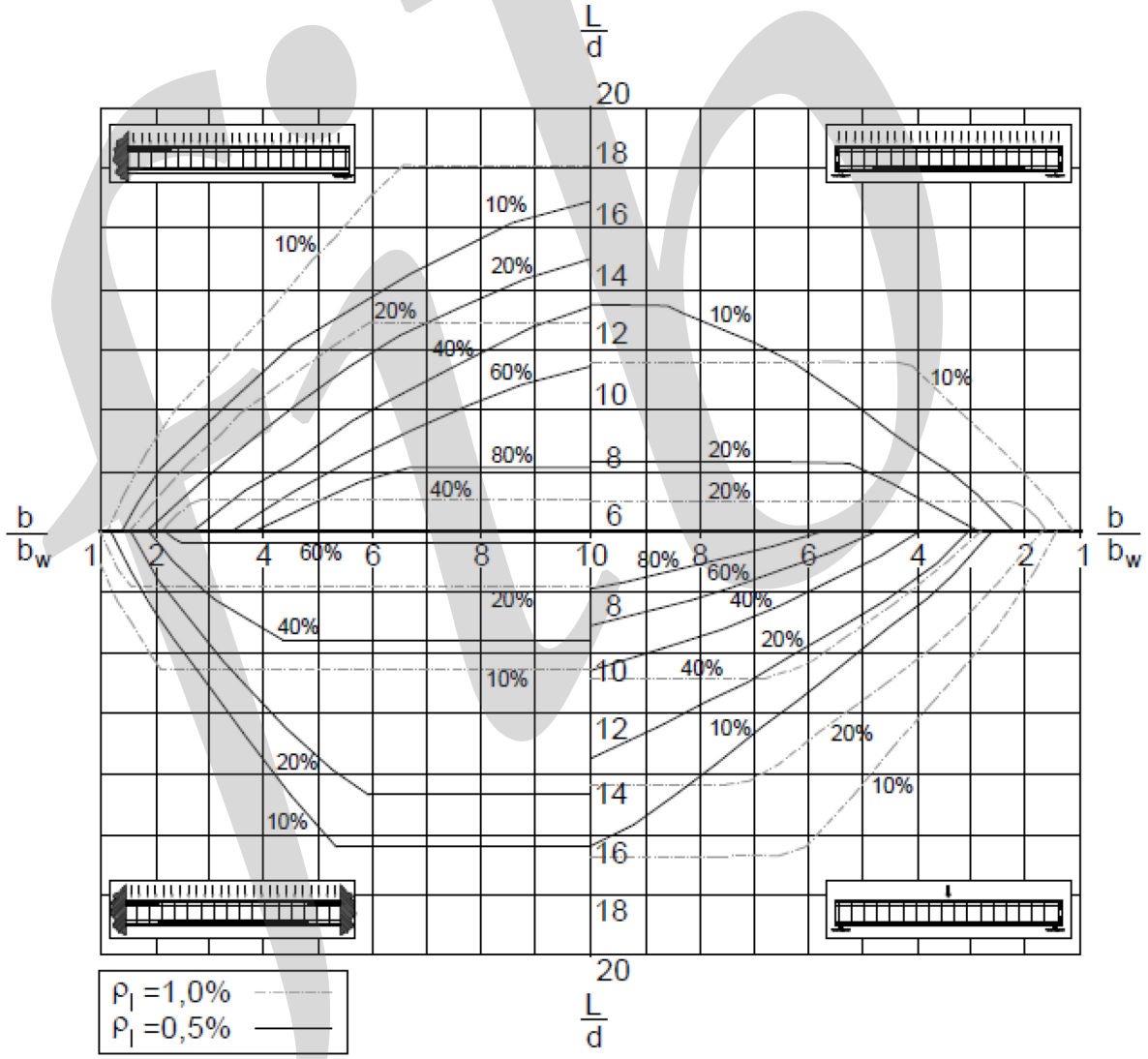


Fig. 6-31 Percentage influence of shear on deflection as a function of the L/d and b/b_w ratios for different static schemes (f_{ck} = 30 N/mm^2)

This document is the intellectual property of the fib – International Federation for Structural Concrete. All rights reserved.
This PDF of fib Bulletin 92 is intended for use and/or distribution solely within fib National Member Groups.

6.3 Slenderness limits

Slenderness limits are defined as the span-to-effective depth ratio (l/d) below which it is not necessary to verify deflections in normal building structures. In MC 2010[6-1] they are an explicit function of:

- The reinforcement ratio, $\rho = (A_s/b_d)$
- The support conditions (simply supported, continuous – end span or interior span –, cantilever)
- The concrete strength

The current formulation, included in MC 2010[6-1] is given in Eq. (6-17)

$$\frac{l}{d} = K\left[11+1.5\sqrt{f_{ck}}\frac{\rho_0}{\rho}+3.2\sqrt{f_{ck}}\left(\frac{\rho_0}{\rho}-1\right)^{3/2}\right] \text{ if } \rho \le \rho_0$$
$$\frac{l}{d} = K\left[11+1.5\sqrt{f_{ck}}\frac{\rho_0}{\rho-\rho'}+\frac{1}{12}\sqrt{f_{ck}}\sqrt{\frac{\rho'}{\rho_0}}\right] \text{ if } \rho > \rho_0 \quad (6\text{-}17)$$

where :

l is the span of the beam

d is the effective depth of the beam

K is a parameter relating the slenderness limit of a simply supported beam to that of beam with different supports conditions

f_{ck} is the characteristic strength of concrete:

ρ is the tensile reinforcement ratio, referred to the reinforcement strictly needed for ULS

ρ' is the compressive reinforcement ratio, referred to the reinforcement strictly needed for ULS

ρ_0 is a model parameter defined in Eq. 6-18

$$\rho_0 = \frac{\sqrt{f_{ck}}}{1'000} \quad (6\text{-}18)$$

In the following paragraphs, the background to the MC 2010[6-1] formulation on slenderness limits is explained, with special emphasis on the limitations of this approach. Following this explanation a proposal for overcoming some of its shortcomings is presented.

6.3.1 How slenderness limits are determined

Fig. 6-32 shows a flowchart which summarizes the procedure which can be followed to obtain the slenderness limit for a given reinforcement ratio. First, a simply supported beam is considered. A value of the reinforcement ratio, for which the slenderness ratio is to be determined (ρ) and a span length (L) are assumed. The section is assumed to be rectangular of arbitrary width b. Assuming a trial value of the effective cross-section depth, d, the ultimate bending moment (M_{Rd}) which the section can resist can be determined. The ultimate factored load (q_{Rd}) can then be obtained by equilibrium conditions.

This document is the intellectual property of the fib – International Federation for Structural Concrete. All rights reserved.
This PDF of fib Bulletin 92 is intended for use and/or distribution solely within fib National Member Groups.

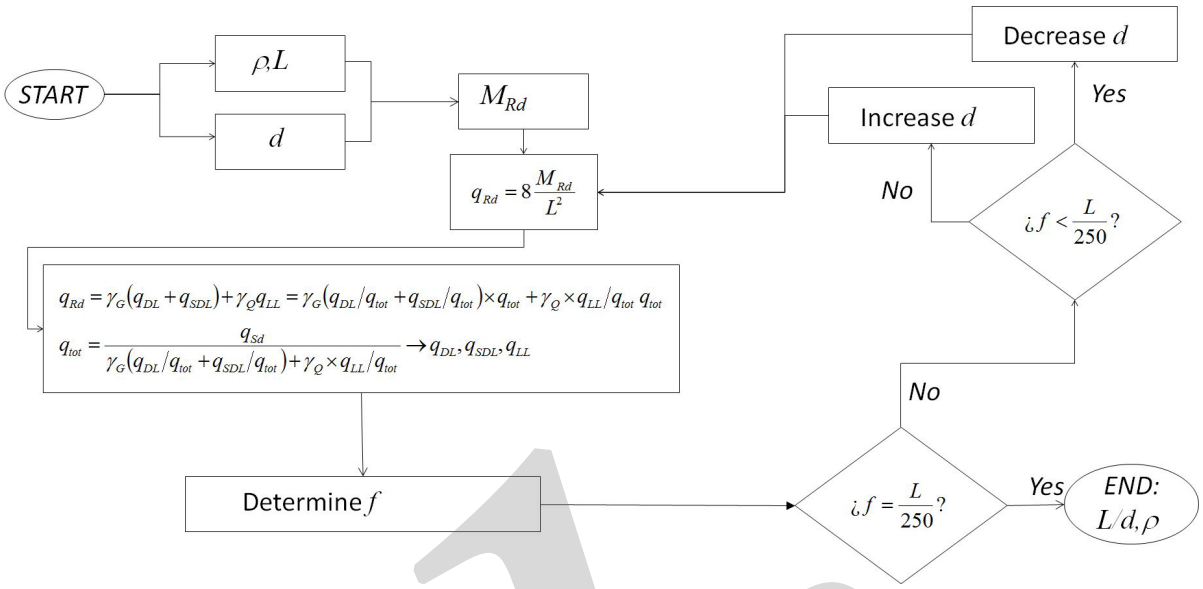


Fig. 6-32 Flowchart for the determination of slenderness limits

In order to continue the process, some values must be assumed for the ratio between self-weight and total load (q_{SW}/q_{tot}), and between superimposed dead load and total load (q_{SDL}/q_{tot}). The ratio between live load and total load (q_{LL}/q_{tot}) follows from $q_{SW}+ q_{SDL}+ q_{LL}= q_{tot}$. If the values of two of these ratios are fixed, it is possible to determine the values of each individual load. Once this is done, the calculation of the deflection can be carried out with any valid method which considers instantaneous plus time-dependent values. For the derivation of the current EN 1992-1-1[6-2] formulation, which was also adopted by MC 2010[6-1], this was done for the quasi-permanent load combination assuming a quasi-permanent combination factor $\psi_2 = 0.3$, and assuming the following load ratios:

- $q_{SW}/q_{tot} = 0.36$
- $q_{SDL}/q_{tot} = 0.24$
- $q_{LL}/q_{tot} = 0.40$

Furthermore, the deflection was determined assuming a certain load history, in which dead load was applied at 10 days, the superimposed dead load at 60 days and the quasi-permanent live load at 365 days[6-22]. This procedure does not take into account early application of the characteristic load which can happen during building stages when the scaffolding is removed from the lower floors to build upper floors[6-23]. Early characteristic load application increases deflections especially for low reinforcement ratios due to reduction in tension-stiffening effects. The premises adopted for the drafting of EN 1992-1-1[6-2]/MC 2010[6-1], (no consideration of early load application combined with the load ratios described above) was done, as a political decision, in order to avoid providing more strict slenderness ratios than those given by ENV 1992-1-1[6-2] or MC90[6-8].

6.3.2 Refining the model

It is considered that the current formulation should be refined by introducing the following improvements:

- Consideration of early application of characteristic loads
- Different load compositions

This document is the intellectual property of the fib – International Federation for Structural Concrete. All rights reserved.
This PDF of fib Bulletin 92 is intended for use and/or distribution solely within fib National Member Groups.

- Consideration of over-reinforcement
- Generalization of factor *K* which relates results computed for a simply supported beam to other support conditions.
- Influence of the deflection limit L/250, L/200, L/300
- In the following paragraphs, proposals are given for each of these improvements. These proposals have been presented by the Spanish Delegation to CEN-TC250/SC2/WG1 which is in charge of drafting a revision of EN 1992-1-1[6-2] to be approved by member countries by the year 2020.

6.3.2.1 Consideration of early application of characteristic loads

In order to correct the current EN 1992-1-1[6-2]/MC 2010[6-1] formulation with regard to the influence of early application of characteristic load, the actual formulation can be multiplied by the following factor:

$$k_{EL} = 1.05\left(1 - e^{-k_{f_{ck,EL}}\frac{\rho}{0.001}}\right) \tag{6-19}$$

where:

$k_{fck,EL}$ is a factor dependent on the concrete strength to be determined using to the following table:

Table 6-3

f_{ck} [MPa]	$k_{fck,EL}$
30	0.50
60	0.30
100	0.25

ρ is the tensile reinforcement ratio.

6.3.2.2 Consideration of load composition

In order correct the current EN 1992-1-1[6-2]/MC 2010[6-1] formulation with regard to the influence of load composition, the following correction is proposed:

$$k_{DL} = 0.7\left[\frac{q_{tot}}{q_{DL}}\right]^{0.65}\left[1 - \left(7.2\cdot10^{-4}\left(\frac{\rho}{0.001}\right)^2 - 5.4\cdot10^{-2}\left(\frac{\rho}{0.001}\right)^2 + 1.05\frac{\rho}{0.001} - 2.67\right)k_{f_{ck,DL}}\right] \tag{6-20}$$

where :

q_{tot} is the total characteristic load, sum of the self-weight, superimposed dead load and live load ($q_{tot} = q_{SW} + q_{SDL} + q_{LL}$)

q_{DL} is the permanent load (sum of the self-weight plus superimposed dead load: $q_{DL} = q_{SW} + q_{SDL}$)

$k_{fck,DL}$ is a factor dependent on the concrete strength to be determined using to the following table:

This document is the intellectual property of the fib – International Federation for Structural Concrete. All rights reserved.
This PDF of fib Bulletin 92 is intended for use and/or distribution solely within fib National Member Groups.

Table 6-4

f_{ck} [MPa]	$k_{fck,EL}$
30	0.010
60	0.0250
100	0.030

ρ is the tensile reinforcement ratio

Furthermore, in order to obtain good numerical results, the coefficient 3.2 in Eq.(6-17) must be changed to a value of 2.0. The proposed formulation, including the effects of early application of characteristic load and load composition is given in Eq.(6-21)

$$\frac{l}{d} = K \cdot k_{EL} \cdot k_{DL} \left[11 + 1.5\sqrt{f_{ck}} \frac{\rho_0}{\rho} + 2\sqrt{f_{ck}} \left(\frac{\rho_0}{\rho} - 1 \right)^{3/2} \right] \text{ if } \rho \le \rho_0$$

$$\frac{l}{d} = K \cdot k_{EL} \cdot k_{DL} \left[11 + 1.5\sqrt{f_{ck}} \frac{\rho_0}{\rho - \rho'} + \frac{1}{12}\sqrt{f_{ck}} \frac{\rho'}{\rho_0} \right] \text{ if } \rho > \rho_0 \qquad (6\text{-}21)$$

Fig. 6-33 to Fig.6-34 show a comparison between values determined using non-linear analysis on a simply supported beam according to flowchart of Fig.6-32 (symbols) and the values obtained by applying Eq. 6-21 for concrete classes C30/37, C60/75 and C100/85. These figures assume that the full characteristic load is applied early on. As can be seen, even though the expression of factor k_{DL} is a bit lengthy, this complexity is compensated by the excellent correlation which is obtained.

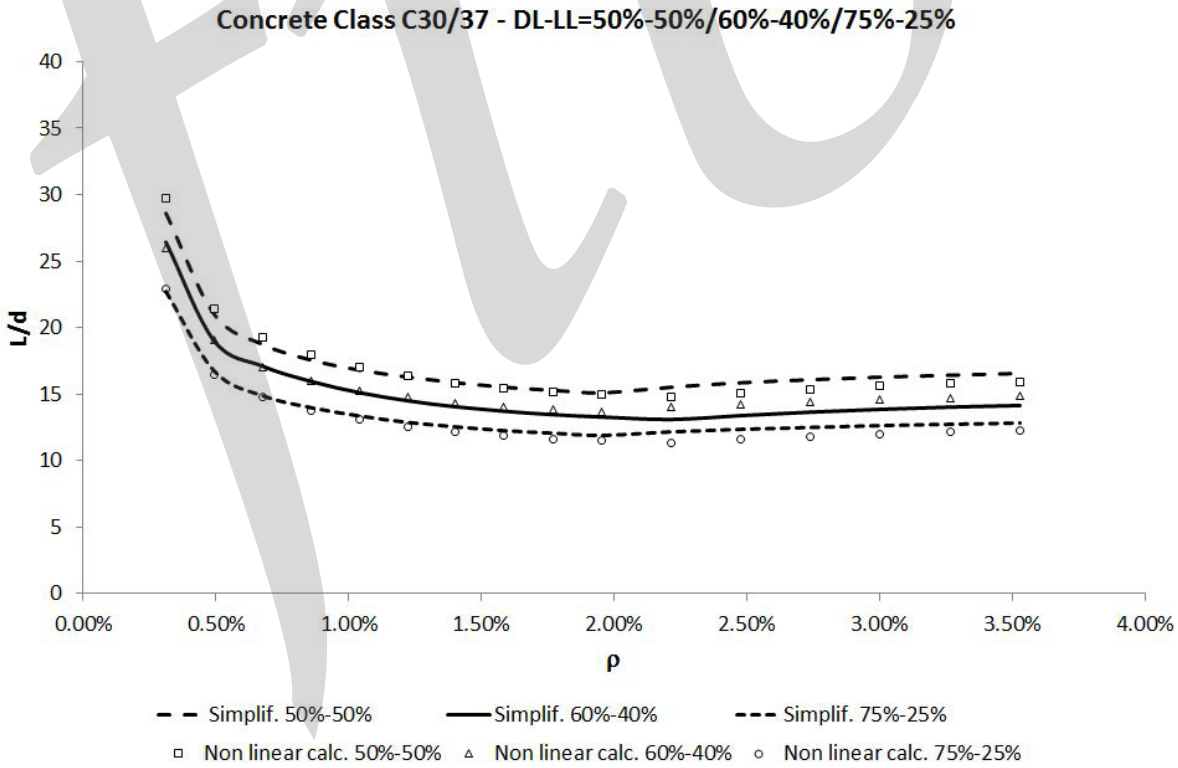


Fig. 6-33 Comparison of slenderness limits obtained by using the proposed formulation (lines) and that obtained by non-linear calculation according to the flowchart of Fig. 6-32 (symbols) for concrete class C30/37 and different load compositions

This document is the intellectual property of the fib – International Federation for Structural Concrete. All rights reserved.
This PDF of fib Bulletin 92 is intended for use and/or distribution solely within fib National Member Groups.

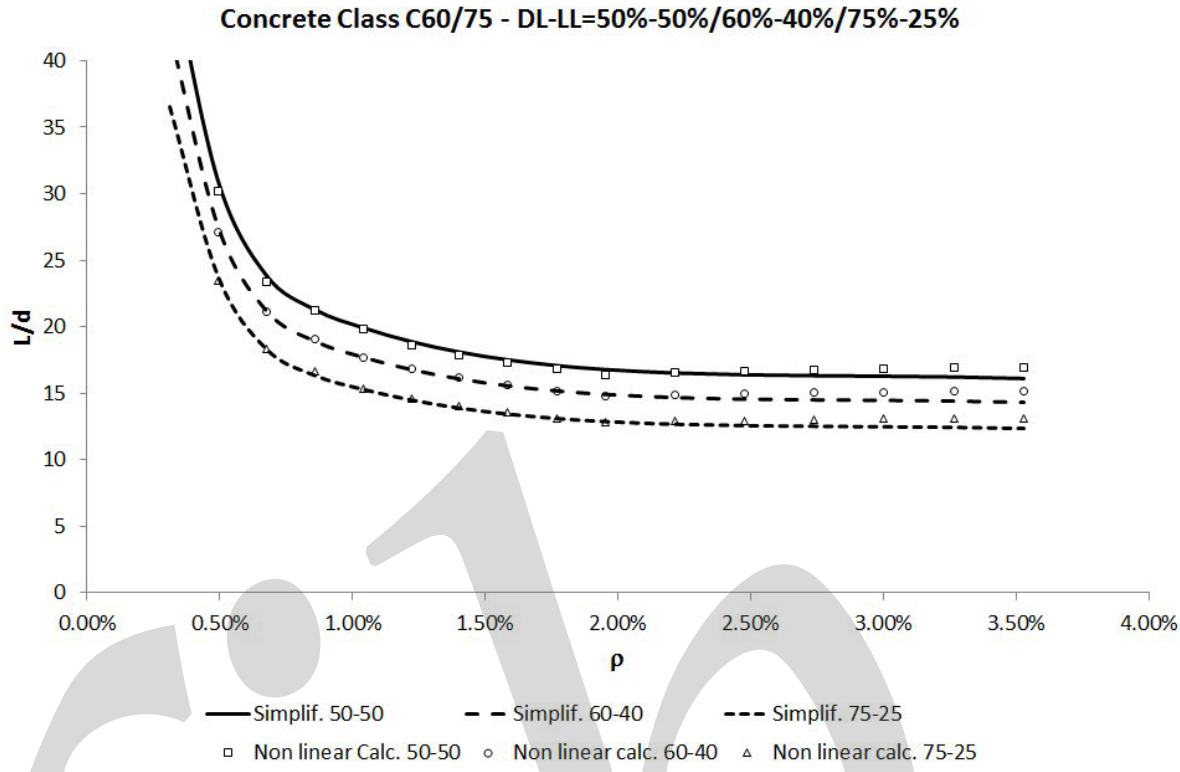


Fig. 6-34 Comparison of slenderness limits obtained by using the proposed formulation (lines) and that obtained by non-linear calculation according to the flowchart of Fig. 6-32 (symbols) for concrete class C60/75 and different load compositions

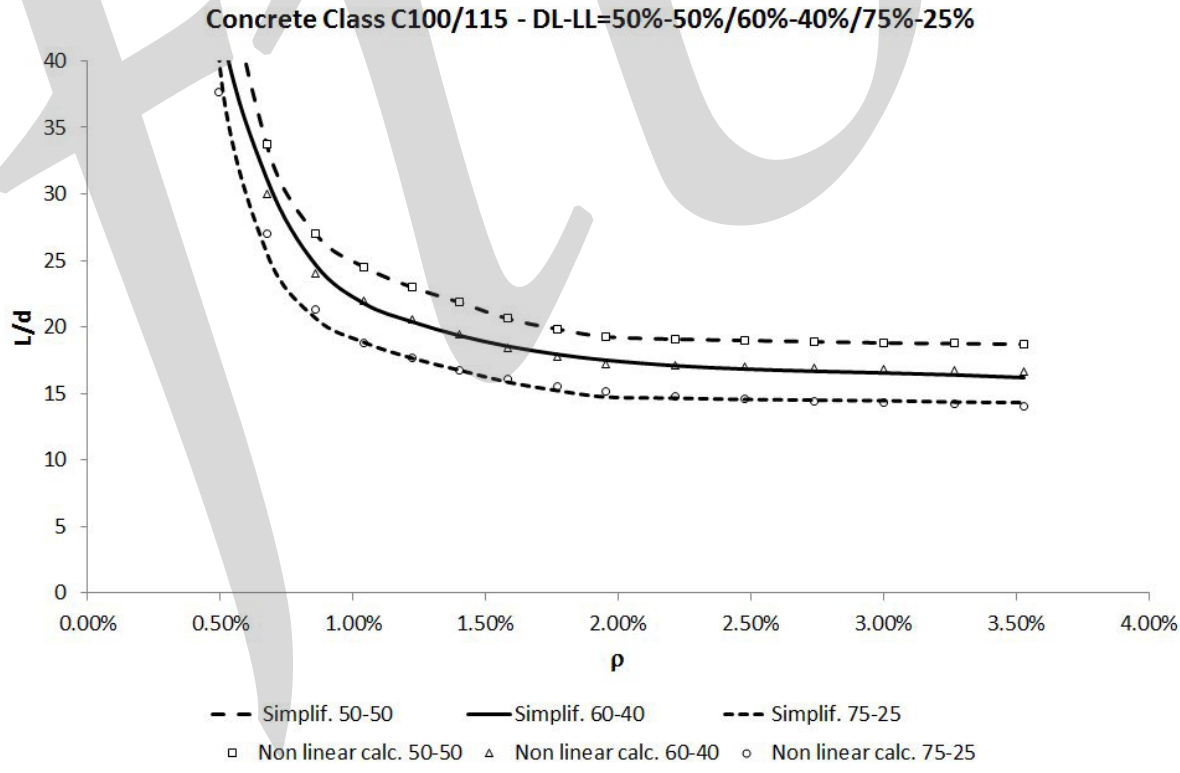


Fig. 6-35 Comparison of slenderness limits obtained by using the proposed formulation (lines) and that obtained by non-linear calculation according to the flowchart of Fig. 6-32 (symbols) for concrete class C30/37and different load compositions

This document is the intellectual property of the fib – International Federation for Structural Concrete. All rights reserved.
This PDF of fib Bulletin 92 is intended for use and/or distribution solely within fib National Member Groups.

6.3.2.3 Consideration of over-reinforcement

If a structure presents deflection problems only in limited parts (for instance areas with large cantilevers), it can be a good idea to provide a significant amount of over reinforcement is such areas in order to comply with deflection limits. For this, it is interesting to quantify how over-reinforcement affects slenderness limits.

In order to take into account this effect in the formulation of slenderness limits, the formulation of Eq. (6-22) is proposed. This formulation has been fitted to a concrete of class C30/37. It may have to be altered with a resistance-dependent coefficient to fit other concrete strengths. This study is pending.

$$\frac{l}{d} = \left(\frac{l}{d}\right)_{\text{EN1992/MC2010}} + 0.03\left(\frac{A_{\text{real}}}{A_{\text{strictly needed}}}\right)^{2} \rho^{-0.7} \qquad (6\text{-}22)$$

where:

A_{real} is the tensile reinforcement actually provided

$A_{strictly\ needed}$ is the reinforcement strictly required to fulfil ULS conditions

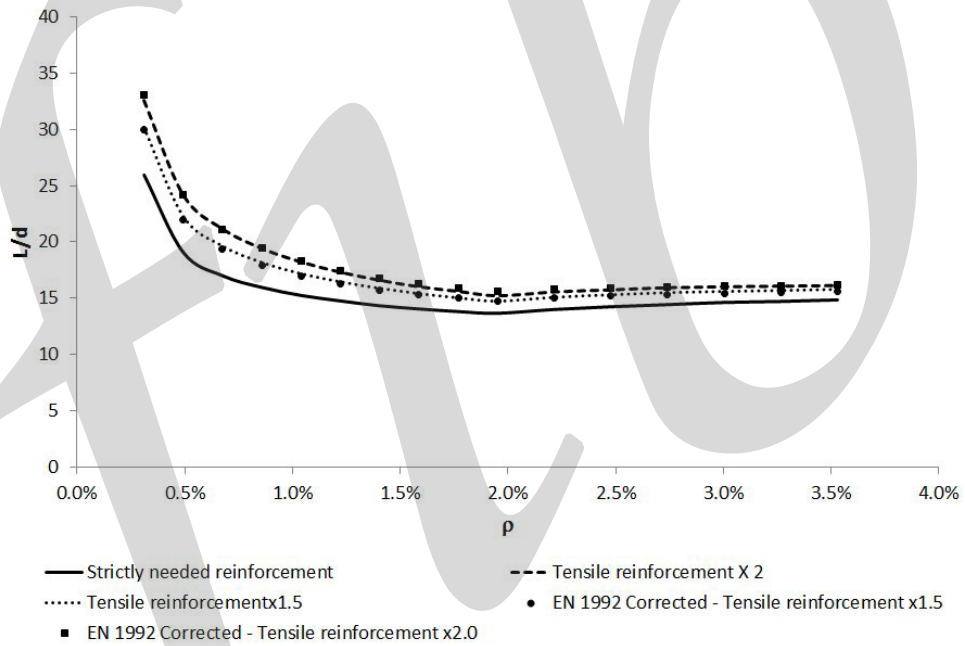


Fig. 6-36 Comparison of slenderness limits obtained by using the proposed formulation (lines) and that obtained by non-linear calculation according to the flowchart of Fig. 6-32 (symbols) taking into account the effect of over-reinforcement (Concrete C30/37)

6.3.2.4 Generalization of *K* factor

Factor *K* in Eq. (6-21) allows the correction of the value of the slenderness limit in order to fit other support conditions. This value is currently given only for a limited number of support conditions and cannot possibly cover all situations which can occur in engineering practice. It is possible, however to determine this value for any structure geometry using linear analysis.

Given a certain span with certain support conditions different from those of a simply supported beam, the ratio between the linear deflection obtained in the structure with General

This document is the intellectual property of the fib – International Federation for Structural Concrete. All rights reserved.
This PDF of fib Bulletin 92 is intended for use and/or distribution solely within fib National Member Groups.

Support Conditions (f_{GSC}) and that obtained for the same load in a Simply Supported beam (f_{SS}) of the same span (l), can be easily determined. Let this value be called a Eq. (6-23).

$$\frac{f_{SS}\left[l\right]}{f_{GSC}\left[l\right]} = a \tag{6-23}$$

The corresponding slenderness limit in the beam with GSC will be given by the condition that for a different span (l^*), the ratio between deflection and span in the simply supported beam with span l and in the beam with GSC with span l^*, will be the same (Eq. (6-24)).

$$\frac{\dfrac{f_{SS}\left[l\right]}{l}}{\dfrac{f_{GSC}\left[l^*\right]}{l^*}} = 1.00 \tag{6-24}$$

By combining Eq. (6-23) and Eq.(6-24), Eq. (6-25) is obtained.

$$\frac{\dfrac{af_{GSC}\left[l\right]}{l}}{\dfrac{f_{GSC}\left[l^*\right]}{l^*}} = 1.00 \rightarrow a\frac{f_{GSC}\left[l\right]}{f_{GSC}\left[l^*\right]}\frac{l^*}{l} = 1.00 \tag{6-25}$$

Finally, since deflections due to distributed loads are proportional to the fourth power of the span, it is concluded that the slenderness limit for a span with GSC is equal to that of a simply supported beam multiplied by the third root of a (see Eq. (6-26)).

$$a\frac{f_{GSC}\left[l\right]}{f_{GSC}\left[l^*\right]}\frac{l^*}{l} = a\frac{l^4}{l^{*4}}\frac{l^*}{l} = a\frac{l^3}{l^{*3}} = 1.00 \rightarrow \frac{l^*}{l} = \sqrt[3]{a} \rightarrow K = \frac{\dfrac{l^*}{d}}{\dfrac{l}{d}} = \sqrt[3]{a} \tag{6-26}$$

6.3.2.5 Effect of allowable deflection limit

With respect to the effect of the allowable deflection limit, it is clear that the decision regarding what the admissible deflection is should be a decision of the owner. All the expressions listed above assume a limit for the total deflection equal to the span divided by 250. It is a pertinent question to ask how these limits would be affected for structures which may be very sensitive to deflections for which a stricter limit may be needed, for example L/300, or how much more slender the structure could be if these limits were relaxed, for instance to L/200.

As it turns out the effect of this variable which will be referred to as a_δ (e.g. $a_\delta = 200$, 250 or 300) is actually, and surprisingly, linear, so it is trivial to adjust the above slenderness limits. In order to understand this linearity, the following reasoning can be followed:

- If the above limits are respected, then deflection obtained for the quasi-permanent load will be $f = L/a_\delta$
- In turn, this deflection will be proportional to the fourth power of the span and to the applied load q see Eq. (6-27):

$$f = \frac{L}{a_\delta} = \alpha_1 \frac{q \cdot L^4}{EI} \tag{6-27}$$

This document is the intellectual property of the fib – International Federation for Structural Concrete. All rights reserved.
This PDF of fib Bulletin 92 is intended for use and/or distribution solely within fib National Member Groups.

- According to Fig. 6-32, q will be proportional to the ultimate bending moment and inversely proportional to the square of the span. Also the ultimate bending moment is constant for a given reinforcement ratio and a given effective height, and so is the equivalent stiffness (EI):

$$f = \frac{L}{a_\delta} = \alpha_1 \frac{q \cdot L^4}{EI} = \alpha_1 \frac{\alpha_2 \frac{M_{Rd}}{L^2} L^4}{EI} = \text{constant} \cdot L^2 \tag{6-28}$$

- From Eq. (6-28) it can be seen that the resulting span (for a given ρ and a given d) is inversely proportional to a_δ and that, given a slenderness limit for a certain value of $a_\delta = a_{\delta 1}$, the corresponding slenderness limit for a different value, $a_{\delta 2}$, of this parameter can be obtained simply by multiplying the previous limit by the ratio $a_{\delta 1}/a_{\delta 2}$ (see Eq. (6-29)).

$$\left.\begin{aligned} f_1 &= \frac{L_1}{a_{\delta 1}} = \text{constant} \cdot L_1^2 \rightarrow L_1 \propto \frac{1}{a_{\delta 1}} \\ f_2 &= \frac{L_2}{a_{\delta 2}} = \text{constant} \cdot L_2^2 \rightarrow L_2 \propto \frac{1}{a_{\delta 2}} \end{aligned}\right\} \frac{L_1}{L_2} = \frac{\frac{L_1}{d}}{\frac{L_2}{d}} = \frac{a_{\delta 2}}{a_{\delta 1}} \tag{6-29}$$

Therefore the limit to the deflection can be taken into account in the proposed formulation simply by introducing yet another coefficient k_a, defined as:

$$k_a = \frac{250}{a_\delta} \tag{6-30}$$

As proof of the above reasoning calculations have been made using non-linear analysis for different values of a_δ and these have been compared to the proposed formula adjusted by using parameter k_a. The results are shown in the following figures. As can be seen the difference is quite important, and owners should start to think about this parameter more often.

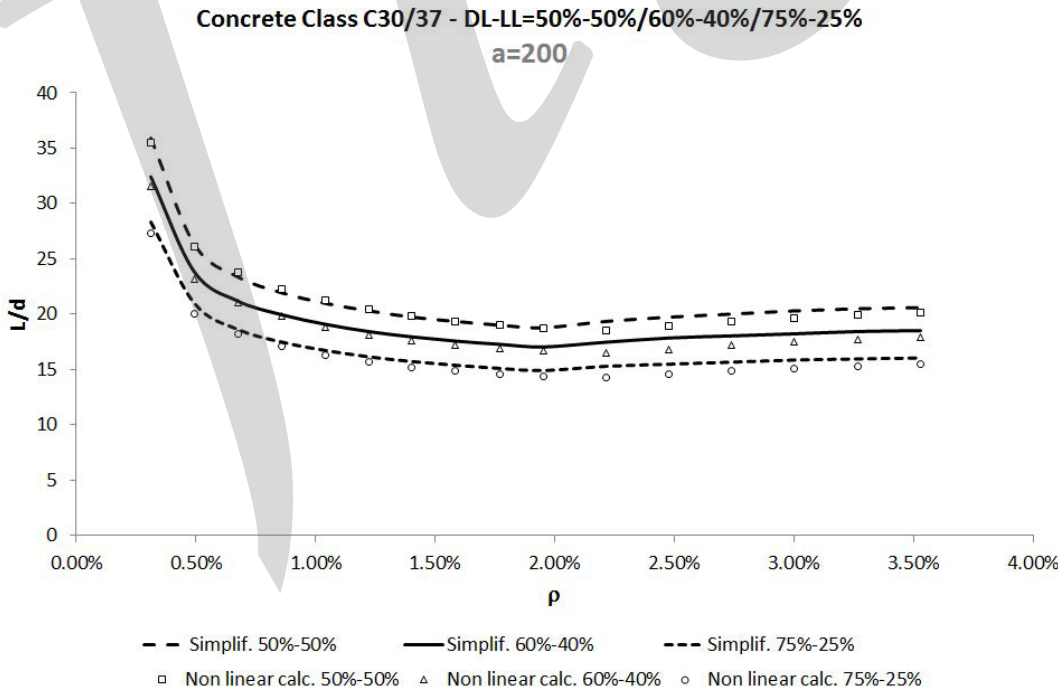


Fig. 6-37 Slenderness limits if $a_\delta = 200$ for different load compositions

This document is the intellectual property of the fib – International Federation for Structural Concrete. All rights reserved.
This PDF of fib Bulletin 92 is intended for use and/or distribution solely within fib National Member Groups.

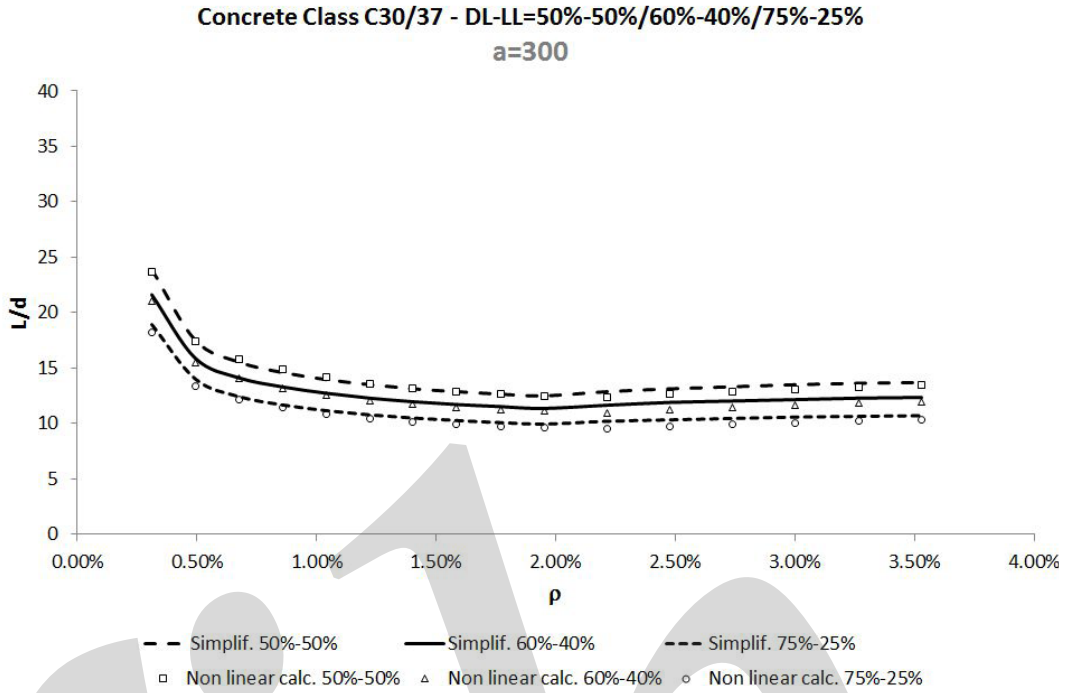


Fig. 6-38 Slenderness limits if $a_\delta = 300$ for different load composition

6.4 The crack width along the concrete cover of reinforced concrete

Structural behaviour of concrete structures is considerably influenced by cracking induced by flexure or direct tension. Cracking has an effect on serviceability, durability and load bearing capacity. In respect of serviceability, the increase of deformations due to the decreased stiffness and the increased permeability of cracked concrete can be mentioned as the most important concerns. The latter can promote the ingress of carbon-dioxide and water solutions towards the reinforcement. Water leakage can result in unacceptable functional or aesthetical conditions. Results of structural cracking can reduce the service life of structures and several literature studies are available in this field. No general conclusion, however, is available on the role of structural cracking and durability; the only observations are that the corrosion of reinforcement is independent from the surface crack widths and the corrosion of reinforcement is accelerated in the presence of chloride ions.

The width of a crack within the concrete cover is different from that of measured at the surface of the structural element. Comprehensive analysis of this behaviour is a gap in the technical literature.

6.4.1 General considerations of crack width and bond in concrete

Structural design of reinforced concrete assumes that the bond is perfect between the steel reinforcement and the concrete, therefore no relative displacement (=slip) is formed between the two components of the composite during loading (i.e. $\varepsilon_c = \varepsilon_s$). With this assumption, internal stresses of any cross section can be calculated by cross sectional analysis of inhomogeneous sections by Bernoulli-Navier hypothesis at any loading condition. The assumption of perfect bond is, however, an over-simplification. In reality, the bond between the concrete and the embedded reinforcement is a function of relative displacement (=slip).

This document is the intellectual property of the fib – International Federation for Structural Concrete. All rights reserved.
This PDF of fib Bulletin 92 is intended for use and/or distribution solely within fib National Member Groups.

Bond between the two materials is provided by contact forces which are proportional to the loading. Relative displacement (=slip) forms during loading due to the different strain capacities and stiffness of concrete and reinforcing bars. By definition, slip is the difference in displacement of steel and concrete sections which coincide before loading and are separated from each other by loading. Slip can be indicated as the integral of the difference between strain of the reinforcement and that of concrete over a bond length l_b as follows:

$$s = u_s(x) - u_c(x) = \int_0^{l_b} \varepsilon_s(x)\, dx - \int_0^{l_b} \varepsilon_c(x) dx \tag{6-31}$$

Bond stress (τ_b) is used to describe the contact forces that are the parallel component of the 3D contact stress vector with the axis of the reinforcement. The bond stress (b) is primarily influenced by slip (s). The bond-slip (τ_b-s) response can be determined by laboratory pull-out tests during which the slips of loaded and non-loaded sections of reinforcing bars are recorded as a function of load (F) over a short bond length. The bond stress is considered as the ratio of the load and the cylindrical contact surface of the reinforcement over the bond length[6-24]:

$$\tau_b(s) = \frac{F(s)}{\varnothing \pi l_b} \tag{6-32}$$

The very basics of the bond-slip response can be summarised by considering a general scheme of the τ_b-s response indicated in Fig. 6-39 for a deformed steel bar. The bond-slip response can be considered as a combination of four mechanisms:

I. Adhesion. Contact resistance due to physical-chemical bond between concrete and reinforcement (corresponding to zero slip).

II. Mechanical interlocking. Ribs of deformed reinforcements are pressed to the surrounding concrete resulting local micro-crushing and slip. The bond stress increases proportionally to loading in a non-linear fashion. Maximum bond stress is the bond strength ($\tau_{b,\max}$).

III. Softening by micro-cracking and micro-crushing. The concrete lugs between the ribs of the reinforcement are gradually deteriorated by the slipping movement of the reinforcement that results a more pronounced micro-cracking in the vicinity of the reinforcement. The bond stress decreases proportionally to slips in a non-linear fashion.

IV. Friction. When slip reaches the magnitude of clear rib spacing of the reinforcement no other bond resistance is available than the friction of the slipping reinforcement over the sheared concrete around it. A residual bond stress can be maintained (τ_{br}). Slips can be increased without limit.

Failure of bond is a function of concrete strength in the case of steel reinforced concrete. The surface of steel reinforcement cannot be damaged during pull-out. Therefore, the bond stresses are considered to be results of concrete strength and rib geometry of the steel reinforcement. Technical literature indicates the bond strength ($\tau_{b,\max}$) and the residual bond stress (τ_{br}) as a function of the square-root of concrete strength as follows:

$$\begin{aligned} \tau_{b,\max} &= k_1 \sqrt{f_{cm}} \\ \tau_{br} &= k_2 \cdot \tau_{b,\max} \end{aligned} \tag{6-33}$$

where k_1 and k_2 are empirical constants regarding the geometry of the reinforcement.

This document is the intellectual property of the fib – International Federation for Structural Concrete. All rights reserved.
This PDF of fib Bulletin 92 is intended for use and/or distribution solely within fib National Member Groups.

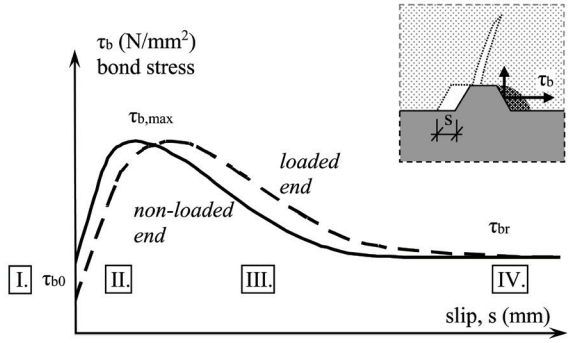


Fig. 6-39 Bond stress vs. slip (τ_b-s) response for deformed reinforcement[6-25]

The bond-slip behaviour can be modelled by a second order differential equation the solution of which generates the distribution of slips over the bond length. Bond stresses can be formulated from slips considering an appropriate relationship between slips and bond stresses. Stresses in the reinforcement and the anchorage length (slip length) can be calculated by the equilibrium of inner forces over the bond length[6-29].

The differential equation of bond-slip:

$$\frac{d^2 s(x)}{dx^2} - K \cdot \tau_b\left[s(x)\right] = 0 \tag{6-34}$$

where:

$$K = \frac{4\left(1-\alpha_e \cdot \rho_{s,ef}\right)}{E_s \cdot \varnothing} \tag{6-35}$$

E_s Young's modulus of reinforcement

$\varnothing$ diameter of reinforcement

$s(x)$ distribution of slips

α_e modulus ratio ($=E_s/E_{ci}$)

$r_{s,ef}$ effective reinforcement ratio ($=A_s/A_{c,ef}$)

where:

$A_{c,ef} = 2{,}5(h\text{-}d)b \le (h\text{-}x)/3$ effective concrete area in tension

The bond law can be that of the CEB-FIB Model Code 1990[6-8]; Bertero, Popov, Eligehausen model:

$$\tau_b = \tau_{bu}\left(\frac{s}{s_m}\right)^{\alpha} \tag{6-36}$$

where

τ_{bu} bond strength

s_m slip at bond strength

α empirical constant ($0 < \alpha < 1$), for deformed steel bar $\alpha = 0{,}40$

This document is the intellectual property of the fib – International Federation for Structural Concrete. All rights reserved.
This PDF of fib Bulletin 92 is intended for use and/or distribution solely within fib National Member Groups.

The solution of the differential equation:

$$s(x)=\left[\frac{2\tau_{bu}\left(1-\alpha_e\cdot\rho_{s,ef}\right)\left(1-\alpha\right)^2}{E_s\cdot\varnothing\cdot s_m^{\alpha}\left(1-\alpha\right)}\right]^{\frac{1}{1-\alpha}} x^{\frac{2}{1-\alpha}} \tag{6-37}$$

The distribution of bond stress:

$$\tau_b(x)=\tau_{bu}\left(\frac{s(x)}{s_m}\right)^{\alpha}=\frac{\tau_{bu}}{s_m^{\alpha}}\left[\frac{2\tau_{bu}\left(1-\alpha_e\cdot\rho_{s,ef}\right)\left(1-\alpha\right)^2}{E_s\cdot\varnothing\cdot s_m^{\alpha}\left(1+\alpha\right)}\right]^{\frac{\alpha}{1-\alpha}} x^{\frac{2\alpha}{1-\alpha}} \tag{6-38}$$

Reinforcement stress can be obtained by the force equilibrium over the length of the element d_x: difference in bond stress is equal to the difference in stress of the reinforcement:

$$\varnothing\pi\tau_b(x)dx=\frac{\varnothing^2\pi}{4}d\sigma_s(x)\Rightarrow\sigma_s(x)=\frac{4}{\varnothing}\int\tau_b(x)dx \tag{6-39}$$

$$\sigma_s(x)=\frac{4\tau_{bu}}{\varnothing\cdot s_m^{\alpha}}\frac{1-\alpha}{1+\alpha}\left[\frac{2\tau_{bu}\left(1-\alpha_e\cdot\rho_{s,ef}\right)\left(1-\alpha\right)^2}{E_s\cdot\varnothing\cdot s_m^{\alpha}\left(1+\alpha\right)}\right]^{\frac{\alpha}{1-\alpha}} x^{\frac{1+\alpha}{1-\alpha}}=D\cdot x^{\frac{1+\alpha}{1-\alpha}} \tag{6-40}$$

The anchorage length (slip length) for any σ_s value:

$$l_b=\left(\frac{\sigma_s}{D}\right)^{\frac{1-\alpha}{1+\alpha}} \quad [\text{mm}] \tag{6-41}$$

Crack width at the surface of the reinforcement can be obtained by the differential equation of bond-slip[6-24]. In the vicinity of cracks the equalisation of steel stress and concrete stress is no longer maintained. The differences in the strains result the opening of the cracks. The crack width at the surface of the reinforcement is the sum of the slips at the two crack surfaces. If s_w denotes the crack spacing over a concrete element then the crack width at the surface of the reinforcement is as follows[6-26]:

$$w=\int_0^{s_w}\left[\varepsilon_s(x)-\varepsilon_c(x)\right]dx=s_1+s_2 \tag{6-42}$$

If bond stresses are neglected then the average crack width can be considered as the integral of the average reinforcement strain over the even crack spacing:

$$w=\int_0^{s_w}\varepsilon_{sm}\cdot dx=s_w\cdot\frac{\sigma_{sm}}{E_s} \tag{6-43}$$

Selecting an appropriate bond law, the crack width at the surface of the reinforcement can be calculated from the differential equation of bond-slip. It can be formulated if the steel stress $\sigma_s(x)$ at the value of $x = l_b$ is introduced into the distribution of slip $s(x)$:

$$w=2\left[\frac{\left(1+\alpha\right)\left(1-\alpha_e\cdot\rho_{s,ef}\right)s_m^{\alpha}\cdot\varnothing}{8\left(1+\alpha_e\cdot\rho_{s,ef}\right)^2}\frac{\sigma_s^2}{\tau_{bu}\cdot E_s}\right]^{\frac{1}{1+\alpha}} \quad [\text{mm}] \tag{6-44}$$

This document is the intellectual property of the fib – International Federation for Structural Concrete. All rights reserved.
This PDF of fib Bulletin 92 is intended for use and/or distribution solely within fib National Member Groups.

The formula indicates that the influencing parameters of the crack width at the surface of the reinforcement are:

- the reinforcement diameter,
- the surface configuration of the reinforcement,
- the Young's modulus of the reinforcement,
- the strength of concrete,
- the magnitude of the effective concrete area in tension
- the stress in the reinforcement, as the most important parameter.

It should be noted that the formula above is valid only if bond stresses are smaller than the bond strength so the slip zones of structural cracks can be considered to be independent from each other (i.e. initial cracking phase).

Fig. 6-40 shows the crack width calculated from the differential equation of bond-slip as a function of the concrete compressive strength and the reinforcement diameter, with the assumption of the initial crack pattern (the member has sections where the slip is equal to zero).

Fig. 6-41 shows the crack width calculated from the differential equation of bond-slip as the function of the concrete compressive strength and the reinforcement diameter, with the assumption of the stabilized crack pattern (the beam has no sections where the slip is equal to zero).

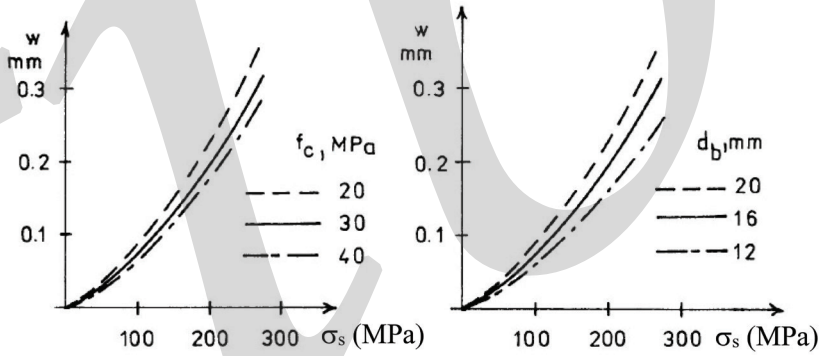


Fig. 6-40 Crack width calculated from the differential equation of bond-slip, with the assumption of the initial crack pattern[6-26]

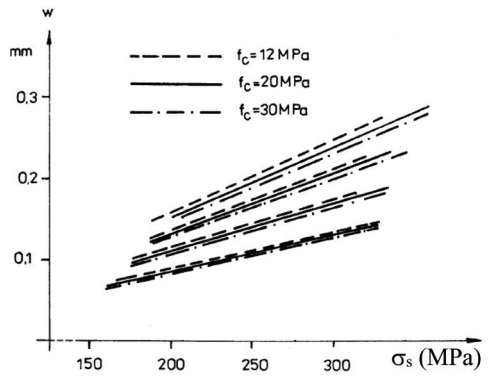


Fig. 6-41 Crack width calculated from the differential equation of bond-slip, with the assumption of the stabilized crack pattern[6-26]

This document is the intellectual property of the fib – International Federation for Structural Concrete. All rights reserved.
This PDF of fib Bulletin 92 is intended for use and/or distribution solely within fib National Member Groups.

Fig. 6-40 and Fig.6-41 are based on the following bond law formula:

$$\tau_b = 2.5\sqrt{f_c}\left(\frac{s}{1.0}\right)^{0.4} \tag{6-45}$$

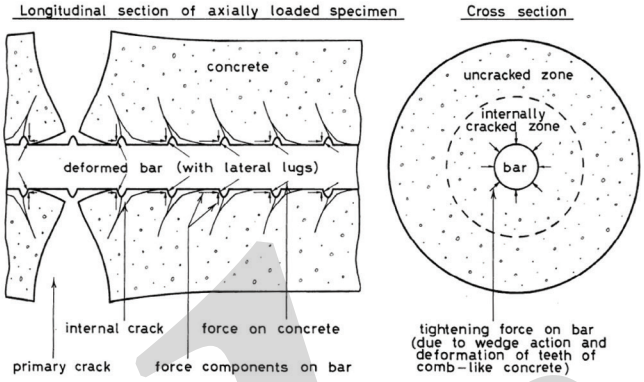


Fig. 6-42 Deformations in the vicinity of the crack[6-27]

6.4.2 Crack width along the concrete cover

Deformations of concrete in the vicinity of the cracks develop as a result of a very complex phenomenon. That can be the reason why no model is available in the technical literature that would allow converting the crack widths at the surface of the reinforcement into the crack widths that appear on the outer surface of the concrete elements.

The schematic representation of the phenomenon is introduced (with distorted, unreal scaling for better visibility) in Fig. 6.4-4[6-27].

Only a limited number of publications are available in technical literature that analyse the crack width along the concrete cover and try to determine what type of relationship could be postulated between the crack widths at the surface of the reinforcement and that of on the outer surface of concrete structures.

During the preparation of present chapter the following studies have been analysed:

- 1965: Broms, B. "Crack width and crack spacing in reinforced concrete members", *ACI Journal* October 1965, pp. 1237-1256[6-28].

- 1968: Husain, S. I. and Ferguson, P. M. *Flexural Crack Widths at the Bars in Reinforced Concrete Beams*. Center for Highway Research, The University of Texas at Austin, Research Report No. 102,1F, 1968[6-29].

- 1989: Yannopoulos, P. J. "Variation of concrete crack widths through the concrete cover to reinforcement". *Magazine of Concrete Research*, 1989, 41, No. 147, 63–68[6-30].

- 2004: Beeby, A. W. "The influence of the parameter ϕ/ρ_{eff} on crack widths". *Structural Concrete*, 2004, 5, No. 2, 71–83[6-31].

- 2006: Tammo, K., Thelandersson, S. "Crack opening near reinforcement bars in concrete structures", *Structural Concrete*, 2006, 7, No. 4, 137–143[6-32].

The open question is illustrated in Fig. 6-43[6-29].

This document is the intellectual property of the fib – International Federation for Structural Concrete. All rights reserved.
This PDF of fib Bulletin 92 is intended for use and/or distribution solely within fib National Member Groups.

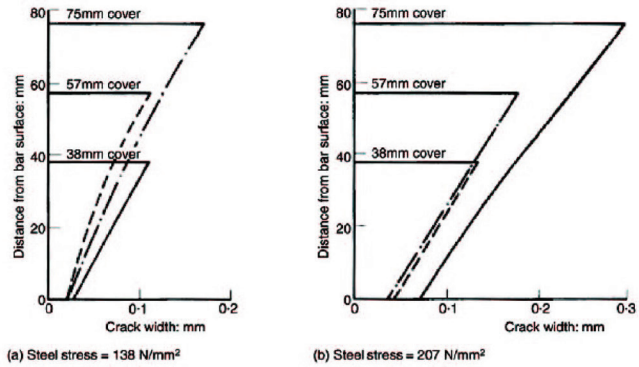


Fig. 6-43 Crack width along the concrete cover[6-29]

Theoretical approaches for modelling of the crack width with simplified calculations are shown in Fig. 6-44[6-33].

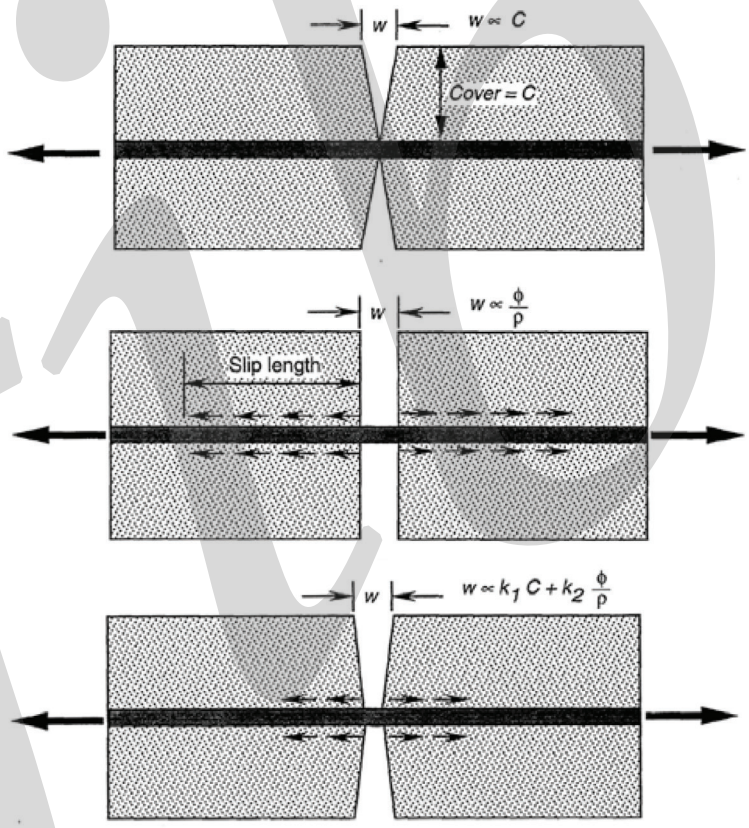


Fig. 6-44 Modelling of the crack width[6-33]

In design standards no direct relationship between the crack width and the extent of concrete cover is provided. Design standards suggest one of the principles that were introduced in Fig. 6-44 to calculate the crack width, but no reference can be found to predict the crack widths at the surface of the reinforcement based on the crack width on the outer surface of the concrete structure.

A summary of the most relevant findings from the references mentioned above is given in the following.

This document is the intellectual property of the fib – International Federation for Structural Concrete. All rights reserved.
This PDF of fib Bulletin 92 is intended for use and/or distribution solely within fib National Member Groups.

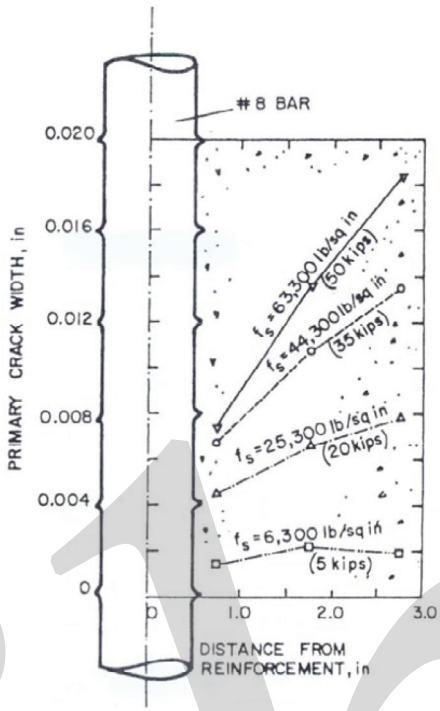


Fig. 6-45 Crack width along the concrete cover[6-28]

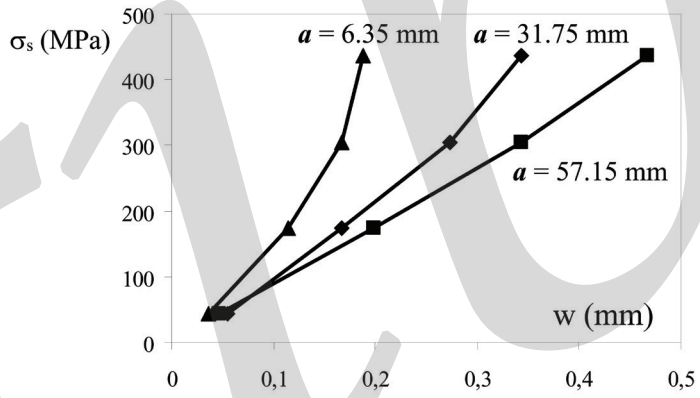


Fig. 6-46 Additional analysis of the results presented in Fig. 6-45[6-28] (*a* denotes the distance from the reinforcement)

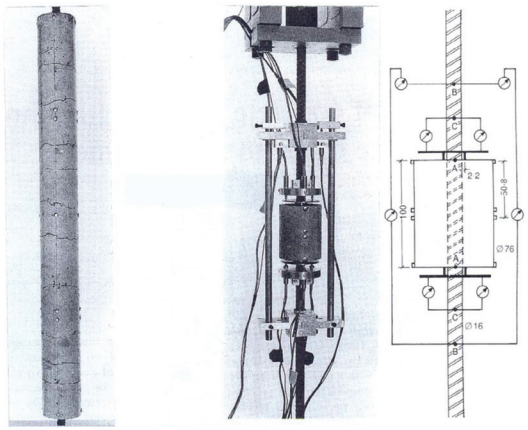


Fig. 6-47 Testing arrangement of the crack width measurement on the surface of the reinforcement and on the outer surface on the concrete member[6-30]

This document is the intellectual property of the fib – International Federation for Structural Concrete. All rights reserved.
This PDF of fib Bulletin 92 is intended for use and/or distribution solely within fib National Member Groups.

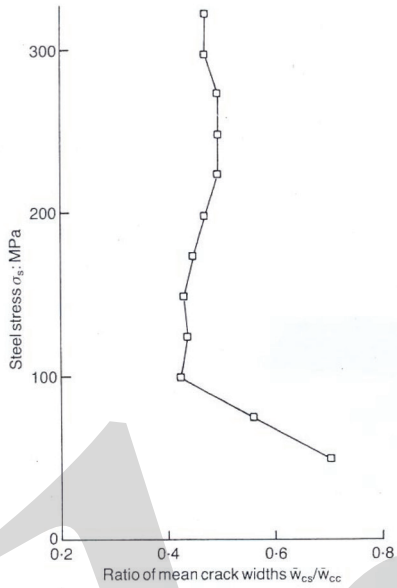


Fig. 6-48 Ratio of the crack widths measured at the surface of the reinforcement and on the outer surface on the concrete member[6-30]

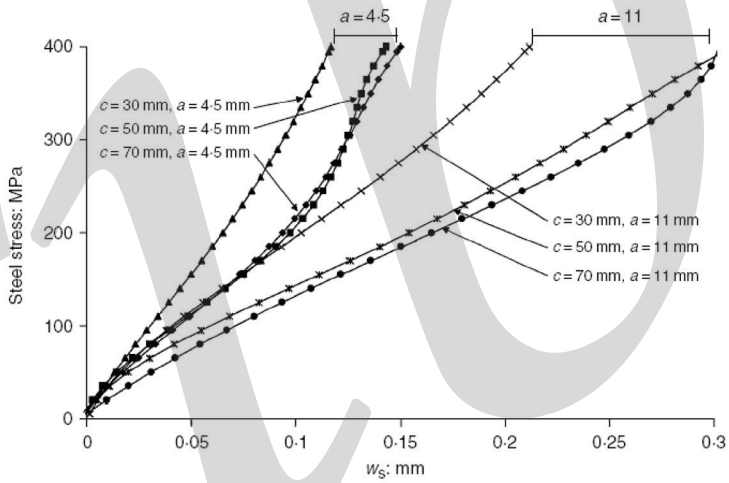


Fig. 6-49 Crack width in different depths along the concrete cover[6-30] (*a* denotes the distance from the reinforcement, and *c* denotes the concrete cover)

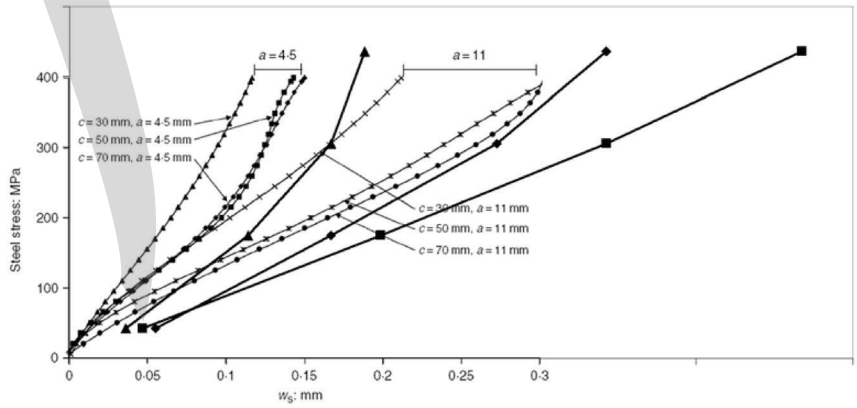


Fig. 6-50 Combination of Fig. 6-46 and Fig.6-49

This document is the intellectual property of the fib – International Federation for Structural Concrete. All rights reserved.
This PDF of fib Bulletin 92 is intended for use and/or distribution solely within fib National Member Groups.

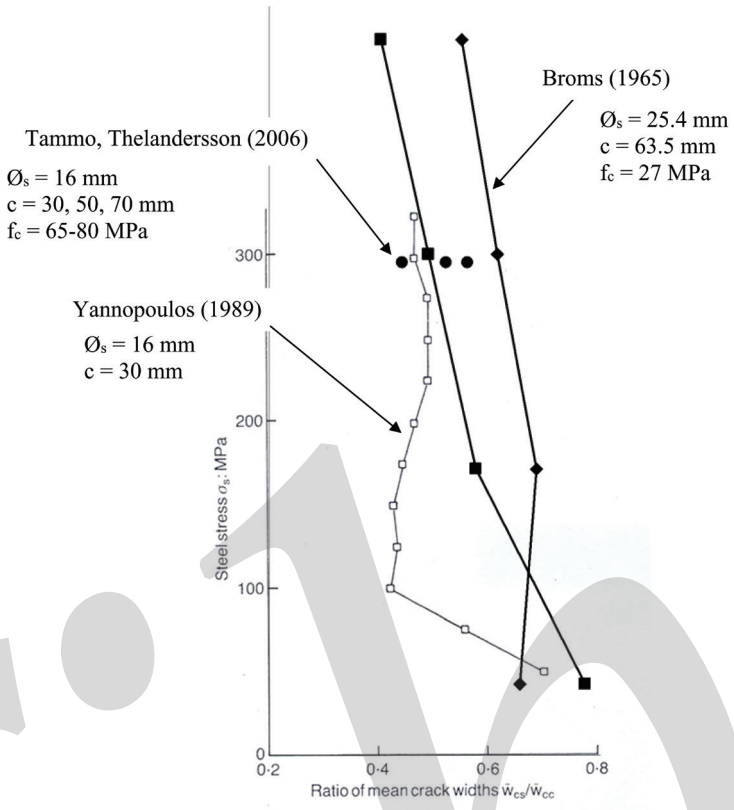


Fig. 6-51 Ratio of the crack widths measured at the surface of the reinforcement and on the outer surface on the concrete members based on the presented results

Based on Fig. 6-51 it can be concluded that according to the technical literature data some kind of proportionality can be found between the crack width at the surface of the reinforcement and on the outer surface on the concrete structure if the validity of the results are restricted to the testing conditions:

$$w_{\text{reinforcement surface}} / w_{\text{concrete surface}} = 0.4 \text{ to } 0.8 \tag{6-46}$$

It should be emphasized that the ratio can be considered as a rough estimate, because in the reality it depends on:

- the concrete cover,
- the load level (steel stress),
- the strength of concrete,
- the Young's modulus of concrete,
- the surface configuration of the reinforcement.

If one would like to interpret the crack width as a function of the distance from the reinforcement (i.e. concrete cover, c); the following theoretical considerations can be taken into account.

If Δw_c denotes the crack width increment that depends on the concrete cover, the crack width can be formulated as:

$$w_{\text{concrete surface}} = w_{\text{reinforcement surface}} + \Delta w_c \tag{6-47}$$

This document is the intellectual property of the fib – International Federation for Structural Concrete. All rights reserved.
This PDF of fib Bulletin 92 is intended for use and/or distribution solely within fib National Member Groups.

According to the above, wreinforcement surface can be determined with the bond law related to the load level, the concrete strength and bond with the solution of the differential equation of bond-slip.

Based on a review of technical literature, assumptions can be formulated only for the concrete cover dependent crack width increment (Δw_c). Design standards and studies from technical literature do not usually give any suggestion of the change of crack width through the concrete cover. Such models can only be found which take into account the concrete cover in an empirical way when calculating the crack width on the concrete surface, but at the same time no crack width on the surface on the reinforcement can be obtained. Some of the models even assume that the size of the crack widths are the same at the surface of the reinforcement, over the concrete cover and on the concrete surface, fully neglecting the additional deformations of the concrete cover that in a real structure results the change of the crack width through the concrete cover.

A possible recommendation for the relationship between the crack width increment and concrete cover is a power function. The graphical representations of this approach can be studied in Fig. 6-52.

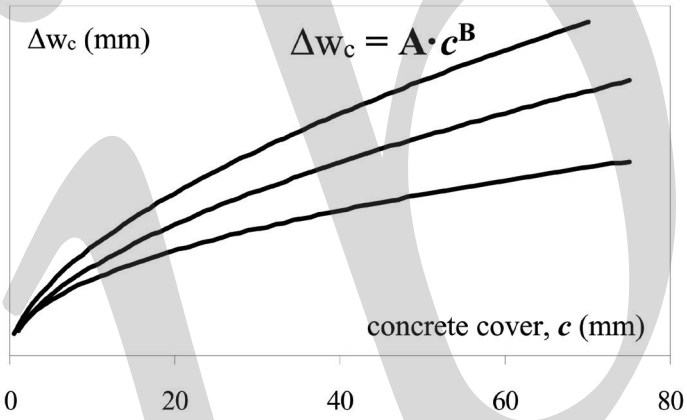


Fig. 6-52 Schematic representation of crack width increment (Δw_c) as a function of the concrete cover

In 2011 the *fib* TG4.1 "Serviceability Models" was working on the semi-analytical solution of proposal presented in Fig. 6-52.

The *fib* Model Code 2010 First Complete Draft[6-34, 6-35] was published in March 2010. Its Chapter 7.6 is the only design aid today that gives a proposal for the relationship of crack width and concrete cover in the following form:

$$w_d^* = w_d + \Delta w_d \tag{6-48}$$

where w_d^* is the crack width on the outer concrete surface, w_d is the crack width at the surface of the reinforcement (this is the slip between the reinforcement and the concrete), Δw_d is the crack width increment due to the additional deformation of the concrete cover. The *fib* Model Code 2010 First Complete Draft[6-34, 6-35] recommends a power function for the change of the crack width along the concrete cover as follows:

$$\Delta w_d = A \cdot c^{\beta} \tag{6-49}$$

This document is the intellectual property of the fib – International Federation for Structural Concrete. All rights reserved.
This PDF of fib Bulletin 92 is intended for use and/or distribution solely within fib National Member Groups.

where:

A = depends on the concrete strength and the effective reinforcement ratio

β = empirical constant ($0 < \beta < 1$)

c = concrete cover

The model of *fib* Model Code 2010 First Complete Draft[6-34, 6-35] is supported by particular experimental results. One study[6-25] refer to this model as well, therefore, results are introduced briefly in the following.

The test specimens were reinforced concrete ties with 900 mm length and 120×120 mm cross section. Reinforcement of one single deformed steel reinforcing bar with a diameter of 20 mm was placed either centrally or asymmetrically in the concrete cross section.

The concrete covers obtained were 20, 40, 60, 80 mm in the specimens with asymmetric layout, and 50 mm in the specimens with central positioning. Self-compacting concrete of f_{cm} = 82.6 N/mm^2 average standard cube compressive strength was used. Specimens were loaded monotonically, deformation controlled (at a loading rate of 0.5 mm/min) with a 600 kN capacity universal testing machine (Instron 1197) up to a stabilized cracking condition with maximum surface crack width of at least 0.30 mm.

The typical test arrangement is given in Fig.6-53. Load-deformation responses were recorded digitally with an HBM Spider8 multi-channel electronic PC measurement unit and a portable computer with HBM Catman professional measurement software. Loading never exceeded the maximum load of 150 kN to avoid yielding of the steel reinforcement. The actual maximum applied load was maintained for 12 to 18 hours during which the structural cracks were injected and the resin was allowed to set. The main focus of the present studies was on the structural cracks that reach the concrete surface to be injected, therefore, the injection was carried out from the surface of the members through plastic injecting packers. As being a preliminary study for the upcoming PU injection tests, the detailed mapping of the internal crack width variation within the concrete cover was targeted during the tests. Therefore, high strength, brittle epoxy resin was selected for the injection. Cracks were sealed at the concrete surface before injection by a rapid set epoxy resin (MC-Quicksolid®) and the injection used a very low viscosity (95 mPa·s), high strength (85 N/mm^2) injection epoxy resin (MC-DUR 1264 KF®). The cracks were maintained in their original, loaded position and the axial load was released only after the resin was allowed to set. Surface crack pattern and surface crack widths were recorded and then the specimens were cut open by a high speed diamond saw to make the crack widths visible throughout the concrete cover. In this way, eight cut surfaces were available for each crack.

Crack widths were recorded by a hand microscope (magnification of 0.01 mm) at every 2 mm along each crack. Readings were recorded on every crack, along all the 8 cut surfaces. Typical detail is shown in Fig. 6-54. The injection material completely filled the cracks, throughout their entire lengths to the reinforcement. The cracks filled with resin can be easily distinguished from the surrounding adjacent concrete.

Concrete compressive strength and Young's modulus tests were also carried out on the same day of the injection to complete the tests.

This document is the intellectual property of the fib – International Federation for Structural Concrete. All rights reserved.
This PDF of fib Bulletin 92 is intended for use and/or distribution solely within fib National Member Groups.



Fig. 6-53 Typical test arrangement[6-25]

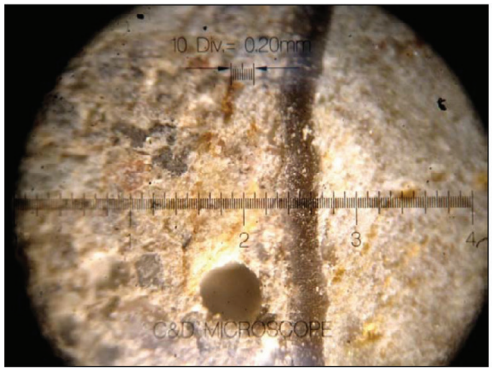


Fig. 6-54 Crack width reading with microscope[6-25]

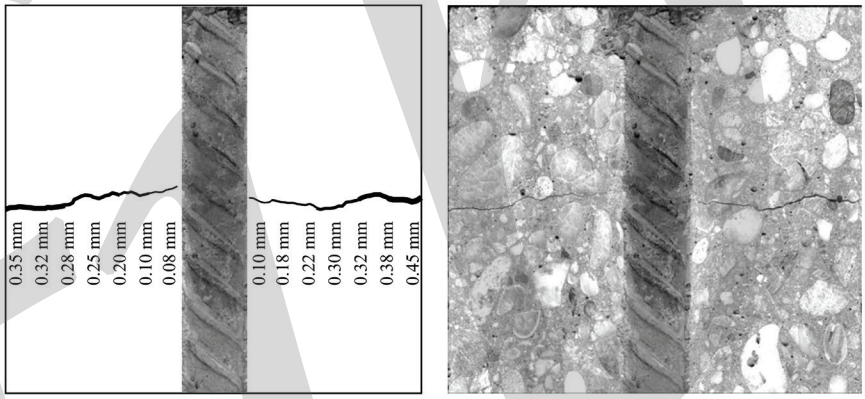


Fig. 6-55 Change of crack width along the concrete cover (c = 50 mm)[6-25]

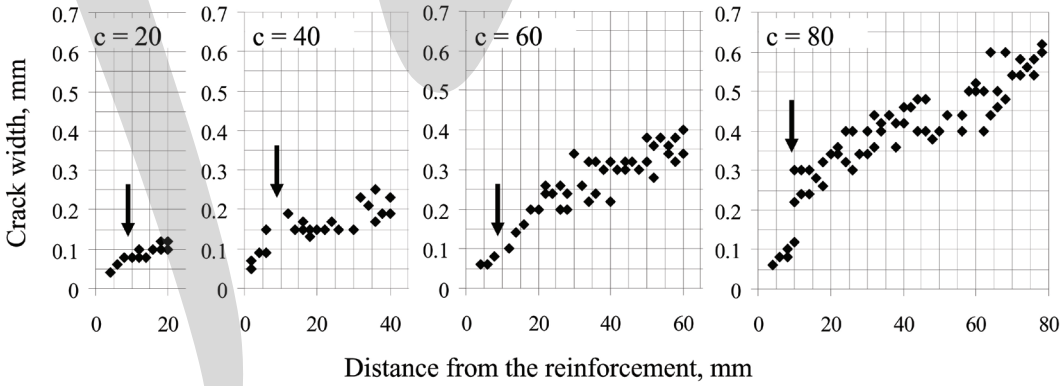


Fig. 6-56 Change of crack width along the concrete cover (c = 20, 40, 60, 80 mm)[6-25]

A typical test result can be studied in Fig. 6-55 (50 mm concrete cover, specimen with central positioning of reinforcement). Fig. 6-56 shows the crack pattern of the specimen with asymmetric positioning of reinforcement (concrete cover: 20, 40, 60, 80 mm).

This document is the intellectual property of the fib – International Federation for Structural Concrete. All rights reserved.
This PDF of fib Bulletin 92 is intended for use and/or distribution solely within fib National Member Groups.

It can be observed that the change of the crack width is remarkable and is not linear along the concrete cover. Results also indicate that the different concrete covers result in different local stiffnesses of the tensile member. Higher stiffness parts apparently collect the deformations and higher crack widths have resulted. If one compares the observed crack widths at a distance of e.g. 20 mm from the steel reinforcement 0.11 mm, 0.15 mm, 0.20 mm and 0.32 mm could be found corresponding to the concrete covers of 20 mm, 40 mm, 60 mm and 80 mm, respectively. On the other hand, the crack width at the level of the steel reinforcement is found to be independent from the actual concrete cover that agrees with the results found in technical literature.

A further remarkable phenomenon can be also seen in Fig. 6-56: the tendency of the change of the crack width is considerably different in the close vicinity of the steel reinforcement (i.e. within a distance of 10 to 15 mm) than in the outer parts of the concrete cover. The apparent limits of these areas are indicated with arrows in the diagrams and seem not to depend on the actual concrete cover. These observations confirm the presence of secondary micro-cracks (i.e. Goto cracks) at the surface of the steel reinforcement (schematically shown in Fig. 6-42). The secondary micro-cracks represent a smeared deformation field in the close vicinity of the steel reinforcement and influence the crack width of the macroscopic structural cracks. Outside this region the deformation of the concrete cover governs the variations of the crack widths.

Results imply that micro-cracks have a strong influence on the deformations of concrete in the vicinity of the reinforcement, hence they also have influence on the crack width at the concrete surface in an indirect way. This influence is not taken into account by either of the theoretical models established for the calculation of the crack width of reinforced concrete structures. Fig. 6-57 shows internal micro-cracks observed and made visible by Goto[6-27] (results belong to σ_s = 294 MPa tensile stress).

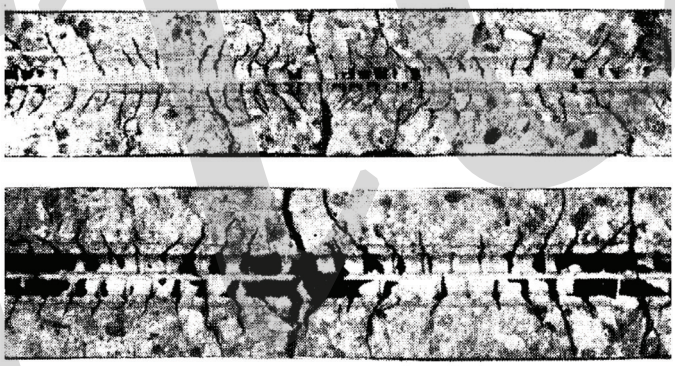


Fig. 6-57 Internal micro-cracks in the vicinity of the reinforcement[6-27]

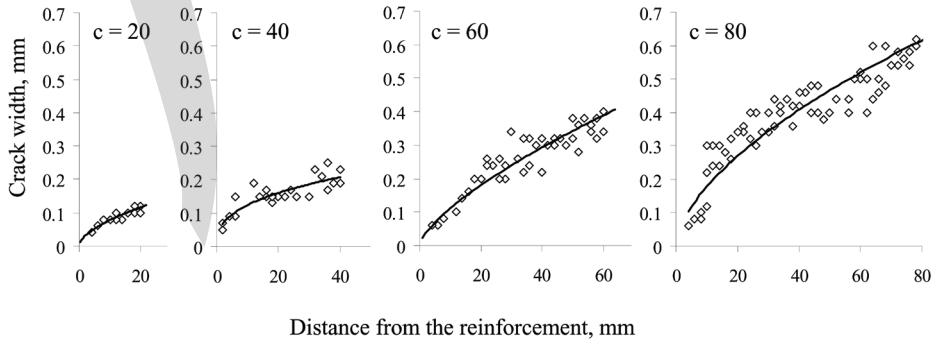


Fig. 6-58 Crack width along the concrete cover; regression functions (c = 20, 40, 60, 80 mm)[6-25]

This document is the intellectual property of the fib – International Federation for Structural Concrete. All rights reserved.
This PDF of fib Bulletin 92 is intended for use and/or distribution solely within fib National Member Groups.

In Fig. 6-58 an estimation can be studied that complete the data of Fig. 6-56 with the proposed function of *fib* Model Code 2010 First Complete Draft[6-34, 6-35,6-25].

According to the observations of the researchers the power of the functions is $\beta = 0{,}4 - 0{,}7$ that confirms the boundary conditions given in the model.

Further considerations are required to determine which load history can be assumed in case of a specific crack or crack width.

Based on the observations of Fig. 6-59 (which shows τ_b-s diagrams obtained from reversed cyclic loading[6-36]) it can be seen that the slip (i.e. crack width at the surface of the reinforcement) does not drop to zero during unloading (i.e. $\sigma_s = 0$ and $\tau_b = 0$). Crack width disappears only as a result of compressive stress.

Unloading, however, can result the change of crack width along the concrete cover compared to the condition when tensile stresses are formed in the concrete member (i.e. $\sigma_s > 0$ and $\tau_b > 0$). In this respect, a schematic illustration is presented in Fig. 6-60.

The schematic illustration of Fig. 6-60 postulates that the proportionality between the crack width at the surface of the reinforcement and that on the outer surface of the concrete structure strongly depends on the actual loading, and hence on the deformations of the structure.

In extreme cases (e.g. in a temporary unloaded condition or during reversed loading) it can happen that no significant difference can be seen between the crack width at the surface of the reinforcement and that on the outer surface of the concrete member, i.e:

$$w_{\text{reinforcement surface}} / w_{\text{concrete surface}} \approx 1.0 \qquad (6\text{-}50)$$

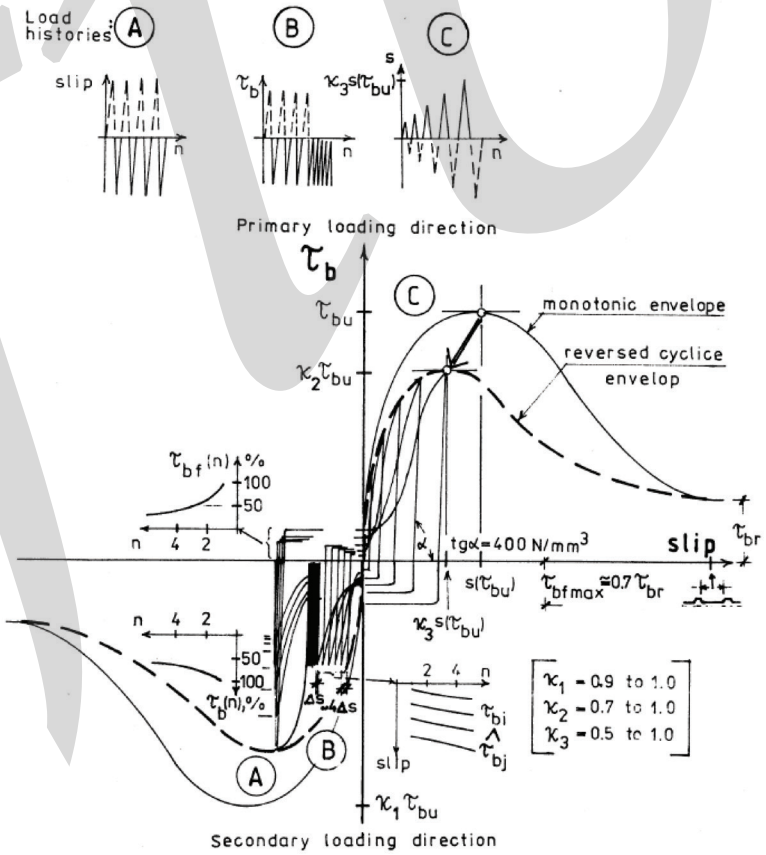


Fig. 6-59 τ_b-s diagrams obtained from/during reversed cyclic loading[6-26]

This document is the intellectual property of the fib – International Federation for Structural Concrete. All rights reserved.
This PDF of fib Bulletin 92 is intended for use and/or distribution solely within fib National Member Groups.

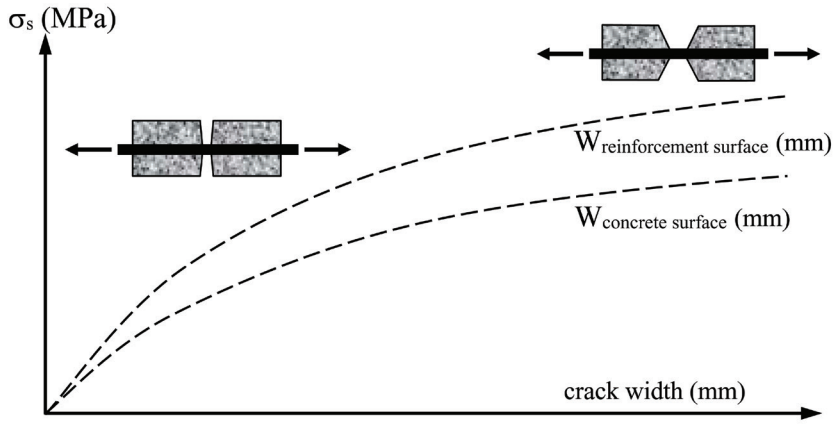


Fig. 6-60 Crack width along the concrete cover (schematic illustration)

The crack width (or the ratio of the crack width at the surface of the reinforcement and that of on the outer surface of the concrete member) can be formulated by the following generalized form:

$$w_{\text{reinforcement surface}} / w_{\text{concrete surface}} = f\left[\sigma_s(t), f_c(t), E_c(t), c, \varnothing_s, \alpha_{sb}\right] \quad (6\text{-}51)$$

where:

$\sigma_s(t)$ actual stress in the reinforcement

$f_c(t)$ actual strength of concrete

$E_c(t)$ actual Young's modulus of concrete

c concrete cover

$\varnothing_s$ diameter of reinforcement

α_{sb} relative rib area of reinforcement.

The variability of the crack width can be considerable along the crack due to the above parameters.

6.4.3 Conclusions and recommendations

Experimental evidence showed that the width of cracks within the concrete cover is different from that of measured at the surface of structural elements. Comprehensive analysis of this behaviour is a gap in the technical literature. Recent design codes do not cover the phenomenon either. Understanding of the behaviour would be essential since cracking can considerably influence the durability of concrete structures due to the change in permeability.

This chapter summarises the most important findings of literature. Based on the observations introduced the following conclusions can be drawn and recommendations can be suggested:

- crack width at the level of the reinforcement depends primarily on the actual stress in the reinforcement and depends on the thickness of the concrete cover only to an extent that generally influences the actual stress in the reinforcement (i.e. stiffness of structural member),

- secondary micro-cracks (Goto cracks) at the surface of the reinforcement represent a smeared deformation field in the close vicinity of the reinforcement and influence the crack width of the macroscopic structural crack,

This document is the intellectual property of the fib – International Federation for Structural Concrete. All rights reserved.
This PDF of fib Bulletin 92 is intended for use and/or distribution solely within fib National Member Groups.

- extension of the micro-cracked zone depends on the relative rib area of the reinforcement and the mechanical properties of concrete,

- the deformation of the concrete cover governs the variations of the crack widths outside the region of the secondary micro-cracks,

- the larger the concrete cover, the larger the crack width at the concrete surface,

- increase of the crack width towards the concrete surface is non-linear,

- the relationship between crack width and concrete cover can be postulated in the following form:

$$w_d^* = w_d + \Delta w_d \tag{6-52}$$

where

w_d^* is the crack width on the outer concrete surface

w_d is the crack width at the surface of the reinforcement (the slip between the reinforcement and the concrete)

Δw_d is the crack width increment due to the additional deformation of the concrete cover given in the form of a power function, $\Delta w_d = A \cdot c^{\beta}$

where

A depends on concrete strength and effective reinforcement ratio

β is an empirical constant ($0 < \beta < 1$)

c is the concrete cover

This document is the intellectual property of the fib – International Federation for Structural Concrete. All rights reserved.
This PDF of fib Bulletin 92 is intended for use and/or distribution solely within fib National Member Groups.

7. Verification of serviceability limit states by numerical simulation

7.1 Introduction

Numerical modelling based on the finite element method and nonlinear constitutive models offers a general method for capturing all features required for realistic description of structural behaviour of reinforced concrete. The material is treated as a composite consisting of concrete and reinforcement in which the stresses are obtained by continuum analysis whereas the requirements of conditions of stress equilibrium and strain compatibility must be fulfilled. Implementation is based on numerical methods, which fulfil the required conditions with certain approximations and thus the quality of the resulting analysis strongly depends on the resolution of the numerical model described by element type and mesh size.

In general a 3D model offers a best representation of reality. It can provide a detail insight in complex situations, such as in so called D regions, where reinforcement detailing can be modelled without simplifying assumptions. However, when appropriate, a dimensional reduction to 2D plane stress, plane strain or rotational symmetry, can be used to reduce the model size while eliminating minor stress components. The limits of such models should be duly acknowledged in the interpretation of results.

Numerical modelling has virtually no limits in reflecting actual boundary conditions and loading scenarios. This is particularly helpful in cases of imposed restraints, or interactions between structures and foundations.

Today, numerical methods are highly developed and offer many advanced methods with various degrees of sophistication. However, in this report the scope is limited only to the displacement-based finite element method, which is most widely used in practice in many commercially available software tools.

Crack development is the most important feature in verification of serviceability states. Therefore, the constitutive model of cracks and its implementation in non-linear finite element analysis should be chosen carefully and validated. A smeared crack approach is typically used for damage by cracks. In this, the discrete cracks are approximated by strain localization within the displacement field of elements. This approach is well suited for reinforced concrete, where many cracks with small spacing occur. The main advantage of this approach is that the crack propagation does not require a mesh refinement.

Discrete crack approach can be applied to a single crack propagation in special cases, such as dams.

In this study we shall describe the two cases of smeared crack models, firstly based on fracture mechanics and secondly based on tension stiffening. They represent two levels of scale applied to concrete fracture. It is recognized that fracture mechanics can effectively handle the cracking only within a certain (small) size range. When extending the analysis to larger sizes, we can adopt an alternative approach based on a tension stiffening behaviour.

This chapter was mainly authored by Červenka.

doi.org/10.35789/fib.BULL.0092.Ch07

This document is the intellectual property of the fib – International Federation for Structural Concrete. All rights reserved.
This PDF of fib Bulletin 92 is intended for use and/or distribution solely within fib National Member Groups.

The present study is focused on the modelling of cracks. Of course, a complete model would consist of other actions, such as multi-axial due to confinement effects, reduction of strength due to cracking, shear resistance of cracked concrete due to aggregate interlock, and others. All these effects may interact and are integrated within a composite model, which is referred to as fracture-plastic constitutive model of concrete. For more details see this study[7-1].

7.2 Crack model based on fracture mechanics

Concrete fracture has been formulated in a study[7-2] in a cohesive crack model. In this model a normal stress on the crack face diminishes gradually with a crack opening, which is called a stress softening. In the course of research development various methods for modelling the stress softening were proposed. Among them the exponential form proposed in this study[7-3] as shown in Fig.7-1 seems to be well suited and sufficiently general. In addition to the stress softening function only two parameters are required for its definition: tensile strength and fracture energy density (area under the curve). The fracture energy G_f describes the energy needed to generate a unit surface of a crack.

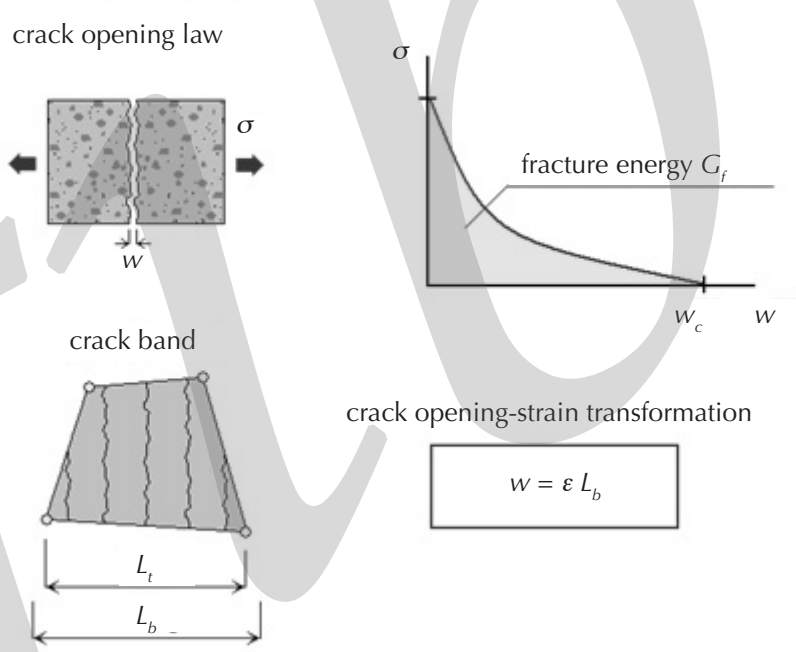


Fig. 7-1 Crack band model. Exponential law[7-3]

The model of cohesive discrete cracking can be implemented within the finite element method with the help of a crack band method proposed in one study[7-4], which ensures a unique dissipation of fracture energy within the finite element representing a discrete cohesive crack, see Fig. 7-1. The crack band L_b , referred as localization limiter, is related to the finite element size L_t and its orientation[7-5]. In a special case of rectangular element and crack parallel with its sides $L_b = L_t$). The appropriate choice of the crack band parameter has a strong effect on the brittleness reflected by the finite element model.

This document is the intellectual property of the fib – International Federation for Structural Concrete. All rights reserved.
This PDF of fib Bulletin 92 is intended for use and/or distribution solely within fib National Member Groups.

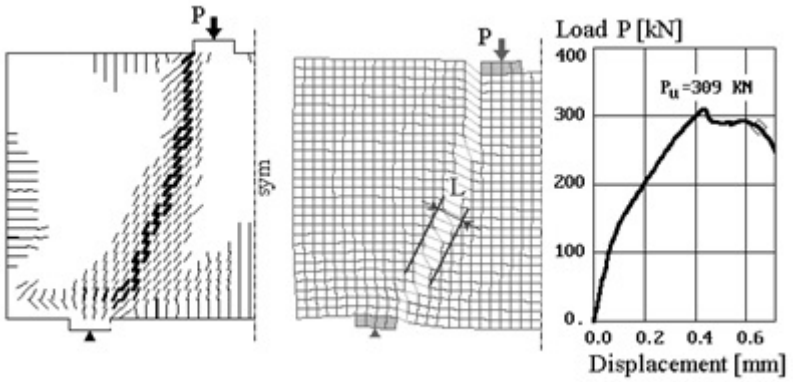


Fig. 7-2 Example of a strain localization in the crack band of a shear wall

Example of a strain localization in a shear wall model is illustrated in Fig. 7-2. The crack band concept mentioned above is used in numerous commercial software tools and has proven to be quite robust for assessment of crack patterns and crack width. Such example is shown in Fig.7-3 where beams tested in this study[7-6] were analysed in 2D plane stress representation. Two types of crack models are compared. A rotated crack model assumes that the crack direction is always aligned with the principal stresses and can rotate during the course of analysis. By definition it has no shear stress on the crack plane and is thus quite simple. To the contrary the fixed crack model defines the crack direction at the instant of crack initiation and keeps it fixed in the consequent analysis. Since the rotated crack model tends to deliver unrealistic crack patterns in some cases the fixed crack model is considered by some authors as a more rational model.

It is interesting to observe quite a good estimate of the crack width by the analysis. It should be noted that the model is based only on crack analysis with no specific model of bond slip. The crack width is calculated in low order isoparametric rectangular elements in integration points and then averaged in elements. The crack width is here a results of strain localization, which develops naturally due to cracking of most stressed locations and a consequent stress redistribution.

These results seem to contradict the state of the art crack model, which is based on a bond stress development along the bar, which in turn defines the crack spacing. It is remarkable that in this analysis no explicit bond slip was considered (perfect bond between bar and concrete). However, this problem can easily be explained if we look more closely at the stress transfer between bars and concrete. The finite element model simulates a bond action by cracking, which is of course a major source of bond slip action. More about bond in finite element modelling can be found in this study[7-7].

This document is the intellectual property of the fib – International Federation for Structural Concrete. All rights reserved.
This PDF of fib Bulletin 92 is intended for use and/or distribution solely within fib National Member Groups.

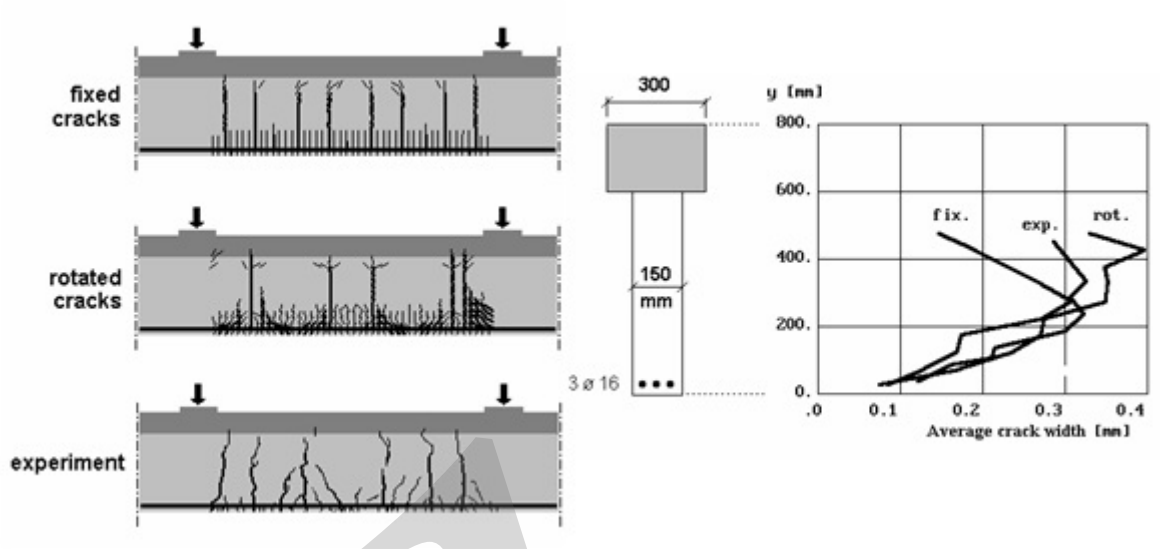


Fig. 7-3 Crack analysis of beam tested in this study[7-6]

The above example also illustrates the need for relatively fine mesh for a fracture mechanics based analysis which may limit the range of application. The crack patterns can be well reproduced by models with solid elements for concrete and embedded truss elements for bars. There should be several elements between cracks to enable sufficient strain localization and generation of separate discrete cracks.

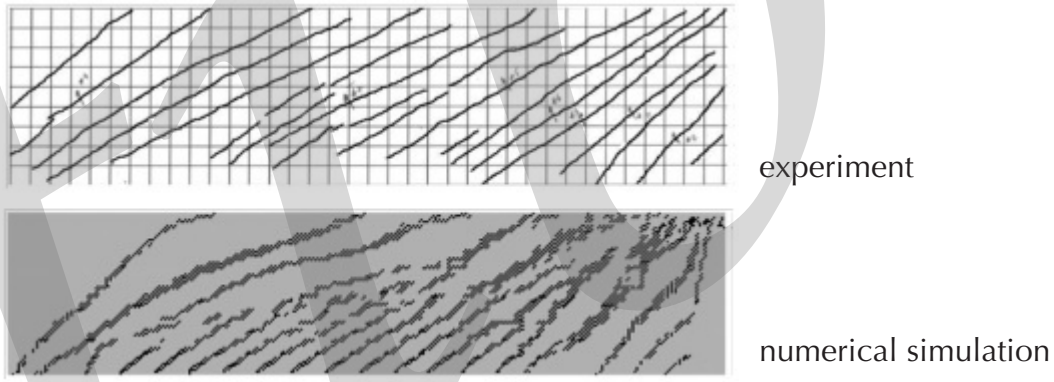


Fig. 7-4 Crack pattern of the shear wall

A verification of the model based on the crack band approach was made possible by the CONCRACK project[7-8]. A real-size shear wall structure was tested, dimensions 4x1x0.15 m, with 1% of orthogonal reinforcement, ø10, spacing 100 mm near both surfaces, and analysed in the bench mark competition. The cracks formed in direction inclined to reinforcement as shown in Fig. 7-4. The mesh size was 50 mm while the crack spacing was about 100 – 150 mm.

The power of numerical simulation can be utilized also in complex cases of exposure to effects of heat due to hydration, shrinkage and restraints provided by boundary conditions. Such a case was also investigated within the CONCRACK project on a reinforced column, cross section 0.8x0.8 m length 9 m. Crack development was simulated in time and the expected life time was estimated based on the projected corrosion rate and crack widths. An example from this project is shown in Fig. 7-5.

This document is the intellectual property of the fib – International Federation for Structural Concrete. All rights reserved.
This PDF of fib Bulletin 92 is intended for use and/or distribution solely within fib National Member Groups.

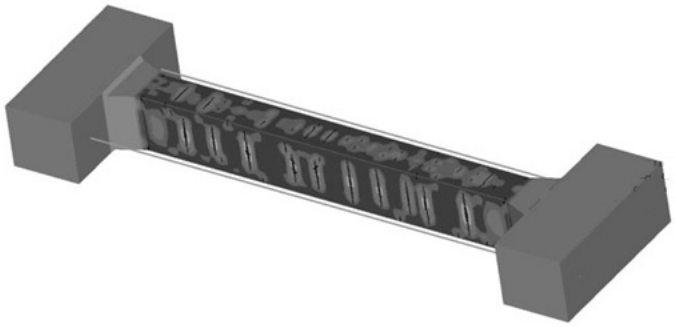


Fig. 7-5 Crack analysis of the massive element subjected to restrained boundary conditions[7-8]

7.3 Crack model based on tension stiffening

As was mentioned above, the fracture mechanics-based model requires a finite element mesh with sufficiently fine resolution in order to capture stress development between cracks and related strain localization. However, in large structures such a detailed model is not practically possible and we have to adopt an approach relying on engineering formulae developed for beams and slabs subjected to bending. In this approach we assume that the average stiffness of the cracked concrete is estimated as a sum of reinforcement and concrete contributions referred to as tension stiffening.

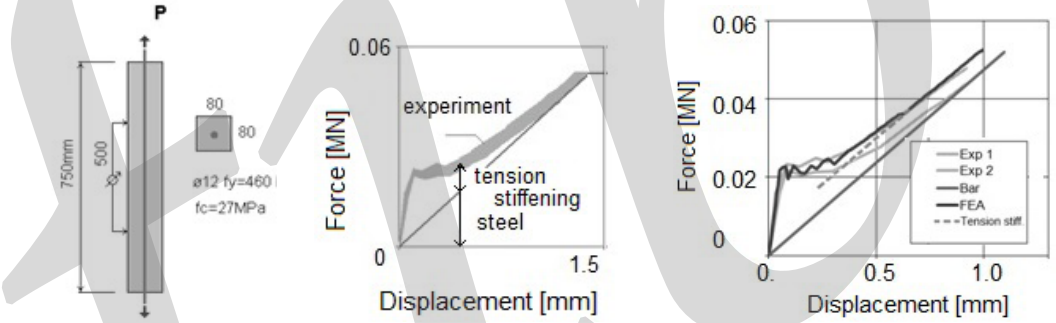


Fig. 7-6 Concrete element with embedded bar under uniaxial tension[7-9]

The effect of tension stiffening is often demonstrated by a tension test of a concrete prismatic element with an embedded bar, such as the one shown in Fig. 7-6[7-9]. A numerical simulation of the test was investigated in a study[7-7] about bond modelling. The effect of tension stiffening as shown in Fig. 7-6(c) can be simulated by a finite element modelling (based on fracture energy). However, with large elements only an average concrete contribution can be considered (marked by dashed line). This is implemented as a concrete stress component on the crack plane, see Fig. 7-7., where e_{cf} is a fracture strain corresponding to the crack opening.

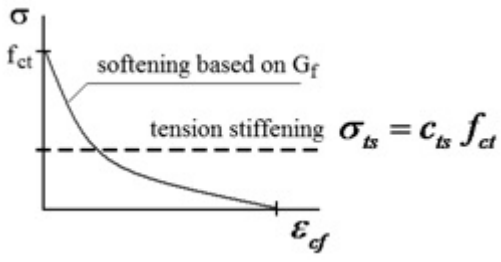


Fig. 7-7 Tension stiffening stress

This document is the intellectual property of the fib – International Federation for Structural Concrete. All rights reserved.
This PDF of fib Bulletin 92 is intended for use and/or distribution solely within fib National Member Groups.

The tension stiffening model can be adopted in combination with the fracture mechanics. Whenever the stress component on the crack face due to the crack band method decreases below the tension stiffening level σ_{ts} then the latter is maintained. The most simple tension stiffening model is constant, representing approximately a fully developed crack pattern. The factor c_{ts} is usually considered as 0.4, but can be lower in order to represent more damage. The approach based on the tension stiffening model is used to obtain strains in cracked zones. These strains are then used for determination of crack width for given crack spacing. The crack spacing for this purpose can be calculated according to the formula for bending $w_d = 2l_{s,\max} \cdot \varepsilon_{ef}$, where $l_{s,\max}$ is a stress development length.

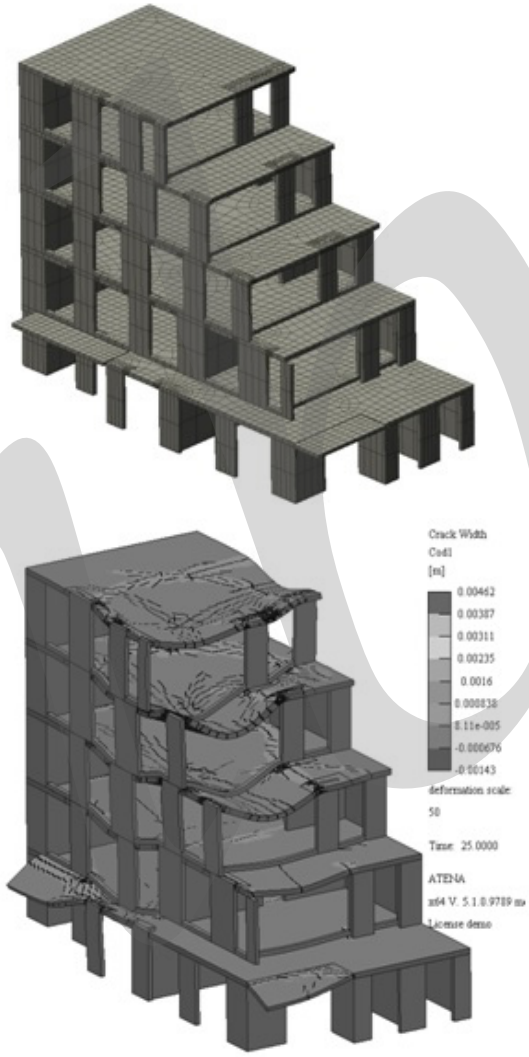


Fig. 7-8 Example of a crack width analysis based on tension stiffening model

An example of a crack analysis of a multi-storey building based on a tension stiffening model is shown in Fig. 7-8. The floor slabs are modelled by layered shell elements. A similar approach is suitable when using beam fibre elements or large solid elements.

This document is the intellectual property of the fib – International Federation for Structural Concrete. All rights reserved.
This PDF of fib Bulletin 92 is intended for use and/or distribution solely within fib National Member Groups.

8. Conclusions

In previous chapters stress analysis, crack width analysis and also deformation analysis were described. All procedures are related to the methods of the limit state approach and to the statements of MC2010[8-1], although some extensions were also mentioned. It is important to note that all procedures are approximate, although the numerical analyses provide high degree of accuracy. However, the results are dependent on input parameters defining the properties of concrete, steel and other applied materials. Many of them are derived from the compressive strength which may be measured quite well. The other values like tensile strength, modulus of elasticity, creep and shrinkage of concrete may be given by direct measurements or derived from compressive strength (class of concrete) indirectly. Then the accuracy of very advanced numerical procedures may become limited.

The other methods described herein are mostly approximate. In spite of it, they are well applicable for design of reliable and durable concrete structures. Serviceability limit states correspond to the actual behaviour of structures. Stresses calculated in concrete and steel inform about the actual level of exploitation of individual materials. The stresses have for a long time been part of main design criteria (theory of allowable stresses, which was used before the limit state design methods were accepted). For experienced designers the knowledge of stresses provides also additional indirect information on possible cracking or sensitivity to deformations, fatigue, etc.

The crack widths calculated using the formulae in this Bulletin can be considered as the widths of nominal cracks. Some cracks wider than the calculated value of the crack width may also be observed in real concrete structures, if the described criteria are satisfied. Crack width is a rather uncertain parameter which should generally also guarantee long-term durability of concrete structures, besides their favourable appearance. There is a never ending discussion, where the crack width should be measured and controlled. For durability, the crack width at the level of the surface of reinforcement is important, but this crack width cannot be measured directly. However, the crack width on the concrete surface is important for appearance and can be measured easily. Thus, the concrete cover layer becomes important for the specification of the crack width at the concrete surface (see section 6.4). For practical reasons, the surface crack width is taken as a criterion of the serviceability limit states.

Cracks induced by mechanical loading (loading by forces) can be directly calculated using the formulae from MC2010[8-1] and from this Bulletin. If cracks induced by restrained deformation are calculated, it is necessary to specify the tensile force or stress, which is the real cause of cracking. The tensile force is dependent on the degree of restraint and on the phenomenon inducing the internal strain. In early ages, the cooling of concrete often represents the primary reason for cracking, particularly in watertight structures. Later, the strains induced by shrinkage develop in time and produce cracks after a longer time period. The calculation of tensile forces is not directly mentioned in this Bulletin, since it is rather a structural issue than the direct crack width analysis. The working party within *fib* TG2.1 will prepare more detailed information on cracking in structures with restrained deformations.

Deflection analysis is thoroughly described in sections 4.3, 6.1 and 6.2. The general method is applicable using the numerical methods. Many commercial computer programs

This chapter was mainly authored by Vítek.

doi.org/10.35789/fib.BULL.0092.Ch08

This document is the intellectual property of the fib – International Federation for Structural Concrete. All rights reserved.
This PDF of fib Bulletin 92 is intended for use and/or distribution solely within fib National Member Groups.

use the method which is here denoted as an interpolation method, when the stiffness of the section or element is calculated by interpolation between the stiffness of the cracked section and the stiffness of the uncracked section. It is important to consider which load is applied. Usually the deflections (mainly long-term deflections) induced by long-term load (quasi-permanent load combination) are calculated, since those deflections are of primary importance for the long term function of the concrete structure. However, it may happen, that only very few cracks or even no cracks appear, if only long-term load is applied. Then the calculated deflections would be seriously underestimated. It is necessary to take into account that the structure could be loaded at higher levels (characteristic or frequent loading combination) which could produce cracks and reduce the stiffness of the structure. Often, the structure is loaded significantly during its construction, and the resulting cracks should be taken into account, when calculating the deflections induced by long-term load. Unfortunately, the pressure of clients aiming at a reduction of costs results in design of rather slender slabs and beams, which become sensitive to deflections. If all influencing factors are not taken into account, the calculated deflections will likely be underestimated. After several years, the users of the structure may suffer from excessive deflections and cracks in non-bearing structures of buildings. Usually, it is rather difficult to stop the slow but steady long-term deflection growth of a too slender element. As it was shown e.g. in chapter 6.3, the strong reinforcement of a slender element has a small impact on the reduced stiffness due to insufficient depth. A thicker slab with reasonable reinforcement is usually more appropriate for robust design than a heavily reinforced thin slab. As shown in section 5.4, the contemporary action of mechanical loading and effects of restrained deformation have to be taken into account. This is typical e.g. for slender slabs of car parks. An incorrect analysis and design may lead to large crack widths and leakage of water through the slabs. The function of such slabs would be impaired, potentially also reducing their durability.

This Bulletin provides extensive information on the analysis of stresses, cracks and deformations. However, for a reasonable design of concrete structures, a wide-ranging approach is most important. It is necessary to take into account the real importance of different serviceability criteria in the entire design process. Information provided here is in support of the design and construction of concrete structures, which should become a unique masterpiece of the design engineer.

This document is the intellectual property of the fib – International Federation for Structural Concrete. All rights reserved.
This PDF of fib Bulletin 92 is intended for use and/or distribution solely within fib National Member Groups.

References

Chapter 2

[2-1] *fib* (2013), *Model Code for Concrete Structures 2010*, Ernst und Sohn, *fib* 2013.

Chapter 3

[3-1] *fib* (2013), *Model Code for Concrete Structures 2010*, Ernst und Sohn, *fib* 2013.

[3-2] DAfStb(2003) – Richtlinie Wasserundurchlässige Bauwerke aus Beton (WU-Richtlinie), Ausgabe Nov. 2003.

[3-3] DAfStb(2006) – Erläuterungen zur DAfStb-Richtlinie Wasser undurchlässige Bauwerke aus Beton, Heft 555, Beuth Verlag, Berlin.

[3-4] ÖVBB (2009) – Richtlinie Wasserundurchlässige Betonbauwerke – Weiße Wannen, Ausgabe März 2009, ÖVBB, Wien, 2009.

[3-5] CEN (2005), EN 1992-3, Eurocode 2: Design of concrete structures: Part 3: Liquid Retaining and containment structures.

[3-6] *fib* (2005) Bulletin No. 32, *Guidelines for the design of footbridges*, *fib* Lausanne, 2005.

Chapter 4

[4-1] *fib* (2013), Model Code for Concrete Structures 2010, Ernst und Sohn, *fib* 2013.

[4-2] Cosenza, E., Debernardi, P.G. (1997), Calculation of stresses, deformations and deflections of reinforced and prestressed concrete elements in service. CEB Bulletin d'Information N.235, Lausanne, pp.105-141.

[4-3] CEB (1997), Serviceability models. CEB Bulletin d'Information N.235, Lausanne.

[4-4] Bažant, Z.P., (1972). "Prediction of concrete creep effects using age-adjusted modulus method". *ACI Journal*, Vol. 69, pp. 212-217.

[4-5] CEB (1984), Manual on cracking and deformations. CEB Bulletin d'Information N.158, Lausanne.

[4-6] Taliano M. (2009), "The improved n-method for the calculation of stresses in service". *Structural concrete*, Vol. 10, pp. 3-13.

[4-7] De Larrard, F. (1996), Extension du domaine des règlements de calcul BAEL/BPEL aux bétons à 80 MPa. Bulletin des Ponts et Chaussées, Numéro spécial XIX.

[4-8] CEB (1993) CEB-FIP Model Code 90. B. d'Inf n°213/214, Thomas Telford, ed., London.

[4-9] CEN (2005), EN 1992-1-1, Eurocode 2: Design of concrete structures: Part 1-1.

[4-10] CEN (1991), ENV 1992-1-1, Eurocode 2. Design of concrete structures. Part 1: General rules and rules for buildings.

[4-11] Beeby, A. W. (2004), The influence of the parameter ϕ/ρ_{eff} on crack widths. *fib Structural Journal*. Vol. 5. No.2., 71-83.

[4-12] Corres Peiretti, H. Petschke, T., Pérez Caldentey A. (2002) *UPM cracking test data base*.

[4-13] Hognestad, E. (1962). High strength bars as concrete reinforcement. Part 2: Control of flexural cracking. Journal of the PCA Research and Development Laboratories, Vol. 4, No. 1. January 1962, pp. 46-63.

This document is the intellectual property of the fib – International Federation for Structural Concrete. All rights reserved.
This PDF of fib Bulletin 92 is intended for use and/or distribution solely within fib National Member Groups.

[4-14] Clark, A.P. (1956), Cracking in Reinforced Concrete Flexural Members. *ACI Journal*, Proc. vol. 27, No. 8, Apr. 1956, pp.851–862.

[4-15] CUR (1994) Dutch Centre for Civil Engineering, Research and Codes Report no. 37 (Out of print).

[4-16] Rüsch, E.., Rehm G. (1963-64), *Versuche mit BetonformStählen*. (1963), pt. II (1963), pt. III (1964). Deutscher Ausschuss für Stahlbeton, No. 140.

[4-17] Krips, M. (1984), *Rissbreitenbeschränkung im Stahlbeton und SpannBeton*. Doctoral thesis, TH Darmstadt.

[4-18] Hartl, G. (1977) – Die Arbeitslinie "Eingebetete Stäbe" bei Erst- und Kurzzeitbelastung, Dissertation, Universität Innsbruck, 1977.

[4-19] Rehm, Eligehausen, Mallée (1976), *Rissverhalten von Stahlbetonkörpern bei Zugbeanspruchung*. Untersuchungsbericht (report).

[4-20] Farra, B., Jaccoud, J.P., 1993, *Influence du Beton et de l'armature sur la fissuration des structures en Beton. Rapport des Essais de Tirants sous déformation imposée de courte durée*. EPFL, Lausanne. Département de Génie Civil, Ecole Polytechnique Fédérale de Lausanne, pub. No. 140.

[4-21] Broms, B. (1965) *Crack width and crack spacing in reinforced concrete members*, ACI Journal October 1965, pp. 1237-1256.

[4-22] Pérez Caldentey, A., Corres Peiretti, H., Peset Irribaren, J. (2010) Estudio de fisuración en muros pantalla. Final Report, research project No. IDI-20080937, funded by CDTI. Ministry of Science and Technology, Spain.

[4-23] Husain, S. I., Ferguson, P. M.(1968), *Flexural Crack Width at the Bars in Reinforced Concrete Beams*. Research report No. 102-1F. Center for Highway Research. Austin, Texas.

[4-24] Borosnyói A., Snóbli I. (2010) *Crack width variation within the concrete cover of reinforced concrete members*, Építőanyag, Journal of the SZTE, Hungarian Scientific Society of the silicate Industry, Vol. 62, No. 3., pp. 70-74.

[4-25] Goto, Y. (1971) *Cracks formed in concrete around deformed tension bars*, ACI Journal, Vol.68, April 1971, pp. 244-251.

[4-26] Jakubovskis, R.; Kaklauskas, G.; Gribniak, V.; Weber, A.; Juknys, M. 2014. "Serviceability analysis of concrete beams with different arrangement of GFRP bars in the tensile zone". *ASCE Journal of Composites for Construction*, 18(5): 04014005-1–10. DOI: 10.1061/(ASCE)CC.1943-5614.0000465.

[4-27] Gómez Navarro, M., (2000) *Concrete Cracking in the Deck of Steel-Concrete Composite Bridges*. PhD Thesis No. 2268, EPFL. Lausanne, 2000.

[4-28] Pérez Caldentey, A., Corres Peiretti, H., Peset Irribaren, J. and Giraldo Soto, A. (2013), *Cracking of RC members revisited: influence of cover, $\varphi/\rho_{s,ef}$ and stirrup spacing – an experimental and theoretical study*. Structural Concrete 01/2013. Nr. 16, pp. 69-78.

[4-29] EN 1992-2 (2005) (English): Eurocode 2: Design of concrete structures - Part 2: Concrete bridges - Design and detailing rules.

[4-30] Ottosen, N.S. (1977) *A failure criterion for concrete*. J. Eng. Mech. Div. ASCE 103, 527 – 535.

[4-31] T. & Fehling, E. (2011), ´Design for serviceability of ultra high performance concrete structures. *High Performance Fiber Reinforced Cement Composites 6 (Eds: Parra-Montesinos, G. J.; Reinhardt, H. W.; Naaman; A. E.), Proceedings of the Sixth International Workshop on High Performance Fiber Reinforced Cement Composites (HPFRCC6)*, pp. 445-452, Ann Arbor, MI, USA, Springer, Dordrecht, 2011.

[4-32] Bergner, H., (1997), *Rissbreitenbeschränkung zwangbeanspruchter Bauteile aus hochfestem Normalbeton,* Deutscher Ausschuss für Stahlbeton, No. 482, Beuth-Verlag, Berlin.

This document is the intellectual property of the fib – International Federation for Structural Concrete. All rights reserved.
This PDF of fib Bulletin 92 is intended for use and/or distribution solely within fib National Member Groups.

[4-33] Vecchio, F. J. and Collins, M.P. (1986) "The Modified Compression-field Theory for Reinforced Concrete Elements subjected to shear", *ACI Journal*, 83(2): 219-231.

[4-34] Kaufmann, W. and Marti, P. (1998) "Structural concrete: Cracked membrane model", *Journal of Structural Engineering*, 124(12):1467-1475.

[4-35] Trost, H. (1967), 'Auswirkungen des Superpositionsprizips auf Kriech und Relaxations Probleme bei Beton und Spannbeton'. *Beton und Stahlbetonbau*, Vol. 62, No. 10, pp. 230-238.

[4-36] Spacone, E., Filippou, F.C. , Taucer, F.F. (1996), 'Fibre Beam-Column Model for Non-Linear Analysis of R/C Frames: Part II. Applications'. *Earthquake Engineering & Structural Dynamics*, Vol. 25, No. 7, pp.727–742.

[4-37] Marí, A., 1984. *Nonlinear geometric, material and time dependent analysis of three dimensional reinforced and prestressed concrete frames*, Department of Civil Engineering. University of California. Berkeley, California.

[4-38] Marí, A.R. & Montaner, J., 2000. Continuous Precast Concrete Girder and Slab Bridge Decks, Proc. *ICE-Strucs. and Buildings*, (140), pp.195–207.

[4-39] Cruz, P.J.S. & Marí, A.R.B., (1994) *Un modelo para el análisis no lineal y diferido de estructuras de hormigón y acero construidas evolutivamente*. Barcelona: Universitar Politècnica de Catalunya. Escola Tècnica Superior d'Enginyers de Camins, Canals i Ports.

[4-40] Marí, A.R. & Valdes, M., 2000. Long-Term behaviour of continuos precast concrete girder bridge model. *ASCE J. Bridge Eng*, 5(1), pp.22–30.

[4-41] Buckle, I.G. & Jackson, A.T. (1981). *A filamented beam element for the non-linear alanysis of reinforced concrete shells with edge beams*, Departament of Civil Engineering, University of Auckland, New Zeland.

[4-42] Bazant, Z.P. & Wu, S.T., 1973. Dirichlet series creep function for ageing concrete. *Journal of Eng. Mechanics Division*, 99, pp.367–387.

[4-43] Chan, E.C., 1982. Nonlinear geometric, material and time dependent analysis of reinforced concrete shells with edge beams, Department of Civil Engineering. University of California. Berkeley, California.

[4-44] Hernandez, H.D. & Gamble, W.L. (1975), *Time-dependent prestress losses in pretensioned concrete construction*, Structural Research Series N. 417, Univ. of Illinois, USA.

[4-45] Kang, Y.J. & Scordelis, A.C., 1980. Nonlinear analysis of prestressed concrete frames. *Journal of Structural Division*, 106, pp.445–462.

[4-46] Kang, Y.J. & Scordelis, A.C., 1990. Non-linear segmental analysis of reinforced and prestressed concrete bridges. . In *3rd International Conference on Short and Medium Spam Bridges*. Toronto (Ontario, Canada), pp. 229–240.

[4-47] Elbadry, M. & Ghali, A., 1990. *User's Manual and Computer Program CPF: Cracked Plane Frames in Prestressed Concrete*, Version 3.0, Research Report No. CE85-2, Department of Civil Engineering, University of Calgary, Calgary (Alberta, Canada), 205 pp.

[4-48] Torres, L. López-Almansa, F., Cahñis, X., Bozzo, L.M. (2003), "A numerical model for sequential construction, repairing and strengthening of 2-D concrete frames". *Engineering Structures*, Vol. 25, No. 3, pp.323–336.

[4-49] Chiorino, M.. & Sassone, M., 1985. Further considerations and updates on time-dependent analysis of concrete structures, Laussane: *fib* Bulletin 52, Lausanne.

[4-50] Gilbert, R., 1988. *Time effects in concrete structures*, Elsevier, Amsterdam.

[4-51] Ghali, A., Favre, R. & Elbadry, M., 2012. *Concrete Structures: Stresses and Deformations – Analysis and Design for Serviceability*, 4th Edition, Spon Press, London, 663 pp.

[4-52] Gilbert, R.I and Ranzi, G., 2011. *Time-dependent behaviour of concrete structures* SponPress, ed., London.

This document is the intellectual property of the fib – International Federation for Structural Concrete. All rights reserved.
This PDF of fib Bulletin 92 is intended for use and/or distribution solely within fib National Member Groups.

[4-53] Elbadry, M., Ghali, A. & Gayed, R., (2014) "Deflection Control of Prestressed Box-Girder Bridges". *Journal of Bridge Eng*, 19(5), 8 pp.

[4-54] Branson, D.E., 1977. *Deformation of Concrete Structures*, New York: McGraw-Hill.

[4-55] Marí, A., Bairán, J.M. & Duarte, N., 2010. Long-term deflections in cracked reinforced flexural members. *Engineering Structures*, Vol. 32, 829-842.

[4-56] Torres, L., López-Almansa, F., Bozzo, L.M. (2004), 'Tension-Stiffening Model for Cracked Flexural Concrete Members'. *ASCE Journal of Structural Engineering*, Vol. 130, No. 8, pp.1242–1251.

[4-57] ACI Committee 318, "Building Code Requirements for Structural Concrete (ACI 318-14). American Concrete Institute, September 2014, ISBN: 978-0-87031-930-32014.

[4-58] CPH (2008), *Instrucción Española del Hormigón Estructural*, Ministerio de Fomento. Centro de Publicaciones, Madrid.

[4-59] Murcia, J., 1991. Análisis aproximado en el tiempo de secciones de hormigón armado en servicio. Propuesta de un nuevo factor de cálculo de flechas diferidas. *Hórmigon y Acero*, 183, pp.19–25.

Chapter 5

[5-1] *fib* (2013), Model Code for Concrete Structures 2010, Ernst und Sohn, *fib* 2013.

[5-2] Ottosen, N.S. (1977) *A failure criterion for concrete*. J. Eng. Mech. Div. ASCE 103, 527 – 535.

[5-3] CEN (2004) Eurocode2. Design of Concrete Structures. Part 1-1: General rules and rules for buildings. EN 1992-1-1, Brussels.

[5-4] Fehling, E., Leutbecher, T. (2003) *Beschränkung der Rissbreite bei kombinierter Beanspruchung aus Last und Zwang*, Beton- und Stahlbetonbau 98 (2003), Vol. 7, S. 377, Verlag Ernst & Sohn.

[5-5] DIN 1045-1: Tragwerke aus Beton, Stahlbeton und Spannbeton - Teil 1: Bemessung und Konstruktion, Deutsches Institut für Normung, Beuth-Verlag 2001-07, 2008-02.

[5-6] Lohmeyer G. and Ebeling K. (2009), *Weisse Wannen - einfach und sicher, Konstruktion und Ausführung wasserundurchlässiger Bauwerke aus Beton*, Bau + Technik Düsseldorf.

[5-7] Marti P., Sigrist V. and Alvarez M. (1997), *Mindestbewehrung von Betonbauten*, Forschungsauftrag Nr. 82/95, Bericht Nr. 529, Bundesamt für Strassenbau, Zürich.

[5-8] Burns C. (2012), *Serviceability analysis of reinforced concrete based on the tension chord model*, IBK Bericht, Nr. 342, ETH Zürich.

[5-9] Marí, A., "Numerical Simulation of the Segmental Construction of Three Dimensional Concrete Frames", *Engineering Structures*, No. 6, Vol. 22, pp 585-596, June 2000.

[5-10] Ghali, A., Favre, R. & Elbadry, M., 2012. *Concrete Structures: Stresses and Deformations – Analysis and Design for Serviceability*, 4th Edition, Spon Press, London, 663 pp.

Chapter 6

[6-1] Cosenza, E., Debernardi, P.G. (1997), *Calculation of stresses, deformations and deflections of reinforced and prestressed concrete elements in service*. CEB Bulletin d'Information N.235, Lausanne, pp.105-141.

[6-2] CEN (2004) Eurocode2. Design of Concrete Structures. Part 1-1:General rules and rules for buildings. EN 1992-1-1, Brussels.

[6-3] *fib* (2013), Model Code for Concrete Structures 2010, Ernst und Sohn, *fib* 2013.

This document is the intellectual property of the fib – International Federation for Structural Concrete. All rights reserved.
This PDF of fib Bulletin 92 is intended for use and/or distribution solely within fib National Member Groups.

[6-4] Debernardi, P.G., Taliano, M. (2010), "Span-to-height ratio limits for prestressed concrete members". *Structural concrete*, Vol. 11, pp. 35-43.

[6-5] Bazant, Z.P., 1972. "Prediction of concrete creep effects using age-adjusted modulus method". *ACI Journal*, Vol. 69, pp. 212-217.

[6-6] CEB (1984), *Manual on structural effects of time-dependent behaviour of concrete*. CEB Bulletin d'Information N.142, Lausanne.

[6-7] CEB (1993), *Structural effects of time-dependent behaviour of concrete*. CEB Bulletin d'Information N.215, Lausanne.

[6-8] Leonhardt, F., Walther, R. (1964), *The Stuggard shear tests*, 1961. Cement and Concrete Association, pp.134.

[6-9] Leonhardt, F., Walther, R. (1967), "Versuche an Plattenbalken mit hoher Schubbeanspruchung". *Deutscher Ausschuss für Stahlbeton*., 152, W. Ernst und Sohn, Berlin.

[6-10] ASCE-ACI Committee 445 (1998). "Recent approaches to shear design of structural concrete". *Journal of Structural Division*; 124: 1375-1417.

[6-11] Pang, X.B.D., Hsu, T.T.C (1995), "Behaviour of reinforced concrete membrane elements in shear". *ACI Structural Journal*, Vol. 92: 665-679.

[6-12] Walraven, J.C., Al-Zubi, N. (1995), "Shear capacity of lightweight concrete beams with shear reinforcement". *Proceedings Symposium on lightweight aggregate concrete*, Sandefjord, Norway, Vol. 1: 91-104.

[6-13] Taylor, H.P.J (1974). "Fundamental Behavior of Reinforced Concrete Beams in Bending and Shear". American Concrete Institute. *Shear in Reinforced Concrete*. SP-42, 43-77.

[6-14] Reineck, K.H. (2002), *Shear design in a consistent design concept for structural concrete based on strut-and-tie models. Design examples for the 1996 FIP recommendations "Practical design of structural concrete". fib* Bulletin, N. 16: 165-186.

[6-15] Guiglia, M. (2005), "Analisi della deformazione a taglio di travi in calcestruzzo armato ad anima sottile". PhD Thesis, Politecnico di Torino (Italy).

[6-16] Debernardi, P.G., Taliano, M. (2002), "Shear deformation of r.c. beams". *Proceedings of the First fib Congress. Concrete Structures in the 21st Century*, Osaka; Vol. 1: 179-188.

[6-17] Debernardi, P.G., Taliano, M. (2006), "Shear deformation in r.c. beams with thin web". *Magazine of Concrete Research*, Vol. 58: 157-171.

[6-18] Vecchio, F. J. and Collins, M.P. (1986) "The Modified Compression-field Theory for Reinforced Concrete Elements subjected to shear", *ACI Journal*, 83(2): 219-231.

[6-19] Debernardi, P.G., Guiglia M., Taliano M. (2011), "Shear strain in B-regions of beams in service". *Engineering structures*, Vol. 33 n. 2, pp. 368-379.

[6-20] CEB (1993) CEB-FIP Model Code 90. B. d'Inf n°213/214, Thomas Telford, ed., London.

[6-21] Debernardi, P.G., Guiglia M., Taliano M. (2012), "Parametric analysis of the influence of shear on the deflection of RC beams in service". *Magazine of concrete research*, Vol. 64 n. 4, pp. 335-350.

[6-22] Corres Peiretti, H., Pérez Caldentey, A., López Agüí, J.C., Erdtbauer J. (2003) *prEN Chapter 7 – Serviceability Limit States. Deflections. Supporting Document*. Eurocode 2 Commentary. The European Concrete Platform ASBL, June 2008.

[6-23] Vollum, R.L. (2009), *Comparison of deflection calculations and span-to-depth ratios in BS 8110 and Eurocode 2*, Magazine of Concrete Research, 2009, 61, No. 6, August, 465–476.

[6-24] Balázs, G. L. (1992*) Load transfer in concrete*, Ph.D. Thesis, Budapest University of Technology, Department of construction materials and engineering (in Hungarian).

This document is the intellectual property of the fib – International Federation for Structural Concrete. All rights reserved.
This PDF of fib Bulletin 92 is intended for use and/or distribution solely within fib National Member Groups.

[6-25] Borosnyói A., Snóbli I. (2010) "Crack width variation within the concrete cover of reinforced concrete members", Építőanyag, *Journal of the SZTE*, Hungarian Scientific Society of the silicate Industry, Vol. 62, No. 3., pp. 70-74.

[6-26] Balázs, G. L. (1993) "Cracking analysis based on slip and bond stresses". *ACI Materials Journal*, July-August 1993, pp. 340-348.

[6-27] Goto, Y. (1971) "Cracks formed in concrete around deformed tension bars", *ACI Journal*, Vol.68, April 1971, pp. 244-251.

[6-28] Broms, B. (1965) "Crack width and crack spacing in reinforced concrete members", *ACI Journal* October 1965, pp. 1237-1256.

[6-29] Husain, S. I., Ferguson, P. M.(1968), "Flexural Crack Width at the Bars in Reinforced Concrete Beams". Research report No. 102-1F. Center for Highway Research. Austin, Texas.

[6-30] Yannopoulos, P. J. (1989) "Variation of concrete crack widths through the concrete cover to reinforcement". *Magazine of Concrete Research*, 1989, 41, No. 147, 63–68.

[6-31] Beeby, A. W. (2004), "The influence of the parameter ϕ/ρ_{eff} on crack widths". *fib Structural Journal*. Vol. 5. No.2., 71-83.

[6-32] Tammo, K., Thelandersson, S. (2006) "Crack opening near reinforcement bars in concrete structures", *Structural Concrete*, 2006, 7, No. 4, 137–143.

[6-33] Carino, N. J., Clifton J. R., (1995) *Prediction of Cracking in Reinforced Concrete Structures*, NIST BFRL, Gaithersburg, 1995.

[6-34] *fib* Bulletin 55, Model Code 2010 – First complete draft, Volume 1, *fib*, Lausanne, 2010.

[6-35] *fib* Bulletin 56, Model Code 2010 – First complete draft, Volume 2, *fib*, Lausanne, 2010.

[6-36] Balázs, G.L. (1991) "Fatigue of bond", *ACI Materials Journal*, November-December 1991, pp. 620-629.

Chapter 7

[7-1] Cervenka, J., Pappanikolaou, V. (2008), "Three dimensional combined fracture-plastic material model for concrete". *Int. J. of Plasticity*, Vol. 24, 12, 2008, ISSN 0749-6419, pp. 2192-2220.

[7-2] Hillerborg A., Modéer M. and Peterson P.E. (1976), "Analysis of crack formation and crack growth in concrete by means of fracture mechanics and finite elements". *Cement Concrete Res.* 6, 1976, 773-782.

[7-3] Hordijk, D.A.,(1991) "Local Approach to Fatigue of Concrete". Ph.D. Thesis, Delft University of Technology, The Netherlands, 1991.

[7-4] Bažant, Z.P., Oh, B. H.: "Crack band theory for fracture of concrete". *Matériaux et Constructions*, Vol.16 – No. 93, 1983, 155-177

[7-5] Slobbe A.T., Hendriks M.A.N., Rots J.G.(2013). *Systematic assessment of directional mesh bias with periodic boundary conditions: Applied to the crack band model. Engineering Fracture Mechanics*, V. 109, September 2013, Pages 186–208.

[7-6] Braam C.R. (1990) - Control of crack width in deep reinforced beams. *Heron* 4 (35), 1990.

[7-7] Jendele, L., Cervenka, J. (2006). "Finite element modeling of reinforcement with bond", *Computers and Structures,* 84, 2006, 1780-1791.

This document is the intellectual property of the fib – International Federation for Structural Concrete. All rights reserved.
This PDF of fib Bulletin 92 is intended for use and/or distribution solely within fib National Member Groups.

[7-8] Cervenka, V. et al. (2014). "ATENA simulation of crack propagation in CONCRACK benchmark". *European Journal of Environmental and Civil Engineering*, Taylor&Francis, Vol.18, Nos.7-8, July-September 2014, p.828-844.

[7-9] Hartl, G. (1977). "Die Arbeitslinie "Eingebetete Stäbe" bei Erst- und Kurzzeitbelastung", Dissertation, Universität Innsbruck, 1977.

Chapter 8

[8-1] *fib* (2013), Model Code for Concrete Structures 2010, Ernst und Sohn, *fib* 2013.

This document is the intellectual property of the fib – International Federation for Structural Concrete. All rights reserved.
This PDF of fib Bulletin 92 is intended for use and/or distribution solely within fib National Member Groups.

The *fib* (International Federation for Structural Concrete - Fédération internationale du béton) is grateful for the invaluable support of the following national member groups and sponsoring members, which contributes to the publication of *fib* technical bulletins, the *Structural Concrete* journal and *fib*-news.

National member groups

UNNOBA - Universidad Nacional del Nor Oeste de la Provincia de Buenos Aires, Argentina
CIA - Concrete Institute of Australia
ÖBV - Österreichische Bautechnik Vereinigung, Austria
GBB-BBG - Groupement Belge du Béton, Belgium
ABCIC - Associação Brasileira da Construção Industrializada de Concreto, Brazil
ABECE - Associação Brasileira de Engenharia e Consultoria Estrutural, Brazil
Université Laval, Canada
Canadian Precast Prestressed Concrete Institute
CCES - China Civil Engineering Society
Cyprus University of Technology
Cyprus Association of Civil Engineers
Česká Betonářská Společnost, Czech Republic
DBF - Dansk Betonforening, Denmark
SB - Suomen Betoniyhdistys, Finland
AFGC - Association Française de Génie Civil, France
DAfStb - Deutscher Ausschuss für Stahlbeton, Germany
Technical Chamber of Greece
University of Patras, Department of Civil Engineering, Greece
Hungarian Group of the *fib*
The Institution of Engineers, India
fib-Indonesia
Department of Technical Affairs, Iran
IACIE - Israeli Association of Construction and Infrastructure Engineers
AICAP - Associazione Italiana Calcestruzzo, Armato e Precompresso, Italy
CTE - Collegio dei tecnici della industrializzazione edilizia, Italy
ITC - CNR, Istituto per le Tecnologie della Costruzione, Italy
ReLUIS, Italy
JCI - Japan Concrete Institute
JPCI - Japan Prestressed Concrete Institute
Administration des Ponts et Chaussées, Luxemburg
fib Netherlands: Betonvereniging
NZCS - New Zealand Concrete Society
NB - Norsk Betongforening / Norwegian Concrete Association
Polish Academy of Sciences, Committee for Civil Engineering, Poland
GPBE - Grupo Português de Betão Estrutural, Portugal
Polytechnic University of Timisoara, Romania
Technical University of Civil Engineering, Romania
University of Transylvania Brasov, Faculty of Civil Engineering, Romania
Association for Structural Concrete, Russia
SNK *fib*, Slovakia
Slovenian Society of Structural Engineers, Slovenia
TCI - The Concrete Institute, South Africa

This document is the intellectual property of the fib – International Federation for Structural Concrete. All rights reserved.
This PDF of fib Bulletin 92 is intended for use and/or distribution solely within fib National Member Groups.

KCI - Korean Concrete Institute, South Korea
ACHE - Asociación Cientifico-Técnica del Hormigon Estructural, Spain
SB - Svenska Betongföreningen, Sweden
Délégation nationale suisse de la *fib*, Switzerland
TCA - Thailand Concrete Association
ITU - Istanbul Technical University, Turkey
NIISK - Research Institute of Building Constructions, Ukraine
Society of Engineers, United Arab Emirates
fib UK: Institution of Structural Engineers, United Kingdom
ASBI - American Segmental Bridge Institute, United States of America
PCI - Precast/Prestressed Concrete Institute, United States of America
PTI - Post-Tensioning Institute, United States of America

Sponsoring members

Strong Force-MGC W.L.L., Bahrain
Liuzhou OVM Machinery Company, China
Shenzhen University, China
Peikko Group Corp., Finland
Consolis, France
ECS - European Engineered Construction Systems Association (formerly VBBF), Germany
FBF - Betondienst, Germany
ISB - Institut für Stahlbetonbewehrung, Germany
MKT - Metall-Kunststoff-Technik, Germany
Progress Group GmbH, Germany
Larsen & Toubro Ltd, ECC Division, India
Katerra India Pvt. Ltd., India
FUJI P. S. Corporation, Japan
IHI Construction Service Company, Japan
Oriental Shiraishi Corporation, Japan
P. S. Mitsubishi Construction Company, Japan
SE Corporation, Japan
Sumitomo Mitsui Construction Company, Civil Engineering Division, Japan
Hilti, Liechtenstein
BBR VT International, Switzerland
Sika Schweiz, Switzerland
VSL International, Switzerland
SSI Span Systems International Co., Ltd., Thailand
CCL Stressing Systems, United Kingdom
CEG – The Consulting Engineers Group, United States of America

This document is the intellectual property of the fib – International Federation for Structural Concrete. All rights reserved.
This PDF of fib Bulletin 92 is intended for use and/or distribution solely within fib National Member Groups.

fib Bulletins published since 1998

1 *Structural Concrete – Textbook on Behaviour, Design and Performance*; Vol. 1: *Introduction, Design Process, Materials*
Manual - textbook (244 pages, ISBN 978-2-88394-041-3, July 1999)

2 *Structural Concrete – Textbook on Behaviour, Design and Performance*; Vol. 2: *Basis of Design*
Manual - textbook (324 pages, ISBN 978-2-88394-042-0, July 1999)

3 *Structural Concrete – Textbook on Behaviour, Design and Performance*; Vol. 3: *Durability, Design for Fire Resistance; Member Design, Maintenance; Assessment and Repair, Practical aspects*
Manual - textbook (292 pages, ISBN 978-2-88394-043-7, December 1999)

4 *Lightweight aggregate concrete: Extracts from codes and standards*
State-of-the-art report (46 pages, ISBN 978-2-88394-044-4, August 1999)

5 *Protective systems against hazards: Nature and extent of the problem*
Technical report (64 pages, ISBN 978-2-88394-045-1, October 1999)

6 *Special design considerations for precast prestressed hollow core floors*
Guide to good practice (180 pages, ISBN 978-2-88394-046-8, January 2000)

7 *Corrugated plastic ducts for internal bonded post-tensioning*
Technical report (50 pages, ISBN 978-2-88394-047-5, January 2000)

8 *Lightweight aggregate concrete*: Part 1 (guide) – *Recommended extensions to Model Code 90*; Part 2 (technical report) – *Identification of research needs*; Part 3 (state-of-art report) – *Application of lightweight aggregate concrete* (118 pages, ISBN 978-2-88394-048-2, May 2000)

9 *Guidance for good bridge design*: Part 1 – Introduction, Part 2 – *Design and construction aspects*
Guide to good practice (190 pages, ISBN 978-2-88394-049-9, July 2000)

10 *Bond of reinforcement in concrete*
State-of-art report (434 pages, ISBN 978-2-88394-050-5, August 2000)

11 *Factory applied corrosion protection of prestressing steel*
State-of-art report (20 pages, ISBN 978-2-88394-051-2, January 2001)

12 *Punching of structural concrete slabs*
Technical report (314 pages, ISBN 978-2-88394-052-9, August 2001)

13 *Nuclear containments*
State-of-art report (130 pages, 1 CD, ISBN 978-2-88394-053-6, September 2001)

14 *Externally bonded FRP reinforcement for RC structures*
Technical report (138 pages, ISBN 978-2-88394-054-3, October 2001)

15 *Durability of post-tensioning tendons*
Technical report (284 pages, ISBN 978-2-88394-055-0, November 2001)

16 *Design Examples for the 1996 FIP recommendations Practical design of structural concrete*
Technical report (198 pages, ISBN 978-2-88394-056-7, January 2002)

17 *Management, maintenance and strengthening of concrete structures*
Technical report (180 pages, ISBN 978-2-88394-057-4, April 2002)

18 *Recycling of offshore concrete structures*
State-of-art report (33 pages, ISBN 978-2-88394-058-1, April 2002)

19 *Precast concrete in mixed construction*
State-of-art report (68 pages, ISBN 978-2-88394-059-8, April 2002)

This document is the intellectual property of the fib – International Federation for Structural Concrete. All rights reserved.
This PDF of fib Bulletin 92 is intended for use and/or distribution solely within fib National Member Groups.

20 *Grouting of tendons in prestressed concrete*
Guide to good practice (52 pages, ISBN 978-2-88394-060-4, July 2002)

21 *Environmental issues in prefabrication*
State-of-art report (56 pages, ISBN 978-2-88394-061-1, March 2003)

22 *Monitoring and safety evaluation of existing concrete structures*
State-of-art report (304 pages, ISBN 978-2-88394-062-8, May 2003)

23 *Environmental effects of concrete*
State-of-art report (68 pages, ISBN 978-2-88394-063-5, June 2003)

24 *Seismic assessment and retrofit of reinforced concrete buildings*
State-of-art report (312 pages, ISBN 978-2-88394-064-2, August 2003)

25 *Displacement-based seismic design of reinforced concrete buildings*
State-of-art report (196 pages, ISBN 978-2-88394-065-9, August 2003)

26 *Influence of material and processing on stress corrosion cracking of prestressing steel – case studies*
Technical report (44 pages, ISBN 978-2-88394-066-6, October 2003)

27 *Seismic design of precast concrete building structures*
State-of-art report (262 pages, ISBN 978-2-88394-067-3, October 2003)

28 *Environmental design*
State-of-art report (86 pages, ISBN 978-2-88394-068-0, February 2004)

29 *Precast concrete bridges*
State-of-art report (83 pages, ISBN 978-2-88394-069-7, November 2004)

30 *Acceptance of stay cable systems using prestressing steels*
Recommendation (80 pages, ISBN 978-2-88394-070-3, January 2005)

31 *Post-tensioning in buildings*
Technical report (116 pages, ISBN 978-2-88394-071-0, February 2005)

32 *Guidelines for the design of footbridges*
Guide to good practice (160 pages, ISBN 978-2-88394-072-7, November 2005)

33 *Durability of post-tensioning tendons*
Recommendation (74 pages, ISBN 978-2-88394-073-4, December 2005)

34 *Model Code for Service Life Design*
Model Code (116 pages, ISBN 978-2-88394-074-1, February 2006)

35 *Retrofitting of concrete structures by externally bonded FRPs*
Technical Report (224 pages, ISBN 978-2-88394-075-8, April 2006)

36 *2006 fib Awards for Outstanding Concrete Structures*
Bulletin (40 pages, ISBN 978-2-88394-076-5, May 2006)

37 *Precast concrete railway track systems*
State-of-art report (38 pages, ISBN 978-2-88394-077-2, September 2006)

38 *Fire design of concrete structures – materials, structures and modelling*
State-of-art report (106 pages, ISBN 978-2-88394-078-9, April 2007)

39 *Seismic bridge design and retrofit – structural solutions*
State-of-art report (300 pages, ISBN 978-2-88394-079-6, May 2007)

40 *FRP reinforcement in RC structures*
Technical report (160 pages, ISBN 978-2-88394-080-2, September 2007)

41 *Treatment of imperfections in precast structural elements*
State-of-art report (74 pages, ISBN 978-2-88394-081-9, November 2007)

42 *Constitutive modelling of high strength / high performance concrete*
State-of-art report (130 pages, ISBN 978-2-88394-082-6, January 2008)

This document is the intellectual property of the fib – International Federation for Structural Concrete. All rights reserved.
This PDF of fib Bulletin 92 is intended for use and/or distribution solely within fib National Member Groups.

43 *Structural connections for precast concrete buildings*
Guide to good practice (370 pages, ISBN 978-2-88394-083-3, February 2008)

44 *Concrete structure management: Guide to ownership and good practice*
Guide to good practice (208 pages, ISBN 978-2-88394-084-0, February 2008)

45 *Practitioners' guide to finite element modelling of reinforced concrete structures*
State-of-art report (344 pages, ISBN 978-2-88394-085-7, June 2008)

46 *Fire design of concrete structures —structural behaviour and assessment*
State-of-art report (214 pages, ISBN 978-2-88394-086-4, July 2008)

47 *Environmental design of concrete structures – general principles*
Technical report (48 pages, ISBN 978-2-88394-087-1, August 2008)

48 *Formwork and falsework for heavy construction*
Guide to good practice (96 pages, ISBN 978-2-88394-088-8, January 2009)

49 *Corrosion protection for reinforcing steels*
Technical report (122 pages, ISBN 978-2-88394-089-5, February 2009)

50 *Concrete structures for oil and gas fields in hostile marine environments*
State-of-art report (36 pages, IBSN 978-2-88394-090-1, October 2009)

51 *Structural Concrete – Textbook on behaviour, design and performance*, Vol. 1
Manual – textbook (304 pages, ISBN 978-2-88394-091-8, November 2009)

52 *Structural Concrete – Textbook on behaviour, design and performance*, Vol. 2
Manual – textbook (350 pages, ISBN 978-2-88394-092-5, January 2010)

53 *Structural Concrete – Textbook on behaviour, design and performance*, Vol. 3
Manual – textbook (390 pages, ISBN 978-2-88394-093-2, December 2009)

54 *Structural Concrete – Textbook on behaviour, design and performance*, Vol. 4
Manual – textbook (196 pages, ISBN 978-2-88394-094-9, October 2010)

55 *fib Model Code 2010, First complete draft* – Volume 1
Draft Model Code (318 pages, ISBN 978-2-88394-095-6, March 2010)

56 *fib Model Code 2010, First complete draft* – Volume 2
Draft Model Code (312 pages, ISBN 978-2-88394-096-3, April 2010)

57 *Shear and punching shear in RC and FRC elements - Workshop proceedings*
Technical report (268 pages, ISBN 978-2-88394-097-0, October 2010)

58 *Design of anchorages in concrete*
Guide to good practice (282 pages, ISBN 978-2-88394-098-7, July 2011)

59 *Condition control and assessment of reinforced concrete structures exposed to corrosive environments (carbonation/chlorides)*
State-of-art report (80 pages, ISBN 978-2-88394-099-4, May 2011)

60 *Prefabrication for affordable housing*
State-of-art report (130 pages, ISBN 978-2-88394-100-7, August 2011)

61 *Design examples for strut-and-tie models*
Technical report (220 pages, ISBN 978-2-88394-101-4, September 2011)

62 *Structural Concrete – Textbook on behaviour, design and performance*, Vol. 5
Manual – textbook (476 pages, ISBN 978-2-88394-102-1, January 2012)

63 *Design of precast concrete structures against accidental actions*
Guide to good practice (78 pages, ISBN 978-2-88394-103-8, January 2012)

64 *Effect of zinc on prestressing steel*
Technical report (22 pages, ISBN 978-2-88394-104-5, February 2012)

65 *fib Model Code 2010*, Final draft – Volume 1
Model Code (350 pages, ISBN 978-2-88394-105-2, March 2012)

This document is the intellectual property of the fib – International Federation for Structural Concrete. All rights reserved.
This PDF of fib Bulletin 92 is intended for use and/or distribution solely within fib National Member Groups.

66 *fib Model Code 2010*, Final draft – Volume 2
Model Code (370 pages, ISBN 978-2-88394-106-9, April 2012)

67 *Guidelines for green concrete structures*
Guide to good practice (56 pages, ISBN 978-2-88394-107-6, May 2012)

68 *Probabilistic performance-based seismic design*
Technical report (118 pages, ISBN 978-2-88394-108-3, July 2012)

69 *Critical comparison of major seismic codes for buildings*
Technical report (216 pages, ISBN 978-2-88394-109-0, August 2013)

70 *Code-type models for structural behaviour of concrete*
State-of-art report (196 pages, ISBN 978-2-88394-110-6, November 2013)

71 *Integrated life cycle assessment of concrete structures*
State-of-art report (62 pages, ISBN 978-2-88394-111-3, December 2013)

72 *Bond and anchorage of embedded reinforcement: Background to the fib Model Code for Concrete Structures 2010*
Technical report (170 pages, ISBN 978-2-88394-112-0, May 2014)

73 *Tall buildings: Structural design of concrete buildings up to 300m tall*
State-of-the-art report (158) pages, ISBN 978-2-88394-113-7, August 2014)

74 *Planning and design handbook on precast building structures*
Manual – textbook (313 pages, ISBN 978-2-88394-114-4, September 2014)

75 *Polymer-duct systems for internal bonded post-tensioning*
Recommendation (172 pages, ISBN 978-2-88394-115-1, December 2014)

76 *Benchmarking of deemed-to-satisfy provisions in standards: Durability of Reinforced Concrete Structures Exposed to Chlorides*
State-of-the-art-report (191 pages, ISBN 978-2-88394-116-8, May 2015)

77 *Corrugated-steel-web bridges*
State-of-the-art-report (110 pages, ISBN 978-2-88394-117-5, December 2015)

78 *Precast-concrete buildings in seismic areas*
State-of-the-art-report (273 pages, ISBN 978-2-88394-118-2, March 2016)

79 *Fibre-reinforced concrete - From design to structural applications*
ACI-*fib* workshop proceedings (480 pages, ISBN 978-2-88394-119-9, May 2016)

80 *Partial factor methods for existing concrete structures*
Recommendation (129 pages, ISBN 978-2-88394-120-5, December 2016)

81 *Punching of structural concrete slabs: Honoring Neil M. Hawkins*
ACI SP-315, ACI-*fib* symposium proceedings (378 pages, ISBN 978-2-88394-121-2, April 2017)

82 *Precast segmental bridges*
Guide to good practice (183 pages, ISBN 978-2-88394-122-9, August 2017)

83 *Precast Tunnel Segments in Fibre-Reinforced Concrete*
State-of-the-art report (162 pages, ISBN 978-2-88394-123-6, November 2017)

84 *Precast insulated sandwich panels*
State-of-the-art report (129 pages, ISBN 978-2-88394-124-3, December 2017)

85 *Towards a rational understanding of shear in beams and slabs*
Technical Report (338 pages, ISBN 978-2-88394-125-0, May 2018)

86 *Safety and performance concepts*
Guide to good practice (357 pages, ISBN 978-2-88394-126-7, August 2018)

87 *2018 fib Awards for Outstanding Concrete Structures*
Bulletin (39 pages, ISBN 978-2-88394-127-4, October 2018)

This document is the intellectual property of the fib – International Federation for Structural Concrete. All rights reserved.
This PDF of fib Bulletin 92 is intended for use and/or distribution solely within fib National Member Groups.

88 *Sustainability of precast structures*
State-of-the-art report (153 pages, ISBN 978-2-88394-128-1, December 2018)

89 *Acceptance of cable systems using prestressing steels*
Recommendation (153 pages, ISBN 978-2-88394-129-8, March 2019)

90 *Externally applied FRP reinforcement for concrete structures*
Technical report (229 pages, ISBN 978-2-88394-131-1, May 2019)

91 *Floating concrete structures*
State-of-the-art report (100 pages, ISBN 978-2-88394-133-5, August 2019)

Abstracts for *fib* Bulletins and lists of available CEB Bulletins and FIP Reports are available on the *fib* website at www.fib-international.org/publications.

This document is the intellectual property of the fib – International Federation for Structural Concrete. All rights reserved.
This PDF of fib Bulletin 92 is intended for use and/or distribution solely within fib National Member Groups.

fib
CEB-FIP

Serviceability Limit State of Concrete Structures

Contents

1 Introduction
2 Requirements for concrete structures in terms of SLS
3 Design criteria of serviceability limit states
4 Rules and explanations
5 Examples
6 Outlook on serviceability limit states
7 Verification of serviceability limit states by numerical simulation
8 Conclusions

ISBN 978-2-88394-136-6

International Federation for Structural Concrete
Fédération internationale du béton
www.fib-international.org

ISSN: 1562-3610